Functional regulation of *Sirt2* during oligodendrocyte development and its requirement during myelination and in an EAE mouse model of multiple sclerosis

A Thesis Submitted to
the College of Graduate and Postdoctoral Studies
in Partial Fulfillment of the Requirements for
the Degree of Doctor of Philosophy
in the College of Pharmacy and Nutrition
University of Saskatchewan
Saskatoon

By

Merlin Premalatha Thangaraj

PERMISSION TO USE

In presenting this thesis in partial fulfillment of the requirements for a Doctor of Philosophy degree from the University of Saskatchewan, I consent that the Libraries of this University may make it freely available for inspection. I further acknowledge that permission for copying this thesis, in whole or in part, for scholarly purposes may be granted by my supervisor Dr. Jane Alcorn. However, any copying, publication, or use of this thesis for financial gain will not be allowed without my written permission. In addition, recognition shall be given to the University of Saskatchewan, as well as myself for any scholarly use that may be made of any data in my thesis.

Requests for permission to copy or make use of information in this thesis in whole or in part should be addressed to:

Dean

College of Graduate and Postdoctoral Studies

University of Saskatchewan

116 Thorvaldson Building, 110 Science Place

Saskatoon, Saskatchewan, S7N 5C9, Canada.

OR

Dean

College of Pharmacy and Nutrition

University of Saskatchewan

104 Clinic Place

Saskatoon, Saskatchewan, S7N 2Z4, Canada.

ABSTRACT

In the central nervous system (CNS), oligodendroglial cells (OLs) form the myelin that ensheaths axons to ensure fast, efficient neurotransmission. Multiple sclerosis (MS) is a chronic demyelinating disease where myelin and myelinating OLs are damaged, making the axons more susceptible to degeneration. The cellular and molecular mechanisms that control the myelinating ability of OLs are largely unknown. The RNA binding protein quaking (QKI) regulates the expression of several myelin specific genes. Sirtuin 2 (SIRT2) is a NAD^+ dependent deacetylase predominantly expressed in OLs. Both *qkI* and *Sirt2* are upregulated during the period of intense CNS myelination *in vivo*; however, it is not known whether these two genes interact to regulate OL differentiation. In the first study, I tested the hypothesis that QKI interacts with *Sirt2* mRNA to promote the expression of SIRT2 in OLs during development. I report for the first time that QKI directly interacts with *Sirt2* mRNA at the 3' untranslated region, protects *Sirt2* mRNA from degradation, and promotes SIRT2 expression in OL lineage cells.

Considering the importance of *Sirt2* in OL differentiation *in vitro*, I hypothesized that loss of *Sirt2* would result in hypomyelination and increase the disease severity in an experimental autoimmune encephalomyelitis (EAE) mouse model of MS. My findings demonstrate that the loss of *Sirt2* results in reduced expression of key myelin genes and a significant reduction in the number of myelinated axons in the CNS *in vivo*. In addition, *Sirt2*$^{-/-}$ mice displayed defects in OL precursor cells (OPC) proliferation and OL differentiation. EAE induction demonstrated that absence of *Sirt2* results in an increased severity of EAE in *Sirt2*$^{-/-}$ mice compared to wild-type mice. These results suggest that *Sirt2* plays a crucial role in OL development and myelination and a protective role in the EAE mouse model of MS. Finally, I investigated the targets through which *Sirt2* could possibly regulate myelination. Cholesterol is

crucial for myelin biogenesis. In neurons, SIRT2 has been implicated in cholesterol biosynthesis by promoting the nuclear translocation of SREBP-2. In this study, I hypothesized that SIRT2 positively regulates the translocation of SREBP-2 into the nucleus in OLs to promote cholesterol biosynthesis. My findings reveal that SREBP-2 and the downstream sterol biosynthesis pathway is not regulated by SIRT2 in OLs during CNS myelination.

Collectively, these findings suggest that QKI regulates the expression of *Sirt2*, which plays a critical role in oligodendrogenesis and myelination of axons in the CNS through SREBP-2/cholesterol-independent mechanism. In addition, *Sirt2* plays a protective role in the EAE mouse model. I believe this research will advance our knowledge in identifying target molecules that regulate the myelinating ability of OLs, leading to the development of potential nutrient and pharmacological therapies for MS.

ACKNOWLEDGEMENTS

I would like to thank my supervisor Dr. Adil J. Nazarali for his constant support, encouragement and guidance. I truly thank him for providing an excellent environment and opportunity to pursue my project. I would like to extend my sincere gratitude to Dr. Jane Alcorn, who kindly accepted to be my supervisor after the sudden demise of Dr. Nazarali. I am grateful for her time and help with my thesis preparation and revisions. I sincerely appreciate the support and help you provided during the most difficult time in the program.

I sincerely thank my co-supervisors Drs. Ronald Doucette and Bogdan Popescu for their mentorship and support during my studies. I also thank my advisory committee members Drs. Darrell Mousseau, Troy Harkness, Phyllis Paterson and Ildiko Badea for their valuable suggestions and support throughout my graduate program. I thank Dr. Jim Eubanks, University of Toronto for agreeing to serve as the external examiner for my defense.

I would like to extend my sincere thanks to Drs. Jane Alcorn, Phyllis Paterson and the College of Pharmacy and Nutrition for their help and support to continue and complete my graduate program after the demise of Dr. Nazarali. I also thank the College of Graduate studies and Research, University of Saskatchewan and Multiple Sclerosis Society of Canada for supporting my graduate studies.

I thank my colleagues Kendra Furber, Paul Iyyanar, LaRhonda Sobchishin, Dennis Okello, Glai Tan, Jotham Gan and Ran Bi for their valuable discussions and friendly help. I also appreciate the technical assistance offered by Ms. LaRhonda Sobchishin for transmission electron microscopy and Ms. Anita Givens for immunohistochemistry. I also thank Ms. Michelle Moroz and the LASU staff especially Ms. Carmen Whitehead for their help with animal maintenance for the research.

I extend my deepest gratitude to my husband Paul P. R. Iyyanar for his support and encouragement to pursue my dream. I also thank my parents, Thangaraj Sangaiah, Clara Thangaraj and my mother in law, Prabhavathy Kadarkarai for their love and moral support.

DEDICATIONS

I would like to dedicate my thesis to my husband Paul P. R. Iyyanar

The manuscripts from this thesis work are dedicated to the memory of my beloved mentors, Drs. Adil J. Nazarali and J. Ronald Doucette, whose values and principles about research and life beyond are an inspiration.

PUBLICATIONS

- **Merlin P. Thangaraj**, Kendra L. Furber, Jotham K. Gan, Shaoping Ji, LaRhonda Sobchishin, J. Ronald Doucette and Adil J. Nazarali. (2017) "RNA-binding Protein Quaking Stabilizes *Sirt2* mRNA during Oligodendroglial Differentiation" *The Journal of Biological Chemistry*, 292; 5166-5182. doi:10.1074/jbc.M117.775544.

- **Merlin P. Thangaraj**, Kendra L. Furber, LaRhonda Sobchishin, Shaoping Ji, J. Ronald Doucette, and Adil J. Nazarali. (2017) "Does Sirt2 Regulate Cholesterol Biosynthesis During Oligodendroglial Differentiation In Vitro and In Vivo?" *Cellular and Molecular Neurobiology*, 38; 329-340. doi:10.1007/s10571-017-0537-6.

TABLE OF CONTENTS

LIST OF FIGURES

LIST OF TABLES

LIST OF ABBREVIATIONS

° C	Degree celsius
AD	Alzheimer's disease
AIP-1	Actin interacting protein 1
ANOVA	Analysis of variance
bp	Base pair
BrdU	5-bromo-2′-deoxyuridine
Caspr	Contactin associated protein
CC	Corpus callosum
CDK	Cyclin-dependent kinase
cDNA	Complementary deoxyribonucleic acid
CFA	Complete Freund's adjuvant
CG4-OL	CG4 oligodendroglial cell line from rat cerebral cortex
CIS	Clinically isolated syndrome
CM	Conditioned medium
CNP	Cyclic nucleotide phosphodiesterase
CNS	Central nervous system
co-IP	co-Immunoprecipitation
DHCR7	7-Dehydrocholesterol reductase
DLFBS	Delipidated fetal bovine serum
DM	Differentiation medium
DM20	Alternatively spliced isoform of PLP
EAE	Experimental autoimmune encephalomyelitis

EM	Electron microscopy
ER	Endoplasmic reticulum
FBS	Fetal bovine serum
FGF	Fibroblast growth factor
FOXO	Forkhead box, class O transcription factor
GM	Growth medium
HD	Huntington's disease
HDAC6	Histone deacetylase 6
HE	Hematoxylin and eosin
HMG-CoA	3-hydroxy-3-methylglutaryl-Coenzyme A
HMGCR	HMG-CoA reductase
HMGCS1	HMG-CoA synthase 1
hnRNPA1	Heterogeneous nuclear ribonucleoprotein A1
HRP	Horse radish peroxidase
IgG	Immunoglobulin G
IPL	Intraperiod line
ISE	Intronic splicing enhancer
jp mice	jimpy mice
kDa	Kilo Dalton
LFB	Luxol fast blue
MAG	Myelin associated glycoprotein
MAP1B	Microtubule associated protein 1B
MBP	Myelin basic protein

md rat	myelin-deficient rat
MDL	Major dense line
MGM	Mixed glial cell medium
min	Minutes
MOG	Myelin oligodendrocyte glycoprotein
MPZ	Myelin protein zero
MS	Multiple sclerosis
mTOR	Mammalian target of rapamycin
NAD	Nicotinamide adenine dinucleotide
Na_v	Voltage-gated sodium channels
Neo	Neomycin
NF155	Neurofascin155
NG2	Neuron-glial antigen 2
NSC	Neural stem cells
ODM	Oligodendrocyte differentiation medium
OGM	Oligodendrocyte growth medium
OL	Oligodendrocyte
Olig2	Oligodendrocyte lineage transcription factor 2
OPC	Oligodendrocyte precursor cell
P	Postnatal day
PBS	Phosphate buffered saline
PCR	Polymerase chain reaction
PD	Parkinson's disease

PDGF	Platelet derived growth factor
PEI	Polyethylenimine
PLP	Proteolipid protein
Plp-ISEdel	Deletion of a critical intronic splicing enhancer of *Plp*
PMD	Pelizaeus-Merzbacher disease
PNS	Peripheral nervous system
PPMS	Primary-progressive MS
PRMS	Progressive-relapsing MS
Pt rabbit	Paralytic tremor rabbit
QKI	Quaking
qk^v/qk^v	*quaking viable* mutant mice
qPCR	Quantitative real time PCR
QRE	Quaking response element
RIS	Radiologically isolated syndrome
RNA	Ribonucleic acid
RNA co-IP	RNA co-immunoprecipitation
rpm	Revolutions per minute
RRMS	Relapsing-remitting MS
rsh	Rumpshaker mouse
RT-PCR	Reverse Transcriptase PCR
s	Seconds
SC	Schwann cells
SCAP	SREBP cleavage activating protein

SCZ	Schizophrenia
SDS	Sodium dodecyl sulphate
SDS-PAGE	Sodium dodecyl sulphate-Polyacrylamide Gel Electrophoresis
SEM	Standard error of the mean
siRNA	Small interference RNA
SIRT2	Sirtuin2
Sirt2$^{-/-}$	*Sirt2* null mice
SPG2	Spastic paraplegia type 2
SPMS	Secondary-progressive MS
SQLE	Squalene epoxidase
SQS	Squalene synthase
SRE	Sterol responsive element
SREBP-2	Sterol-regulatory-element-binding protein-2
TMEV	Theiler's murine encephalomyelitis virus
UTR	Untranslated region
VZ/SVZ	Ventricular / subventricular zone
WT	Wild-type mouse

Note:

Word in *Italics* denotes the gene or mRNA form (eg. *Sirt2* gene)

Word in UPPERCASE letters denotes the protein form (eg. SIRT2 protein)

1. GENERAL INTRODUCTION

Oligodendrocytes (OLs) are the myelin forming glial cells in the central nervous system (CNS) (Baumann and Pham-Dinh, 2001; Bradl and Lassmann, 2010). In the CNS, OL precursor cells (OPCs) originate from the ventricular/subventricular (VZ/SVZ) zones, and proliferate, migrate and eventually differentiate into mature OLs (Baumann and Pham-Dinh, 2001; Bergles and Richardson, 2015). The mature OLs extend their plasma membrane rich in lipids and proteins to ensheath axons with a compact, multilayered membranous myelin sheath (Baumann and Pham-Dinh, 2001; Pfeiffer et al., 1993; Simons and Nave, 2015). Myelination is essential for fast, efficient conduction of action potentials from neuronal cell bodies to synaptic terminals. During demyelination (myelin loss) or axonal injury OPCs are recruited and induced to differentiate to promote remyelination. However, both myelination and remyelination are impaired in multiple sclerosis (MS). MS, a chronic demyelinating disease caused by an immune reaction against myelin and myelin forming OLs (Hanafy and Sloane, 2011; Miron et al., 2011; Kotter et al., 2011). MS results in non-traumatic neurological disability in adults between 20 to 50 years old, with a prevalence high in North America and Europe (140 and 108 in 100,000 population, respectively) and low in Sub-Saharan Africa and East Asia (2.1 and 2.2 in 100,000 population, respectively) (Multiple Sclerosis International Federation, 2013). The cellular and molecular mechanisms regulating OL to myelinate axons is of critical importance in understanding effective repair in MS.

The RNA binding protein quaking (QKI) plays an important role in myelination by post-transcriptionally regulating several myelin specific genes (Li et al., 2000; Wu et al., 2002; Zhao et al., 2006a, b; Zhao et al., 2010). QKI regulates splicing, stabilization, subcellular localization and/or translation efficiency of the target mRNA. The *quaking viable* (qk^v/qk^v) mutant mouse,

which harbors a one megabase deletion upstream of *qkI* locus, exhibits hypomyelination in the CNS mainly due to a defect in OL maturation (Chenard and Richard, 2008; Hardy, 1998a, b). QKI has been reported to interact with target mRNAs such as myelin basic protein (*Mbp*) (Larocque et al., 2002; Li et al., 2000; Ryder and Williamson, 2004), proteolipid protein (*Plp1)* (Wu et al., 2002), myelin associated glycoprotein (*Mag)* (Wu et al., 2002), cyclin dependent kinase inhibitor $p27^{Kip1}$ (Larocque et al., 2005), actin interacting protein 1 (*Aip-1*) (Doukhanine et al., 2010), microtubule associated protein 1B (*Map1B*) (Zhao et al., 2006a) and heterologous nuclear ribonucleoprotein A1 (*hnRNPA1*) (Zearfoss et al., 2011) in OLs.

Sirtuin 2 (SIRT2) is a class III NAD^+-dependent deacetylase predominantly expressed in the cytoplasm of OLs (North et al., 2003). Interestingly, the expression of SIRT2 protein but not mRNA is impaired in the qk^v/qk^v mutant mice (Zhu et al., 2012). Furthermore, SIRT2 expression is reduced in the myelin sheath of *Plp* null mice, which lacks both PLP and DM20 (Werner et al., 2007) and *Plp*-ISEdel (deletion of intronic splicing enhancer of *Plp*) mutant mice in which PLP is selectively reduced but not DM20 (Zhu et al., 2012). Moreover, no putative QKI binding sites have been previously identified in *Sirt2* mRNA. Thus, it was postulated that QKI indirectly regulates SIRT2 through PLP (downstream target of QKI), which aids in the transport of SIRT2 into the myelin sheath (Zhu et al., 2012). However, the molecular mechanism that governs the direct or indirect interaction between QKI and *Sirt2* during OL development has not been elucidated (Objective 1). In this thesis, I have investigated the post-transcriptional regulation of *Sirt2* by QKI in CG4-OL cells and primary OL cells by RNA co-immunoprecipitation. Results reveal that QKI binds to all the three variants of *Sirt2* mRNA at the 3' untranslated region (UTR) through a common quaking response element (QRE) at 1853bp. My findings indicate that QKI interacts directly with *Sirt2* mRNA to regulate its expression during OL development.

In addition to investigating the regulation of *Sirt2* by QKI, I explored the role of *Sirt2* during OL development, myelination and in MS. Our group has previously demonstrated that *Sirt2* is essential for the OL process formation and plays a role in the maturation of OLs *in vitro* (Ji et al., 2011). Moreover, SIRT2 is upregulated during the peak period of myelination in the CNS (Southwood et al., 2007) as well as in the peripheral nervous system (PNS) (Beirowski et al., 2011). In addition, studies on myelin proteome revealed that the isoform SIRT2.2 integrates into myelin in close proximity to PLP and the alternatively spliced isoform of PLP (DM20) and is localized in paranodal loops (Li et al., 2007a; Southwood et al., 2007; Werner et al., 2007). Interestingly, the expression profile of SIRT2 is similar to that of MBP and myelin protein zero (MPZ) in the CNS and PNS, respectively (Ji et al., 2011; Beirowski et al., 2011). However, the role of *Sirt2* in CNS myelination and in the disease severity of experimental autoimmune encephalomyelitis (EAE), a mouse model of MS, has not been investigated (Objective 2). Here, I examined the impact of loss of *Sirt2* in myelination and in the disease severity of EAE using *Sirt2* knockout (*Sirt2*$^{-/-}$) mice. Loss of *Sirt2* was associated with reduced myelin gene expression, hypomyelination and an increased disease severity in the EAE mouse model.

Cholesterol represents one of the major components of myelin and defects in cholesterol synthesis significantly impair myelination (Norton and Poduslo, 1973a; Saher et al., 2005; Saher and Simons, 2010; Mathews et al., 2014). Interestingly, *Sirt2* plays a role in the sterol biosynthesis mediating the nuclear translocation of sterol regulatory element binding protein (SREBP)-2 (Luthi-Carter et al., 2010; Taylor et al., 2011). SREBP-2 is a key transcription factor that enters into the nucleus under low intracellular sterol levels and binds to sterol responsive element (SRE) inducing genes encoding enzymes involved in cholesterol biosynthesis (Amemiya-Kudo et al. 2002; Eberlé et al. 2004; Horton et al. 2002; Horton et al. 2003).

Inactivation of enzymes involved in cholesterol biosynthesis such as squalene synthase (SQS) and HMG-CoA synthase 1 (HMGCS1) results in reduced myelin gene expression (Mathews et al., 2014; Saher et al., 2005). Overexpression of *Sirt2* increases MBP expression and facilitates arborization of OLs *in vitro* (Ji et al., 2011). It is not known if these changes are due to increased translocation of SREBP-2 into the nucleus by SIRT2 (Objective 3). To address this, I utilized *Sirt2*$^{-/-}$ mutant mice to investigate the role of *Sirt2* in regulating cholesterol biosynthesis *in vivo* and *in vitro* in the developing CNS white matter and primary OL cultures, respectively. In addition, I evaluated the impact of loss or gain of function of *Sirt2* on the expression of cholesterol biosynthetic genes, cholesterol content and nuclear translocation of SREBP-2 using CG4-OLs. My findings suggest that *Sirt2* is not involved in the regulation of SREBP-2 dependent cholesterol biosynthesis in OLs during CNS myelination.

1.1 Hypotheses

1. QKI binds, interacts, and stabilizes *Sirt2* mRNA at the 3' UTR to induce expression of *Sirt2*.
2. *Sirt2* is a positive regulator of OL differentiation and myelination by facilitating the expression of myelin specific genes. *Sirt2* plays a protective role in the EAE mouse model of MS by improving myelin repair.
3. SIRT2 facilitates the translocation of SREBP-2 from cytoplasm into nucleus and promotes cholesterol biosynthesis.

1.2 Objectives

1. To elucidate the post-transcriptional regulation of *Sirt2* transcripts by QKI during OL development *in vitro*.
2. To determine the impact of loss of function of *Sirt2* in CNS myelination, OL development, and on the disease severity of the EAE mouse model of MS.
3. To investigate the impact of *Sirt2* in cholesterol biosynthesis during OL differentiation *in vivo* and *in vitro*.

2. REVIEW OF LITERATURE

Myelination is an essential biological process required for the proper development and functioning of the vertebrate nervous system (Nave and Werner, 2014). Myelin is a multilayered membranous sheath formed by glial cells such as oligodendrocytes (OLs) in the CNS and by Schwann cells (SC) in the PNS. OLs and SCs differ in their developmental origin and capability to myelinate axons. OLs arise from the subventricular zone and SCs arise from the neural crest (Jessen and Mirsky, 2005; Levison and Goldman, 1993; Luskin and McDermott, 1994; Ndubaku and de Bellard, 2008). One OL can myelinate up to 60 axons (1:60) (Remahl and Hildebrand, 1990) whereas one SC can myelinate only one internode of one axon (1:1). In addition, there are also differences in the composition of structural proteins constituting the myelin sheath in the CNS and the PNS (Nave and Werner, 2014). In this literature review, I will mainly focus on the CNS myelination by OLs.

2.1 Oligodendrocyte development and myelination

In developing CNS, the OPCs develop from the neuroepithelial precursor cells or neural stem cells (NSC) that originate in dorsal and ventral regions of brain and spinal cord (Kessaris et al., 2006; Vallstedt et al., 2005; Bergles and Richardson, 2015). The progression of OPCs to mature myelinating OL is a complex and dynamic process regulated by transcription factors, growth factors, epigenetic factors and extrinsic signals (Emery, 2010; Emery and Lu, 2015). In the mouse spinal cord, the first set of OPC arise from the ventral ventricular zone at embryonic stage (E) 12.5 and then after 2 days a second set of OPCs arise from the dorsal ventricular zone (Warf et al, 1991; Lu et al., 2002; Fogarty et al., 2005; Cai et al., 2005). In the brain, the first set of OPC is generated from the ventral forebrain in the medial ganglionic eminence and anterior

entopeduncular area around E12.5. These OPCs migrate and populate the cerebral cortex. The second set of OPC is derived from the lateral and caudal ganglionic eminences around E15.5. The third set of OPC is generated locally in the cortex around birth (Kessaris et al., 2006). During postnatal development, OPCs continue to develop from NSC that arise from the subventricular zones and populate cortex (Levison and Goldman, 1993; Luskin and McDermott, 1994; Baumann and Pham-Dinh, 2001; Nicolay et al., 2007). Although the ventrally and dorsally derived OPCs display similar electrical properties, they had different migration, settling and differentiation patterns (Tripathi et al., 2011; Crawford et al., 2016). Oligodendrocyte lineage transcription factor 2 (Olig2) plays a critical role in the specification of NSCs to OPCs (Lu et al., 2002; Ligon et al., 2006). Once specified OPCs with bipolar morphology proliferate and express progenitor cell markers such as the platelet-derived growth factor receptor alpha (PDGFRα) and neuron-glial antigen 2 (NG2) proteoglycan (Nishiyama et al., 1996; Levine et al., 2001; Marques et al., 2016). These proliferating OPCs migrate to the site of myelination through vasculature (Tsai et al., 2016) and transform into intermediate immature OLs displaying a multipolar morphology with oligodendrocyte cell surface antigen-4 (O4) expression. Finally, the immature OLs differentiate into myelinating OLs that express mature OL markers such as myelin basic protein (MBP), proteolipid protein (PLP) and other myelin structural proteins (Marques et al., 2016). The myelin structural protein expression in the differentiated OL is mediated by transcription factors such as Olig1 (Xin et al., 2005; Li et al., 2007b), Olig2 (Lu et al., 2002; Liu et al., 2007), Sox10 (Stolt et al., 2002; Liu et al., 2007; Li et al., 2007b) and myelin gene regulatory factor (Emery et al., 2009). Deletion of each individual transcription factor impaired myelin structural protein expression, indicating that all these transcription factors play a non-redundant role to promote OL differentiation and myelination (Emery and Lu, 2015). The

myelinating OLs extend their plasma membrane to encapsulate axons (Fig. 2.1) (Pfeiffer et al., 1993; Simons and Nave 2015; Snaidero and Simons, 2017).

After establishing contact with an appropriate axon, the glial membrane starts to wrap the axon, leaving an inner tongue of cytoplasm (plasmalemma) close to the axon surface, which forms the inner mesoaxon (periaxonal layer). This inner tongue continues to grow under the previously deposited membrane leading to the formation of a multilayered myelin sheath (Snaidero et al., 2014). The newly formed myelin membranes extend laterally, constituting the paranodal loops (Snaidero et al., 2014). The paranodal loops are attached to the axon by neurofascin155 (NF155), contactin and contactin associated protein (caspr) (Simons and Trajkovic, 2006; Pedraza et al., 2009). As it continues to wrap, the plasmalemma fuses to form a condensed cytoplasmic membrane structure, which appears dark under the electron microscope and is called the major dense line (MDL). The closely opposed outer surface of the glial membrane appears lighter and is called the intraperiod line (IPL). Towards the end of wrapping, the plasmalemma leaves a loop forming the outer mesoaxon (abaxonal layers) (Soldan and Pirko, 2012; Simons and Nave, 2015; Snaidero and Simons, 2017). Thus, under the electron microscope, the myelin sheath is visualized as having a compact region (MDL and IPL) and a non-compact region (mesoaxon and paranodal loops) (Nave and Werner, 2014). The region of axon that is covered by myelin forms the internode (Fig. 2.2). The space between two internodes that is left uncovered by myelin constitutes the nodes of Ranvier enriched in voltage-gated sodium channels (Na_V) (Quarles et al., 2006; Soldan and Pirko, 2012). The Na_V channels, which are diffusely distributed, become clustered at the nodes of Ranvier by oligodendrocyte protein or oligodendroglial contact with the axon and aids in fast and efficient action potential propagation (Kaplan et al., 1997; Kaplan et al., 2001; Simons and Trajkovic, 2006; Freeman et a., 2016).

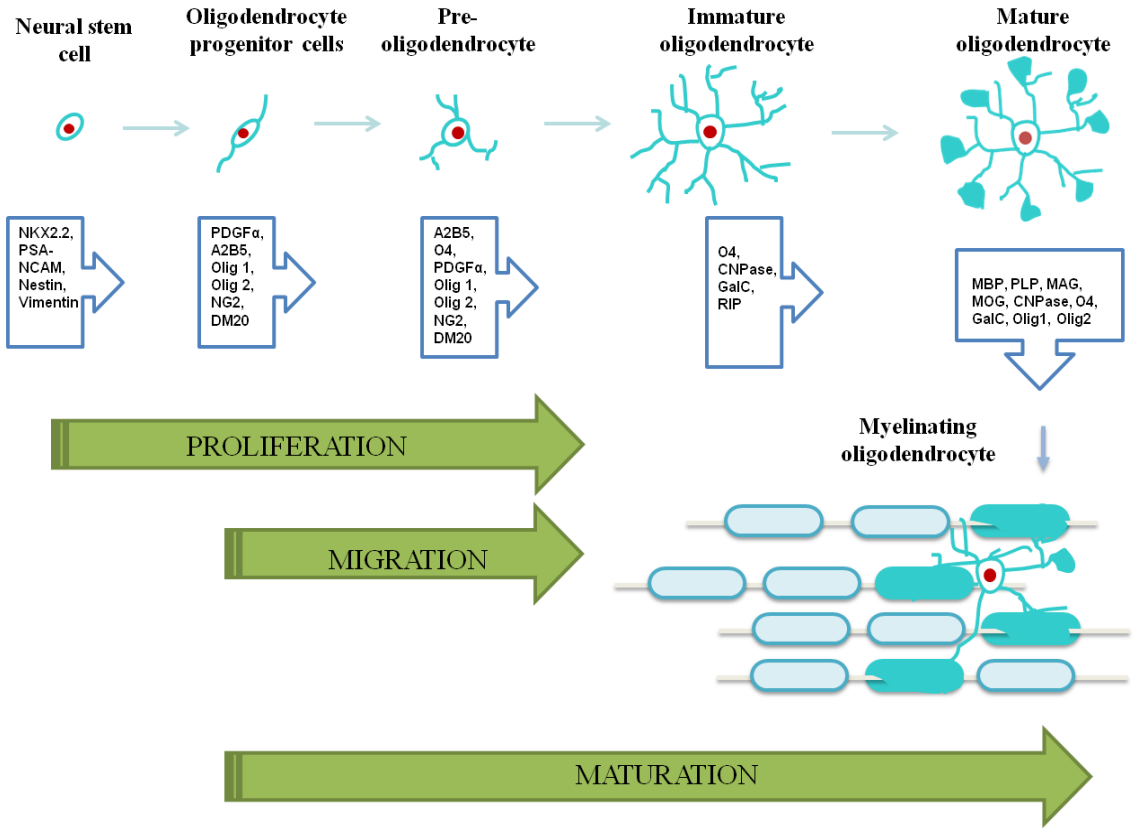

Figure 2.1: Schematic representation of developmental stages involved in OL development. OL development initiates with NSC and OPC, which undergo proliferation and express stage-specific markers while progressing to the pre-oligodendrocyte stage. The pre-oligodendrocytes with bipolar morphology migrate and develop into immature OLs with a multipolar morphology. These immature OLs differentiate to extend multiple cellular processes to wrap nearby axons with myelin, during which they express myelin specific markers such as MBP, PLP and MAG. Stage-specific markers are indicated in boxes (adapted from Baumann and Pham-Dinh, 2001).

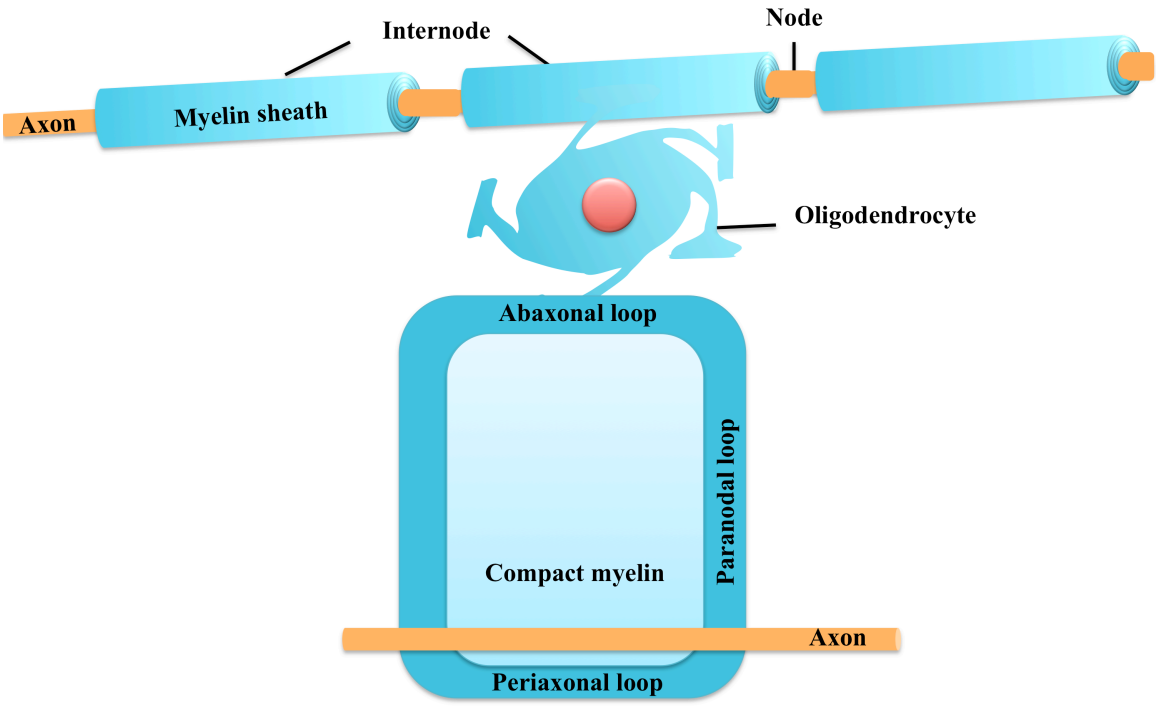

Figure 2.2: Myelin sheath in the CNS. Axons in the CNS are wrapped around by OLs. The part of the axon covered by myelin forms the internode, and the uncovered part of the axon forms the Node of Ranvier. The spiraling of the myelin sheath starts at the inner mesoaxon (periaxonal loop), which fuses and continues to wrap as compact myelin and ends with non-compact outer mesoaxon (abaxonal loop) (adapted from Soldan and Pirko, 2012).

2.2 Myelin proteins and their impact on myelin structure

Myelin is composed of approximately 70% lipids and 30% proteins (Quarles et al., 2006). Myelin forms as protein–lipid–protein-lipid-protein structure (Morell and Quarles, 1999). MBP and PLP constitute the major myelin structural proteins (Table 2.1). The role of myelin structural proteins in CNS myelination is complex and unique with each protein mutation displaying a difference in ultrastructural myelin changes, motor function and coordination. In addition, different types of mutations of the same gene (e.g. *Plp*) exhibit structural and functional differences.

2.2.1 Myelin basic protein (MBP)

MBP constitutes 8% of the total myelin proteome in the mouse CNS (Table 2.1) (Jahn et al., 2009). It is an intrinsic cytosolic protein expressed in the inner surface of the OL membrane forming the MDL (Readhead et al., 1990). MBP is encoded as a product of a large gene complex called Golli (Genes of Oligodendrocyte Lineage), which has 11 exons and 3 transcription start sites (Campagnoni et al., 1993; Givogri et al., 2001). The region downstream of transcription start site 3 has seven exons (exon I to VII) and encodes classic MBP isoforms of molecular masses 21.5, 18.5, 17 and 14 kDa as a result of alternative splicing of the primary mRNA transcript (de Ferra et al., 1985; Takahashi et al., 1985; Givogri et al., 2001). Among the four isoforms, 14 kDa and 18.5 kDa MBP isoforms lacking exon II are the most abundant in CNS (Akiyama et al., 2002). The positively charged MBP associates with negatively charged oligodendroglial phospholipids and facilitates the compaction of myelin sheath (Hu et al., 2004; Boggs, 2006; Muller et al., 2013; Harauz and Boggs, 2013). The *Mbp* mRNA is transported through RNA transport granules from the site of synthesis to the myelin compartment where

localized translation occurs (Colman et al., 1982; Muller et al., 2013). The transport requires OL cytoskeleton, microtubules and kinesin motors. Disruption of microtubule dynamics or kinesin restricts translocation of *Mbp* mRNA and results in failure in myelin sheath compaction (Lyons et al., 2009).

Several studies on naturally occurring *Mbp* mutants have rendered extensive knowledge on the role of *Mbp* in CNS myelination (Table 2.2 and 2.3). In general, all *Mbp* mutants exhibit hypomyelination, tremor and shortened life span (Chernoff, 1981; Matthieu et al., 1992), underlining the critical role played by this gene in the functioning of the vertebrate CNS. One of the well-known naturally occurring *Mbp* mutants is the *shiverer* mutant mouse, where exon two to seven is deleted (Roach et al., 1985) resulting in complete absence of MBP expression (Jacque et al., 1983). Hypomyelination is observed only in the CNS but not in PNS. Furthermore, the CNS myelin is not compact with complete absence of MDL (Readhead and Hood, 1990).

Myelin deficient mouse (*mld*) is another *Mbp* mutant mouse where the *Mbp* locus has two tandem *Mbp* genes. In this *mld Mbp* locus, the upstream gene at the 3' end from exon three to seven is in reverse orientation (Popko et al., 1987). In *mld* mice, the *Mbp* transcripts are abnormally unstable leading to reduced levels of *Mbp* mRNA levels (Popko et al., 1987). Conversely, with increasing age the *Mbp* mRNA levels recover to some extent albeit lower than in the wild-type, resulting in compaction of myelin in some axons (Matthieu et al., 1980; Matthieu et al., 1984).

2.2.2 Proteolipid protein (PLP)

The PLP is the most abundant protein in the CNS myelin. PLP constitutes 17% of the total myelin proteome (Table 2.1) (Jahn et al., 2009). *Plp* gene is present on the X-chromosome with seven exons, which gives rise to two proteins (PLP and DM20) due to the 5' splice site present in exon 3. PLP is a 30 kDa protein and its alternatively spliced isoform DM20 is a 26.5 kDa protein, which differs from PLP by lacking 35 amino acids (aa) (Nave et al., 1987). PLP is present in the extracellular membrane of OL forming the IPL (Barkovich, 2000). In mouse, bovine and human CNS, DM20 protein is expressed prior to PLP protein during development (LeVine et al., 1990). However, with development, PLP becomes the predominant protein in the CNS (LeVine et al., 1990). All the *Plp* mutations are inherited in an X-linked manner (Willard & Riordan, 1985). In humans, mutation in *Plp* has been associated with X-linked dysmyelinating leukodystrophies, Pelizaeus-Merzbacher disease (PMD) and spastic paraplegia type 2 (SPG2). Similar to *Mbp*, *Plp* has also been studied extensively with several naturally occurring and transgenic mutant lines (Table 2.2 and 2.3). These mutants provide models for PMD/SPG2 with varying clinical presentation.

In jimpy (*jp*) mice, a naturally occurring point mutation within intron four of the *Plp* gene results in aberrant splicing of exon five, causing a frameshift in the translation that gives rise to a protein with a truncated C-terminus (Dautigny et al., 1986; Nave et al., 1987; Hudson et al., 1987). This causes misfolding of PLP and DM20 and eventually gets degraded after synthesis (Roussel et al., 1987). In *jp* mice, less than 5% of the axons are myelinated, which are ultrastructurally abnormal (Duncan et al., 1989). In addition, there is an increase in the number of immature OLs and increased apoptosis of differentiated OLs (Knapp et al., 1986; Skoff, 1995).

The myelin-deficient *(md)* rat is another *Plp* mutant rodent that exhibits severe hypomyelination in the CNS similar to *jp* mice (Dentinger et al., 1982). These rats are characterized by a point mutation (A-C transversion) in exon three of the *Plp* gene, which causes a threonine to proline (T75P) substitution. This mutation induces a conformational change and disrupts the integration of PLP within the membrane (Boison and Stoffel, 1989). The offspring develop tremors, ataxia and seizures, and die after 24-28 days (Boison and Stoffel, 1989). Furthermore, at 17-20 days of age these rats display axonal swellings (Dentinger et al., 1982). Most of the axons are unmyelinated and only a few are myelinated with non-compact myelin like loops of membrane (Dentinger et al., 1982; Duncan et al., 1987).

In addition to the *jp* mouse and the *md* rat, importance of the *Plp* gene was studied using Rumpshaker (*rsh*) mouse (Griffiths *et al*., 1990), Shaking pup (Nadon *et al*, 1990) and paralytic tremor (*Pt*) rabbit (Tosic *et al*., 1993), all of which have unique missense mutations of the *Plp* gene causing single amino acid substitutions. In all these mutants, distinction between IPL and MDL is lost with less compaction at the IPL. Interestingly, the CNS is severely affected with very little defects noted in the PNS in these *Plp* mutants, highlighting the predominant role of PLP in CNS.

In addition to spontaneous mutants, the *Plp* gene was studied with two lines of mice with targeted mutations. In *Plp* deficient mice, the splice site at exon three is disrupted leading to aberrant splicing of the primary transcript. Small diameter axons were unmyelinated while the myelin in the myelinated axons was uncompacted with normal MDL and missing IPL (Boison and Stoffel, 1994). In $Plp^{-/-}$ mice, the translation start site was disrupted (Klugmann et al., 1997). In contrast to the naturally occurring *rsh* mutant that showed defects in motor performance as early as six months of age (Klugmann et al., 1997), $Plp^{-/-}$ mice displayed motor defect only after

16 months of age (Griffith et al., 1998). Myelin compaction was normal with condensed IPL resembling MDL in *Plp*$^{-/-}$ mice. However, axonal swellings and degeneration was observed more predominantly in small caliber axons in the *Plp*$^{-/-}$ mice (Griffith et al., 1998; Rosenbluth et al., 2006).

In addition, deletion of the intronic splicing enhancer (ISE) in *Plp* (*Plp*-ISEdel mutant mouse) reduced *Plp* /*Dm20* mRNA and protein ratio (Wang et al., 2008). Furthermore, the myelin sheath of *Plp*-ISEdel mutant mice was ultrastructurally abnormal with rare axonal degeneration (Wang et al., 2008). In addition, axonal injury and gliosis were increased during two to four months of age in *Plp*-ISEdel mutant mice (Bachstetter et al., 2013). In humans, deletion of a 19 bp sequence within intron three of the *Plp* reduced the *Plp*/*Dm20* mRNA ratio and was associated with myelin instability and axonal loss (Hobson et al., 2002).

2.2.3 Myelin-associated glycoprotein (MAG)

MAG is a 100 kDa glycoprotein that is enriched in the inner tongue (adaxonal) of the oligodendrocyte membrane (Quarles et al., 2006). MAG constitutes 1% of the myelin proteome (Table 2.1) (Jahn et al., 2009). *Mag* is located on chromosome 7 and has 13 exons (Barton et al., 1987). Exon 12 harbors a stop codon and alternative splicing of exon 12 generates an isoform with longer C-terminus, L-MAG (lacks exon 12) and another isoform with truncated C-terminus, S-MAG (Lai et al., 1987). L-MAG predominates early in development during active myelination of the CNS whereas S-MAG increases during development and becomes predominant in adults (Lai et al., 1987). In the *Mag*$^{-/-}$mice, myelination in the PNS is affected more severely compared to the CNS (Li et al., 1994). Subtle ultrastructural abnormalities such as shortened periaxonal collar and double myelin sheath are observed in the CNS, with an increase in severity with aging

(Uschkureit et al., 2000). Loss of *Mag* results in increased MBP expression only in the PNS but not in the CNS (Li et al., 1994; Uschkureit et al., 2000).

A better understanding of the role of *Mag* in myelination was achieved by generating double and triple knockout with *Plp* and *Mbp* (Table 2.3) (Uschkureit et al., 2000). In $Plp^{-/-}Mag^{-/-}$ double mutant mice, axon degeneration is observed with cognitive and motor defects. In $Plp^{-/-}$ $Mbp^{-/-}Mag^{-/-}$ triple mutant mice, hypomyelination is observed with pseudomyelin. Both $Plp^{-/-}$ mice and $Mag^{-/-}$mice exhibit normal phenotypic, while $Plp^{-/-}Mag^{-/-}$ double mutants exhibit tremor beginning at four weeks of age. However, single ($Plp^{-/-}$mice and $Mag^{-/-}$mice) and double mutants ($Plp^{-/-}Mag^{-/-}$ mice) possess normal life span (Uschkureit et al., 2000). Conversely, $Mbp^{-/-}$ (*shiverer*) mutants die around 3 months of age, while $Plp^{-/-}Mbp^{-/-}Mag^{-/-}$ triple mutants have a life span of around 7-9 months (Uschkureit et al., 2000). Axonal degeneration occurred at later stage of life in $Plp^{-/-}$ mice (Griffiths et al., 1998) while in double mutants axonal degeneration occurs at postnatal day (P) 40 (Table 2.3). Furthermore, in $Mbp^{-/-}$ (*shiverer*) mutants, OLs were unable to wrap axons, whereas in $Plp^{-/-}$ $Mag^{-/-}$ double mutants and in $Plp^{-/-}Mbp^{-/-}$ $Mag^{-/-}$ triple mutants, OLs wrap large axons with few lamellae (Uschkureit et al., 2000). To sum up, deletion of *Mag* in $Plp^{-/-}$ or $Plp^{-/-}Mbp^{-/-}$ double mutants causes an early onset of axon degeneration and shortened lifespan (Table 2.3) (Uschkureit et al., 2000).

2.2.4 Myelin oligodendrocyte glycoprotein (MOG)

MOG is a 28 kDa glycoprotein present in the outer tongue (abaxonal) of the oligodendrocyte membrane (Brunner et al., 1989). Similar to MAG, MOG constitutes 1% of the total myelin proteome (Table 2.1) (Jahn et al., 2009). MOG protein belongs to the immunoglobulin superfamily and the *Mog* gene is located within the major histocompatibility

complex gene locus (Pham-Dinh et al., 1993). MOG protein expression initiates during the onset of myelination and hence is considered a marker of OL maturation (Scolding et al., 1989). However, *Mog* null mice did not show any physical, behavioral, myelin structural or axonal abnormalities (Delarasse et al., 2003).

2.2.5 2', 3'-Cyclic nucleotide 3'-phosphodiesterase (CNP)

CNP is another myelin protein, which constitutes about 4% of the total myelin proteome (Table 2.1) (Jahn et al., 2009). *Cnp* encodes two protein isoforms due to the presence of alternative translation start sites in exons one and two. The protein isoforms appear as a doublet with a molecular mass of 46 kDa and 48 kDa (O'Neill et al., 1997). The enzymatically active CNP hydrolyzes 2', 3'-cAMP preferably, in addition to cGMP, cCMP and cUMP. CNP is predominantly present in the soma of OLs (Nishizawa et al., 1985) and hence, is associated with the non-compact regions such as the inner mesaxon and paranodal loops (Braun et al., 1988; Trapp et al., 1988). Disruption of *Cnp* in mice leads to axonal swelling and neurodegeneration with increased reactive gliosis (Lappe-Siefke et al., 2003). In addition, motor performance is reduced at six months of age and the mortality increased around 13 months of age (Table 2.3) (Lappe-Siefke et al., 2003). Recently, CNP was reported to associate with actin cytoskeleton to counteract membrane compaction by MBP, thereby maintaining the cytoplasmic channels within the myelin compartment (Snaidero et al., 2017).

Table 2.1: Relative abundance of myelin proteins in CNS determined by mass spectrometry

Myelin protein	**Percentage (%) in CNS myelin proteome**	**Localization**	**Function**
Proteolipid protein (PLP)	17%	Compact myelin	• Extracellular membrane protein • Forms the intraperiod line • Compaction
Myelin basic protein (MBP)	8%	Compact myelin	• Intracellular membrane protein • Forms the major dense line • Adhesion and Compaction
Cyclic nucleotide phosphodiesterase (CNP)	4%	Noncompact myelin	• 2', 3'-cAMP metabolism • Counteract membrane compaction
Myelin oligodendrocyte glycoprotein (MOG)	1%	Abaxonal layer	• Maintenance of myelin integrity
Myelin-associated glycoprotein (MAG)	1%	Noncompact myelin	• Maintenance of myelin integrity
Sirtuin 2 (SIRT2)	1%	Noncompact myelin	• Deacetylase • OL maturation

Table 2.2: Spontaneous mutations of myelin specific genes and their impact on myelination

Names of mutants	Affected gene	Inheritance	Observed defects	References
Jimpy mouse (*jp*), rumpshaker mouse (*rsh*), myelin-deficient (*md*) rat, shaking pup, paralytic tremor (*Pt*) rabbit	Proteolipid protein (*Plp*)	X-linked	• Hypomyelination in the CNS • Variable degrees of oligodendrocyte death • Decreased compaction at IPL	Quarles et al., 2006; Campagnoni and Skoff, 2001; Dentinger et al., 1982; Duncan et al., 1989
Shiverer mouse, myelin deficient (*mld*) mouse	Myelin basic protein (*Mbp*)	Autosomal recessive	• Severe CNS hypomyelination • Tremor • Shortened life span • Failure in the compaction of MDL	Quarles et al., 2006; Campagnoni and Skoff, 2001; Chernoff, 1981; Matthieu et al., 1992; Readhead and Hood, 1990
quaking viable mouse (qk^v/qk^v)	Quaking (*qkI5*, *qkI6* and *qkI7*)	Autosomal recessive	• Severe CNS hypomyelination • Lack of compaction and poorly developed nodes • Defect in oligodendrocyte development • Tremor at the caudal part of the trunk	Sidman et al., 1964; Wisniewski and Morell, 1971; Hardy, 1998a; Chenard and Richard, 2008).

Table 2.3: Phenotype and morphology changes in the myelin of mutant mice

Transgenic lines	Morphology of myelin	Morphology of axons	Phenotype	Life span
[a]*Mbp*$^{-/-}$	• Hypomyelination in CNS • Increase in the number of OLs	• Not altered compared to wild-type	• Tremor • Lack of motor coordination	3-4 months
[a]*Plp*$^{-/-}$	• Dissociation of IPL • Decompact myelin membrane	• Late onset of degeneration in CNS	• Normal phenotype	>24 months
[a]*Mag*$^{-/-}$	• Reduced cytoplasmic collar • Doubled myelin sheaths in CNS	• Late onset of degeneration in CNS	• Normal phenotype	>24 months
[a]*Plp*$^{-/-}$*Mbp*$^{-/-}$	• Hypomyelination in CNS • Pseudomyelin in CNS • Increase in the number of OLs	• Late onset of degeneration in CNS	• Tremor • Lack of motor coordination	>24 months
[a]*Plp*$^{-/-}$*Mag*$^{-/-}$	• Dissociation of IPL • Decompact myelin membrane	• Early onset of degeneration in CNS	• Tremor • Lack of motor coordination	>24 months
[a]*Plp*$^{-/-}$*Mbp*$^{-/-}$ *Mag*$^{-/-}$	• Hypomyelination in CNS • Pseudomyelin in CNS • Increase in the number of OLs	• Early onset of degeneration in CNS	• Tremor • Lack of motor coordination	7-9 months
[b]*Cnp*$^{-/-}$	• Disrupts non compact myelin regions (mesoaxon and paranodal loops) • Increased reactive gliosis	• Axonal swelling and neurodegeneration	• Normal phenotype	13 months

Data published in [a] Uschkureit et al., 2000; [b]Lappe-Siefke et al., 2003

2.3 Demyelination

Loss of myelin forming OLs or the myelin sheath results in demyelination (Love, 2006; Kotter et al., 2011; Miron et al., 2011). Demyelination slows down the action potential propagation along axons, which eventually leads to axonal degeneration. In the CNS, demyelination is caused by several factors such as inflammation, viral infections, metabolic problems, hypoxia and focal compression (Love, 2006). However, the inflammatory demyelinating disease, multiple sclerosis (MS), is the most prevalent in the CNS (Hanafy and Sloane, 2011; Kotter et al., 2011; Miron et al., 2011).

2.3.1 Multiple sclerosis

MS is the leading cause of neurological disability in adults between the age of 20-50 and appears to be three times more common in females (Milo and Miller, 2014). MS has an incidence rate of 140 and 108 in 100,000 in North America and Europe, respectively (Multiple Sclerosis International Federation, 2013). Canada has one of the highest incidences of MS in the world (World Health Organization, 2008). MS is a complex disease caused by genetic susceptibility, immune system's attack and environment (Gross and Jager, 2011). However, the exact pathogenic mechanism underlying the cause of disease is not yet fully understood. MS is characterized as a prototypic immune-mediated disorder of the CNS mediated by autoreactive T cells against myelin proteins (Hafler et al., 2005; Compston and Coles, 2008). Upon entry into the CNS, these myelin-reactive T cells cause multiple areas of inflammation, demyelination, glial scarring (sclerosis), perivascular leukocyte infiltration, axonal damage and neuronal loss leading to the formation of lesions in brain and spinal cord (Frohman et al., 2005; Peterson and Fujinami, 2007; Milo and Miller, 2014). Demyelinating lesions display heterogeneity in the pathology and

are categorized into four distinct patterns (pattern I to IV). These include macrophage associated demyelination in pattern I, complement and antibody mediated demyelination in pattern II, lesions with oligodendrocyte apoptosis as pattern III and lesions with oligodendrocyte degeneration as pattern IV (Lucchinetti et al., 2000)

2.3.2 Clinical subtypes of MS

The clinical course of MS is classified into four different types based on the progression and recovery of the disease (Lublin and Reingold, 1996; Hurwitz, 2009) (Fig. 2.3):

1. Relapsing-remitting MS (RRMS):

Nearly 85% of MS patients develop this form of MS at early onset (Jacobs et al., 1999). These patients generally recover after the first few weeks of attack, but the recovery is generally incomplete. This type of MS is characterized by inflammation, demyelination, axonal transaction and remyelination (Lublin and Reingold, 1996). With prolonged disease, plaques are formed in the white matter of the brain (Thompson et al., 1990).

2. Secondary-progressive MS (SPMS):

RRMS after prolonged progression of the disease could be transformed into SPMS (Hurwitz, 2009). Approximately 50% of RRMS cases transform to SPMS after 10 years (Milo and Miller, 2014). Severity of the motor dysfunction increases with enlarged ventricles. Thinning of corpus callosum (CC) occurs with atrophy in the whole brain and spinal cord (Lublin and Reingold, 1996).

3. Primary-progressive MS (PPMS):

This type of MS is characterized by gradual progression of the symptoms without any sign of relapses interrupted with brief periods of remittance (Lublin and Reingold, 1996). These patients have difficulties in walking and other motor dysfunction. Lesions in the brain are small; however, spinal cord lesions are large and numerous (Lublin and Reingold, 1996). PPMS is most commonly seen in males and older patients (Hurwitz, 2009).

4. Progressive-relapsing MS (PRMS):

These patients experience a gradual worsening of the disease from onset accompanied by progressive relapses with or without remittance (Lublin and Reingold, 1996). This type of MS is rare and occurs in about 5% of the MS patients (Jacobs et al., 1999).

Recently, additional subtypes such as clinically isolated syndrome (CIS) and radiologically isolated syndrome (RIS) were included in clinical MS subtypes (Milo and Miller, 2014; Lublin et al., 2014). CIS refers to first clinical presentation of neurological disability or inflammatory demyelination that could potentially be MS. The RIS subtype is categorized based on findings with imaging which shows MS lesions without any clinical symptoms (Milo and Miller, 2014; Lublin et al., 2014).

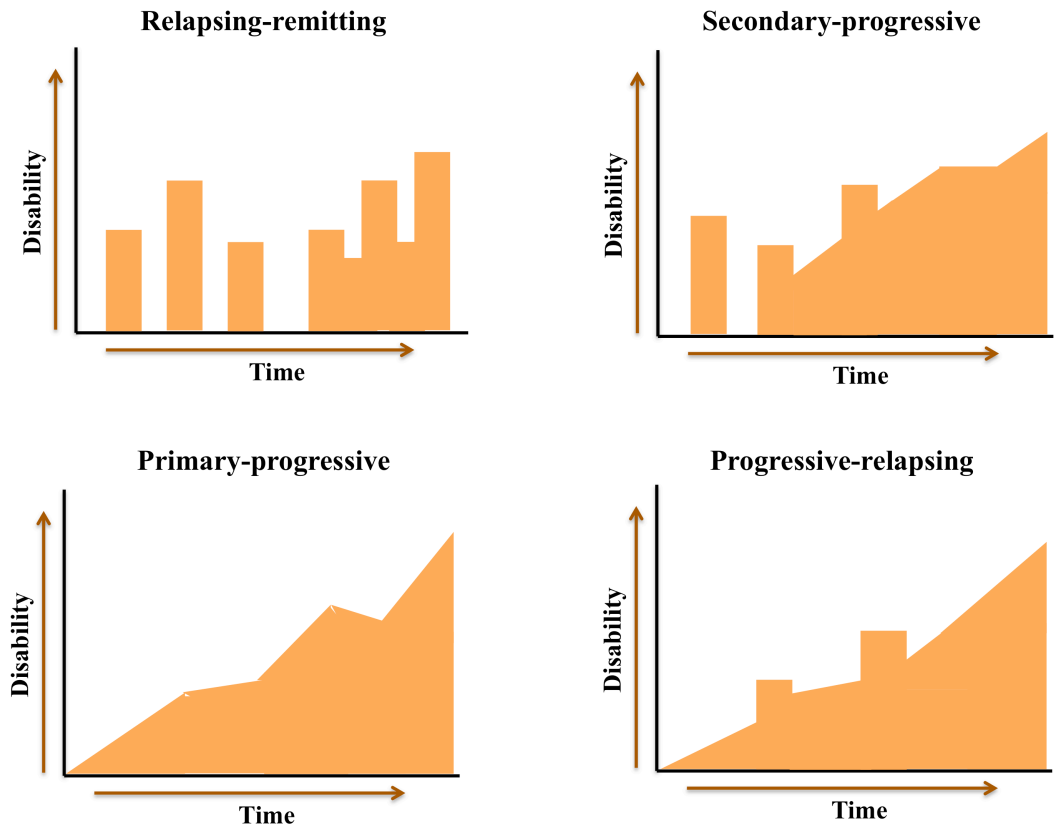

Figure 2.3: Clinical subtypes of multiple sclerosis. MS is classified into four forms depending on the clinical characteristics. Relapsing-remitting MS (RRMS) develops during the initial stages of MS and is characterized by relapse with subsequent impairment in recovery. Prolonged progression of RRMS results in Secondary-progressive MS (SPMS). Primary-progressive MS (PPMS) is characterized by gradual progression with or without infrequent relapses with short periods of remittance. Continued progression of the disease worsens the condition resulting in Progressive-relapsing MS (PRMS), which is accompanied by minor relapses (adapted from Lublin and Reingold, 1996).

2.3.3 Animal models of MS

Three animal models are commonly used to study MS. These include: 1) experimental autoimmune encephalomyelitis (EAE), 2) Theiler's murine encephalomyelitis virus (TMEV)-induced demyelination, and 3) chemical-induced demyelination. EAE is the most widely used animal model as it reflects many clinical, immunological and pathological features of human MS (Gold et al., 2006; Simmons et al., 2013; Bittner et al., 2014). EAE is a T cell-mediated disease that targets the myelin sheath in the white matter (Goverman et al, 2005). EAE is induced by immunization with crude brain tissue or proteins and peptides (active induction) derived from components of the CNS such as MOG, PLP, or MBP (Fritz et al., 1983; Amor et al., 1993; Amor et al., 1994; Gold et al., 2006; Mix et al., 2010; Bittner et al., 2014; Procaccini et al., 2015). EAE is also induced via adoptive transfer of activated myelin-specific T cells isolated from immunized animals into naive recipients (Linington et al., 1993; Mannara et al., 2012). In order to increase susceptibility, *Bordetella pertussis* toxin is injected, which may induce hyperacute EAE (Kamradt et al., 1991). The exact mechanism by which pertussis toxin provokes EAE has not been fully elucidated but non-selective expansion of T cells and vascular changes in the CNS may occur, which in turn results in the breakdown of the blood-brain-barrier and increased interferon-γ production (Hofstetter et al., 2002).

EAE can be provoked as an acute, chronic, or relapsing-remitting disease course that is dependent on the type of antigen, dosage of antigen, method of induction and type of animal used (Berard et al., 2010; Mix et al., 2010; Procaccini et al., 2015). For example, immunization of SJL/J mice with $PLP_{139-151}$ peptide induces a relapsing-remitting subtype (Tuohy et al., 1989); immunization of C57BL6/J mice with MOG_{35-55} peptide at higher dose induces chronic disease (Tompkins et al., 2002), while at a lower dose, a relapsing-remitting disease course is induced

(Berard et al., 2010). In addition to the classical myelin proteins and peptides, paranodal protein NF155 (Mathey et al., 2007) and non-myelin components such as neuronal membrane protein NF186 (Mathey et al., 2007), neuronal cytoskeletal protein neurofilament M (Krishnamoorthy et al., 2009) and astrocyte protein S100β (Kojima et al., 1997) are reported to promote the autoimmune pathogenesis of EAE.

EAE induction results in extensive demyelination, axonal and neuronal loss, microglial activation and marked gliosis (Hampton et al., 2008; Berard et al., 2010; Mix et al., 2010). Hence, EAE models are widely used to investigate the pathological mechanisms responsible for disease progression, neurodegeneration and for the development of therapy for neuroprotection. EAE models have been criticized recently because of the failure in reproducing therapies in human MS (Longbrake and Racke, 2009; Baker and Amor, 2014; Procaccini et al., 2015). This could be attributed to genetic and environmental factors that contribute to the complexity of MS in humans. Remyelination does not occur properly in EAE models because of infiltrating macrophages and microglia in the lesions (Procaccini et al., 2015). In addition, EAE was reported to primarily affect spinal cord white matter rather than brain as seen in human MS. However, forebrain demyelination has been reported recently in MOG induced chronic EAE (Mangiardi et al., 2011; Girolamo et al., 2011).

Theiler's murine encephalomyelitis virus is single stranded RNA picornavirus that can replicate and persist within the CNS (Denic et al., 2011; Mecha et al., 2013). Although Epstein-Barr virus infection has been linked to MS as an environmental risk factor (Ascherio et al., 2001; Ascherio and Munger, 2007), persistent viral infection of the CNS has not been reported in humans. TMEV induces early acute disease followed by chronic progressive demyelination in mice similar to MS pathology. However, TMEV induces demyelination only in mice and not in

other rodents or primates (Denic et al., 2011). In TMEV induced demyelination, axonal damage occurs first followed by inflammatory demyelination (Tsunoda et al., 2003; Tsunoda et al., 2007) whereas in MS demyelination precedes axonal damage.

To study remyelination following demyelination, chemical induced demyelination using cuprizone and lysolecithin are used (Blakemore and Franklin, 2008). Cuprizone (biscyclohexanone-oxaldihydrazone) is a copper chelator, which is usually administered through the diet of mouse or rat. Cuprizone specifically targets mature OL by inhibiting copper-dependent mitochondrial enzymes that disturb energy metabolism in OLs, resulting in OL cell death and demyelination followed by activation of astrocyte and microglia (Benardais et al., 2013). Removal of cuprizone from the diet induces remyelination (Matsushima ad Morell, 2001). Lysolecithin is an activator of phospholipase A2, which is injected (mouse, rat and primate) to induce focal areas of demyelination (Blakemore and Franklin, 2008). However, the chemical induced demyelination does not reflect inflammatory demyelination in MS (Blakemore and Franklin, 2008).

2.4 Quaking

Given the role played by the myelin structural genes in compact myelin biogenesis and the importance of myelin and myelin forming OLs in MS, it is pertinent to understand the regulation of these myelin structural genes during OL development and myelination. The RNA binding protein, quaking (QKI), is known to control the expression of several myelin transcripts either directly or indirectly for proper OL development and myelination (Chen et al., 2007b; Larocque et al., 2005; Li et al., 2000; Wu et al., 2002; Zhao et al., 2006a; Zhao et al., 2010). Hence, QKI is considered to be a master regulator of myelin specific gene expression.

The *quaking (qkI)* gene contains nine exons (Kondo et al., 1999), which gives rise to three major isoforms due to alternative splicing such as QKI-5, QKI-6, and QKI-7 (Ebersole et al., 1996). All the three isoforms have the same conserved QUA1, KH (hnRNP K homology) and QUA2 domains in the N-terminus, which plays a role in RNA binding and dimerization (Ebersole et al., 1996; Kondo et al., 1999; Wu et al., 1999; Beuck et al., 2012). However, the three isoforms carry distinct C-terminus that determines their subcellular localization (Wu et al., 1999). QKI-5 alone has the nuclear localization signal in the C-terminal (Wu et al., 1999) and is present in the nucleus while QKI-6 and QKI-7 are present in the cytoplasm. Since all the QKI isoforms have the same RNA binding domain, they may have similar selectivity and affinity towards their target transcripts (Galarneau and Richard, 2005). QKI selectively binds to the QKI Response Element (QRE) with the sequence ACUAAY or AUUAAY within the 3'UTR of its target mRNA (Ryder and Williamson, 2004; Galarneau and Richard, 2005; Hafner et al., 2010). QKI plays a role in pre-mRNA splicing, mRNA localization, transport, mRNA stability, and translation efficiency of the target transcripts (Galarneau and Richard, 2009).

Quaking viable (qk^v/qk^v) mutant mice carries a deletion of ~1.1 Mbp region in chromosome 17 upstream of *qkI* gene which includes the promoter region of the *qkI* gene (Ebersole et al., 1996), part of the *Parkin* gene and the entire *Parkin* coregulated gene (Lockhart et al., 2004; Lorenzetti et al., 2004a; Lorenzetti et al., 2004b). These qk^v/qk^v mutant mice display a quaking phenotype with increased tremor at the caudal part of the trunk (Sidman et al., 1964). These mice are characterized by severe hypomyelination with thin myelin sheath, lack of compaction and poorly developed nodes (Wisniewski and Morell, 1971). In addition, there is reduction in the expression of myelin proteins and number of mature OLs in the CNS (Table 2.2) (Hardy, 1998a; Chenard and Richard, 2008). The dysmyelination and tremor phenotype observed

in qk^v/qk^v mutant mice is caused by deletion of the *qkI* locus, as *Parkin* null mice do not display these phenotypes (Itier et al., 2003).

The *qkI* gene is located on chromosome 6q26 in humans, which lies within the region of 6q25-6q27, a susceptibility locus associated with schizophrenia (SCZ) (Lindholm et al., 2001). In addition, a 0.5 Mb haplotype region which was found to be inherited among the SCZ patients lies within the *qkI* gene (Aberg et al., 2006a). Furthermore, the mRNA expression of *qkI-7* was severely reduced in the SCZ brains (Aberg et al., 2006a), suggesting a post-transcriptional misregulation of *qkI* and its importance in the etiology of SCZ. Additionally, many of the defects observed in qk^v/qk^v mutant mice such as a lack of compaction of the myelin sheath and a reduction in the number of myelin lamellae have also been observed in patients with SCZ (Takahashi et al., 2011). Recently, the structural abnormalities in nodal, internodal and paranodal region with altered myelin thickness, uncompact myelin and abnormal distribution of ion channel complexes in the SCZ brains similar to that of qk^v/qk^v brains was proposed to be the reason for functional impairment in SCZ patients (Rosenbluth and Bobrowski-Khoury, 2013). Furthermore, several myelin-associated genes, which are downstream targets of QKI, were downregulated in the white matter of SCZ patients, including *Mbp*, *Plp* and *Mag* (Aberg et al., 2006a; Aberg et al., 2006b).

2.4.1 Expression pattern of QKI during OL development

The expression of QKI is abundant in myelinating glial cells in CNS as well as in PNS (Hardy et al., 1996). Expression of *qkI* mRNA transcripts, *qkI-5* and *qkI-6* are detected early in embryonic development at E7.5 in neuroepithelium of head folds (Ebersole et al., 1996). The QKI-5 isoform is expressed earliest during embryonic and fetal development, with expression

decreasing during the peak of myelination (3-4 weeks in rodents and 2-3 years in humans) (Ebersole et al., 1996; Lauriat et al., 2008). In contrast, QKI-6 and QKI-7 are not expressed until closer to birth, with highest expression at the peak of myelination. The expression of QKI-6 and 7 increases with increase in age both in mice and humans (Ebersole et al., 1996; Lauriat et al., 2008). In addition, *in vitro* differentiation of primary OL cells showed increase in the expression of QKI-6 and QKI-7 as the OLs differentiate, whereas the expression of QKI-5 decreased during OL differentiation (Tyler et al., 2011). This is consistent with the findings that QKI-6 and QKI-7 play a potential role in promoting the maturation of OLs and myelination (Chen et al., 2007b).

Expression of QKI in the NSCs has been found to switch the NSC from neurogenesis to gliogenesis (Hardy, 1998b). During neuron-glia fate specification, a subpopulation of NSCs in the VZ expressing high levels of QKI-5 migrates away and enters the glial pathway expressing the markers of OL progenitor cells. In addition, the expression of *qkI* is silenced in the cells that are determined to become neurons (Hardy, 1998b). Furthermore, the cytoplasmic isoforms QKI-6 and QKI-7 have also been demonstrated to promote glial cell fate specification from multipotent neural progenitors *in vivo* in mice (Larocque et al., 2005).

2.4.2 Role of QKI in fine-tuning OL differentiation

The importance of QKI in OL differentiation has been demonstrated using knockdown and overexpression studies both *in vitro* and *in vivo* (Larocque *et al*., 2005; Chen et al., 2007b). All three isoforms of QKI promote OL differentiation with varying efficiency (Chen et al., 2007b). QKI plays a role in OL differentiation by regulating cell cycle and cytoskeletal organization.

2.4.2.1 QKI in cell cycle control

OL differentiation is initiated soon after OLs exit cell cycle and cease to proliferate. Cyclin-dependent kinase (CDK) inhibitors turn off the cell cycle (Sherr and Roberts, 1999). CDK inhibitor $p27^{Kip1}$ is involved in promoting cell cycle exit and differentiation in OLs (Casaccia-Bonnefil et al., 1997). The *p27^{Kip1}* mRNA harbors QRE that allows QKI to bind, stabilize and increase $p27^{Kip1}$ protein expression (Larocque et al., 2005) (Fig. 2.4). Although $p27^{Kip1}$ can effectively arrest cell cycle, ectopic expression of $p27^{Kip1}$ alone is not sufficient to promote OL differentiation (Tang et al., 1999). In addition, loss of *p27^{Kip1}* increases the number of proliferating OLs and reduced the number of differentiating OLs but did not alter the initiation of OL differentiation (Casaccia-Bonnefil et al., 1997; Casaccia-Bonnefil et al., 1999). This indicates that *qkI* could regulate the expression of additional target mRNA that promotes cell cycle arrest and OL differentiation.

2.4.2.2 QKI in reorganization of cytoskeleton and process outgrowth

In addition to cell cycle arrest, OL differentiation involves process outgrowth, which is characterized by cytoskeletal rearrangements (Bauer et al., 2009; Michalski and Kothary, 2015). Cytoskeletal rearrangements involve continuous polymerization and depolymerization of the cytoskeletal proteins through addition or removal of monomer units (Fletcher and Mullins, 2010). Process outgrowth in OL is regulated by increased levels of proteins involved in polymerization and decreased levels of proteins involved in depolymerization (Liu et al., 2003). Actin interacting protein 1 (AIP-1) plays a role in actin disassembly and inhibits OL differentiation (Doukhanine et al., 2010). *Aip-1* mRNA contains QRE at the 3′ UTR that facilitates the binding of QKI (Doukhanine et al., 2010). Interestingly, *qk^{v}/qk^{v}* mutant mice had

increased levels of AIP-1 expression in OLs (Doukhanine et al., 2010). Overexpression of *qkI* destabilizes the *Aip-1* mRNA and reduced the abundance of *Aip-1* mRNA (Fig. 2.4).

Another target of QKI that plays a role in cytoskeletal organization of OL is microtubule associated protein 1B (MAP1B). The 3′ UTR of *Map1B* comprises several QREs, which aid in interaction with QKI (Zhao et al., 2006a). Overexpression of *qkI* increases the expression of MAP1B, whereas knockdown of *qkI* reduces the expression of MAP1B in OLs (Fig. 2.4). This indicates that QKI interacts with *Map1B* during OL differentiation and increases its protein expression (Zhao et al., 2006a). Although MAP1B is expressed both in neurons and OLs, expression of QKI exclusively in OLs offers OL specific MAP1B regulation and not in neurons (Zhao et al., 2006a). It is plausible that QKI might interact with several other cytoskeletal proteins to regulate the morphological changes in OLs, but this remains to be explored.

2.4.3 Role of QKI in myelination

QKI has been proposed to control myelination by regulating stability, splicing and localization of target mRNAs (Fig. 2.4).

2.4.3.1 mRNA stability

In addition to the aforementioned mRNAs such as *Map1B* (Zhao et al., 2006a), *Aip-1* (Doukhanine et al., 2010) and $p27^{Kip1}$ (Larocque et al., 2005), QKI is involved in the stabilization of myelin specific genes such as *Mbp, Plp* and *Mag* for proper myelinogenesis (Li et al., 2000; Roth et al., 1985; Sorg et al., 1986; Sorg et al., 1987; Wu et al., 2002; Zhao et al., 2010). The ratio of MBP isoform 14/21.5 (higher 14kDa MBP and lower 21 kDa MBP expression) is considered an index of myelin maturation, which increases during the peak of myelination (Campagnoni et al., 1978). In qk^v/qk^v mutant mice, the quantity of *Mbp* mRNA in the myelin is

reduced and there is isoform preferential destabilization of *Mbp* mRNA encoding 14 kDa protein (Li et al., 2000). The removal of 3′ UTR in the *Mbp* mRNA *in vitro* reduces its interaction with QKI, suggesting that 3′ UTR in the *Mbp* mRNA is stabilized by the QKI interaction (Li et al., 2000). The expression of *Plp* mRNA is also reduced in qk^v/qk^v mutant mice, implicating the role of QKI in stabilizing *Plp* mRNA (Sorg et al., 1987). Interestingly, transgene overexpression of *qkI-6* in qk^v/qk^v mutant mice was able to rescue the destabilization of *Mbp* and *Plp* mRNA with higher efficiency towards *Mbp* compared to *Plp* mRNA (Zhao et al., 2006b).

Recently, QKI has been shown to bind to mRNAs of other RNA binding proteins such as heterologous nuclear ribonucleoprotein A1 (hnRNPA1) (Zearfoss et al., 2011). QKI binds to the QRE present in the 3′ UTR of *hnRNPA1* mRNA, stabilizes the mRNA and inhibits its translation (Zearfoss et al., 2011). Stabilization mediated by QKI can either promote ($p27^{Kip1}$) or inhibit (*hnRNPA1*) the downstream translation of target mRNA to protein (Larocque et al., 2005; Zearfoss et al., 2011). In addition, QKI-6 stabilizes and represses the expression of two canonical splicing factors, hnRNPF and hnRNPH (Mandler et al., 2014). Repression of *hnRNPF* and *hnRNPH* facilitates QKI-6 to regulate the alternative splicing of polyguanine containing transcripts and rescue aberrant splicing in qk^v/qk^v mutant (Mandler et al., 2014).

2.4.3.2 Localization of myelin transcripts

The transcription of *Mbp* increases during the active phase of myelination. The synthesized mRNA is transported along the OL processes into the myelin, where it is translated and incorporated into the myelin sheath (Ainger et al., 1993). It is pertinent to note that the OLs in the qk^v/qk^v mutants are defective in exporting *Mbp* mRNA from the nucleus (Barbarese, 1991). All three QKI isoforms have been shown to directly bind to *Mbp* mRNA and control the

subcellular localization of *Mbp* transcripts (Larocque et al., 2002). Overexpression of QKI-5 in primary mouse OL cultures results in the retention of *Mbp* mRNA in the nucleus, which results in lower protein expression and reduced levels of mRNA transport to OL processes (Larocque et al., 2002). The presence of QKI-6 and QKI-7 releases the QKI-5 mediated nuclear retention of *Mbp* mRNA (Larocque et al., 2002).

2.4.3.3 Regulation of alternative splicing

QKI can regulate the splicing of *Mbp, Plp* and *Mag* mRNA (Wu et al., 2002; Zhao et al., 2010). Homozygous qk^v/qk^v mutants display an imbalance in the ratio of alternative splice variants for *Mbp*, *Plp,* and *Mag*. In qk^v/qk^v mutant, dysregulated splicing results in reduction of the L-MAG (Fujita et al., 1988; Fujita et al., 1990; Wu et al., 2002; Zhao et al., 2010). The nuclear isoform QKI-5 binds to the 53 nucleotide QRE in the intronic region of *Mag* and represses the inclusion of exon 12 (Wu et al., 2002). Furthermore, cytoplasmic isoform QKI-6 also can bind to and rescue the dysregulated MAG splicing (Zhao et al., 2010). Additionally, QKI is also found to modulate the splicing of *Mag* indirectly by regulating the expression of hnRNPA1, which is expressed highly in qk^v/qk^v mutant mice (Zhao et al., 2010; Zearfoss et al., 2011). Microarray analysis revealed that a subset of QKI targets is co-regulated by hnRNPA1, suggesting that hnRNPA1 is an important target of QKI in regulating myelin specific gene expression (Zearfoss et al., 2011).

Since the QKI isoforms vary only in their C-terminus, the distinctive functional differences between the three isoforms is largely attributed to the location of the target mRNA, combined with differences in spatial and temporal expression of the three isoforms (Larocque et al., 2002; Zhao et al., 2010).

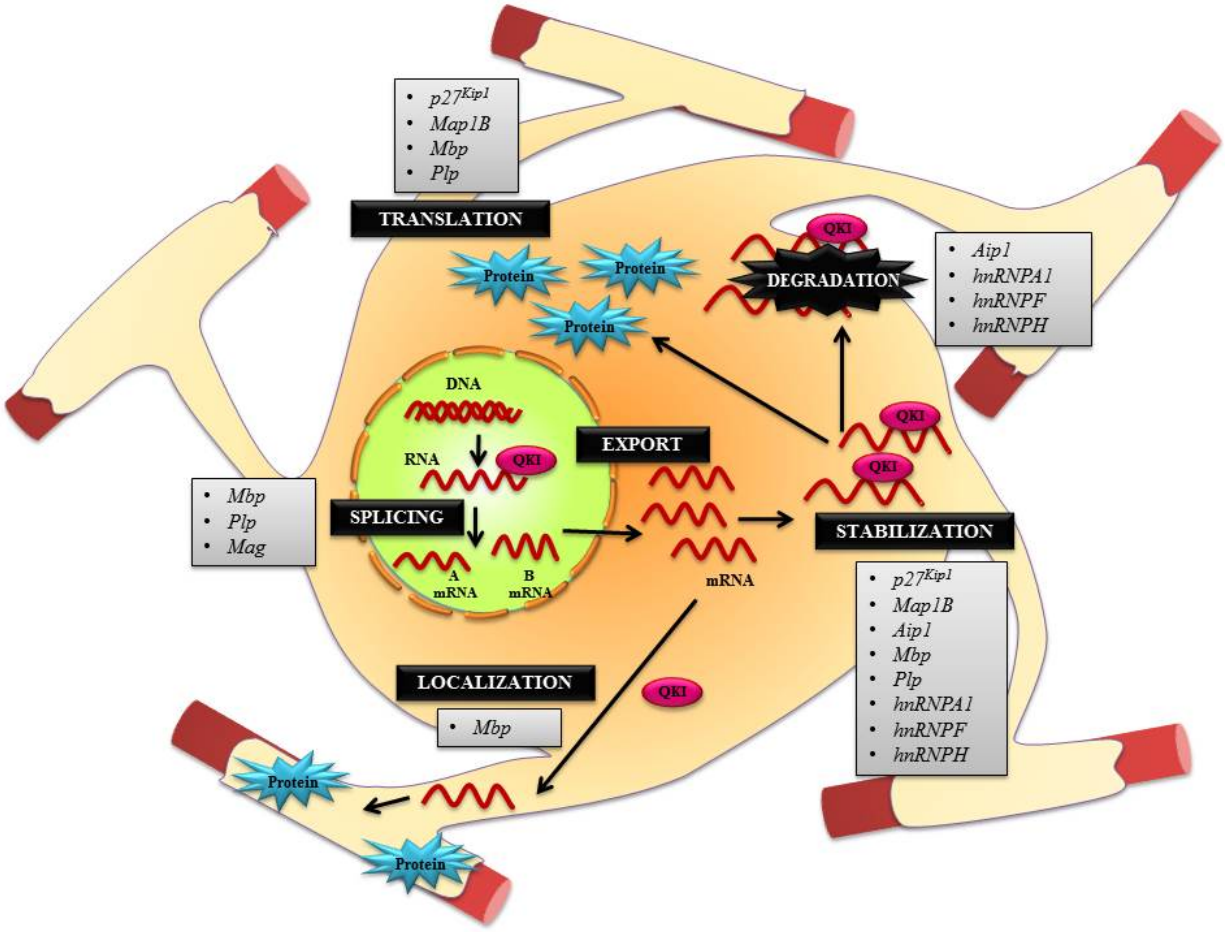

Figure 2.4: Potential roles of quaking in oligodendrocyte differentiation and myelination. In OLs, QKI post-transcriptionally regulates the expression of several genes necessary for OL differentiation by four different mechanisms (indicated in black boxes), which include mRNA stabilization, splicing, sub-localization and export. Stabilization of mRNA by QKI results in either mRNA degradation or increased translation. The target mRNAs of QKI are indicated in the grey box beside each mechanism.

In addition to myelin structural proteins (MBP and PLP), sirtuin 2 (SIRT2) protein expression is also reduced in the myelin sheath of qk^{v}/qk^{v} mice throughout development and into adulthood (Zhu et al., 2012). QKI regulates the transport of SIRT2 to myelin through PLP (Zhu et al., 2012). Yet, the relationship between QKI and *Sirt2* during OL differentiation is largely unknown.

2.5 Sirtuin2

Sirtuin2 (SIRT2) is predominantly expressed in the cytoplasm of OLs (North et al., 2003; Li et al., 2007a) and constitutes 1% of the myelin proteome (Jahn et al., 2009).

2.5.1 Mammalian sirtuins

Sirtuins (SIRTs) are class III protein deacetylase enzymes, which depend on the cofactor nicotinamide adenine dinucleotide (NAD^{+}) for their enzymatic activity (Brachmann et al., 1995; Frye, 2000; Michan and Sinclair, 2007). SIRTs are evolutionarily conserved from bacteria to mammals (Brachmann et al., 1995; Frye, 2000; North et al., 2003). In mammals, seven SIRTs (SIRT1 to SIRT7) have been identified that are classified based on their homology to yeast Sir2 (silent information regulator 2) protein (Blander and Guarente, 2004; Frye, 2000). All the SIRTs have a conserved NAD^{+}-dependent catalytic core domain comprised of 275 aa, which display either NAD^{+}-dependent deacetylase activity and/or mono-ADP-ribosyltransferase activity (Fig. 2.5). The flanking N-terminal and C-terminal regions of SIRTs vary in length and amino acid sequence. The mammalian SIRTs are heterogeneously localized in sub-cellular compartments with differing deacetylase and/or ADP-ribosyltransferase activity (Fig. 2.6). SIRT1, SIRT6 and SIRT7 are mainly localized in the nucleus (Frye, 2000; Michishita et al., 2005), whereas SIRT2 is localized in the cytoplasm (North et al., 2003; Michishita et al., 2005). SIRT3, SIRT4 and

SIRT5 are localized in mitochondria (Michishita et al., 2005). SIRT1 and SIRT2 are reported to shuttle between the nucleus and cytoplasm (Tanno et al., 2007; North and Verdin, 2007a). In addition to different sub-cellular localizations, the mammalian SIRTs are differentially expressed in various organs and tissues (Kelly, 2010). This suggests that SIRTs may have different target substrates and may affect a broad range of cellular functions (Haigis and Sinclair, 2010).

Among all the SIRTs, *Sirt2* is abundantly expressed in the CNS at mRNA and protein levels (Sidorova-Darmos et al., 2014), and it is the only SIRT protein that is present in the myelin sheath (Werner et al., 2007).

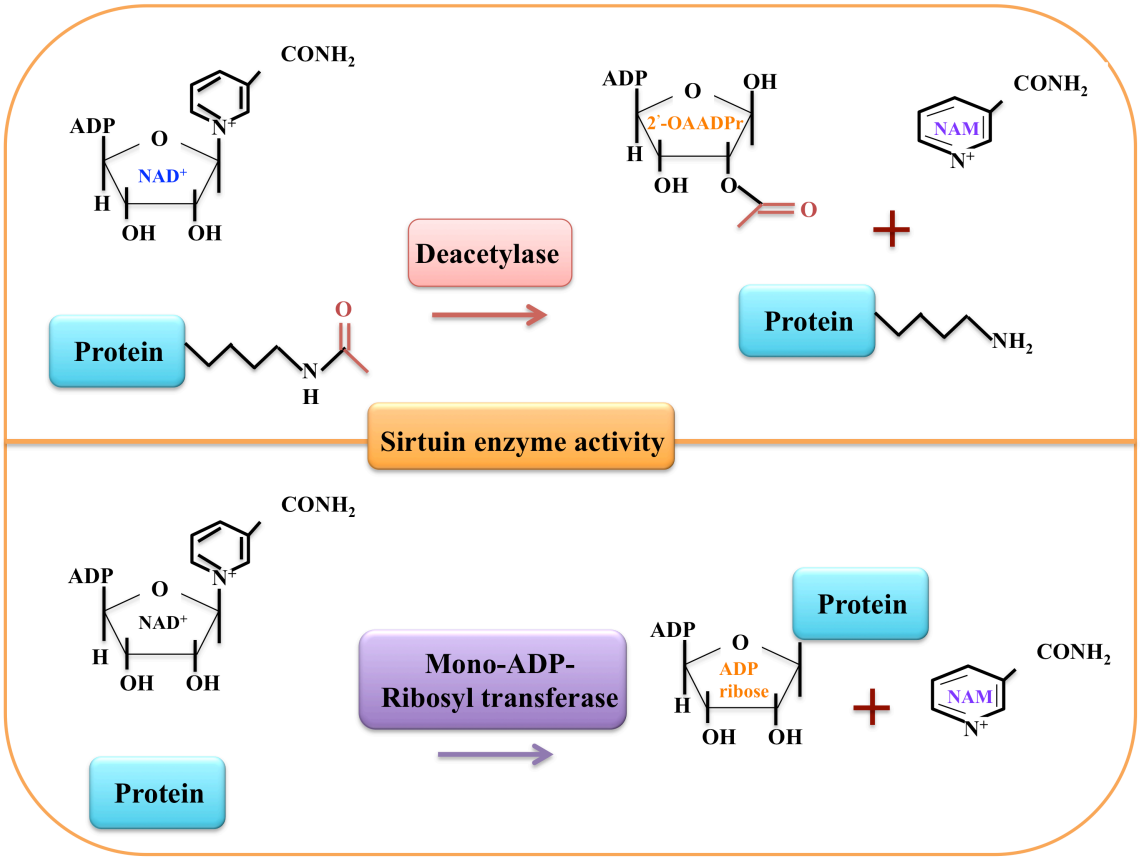

Figure 2.5: Sirtuin enzymatic activities. NAD^+-dependent deacetylation and mono-ADP-ribosyltransferase activity of sirtuins. Both deacetylation and ADP-ribosylation occur in the presence of NAD^+. The acetylated lysine residue of the target protein serves as substrate for sirtuin deacetylation. NAD^+ and acetylated protein are converted to free lysine side chain, nicotinamide (NAM) and 2'-O-acetyl-ADP-ribose (2'-OAADPr). (adapted from Michan and Sinclair, 2007)

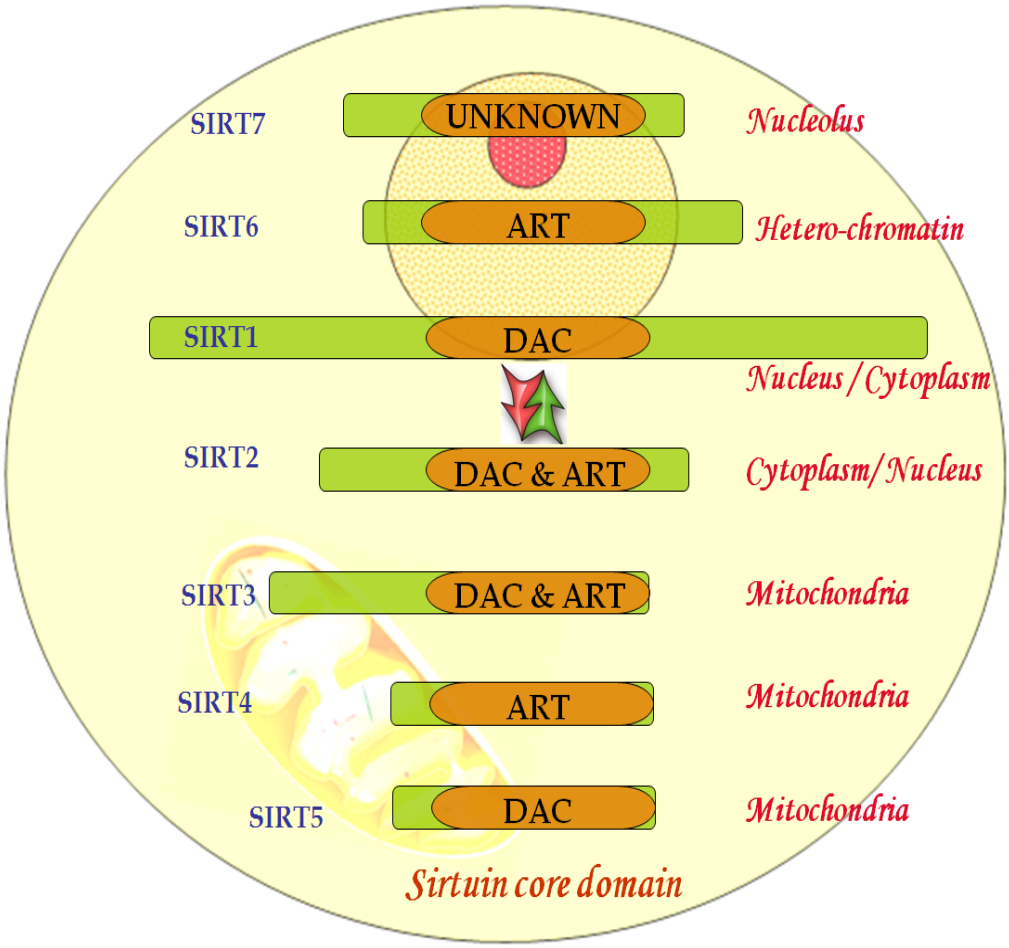

Figure 2.6: Catalytic core domain and subcellular localization of mammalian SIRTs. Diagrammatic representation of the domains and localization of mammalian SIRTs (SIRT1 to SIRT7) within a cell. The conserved NAD^+-dependent catalytic core domain performs either a deacetylase (DAC) and/or mono-ADP-ribosyltransferase (ART) activity depending on their sub-cellular localization and biological function. SIRT1 and SIRT2 shuttle between nucleus and cytoplasm (indicated by arrow). SIRT3, SIRT4 and SIRT5 are localized in the mitochondria, while SIRT7 is localized in the nucleolus.

2.5.2 Organization of *Sirt2* gene and its isoforms

The *Sirt2* gene is located on chromosome 19 in humans and on chromosome 7 in mice. The full length *Sirt2* gene contains 16 exons in both human and mouse (Fig. 2.7) (Voelter-Mahlknecht et al., 2005; Maxwell et al., 2011). The *Sirt2* mRNA is alternatively spliced between exons two to four giving rise to three isoforms of SIRT2 protein with different amino termini (Maxwell et al., 2011). In mice, *Sirt2* variant 1 (*Sirt2.1*) contains all 16 exons encoding SIRT2.1 protein (389 aa) with a molecular weight of 43 kDa (Maxwell et al., 2011). The *Sirt2* variant 2 (*Sirt2.2*) is spliced at exon two and the resulting frameshift introduces a premature stop codon in exon three. Translation of *Sirt2.2* variant initiates at a downstream start site present in exon four giving rise to SIRT2.2 protein (352 aa) with a molecular weight of 39.5 kDa. This SIRT2.2 is the most abundant isoform in the CNS white matter (Werner et al., 2007; Zhu et al., 2012) and the only isoform integrated into myelin sheath (Werner et al., 2007). *Sirt2* variant 3 (*Sirt2.3*) has 13 exons (lacking exon two, three and four) encoding SIRT2.3 protein (319 aa) with a molecular weight of 35.5 kDa. SIRT2.3 increases with age in brain and spinal cords (Maxwell et al., 2011). Crystal structure of the catalytic core of SIRT2 contains two domains, i) a large α/β Rossmann fold domain (six parallel beta strand linked to alpha helices on either sides) and ii) a small Zn^{2+} binding domain (most diverse region between sirtuins) (Finnin et al., 2001). These two domains are connected by four polypeptide chain loops, which form a gap where the acetylated substrates and the NAD bind (Finnin et al., 2001; Sanders et al., 2010). However, the sub-cellular localization, substrate specificity and the functional significance of SIRT2 isoforms are yet be characterized.

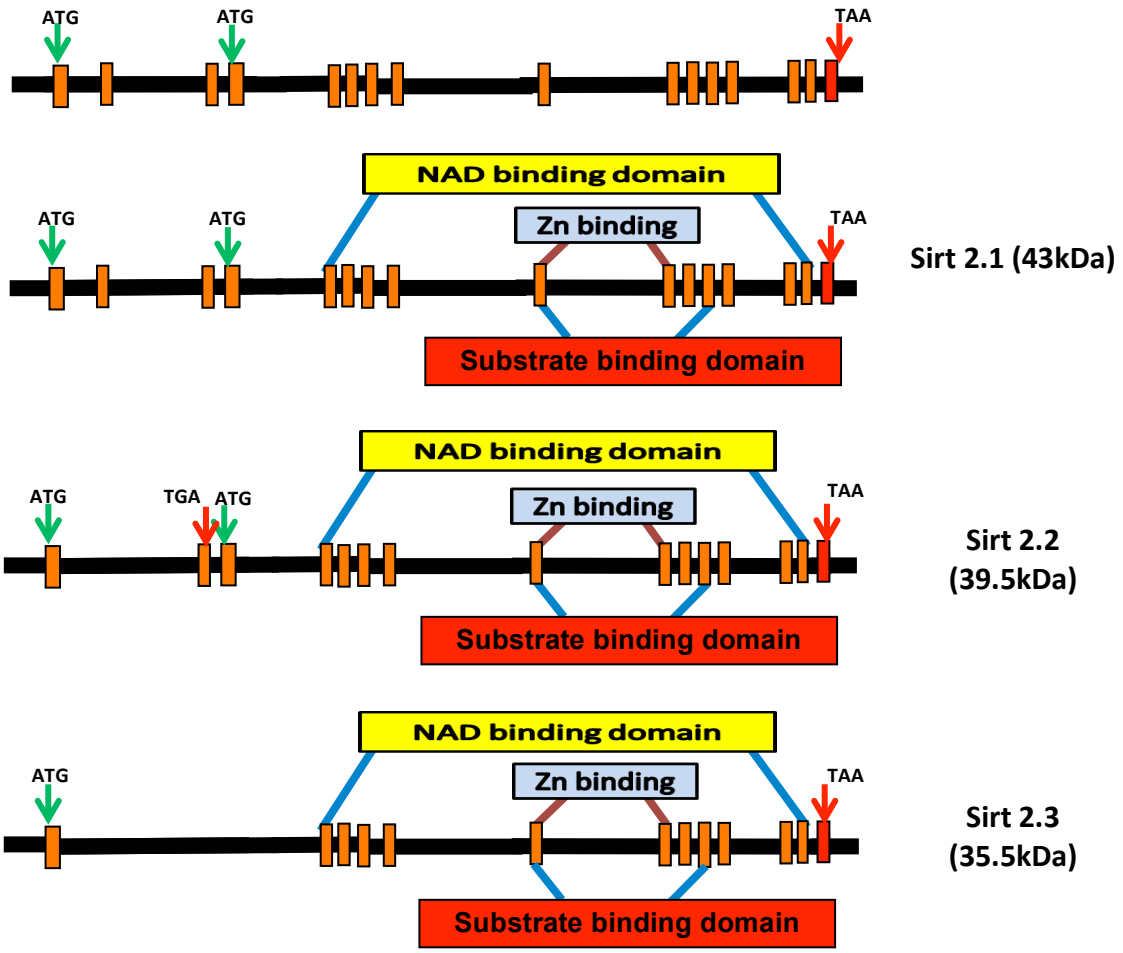

Figure 2.7: Structural organization of mammalian *Sirt2* gene and its splice variants. The genomic organization of mammalian *Sirt2* gene showing the relative position of exons, introns and translation start sites (ATG). The gene organization of *Sirt2* splice variants are shown in the lower panel. The catalytic core domain of the SIRT2 protein is encoded by sequences from exon 5 to exon 15. The Zinc binding module (exon 9 and exon 10) and the substrate binding (exon 9 to exon 12) region are present within the catalytic domain.

2.5.3 Interacting partners, substrates, and downstream effectors of SIRT2

In the CNS, SIRT2 is predominantly expressed by OLs in the cytoplasm where it deacetylates α-tubulin at lysine 40 (K40) (Li et al., 2007a). Given that reversible acetylation of tubulin modulates microtubule dynamics (Zilerman et al., 2009), SIRT2 could possibly play a role in cytoskeletal organization. SIRT2 was found to interact with histone deacetylase 6 (HDAC6) in microtubules to deacetylate α-tubulin in HeLa cells and 293T cells (North et al., 2003). However, HDAC6 is expressed only by neurons in the CNS (Southwood et a., 2007), indicating that this interaction does not occur in OLs. In our laboratory it was demonstrated that the homeodomain transcription factor NKX2.2 binds to the promoter region of *Sirt2* in the presence of HDAC1 and represses SIRT2 expression in OPCs (Ji et al., 2011).

SIRT2 is localized in the cytoplasm throughout the cell cycle and translocates into the nucleus during G2/M transition phase (Dryden et al., 2003; North and Verdin, 2007a; North and Verdin, 2007b), where it deacetylates histone H4 at lysine 16 (H4K16) at a global level. Knock down of *Sirt2* increases acetylated H4K16, which promotes mitotic exit (Vaquero et al., 2006). In addition, SIRT2 deacetylates H3K56 (Das et al., 2009) and H3K9 (Vaquero et al., 2006) to promote chromatin condensation. However, the acetylation of histones H3 and H4 are not altered in OLs transfected with *Sirt2* (Li et al., 2007a).

Although α-tubulin is the only known substrate of SIRT2 in the CNS (Li et al., 2007a), other interacting partners and substrates of SIRT2 have been identified using cancer cell lines and mouse fibroblast cells (Jin et al., 2008; Bae et al., 2004; Jing et al., 2007; Wang et al., 2007; Wang and Tong, 2009; Rothgiesser et al., 2010; Wang et al., 2014;Xu et al., 2014). SIRT2 can interact with 14-3-3 β/γ in HEK293 cells, which allows SIRT2 to deacetylate and inhibit the

transcriptional activity of p53 (Jin et al., 2008). Interaction of SIRT2 with homeobox transcription factor A10 (HoxA10) suggests the role of SIRT2 in mammalian development (Bae et al., 2004). Furthermore, SIRT2 interacts with Forkhead box, class O1 transcription factor (FOXO1) in the nucleus to modulate adipocyte differentiation (Jing et al., 2007; Wang and Tong, 2009). SIRT2 deacetylates FOXO1, which inhibits Akt/PKB mediated phosphorylation of FOXO1 at Ser253 and retains FOXO1 in the nucleus. Deacetylated FOXO1 binds to peroxisome proliferator-activated receptor γ (PPARγ) and transcription factor CCAAT enhancer binding protein α (C/EBPα), which in turn represses the expression of adipocyte differentiation markers and inhibits adipocyte differentiation (Jing et al., 2007; Wang and Tong, 2009).

SIRT2 has been implicated in inflammation, oxidative stress response and metabolism (Rothgiesser et al., 2010; Wang et al., 2007; Wang et al., 2014; Xu et al., 2014). SIRT2 deacetylates the p65 subunit of nuclear factor kappa B transcription factor (NF-κB), which down-regulates the expression of NF-κB dependent genes in mouse embryonic fibroblasts (Rothgiesser et al., 2010). During oxidative stress, SIRT2 deacetylates FOXO3a and promotes the expression of FOXO3a downstream targets such as p27kip1, MnSOD (manganese superoxide dismutase) and Bim to reduce cellular levels of reactive oxygen species in NIH 3T3 cells (Wang et al., 2007). SIRT2 has also been reported to interact with metabolic enzymes, glucose 6-phosphate dehydrogenase (Wang et al., 2014) and phosphoglycerate mutase (Xu et al., 2014) to counteract oxidative damage.

In addition, the activity of SIRT2 is modulated by post-translational modifications such as phosphorylation and acetylation. CDK such as cyclin B-CDK1, cyclin E-CDK2, cyclin A-CDK2 and p35-CDK5 phosphorylate SIRT2 at a consensus sequence located in the C terminus, serine 368 in SIRT2.1 and at serine 331 in SIRT2.2. Phosphorylation by CDK inhibits the

catalytic activity of SIRT2 and interferes with its functions such as cell adhesion, cell migration, neurite outgrowth and growth cone motility (North and Verdin, 2007b; Pandithage et al., 2008). SIRT2 is predicted to have AKT phosphorylation sites (Jin et al., 2008). SIRT2 is dephosphorylated by the phosphatase CDC14B, which results in ubiquitination and 26S proteosome mediated degradation of SIRT2 leading to mitotic exit (North and Verdin, 2007b; Inoue et al., 2007). Furthermore, SIRT2 is acetylated by p300, which attenuates the deacetylation activity of SIRT2 (Han et al., 2008).

2.5.4 SIRT2 in oligodendrogenesis

SIRT2 deacetylates α-tubulin and modulates the cytoskeleton during oligodendrogenesis (Li et al., 2007a; Tang and Chua, 2008). There are controversies in the regulatory role of *Sirt2* in OL differentiation. Initially, it was reported that *Sirt2* prevents OL differentiation through tubulin deacetylation (Li et al., 2007a). These observations were made using gene overexpression and knockdown *in vitro* (Li et al., 2007a). However, OLs with endogenous higher expression of *Sirt2* displayed complex process outgrowth (Li et al., 2007a). In addition, SIRT2 was found to be colocalized with CNPase and identified as an early OL differentiation marker (Southwood et al., 2007). In our laboratory, it was shown that *Sirt2* promotes OL differentiation and enhances OL arborization with an increase in MBP expression in CG4-OL cells (Ji et al., 2011). These findings suggest that *Sirt2* promotes OL differentiation. Moreover, SIRT2 deacetylates H3K56 (Das et al., 2009), and a decrease in the levels of acetylated H3K56 has been reported to initiate differentiation (Xie et al., 2009). This correlates with our findings that the expression of SIRT2 continues to increase as CG4-OLs differentiate and its expression remains prominent in adult CNS (Ji et al., 2011).

Disruption of microtubules using nocodazole or colchicine inhibits the transport of *Mbp* mRNA (Carson et al., 1997) and incorporation of PLP into myelin sheath (Bizzozero et al., 1982). In addition, increased microtubule polymerization compromises OL process outgrowth (Song et al., 1999). Thus, normal microtubule structure is critical for the transport of myelin components and process extension in OLs (Song et al., 1999). During oligodendrogenesis, SIRT2 modulates the microtubule dynamics by deacetylating α-tubulin (Li et al., 2007a). Hence, SIRT2 may also function in modulating microtubule-based vesicular transport, which is critical during differentiation and myelin formation (Tang and Chua, 2008). SIRT2 may also regulate OL differentiation and myelin formation by modulating the acetylation status of other myelin proteins (Werner et al., 2007).

Moreover, SIRT2 is upregulated during the peak period of myelination in the CNS (Southwood et al., 2007) as well as in the PNS (Beirowski et al., 2011). Interestingly, the expression profile of SIRT2 is similar to that of MBP and MPZ in CNS and PNS, respectively (Ji et al., 2011; Beirowski et al., 2011). In addition, studies on myelin proteome revealed that the isoform SIRT2.2 integrates into the myelin sheath (Werner et al., 2007) in close proximity to PLP and DM20 near paranodal loops (Li et al., 2007a; Southwood et al., 2007). The transport of SIRT2 into the myelin sheath is mediated by PLP (Werner et al., 2007; Zhu et al., 2012). The localization of SIRT2 in paranodal loops suggests that SIRT2 may be involved in axo-glial interaction and axonal integrity (Werner et al., 2007). In Schwann cells, knockout of *Sirt2* delays myelin formation by regulating the activity of the polarity complex signaling component aPKC via deacetylation of Par-3 (Beirowski et al., 2011). In addition, loss of *Sirt2* in PNS results in extensive outfoldings in compact myelin close to paranodes (Beirowski et al., 2011).

2.5.5 SIRT2 and signaling molecules in CNS myelination

The serine/threonine kinase AKT is involved in regulating many vital cellular functions. In the transgenic mouse *Plp*-Akt-DD (phosphorylation of aspartic acid residues at Thr^{308} and Ser^{473}), the constitutive activation of AKT1 throughout the OL lineage leads to enhanced myelination with increased thickness and increased expression of major myelin genes such as *Plp*, *Mog* and *Mbp* (Flores et al., 2008). Further, the activation of mammalian target of rapamycin (mTOR) and its downstream substrate p70 S6 Kinase and S6 ribosomal protein are increased in *Plp*-Akt-DD mice (Narayanan et al., 2009). In addition, when mTOR signaling is inhibited *in vivo* with chronic rapamycin treatment, the hypermyelination and the associated changes are all rescued (Narayanan et al., 2009). Conditional knockout of mTOR in the OLs using CNP-cre-$mTOR^{fl/fl}$ mice exhibits hypomyelination in CNS (Wahl et al., 2014). This indicates that Akt-mTOR signaling plays a critical role in CNS myelination (Narayanan et al., 2009). In addition to AKT-mTOR, ERK 1/2 is also involved in myelin compaction during the active stages of myelination in the spinal cord, with negligible roles in OPC proliferation and OL differentiation (Ishii et al., 2012).

Although the role of SIRT2 in the signaling pathways that promote myelination has not been studied in OLs, a few studies in other cell types have demonstrated the interaction of SIRT2 with these signaling molecules. In myeloid leukemia cells, it has been demonstrated that the deacetylase activity of SIRT2 activates protein kinase B/AKT (Dan et al., 2012). Moreover, when SIRT2 or its activator, nicotinamide phosphoribosyl transferase (NAMPT- key enzyme involved for the synthesis of NAD^{+}) is inhibited, acetylation of protein kinase B/AKT increases, which in turn inhibits protein kinase B/AKT activity (Dan et al., 2012). Furthermore, SIRT2 is found to interact with AKT in an AMP-activated kinase dependent manner *in vitro* in fibroblast

and cancer cell lines (Ramakrishnan et al., 2014). AMP-activated kinase phosphorylates SIRT2 at Thr^{101}, which mediates the interaction of SIRT2 with AKT and this interaction enhances AKT activity (Ramakrishnan et al., 2014). In addition to AKT, SIRT2 interacts with ERK1/2 in human embryonic kidney cells (Choi et al., 2013). Interestingly, this interaction increases SIRT2 protein expression with high stability and increases deacetylase activity (Choi et al., 2013). SIRT2 also increases the phosphorylation and activation of ERK1/2, which enhances the expression of cell cycle regulatory proteins such as cyclinD1 and CDK2 to promote cell proliferation in myoblast cells (Wu et al., 2014).

2.5.6 SIRT2 in neuroprotection

In addition to OLs, SIRT2 is expressed in neurons in the CNS (Southwood et al., 2007; Suzuki and Koike, 2007; Pandithage et al., 2008; Maxwell et al., 2011). Pharmacological or genetic inhibition of SIRT2 has neuroprotective effects against neurodegenerative diseases such as Parkinson's (PD) (Outeiro et al., 2007), Alzheimer's (AD) (Silva et al., 2017) and Huntington's (HD) (Luthi-Carter et al., 2010) disease. PD is characterized by loss of dopaminergic neurons and aggregation of α-synuclein to form Lewy bodies in the substantia nigra (Beitz, 2014). Pharmacological inhibition of SIRT2 in neuroglioma cells transfected with α-synuclein and in a *Drosophila* model of PD displays dose-dependent protective effects (Outeiro *et al*., 2007). Silencing *Sirt2* in cellular models of PD rescued the α-synuclein mediated cell death, suggesting that SIRT2 inhibition could be a useful strategy in combating PD (Outeiro et al., 2007). The inhibition of *Sirt2* might also increase the stabilization of α-tubulin (by increased tubulin acetylation), which could lead to stronger interactions with α-Syn through microtubules, stabilizing the formation of larger protein aggregates that are less toxic (Outeiro et al., 2007). In contrast, SIRT2 inhibition in oxidative stress induced α-synuclein aggregation

enhanced cell death, while overexpression of SIRT2 protected neural cells from α-synuclein mediated toxicity (Singh et al., 2017).

In AD cells containing patient mitochondrial DNA and in AD brain, expression of SIRT2 is high with an increase in tubulin deacetylation, which leads to amyloid-β accumulation (Silva et al., 2017). Loss of SIRT2 in AD cells recovers the microtubule assembly and cell survival by eliminating amyloid-β (Silva et al., 2017). In Huntington's disease model, SIRT2 inhibition using pharmacological inhibitors AK-1 and AGK2 rescue neuronal death in a dose-dependent manner whereas overexpression of *Sirt2* counteracts neuroprotection (Luthi-Carter et al., 2010). Molecular pathway analysis and gene ontology classification revealed that this neuroprotection is mediated by downregulation of genes involved in cholesterol biosynthesis (Luthi-Carter et al., 2010).

2.6 Cholesterol

Cholesterol is the major lipid component of myelin, constituting around 25% of total myelin lipids (Norton and Poduslo, 1973a; Saher and Simons, 2010). Cholesterol is supplied to the cell by *de novo* synthesis or by uptake from circulation (Saher et al., 2011). However, in brain, cholesterol is mainly supplied by *de novo* synthesis (Jurevics and Morell, 1995; Jurevics et al., 1997) as the blood brain barrier prevents the uptake of cholesterol from circulation (Dietschy and Turley, 2004).

2.6.1 Cholesterol biosynthesis in brain

Myelin accounts for around 80% of brain cholesterol (Dietschy and Turley 2004; Muse et al. 2001). In the brain, cholesterol needed for myelin biogenesis is primarily produced by OLs (Jurevics and Morell, 1995; Jurevics et al., 1997) with little being imported from circulation

(Dietschy and Turley, 2004). In mice, the brain cholesterol concentration is about 3.5 mg/g at birth, which increases during the peak of myelination and is tripled (12 mg/g) three weeks after birth (Dietschy and Turley, 2004). Cholesterol synthesis occurs through the isoprenoid biosynthetic pathway, which starts with the conversion of acetyl-CoA to 3-hydroxy-3-methylglutaryl-CoA (HMG-CoA). HMG-CoA is converted into mevalonate by HMG-CoA reductase, which is the rate-limiting step in cholesterol biosynthesis. Mevalonate is then converted into 3-isopentenyl pyrophosphate and farnesyl pyrophosphate. The conversion of farnesyl pyrophosphate into squalene by squalene synthase (SQS) is the first committed step in the isoprenoid biosynthetic pathway to form cholesterol. Squalene undergoes a series of enzymatic reaction to form cholesterol (Saher et al., 2011).

2.6.2 Importance of cholesterol in myelination

In mouse, conditional mutation of *Sqs* gene in OLs reduced myelin specific gene expression and severely delayed myelination (Saher et al., 2005). Similarly, mutation of Hmg-CoA synthase 1 (*Hmgcs1*) in zebrafish impaired myelin specific gene expression and axon wrapping (Mathews et al., 2014; Mathews and Appel, 2016). In addition, usage of the cholesterol lowering drug, statin, which inhibits HMG-CoA reductase reduced myelin specific gene expression and process outgrowth in OLs (Miron et al., 2007; Smolders et al., 2010). Besides being an important component of the myelin membrane, cholesterol aids in the transport and sorting of PLP and DM20 to promote tight compaction and myelin assembly (Saher and Simons, 2010; Saher et al., 2005; Saher et al., 2009; Simons et al., 2000; Werner et al., 2013). Hence, the availability of cholesterol is a rate-limiting factor for OL process outgrowth and myelination (Saher et al., 2005; Saher and Stumpf, 2015; Mathews et al., 2014; Mathews and Appel, 2016).

2.6.3 Sterol regulatory element binding protein (SREBP)-2

Cholesterol biosynthesis occurs under the control of a transcription factor, sterol regulatory element binding protein (SREBP)-2 (Brown and Goldstein, 1997; Amemiya-Kudo et al., 2002; Eberlé et al., 2004). SREBP-2 is produced as an inactive precursor containing three domains, 1) NH2-terminal domain harboring the basic helix-loop-helix-leucine zipper region, 2) hydrophobic transmembrane-spanning segment, and 3) a COOH- terminal domain (Horton et al., 2002). The SREBP-2 precursor is bound to the endoplasmic reticulum (ER) along with SREBP cleavage activating protein (SCAP) (Yabe et al., 2002; Yang et al., 2002). When the cellular concentration of cholesterol is low, the SREBP-SCAP complex is released from the ER and enters the golgi apparatus (Yabe et al., 2002; Yang et al., 2002). In the golgi apparatus, the precursor SREBP-2 is cleaved by two proteases, site-1 protease and site-2 protease (Sakai et al., 1996; Wang et al., 1994). This releases the NH2-terminal domain of SREBP-2, which translocates to the nucleus (nSREBP-2) and binds to sterol responsive elements (SREs) in the target genes encoding cholesterogenic enzymes (Amemiya-Kudo et al., 2002; Eberlé et al., 2004; Horton et al., 2002). However, excess sterol negatively regulates cholesterol synthesis by retaining SREBP-SCAP complex in the ER and inhibiting SREBP processing (Wang et al., 1994; Yang et al., 2002).

2.6.4 *Sirt2* in cholesterol biosynthesis

Acetylation and deacetylation of lysine residues within the DNA binding domain of SREBPs can modulate SREBP activity and downstream target gene expression (Giandomenico et al., 2003; Ponugoti et al., 2010; Walker et al., 2010). In neuronal cells, overexpression of *Sirt2* promotes cholesterol biosynthesis by facilitating the nuclear translocation of SREBP-2 (Luthi-

Carter et al., 2010; Taylor et al., 2011). In addition, pharmacological inhibition using SIRT2 specific inhibitors, AGK2, AK-1 and AK-7, retained SREBP-2 in the cytoplasm, which reduced the expression of genes encoding enzymes involved in cholesterol biosynthesis and total cholesterol content (Luthi-Carter et al., 2010; Taylor et al., 2011). Similarly, overexpression of deacetylase-deficient *Sirt2* mutant (Sirt2H150Y) impaired nuclear translocation of SREBP-2 and cholesterol biosynthesis (Luthi-Carter et al., 2010). This indicates that deacetylase activity is crucial for the nuclear translocation of SREBP-2. However, SREBP-2 translocation and cholesterol synthesis was not altered in the whole brain of *Sirt2* knock-out mice (Bobrowska et al., 2012). This difference could be cell type specific. Therefore, it remains to be understood if SIRT2 regulates SREBP-2 in OLs during myelination.

Preamble to Chapter 3: QUAKING PROMOTES THE EXPRESSION OF SIRT2 DURING OLIGODENDROGLIAL DIFFERENTIATION

Rationale: SIRT2 is a NAD^+ dependent deacetylase, predominantly expressed in OLs. Previous work from our group showed that *Sirt2* is essential for OL differentiation *in vitro* using CG4-OLs, although the mechanism involved in regulating the expression of SIRT2 during oligodendrogenesis is largely unknown. The RNA binding protein Quaking (QKI) regulates the expression of several myelin specific genes either directly or indirectly. Moreover, SIRT2 protein is absent in qk^v/qk^v mutant mice. It is not clear whether QKI protein directly interacts with *Sirt2* mRNA to modulate OL development. In this study, I investigated the molecular mechanism by which QKI regulates the expression of SIRT2 during OL development.

Publication

Merlin P. Thangaraj, Kendra L. Furber, Jotham K. Gan, Shaoping Ji, LaRhonda Sobchishin, J. Ronald Doucette and Adil J. Nazarali. (2017) "RNA-binding Protein Quaking Stabilizes *Sirt2* mRNA during Oligodendroglial Differentiation" *The Journal of Biological Chemistry*, 292; 5166-5182. doi:10.1074/jbc.M117.775544.

Contribution statement

I designed and performed the experiments to investigate how QKI regulates SIRT2 expression in oligodendrocytes. The data generated are shown in figures 1-8 of the manuscript. Kendra L. Furber, Jotham K. Gan, Shaoping Ji and LaRhonda Sobchishin contributed to the data generated using QKI-5 isoform shown in figures 9 and 10 of the manuscript. Adil J. Nazarali and J. Ronald Doucette conceived and coordinated the study. In this chapter, I am presenting only the data I generated (Figure 3.1-3.12).

3. QUAKING PROMOTES THE EXPRESSION OF SIRT2 DURING OLIGODENDROGLIAL DIFFERENTIATION

3.1 Summary

Myelination is controlled by timely expression of genes involved in the differentiation of OPCs into myelinating OLs. SIRT2, a NAD^+-dependent deacetylase, plays a critical role in OL differentiation by promoting both arborization and downstream expression of myelin specific genes *in vitro*. However, the mechanisms involved in regulating SIRT2 expression during OL development are largely unknown. The RNA binding protein Quaking (QKI) plays an important role in myelination by post-transcriptionally regulating the expression of several myelin specific genes. In qk^v/qk^v mutant mice, SIRT2 protein is severely reduced; hence, I hypothesized that QKI interacts with *Sirt2* mRNA to regulate OL differentiation. Here, I report for the first time that QKI directly binds to *Sirt2* mRNA via a common quaking binding site located in the 3' UTR to control SIRT2 expression in OL lineage cells. This interaction is associated with increased stability and longer half-lives of *Sirt2.1* and *Sirt2.2* transcripts leading to increased accumulation of *Sirt2* transcripts. Consistent with this, overexpression of *qkI* promoted the expression of SIRT2 protein. Collectively, this study demonstrates that QKI directly plays a crucial role in the post-transcriptional regulation and expression of *Sirt2* to facilitate OL differentiation.

3.2 Introduction

OLs are the myelinating glial cells in the CNS. In the mammalian cortex, OPCs originating from the VZ/SVZ proliferate, migrate, and eventually differentiate into mature, myelinating OLs (Baumann and Pham-Dinh, 2001; Emery and Lu, 2015; Nicolay et al., 2007). The RNA-binding protein QKI is expressed by glial progenitors (Hardy, 1998a). QKI controls OL development and myelination by governing the post-transcriptional regulation of several myelin-specific transcripts (Chen et al., 2007b; Larocque et al., 2002; Wu et al., 2002; Li et al., 2000; Zhao et al., 2006a; Zhao et al., 2010). The qk^v/qk^v mutant mouse (Sidman et al., 1964) carries a spontaneous one megabase pair deletion in the upstream of *qkI* locus covering a part of the *Parkin* gene, entire *Parkin* co-regulated gene and the promoter/enhancer region of the *qkI* gene (Ebersole et al., 1996; Lockhart et al., 2004; Lorenzetti et al., 2004a; Lorenzetti et al., 2004b). In qk^v/qk^v mutant mouse there is OL specific decrease in the expression of QKI, which leads to severe hypomyelination in the CNS (Hardy et al., 1996; Lu et al., 2003).

qkI encodes three alternatively spliced transcripts, *qkI-5*, *qkI-6*, and *qkI-7*. All three variants contain exons encoding common QUA1 – K homology (KH) – QUA2 domains in the N- terminal that confer RNA binding specificity and dimerization (Ebersole et al., 1996; Kondo et al., 1999; Chen and Richard, 1998). QKI interacts with target mRNAs that possess a specific quaking response element (QRE) ACUAAY[N1-20]UAAY (Galarneau and Richard, 2005) or its variant AUUAAY (Wu et al., 2002). In OLs, efficient binding of QKI to QREs has been reported for transcripts of *Mbp* (Larocque et al., 2002; Li et al., 2000; Galarneau and Richard, 2005; Ryder and Williamson, 2004), *Mag* (Wu et al., 2002), $p27^{Kip1}$ (Larocque et al., 2005), *Aip-1* (Doukhanine et al., 2010), *Map1B* (Zhao et al., 2006b) and *hnRNPA1* (Zearfoss et al., 2011). This interaction alters the stability of the target mRNAs, which can lead to either a promotion or

inhibition in the downstream translation of the protein products, as is the case for *p27*^{Kip1} (Larocque et al., 2005) or *Aip-1* (Doukhanine et al., 2010), respectively. In addition to stabilizing the target mRNA, QKI has been demonstrated to regulate alternative splicing of *Mag* (Wu et al., 2002; Zhao et al., 2010), and an altered ratio of splice variants for *Mag* (Fujita et al., 1990) and *Mbp* (Li et al., 2000) are found in the *qk*^{v}/*qk*^{v} mutants. *qk*^{v}/*qk*^{v} mice also show a mislocalized pattern of *Mbp*, with its confinement to the nucleus (Larocque et al., 2002; Li et al., 2000). Thus, QKI proteins interact with target transcripts at multiple levels to control gene expression during oligodendroglial differentiation.

Similar to myelin structural proteins (MBP and PLP), SIRT2 protein expression is also reduced in *qk*^{v}/*qk*^{v} mice (Zhu et al., 2012). Mammalian SIRT2 is a class III NAD^{+}-dependent deacetylase (North et al., 2003), which is predicted to give rise to three isoforms, SIRT2.1, SIRT2.2, and SIRT2.3 (Maxwell et al., 2011). SIRT2 isoforms differ in the amino terminal but the functions of these isoforms are not yet clearly identified. However, SIRT2.2 is the most abundant isoform in OLs (Ji et al., 2011, Zhu et al., 2012) and is the only isoform incorporated into the myelin sheath (Werner et al., 2007). SIRT2.1 is expressed in non-neuronal cells and expression of SIRT2.3 increases with age in brain and spinal cord (Maxwell et al., 2011). SIRT2 is enriched in brain and spinal cord tissue, predominately localized in the paranodal regions of the CNS myelin sheath (Li et al., 2007a; Werner et al., 2007; Southwood et al., 2007). During OL differentiation, SIRT2 is expressed early, prior to the expression of myelin specific genes (Zhu et al., 2012; Southwood et al., 2007; Ji et al., 2011), promoting differentiation at both the cellular and molecular level (Ji et al., 2011). In addition to the *qk*^{v}/*qk*^{v} mice, SIRT2 expression is reduced in the *Plp* null mice (Werner et al., 2007) and *Plp*-ISEdel mutant mice (Zhu et al., 2012). In *Plp* mutants, the loss of SIRT2 is observed primarily in the myelin sheath (Zhu et al., 2012;

Werner et al., 2007) but not in OPCs or OL cell bodies (Zhu et al., 2012). Moreover, no putative QREs have previously been identified in *Sirt2* mRNA. Thus, it was postulated that QKI indirectly regulates SIRT2 expression during CNS myelination through co-transport with PLP into the myelin sheath (Zhu et al., 2012).

To further investigate the relationship between *qkI* and *Sirt2* in OL development, I used the CG4-OL cell line derived from neonatal rat forebrain O-2A progenitors and mouse primary OLs that undergo defined stages of differentiation under controlled media conditions (Ji et al., 2011; Louis et al., 1992a; Louis et al., 1992b; Wang et al., 2011; Chen et al., 2007a; Niu et al., 2012). Coordinated expression of QKI and SIRT2, was observed during differentiation. Thus, I sought to delineate the molecular mechanism that governs the direct or indirect interaction between the RNA binding protein QKI and *Sirt2* during OL development. My findings demonstrate that there is a direct interaction between QKI and *Sirt2* mRNA in OL progenitors and differentiating OLs. The binding site for QKI was mapped to the QRE ACUAAC at 1853-1858 bp in the 3' UTR of *Sirt2* mRNA. My findings indicate that *Sirt2* is a direct target of QKI. Binding of QKI to *Sirt2* mRNA increases the post-transcriptional stability of *Sirt2* mRNA and controls its availability for translation.

3.3 Materials and Methods

3.3.1 CG4-OL cell culture

CG4-OL is a O-2A progenitor cell line derived from rat brain and was cultured as previously described (Ji et al., 2011; Louis et al., 1992a; Louis et al., 1992b; Wang et al., 2011). Briefly, the CG4-OL cells were cultured on poly-D-lysine (Sigma) coated tissue culture dishes and maintained as undifferentiated progenitors in growth medium (GM) containing Dulbecco's

modified Eagle's medium (DMEM), 50 μg/mL transferrin, 5 μg/mL insulin, 9.8 ng/mL biotin, 50 ng/mL selenium, 1% antibiotic antimycotic solution and 30% B104 conditioned medium (CM) (Ji et al., 2011; Wang et al., 2011). Differentiation of CG4-OL cells was induced by culturing in differentiation medium (DM) containing 2% fetal bovine serum (FBS) instead of B104 CM (Ji et al., 2011; Wang et al., 2011). Transfection was carried out using Lipofectamine 2000 (Invitrogen) or polyethylenimine (PEI) (Polysciences) in serum free / antibiotic free media. For growth conditions (GM), cells were harvested 48 hours (h) after transfection for RNA and protein extraction. For differentiation (DM), transfections were performed on day 0, day 2, day 4, to maintain consistent levels of overexpression throughout six days of experimental timeline.

3.3.2 Primary OL cell culture and electroporation

Primary OLs were prepared from C57BL/6 mice at P1, as previously described (Chen et al., 2007a; Niu et al., 2012). Briefly, mixed glial cells were prepared from the meninges free cortices isolated from neonatal mouse pups. The dissected cortices were digested with Accumax solution (Sigma) and passed through a 70 μm nylon cell strainer. The filtered cell suspensions were plated on poly-D-lysine (Sigma) coated T75 tissue culture flasks and maintained as mixed glial cells in mixed glial medium (MGM) containing DMEM/F12, 10% FBS and penicillin-streptomycin solution. Half of the culture medium was changed every other day. After seven days, to enrich OLs in the mixed glial cells, MGM was replaced with OL growth medium (OGM) containing 10 ng/mL biotin, 5 μg/mL insulin, 50 μg/mL transferrin, 2 mM glutamine, 30 nM sodium selenite, 0.1% BSA, 10 nM hydrocortisone, 1% penicillin-streptomycin solution in DMEM/F12 and 30% of B104 conditioned medium. After 14 days, primary OLs were shaken off (at 200 rpm; 37°C) from the mixed glial cultures and plated in the OGM supplemented with 10 ng/mL human recombinant platelet-derived growth factor (PDGF-AA) (Peprotech) and 10 ng/mL basic

fibroblast growth factor (bFGF) (Peprotech). To induce differentiation, purified primary OLs were plated in OL differentiation medium (ODM) containing 10 ng/mL biotin, 5 μg/mL insulin, 50 μg/mL transferrin, 2 mM glutamine, 30 nM sodium selenite, 0.1% BSA, 10 nM hydrocortisone, 1% penicillin-streptomycin solution in DMEM/F12, 5 μg/mL *N*-acetyl-L-cysteine and 1% FBS. Transfections were carried out by electroporation (Amaxa nucleofection apparatus, Lonza) in 3-5 x 10^6 primary OLs using Ingenio electroporation solution (Mirus Bio LLC). Primary OLs were resuspended in OGM (supplemented with PDGF-AA+bFGF) or ODM and harvested 6 days after electroporation for protein and RNA extraction. Animal use was approved by the University of Saskatchewan's Animal Research Ethics Board, and adhered to the Canadian Council on Animal Care guidelines for humane animal use.

3.3.3 Vector construct and site directed mutagenesis

The common coding region of *qkI* (908 bp) spanning from 489 bp (exon 1) to 1417 bp (exon 6) containing the RNA binding and dimerization domains (QUA1-KH-QUA2) (Ebersole et al., 1996; Kondo et al., 1999) was amplified by PCR using the forward 5'-AAGGGATCCGAATATGGTCGGGGAAATG-3' and reverse 5'-GTGGAATTCACACCACTGGGTTCAAT-3' primers and cloned into pcDNA 3.1/His between *BamHI* and *EcoRI* restriction sites. The 3' UTR of *Sirt2* mRNA was amplified using the forward 5'-CGCTCTAGACAGTAACCATGACCTCCCG -3' and reverse 5'-ACGCTCTAGACATGGTTAGTTGCTTTGT -3' primers and cloned into pGL3-promoter luciferase vector (Promega) at *XbaI* site. The two putative QREs in the 3' UTR of *Sirt2* mRNA at 1639 bp (*Sirt2* 3' UTR-Mut1) and/or 1853 bp (*Sirt2* 3' UTR-Mut2) were mutated using QuikChange Lightning kit (Agilent Technologies) with the primers, *Sirt2* 3' UTR-Mut1; 5'-

GCGGGGTAGGGTCGATTGATTTAGCCATAGGCC-3' and 5'-GGCCTATGGCTAAATCAATCGACCCTACCCCGC-3' and *Sirt2* 3' UTR-Mut2; 5'-GCCCCGACTCTAGACATGGCTCGATGCTTTGTTTTG-3' and 5'-CAAAACAAAGCATCGAGCCATGTCTAGAGTCGGGGC-3'.

3.3.4 Luciferase reporter assay

CG4-OL cells maintained in GM were seeded in a white opaque 96-well plate (Costar, 3610) and were co-transfected with pcDNA vector or pcDNA-*qkI* expression vector along with *Sirt2* 3' UTR luciferase vector (pGL3-*Sirt2* 3' UTR) or putative QREs mutated *Sirt2* 3' UTR luciferase vector (pGL3-*Sirt2* 3' UTR- Mut1 or pGL3-*Sirt2* 3' UTR- Mut2 or pGL3-*Sirt2* 3' UTR-Mut1*Mut2). pRL-CMV renilla luciferase vector was used as a control for normalizing transfection efficiency. Dual-Glo luciferase assay system (Promega) was used to measure the luciferase activity of cells co-transfected with *qkI* overexpression vector and wild-type or mutated *Sirt2* 3' UTR luciferase vectors. Luciferase assay was performed according to the manufacturer's instruction. Briefly, 48 h after transfection, equal volume of Dual-Glo reagent was added to the cells in culture medium to measure the firefly luminescence. Subsequently, Dual-Glo Stop & Glo reagent was added to inactivate firefly luciferase activity and measure the renilla luciferase activity. Relative luciferase activity was calculated by normalizing the firefly luciferase values to its respective renilla luciferase values. Data were normalized to the *Sirt2* 3' UTR co-transfected with pcDNA control vector and represented as percentage luciferase activity.

3.3.5 RNA isolation, reverse transcription-PCR (RT-PCR) and quantitative real time-PCR (qPCR)

Total mRNA from the CG4-OL cells was isolated using Aurum total RNA mini kit (BioRad) as per the manufacturer's protocol. First strand cDNA synthesis (Reverse transcription) was performed with 500 ng – 1 μg of total RNA using the Quantitect Reverse Transcription Kit (Qiagen) or High-Capacity cDNA Reverse Transcription kit (Applied Biosystems) with random primers. RT-PCR was carried out as described before (Ji et al., 2011). The following primer pairs were used: (i) *Sirt2* forward 5′-AGCAAGGCACCACTAGCCACC-3′ and reverse 5′-TGTTCCTCTTTCTCTTTGGTC-3′; and (ii) *Gapdh* forward 5′-ACCACAGTCCATGCCATCAC-3′ and reverse 5′-TCCACCACCCTGTTGCTGTA-3′. PCR products were visualized on RedSafe stained 1% agarose gel and integrated density values were determined for each band with AlphaView® imaging software.

qPCR was carried out according to Doucette et al., (2010), using SYBR select master mix (Applied Biosystems) in Step one Real Time PCR System (Applied Biosystems) with gene specific primers. For analyzing the total *Sirt2* mRNA levels, primers were the same as above and for total *qkI* mRNA levels, forward primer, 5′- TGAATGGCACCTACAGAGAC-3′ and reverse primer, 5′- CAAAGGCATTATGGTAGGGC-3′ were used. For quantifying the levels of *Sirt2* variants, common reverse primer 5′-GGGGAGCGGAAGTCAGGGAT-3′ was used in combination with variant specific forward primer, *Sirt2.1*, 5′-CAGGAGGCTCAGGATTCAGAC-3′; *Sirt2.2*, 5′-CCCAGGATTCAGACTCGGACA-3′; *Sirt2.3*, 5′-CTGCTCCCCGTCGCAGGGTC -3′. The expression levels of β-actin (Forward 5′-ATTGTAACCAACTGGGACG-3' and reverse 5'-TTGCCGATAGTGATGACCT-3') and 18s ribosomal RNA (18s rRNA) (forward 5′-CGCGGTTCTATTTTGTTGGT-3' and reverse 5′-

AGTCGGCATCGTTTATGGTC-3') were used as endogenous control. The relative levels of transcripts were determined by threshold cycle differences ($2^{-\Delta\Delta CT}$) of target normalized to the endogenous control as previously described (Doucette et al., 2010).

3.3.6 RNA co-immunoprecipitation (RNA co-IP)

Immunoprecipitation of mRNA-protein complexes was performed according to (Peritz et al., 2006). The cells were harvested, either in GM or after DM-day 6, and lysed with polysome lysis buffer. The mixture was precleared with protein A agarose beads before immunoprecipitation to remove nonspecific binding to the beads. Subsequently, the supernatant was incubated with 10 μg of rabbit monoclonal anti-QKI antibody (Abcam: ab126742) or normal rabbit anti- IgG (Millipore: 12-370) overnight at 4°C. The following day, fresh protein A agarose beads were added and incubated for 4 h at 4°C. After immunoprecipitation, the beads were collected and washed four times with polysome lysis buffer and then with polysome lysis buffer containing 1 M urea. Next, 0.1% SDS and 30 μg proteinase K were added to the immunoprecipitated beads and heated at 50°C for 30 min to retrieve the protein-RNA complex. RNA isolation and qPCR was performed, as described above.

3.3.7 mRNA stability assay

CG4-OL cells maintained in GM were transfected with pcDNA vector or pcDNA-*qkI* expression vector and the stability of *Sirt2* mRNA variants were examined by treating the cells with actinomycin D (Sigma) (Larocque et al., 2005; Doukhanine et al., 2010; Zhao et al., 2006). After 48 h of transfection, actinomycin D (10 μg/mL) was added to cells and total RNA was extracted at indicated time points (0, 15, 30, 60 and 120 min). RNA isolation and qPCR was performed, as described above. Half-life ($t_{1/2}$) of *Sirt2* mRNA variants were calculated as the time required for

each mRNA variant to reduce to 50% after actinomycin D treatment from its initial abundance at time 0 min. Half-lives ($t_{1/2}$'s) were determined by nonlinear regression analysis (Baudouin-Legros et al., 2005).

3.3.8 Western blot analysis

Total protein was extracted from CG4-OL cells using RIPA lysis buffer (150 mM NaCl, 0.5% SDS, 1% Trition-100, 0.1% deoxycholate, 10 mM Tris-HCl [pH 7.2], 5 mM EDTA) at 4°C. Protein quantification, electrophoresis, and subsequent protein detection was performed as described previously (Ji et al., 2011). Briefly, proteins (20-40 µg) were separated on 12% SDS-PAGE and transferred to a PVDF membrane. Immunoblot was performed with the following primary antibodies: anti-QKI (1:1000, Abcam), anti-SIRT2 (1:3000, Sigma), anti-MBP (1:1000, Sternberger Monoclonals), anti-β-tubulin (1:1000, Developmental Studies Hybridoma) and anti-GAPDH (1:10000, Sigma). Secondary antibodies utilized were goat anti-rabbit IgG- horse radish peroxidase (HRP) conjugate (1:3000, BioRad), and goat anti-mouse IgG-HRP conjugate (1:3000, BioRad). Bands visualized with Clarity™ Western ECL Substrate (BioRad). Densitometric analyses were carried out using Alpha View Imaging software.

3.3.9 Statistical analysis

All data are presented as mean ± standard error of the mean (SEM). Statistical analyses were performed using Student's t-test or ANOVA with Bonferonni's multiple comparisons post-test (Prism® Software Corporation) as indicated in the figure legends.

3.4 Results

3.4.1 Expression of QKI and Sirt2 increase during OL differentiation

In this study, I sought to delineate the molecular interaction between *qkI* and *Sirt2* in OPC proliferation (i.e., growth media; GM) and OL differentiation (i.e., differentiation media; DM). The expression patterns of mRNA and proteins of both QKI (Fig. 3.1) and Sirt2 (Fig. 3.2) increased in CG4 cells over six days of differentiation. Expression of *qkI* mRNA (Fig. 3.1A) gradually increased with differentiation with a ~3-fold increase observed by day 6. There was a corresponding increase in expression of the QKI protein product QKI-6 isoform (~ 2 fold increase at DM-day 6) but not of QKI-5 or QKI-7, which co-migrate on the immunoblot (Fig. 3.1B, C).

The *Sirt2.2* variant was the most abundant transcript in CG4-OL cells with ~4.5-fold and ~2700-fold greater expression than *Sirt2.1* and *Sirt2.3*, respectively, under growth conditions (Fig. 3.2A). Expression of *Sirt2.2* mRNA increased ~8-fold within 24h under differentiation conditions and was maintained through to day 6. Similarly, *Sirt2.1* and *Sirt 2.3* mRNA expression increased throughout differentiation. SIRT2.2 was also the most abundant protein isoform in CG4-OL cells (Fig. 3.2B). Expression of SIRT2.2 protein increased ~2.5-fold by day 3 and was maintained through to day 6 (Fig. 3.2C). Although *Sirt2.1* and *Sirt2.3* mRNA increased during differentiation, this did not translate to an increase in the SIRT2.1 or SIRT2.3 protein products. The coordinated expression patterns of *qkI* and *Sirt2* during OL differentiation suggest that these two genes may interact, either directly or indirectly, to promote OL differentiation.

A

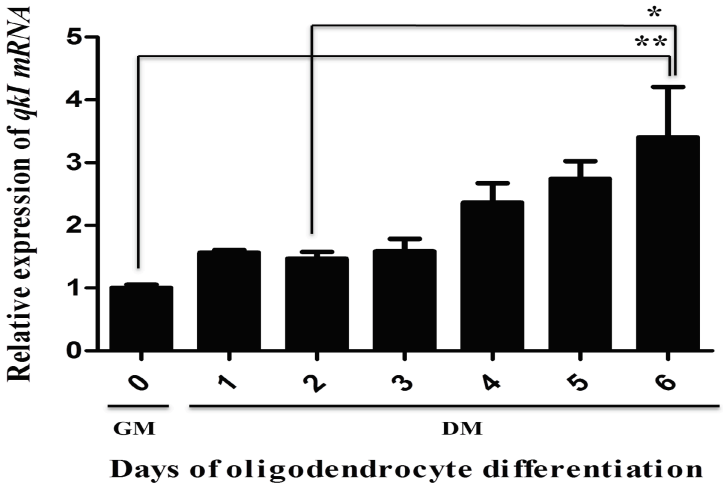
Relative expression of qkI mRNA
5
4
3
2
1
0
*
**
0
1
2
3
4
5
6
GM
DM
Days of oligodendrocyte differentiation

B

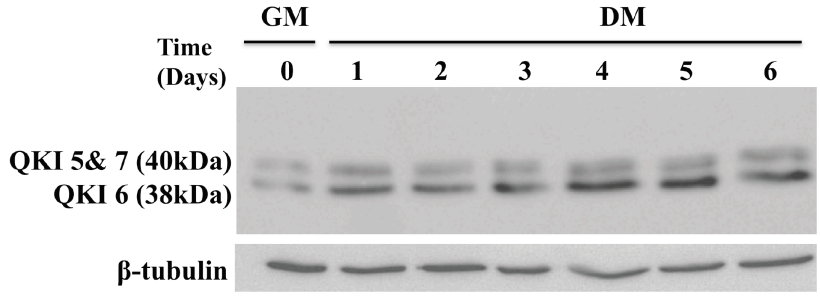
GM
DM
Time
(Days)
0
1
2
3
4
5
6
QKI 5& 7 (40kDa)
QKI 6 (38kDa)
β-tubulin

C

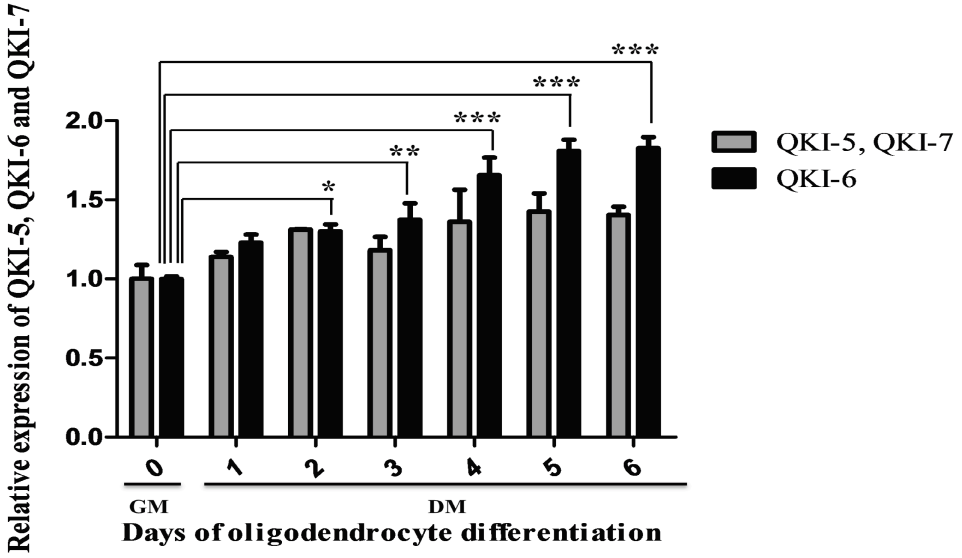
Relative expression of QKI-5, QKI-6 and QKI-7
2.0
1.5
1.0
0.5
0.0
*
**
***
***
***
0
1
2
3
4
5
6
GM
DM
Days of oligodendrocyte differentiation
QKI-5, QKI-7
QKI-6

Figure 3.1: Expression of *qkI* mRNA and protein increases during differentiation. CG4-OL progenitor cells undergo high rates of proliferation in growth medium (GM) followed by differentiation into mature, pre-myelinating OLs when transferred to differentiation medium (DM). Whole cell lysates were collected at 24 h intervals during differentiation (day 0, 1, 2, 3, 4, 5 and 6). **(A)** Quantitative Real time PCR was carried out to analyze the changes in the mRNA levels of *qkI* (n=3 biological replicates). A gradual increase in *qkI*, expression was observed over the 6 day experimental timeline. Data were normalized to *β-actin* and represented relative to day 0 (mean±SEM; one-way ANOVA *$p < 0.05$, **$p < 0.01$). **(B)** Representative immunoblot showing a corresponding increase in QKI protein expression over the course of 6 day differentiation. **(C)** Densitometric analysis of immunoblots (n=3 biological replicates) shows QKI-6 is the predominate isoform expressed during OL differentiation. Data were normalized to β-tubulin and represented relative to the respective isoform at day 0 (mean±SEM; two-way ANOVA *$p < 0.05$, **$p < 0.01$, ***$p < 0.001$).

A

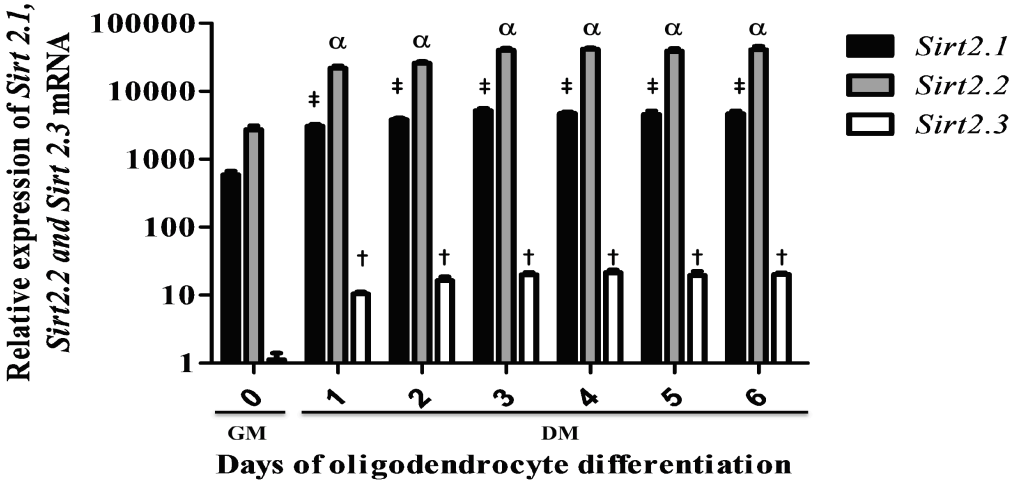
Relative expression of Sirt 2.1, Sirt2.2 and Sirt 2.3 mRNA
100000
10000
1000
100
10
1
Sirt2.1
Sirt2.2
Sirt2.3
GM
DM
Days of oligodendrocyte differentiation

B

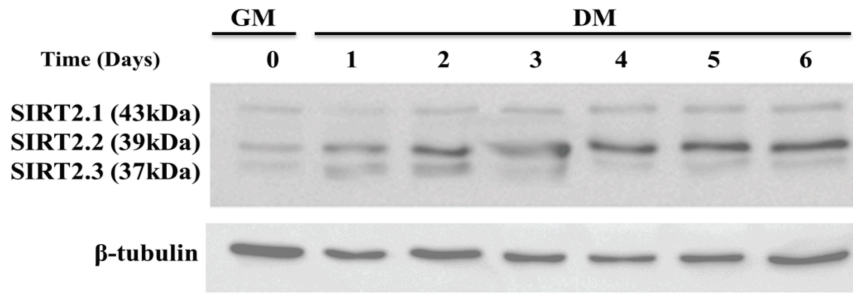
GM
DM
Time (Days)
0
1
2
3
4
5
6
SIRT2.1 (43kDa)
SIRT2.2 (39kDa)
SIRT2.3 (37kDa)
β-tubulin

C

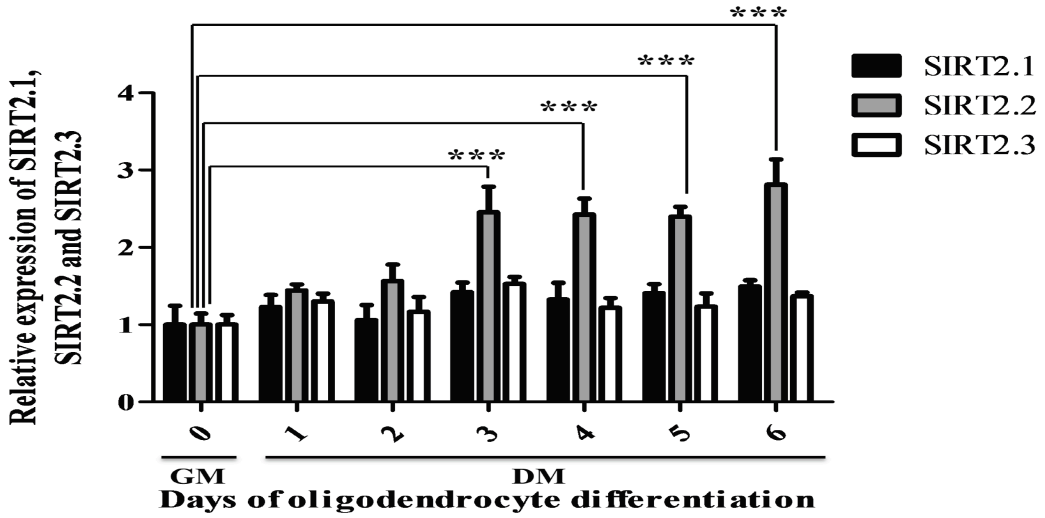
Relative expression of SIRT2.1, SIRT2.2 and SIRT2.3
SIRT2.1
SIRT2.2
SIRT2.3
GM
DM
Days of oligodendrocyte differentiation

Figure 3.2: Expression of *Sirt2* mRNA and protein increases during differentiation. CG4-OL progenitor cells in growth medium (GM) were transferred to differentiation medium (DM) and whole cell lysates were collected at 24 h intervals (day 0, 1, 2, 3, 4, 5 and 6). **(A)** *Sirt2* mRNA expression increases under differentiation conditions. *Sirt2.2* mRNA is the most abundant transcript expressed in CG4-OL cells and increases by day 1 of differentiation. qPCR data (n=3 biological replicates) were normalized to *β-actin* and represented relative to *Sirt2.3* variant at day 0 (mean±SEM; two-way ANOVA). ‡ denotes *Sirt2.1* mRNA with $p < 0.001$; α denotes *Sirt2.2* mRNA with $p < 0.001$ and † denotes *Sirt2.3* mRNA with $p < 0.001$ relative to their respective variants at day 0 **(B)** Representative immunoblot showing a corresponding increase in SIRT2 protein expression over the course of differentiation. **(C)** Densitometric analysis of immunoblots (n=3 biological replicates) reveal that SIRT2.2 is the predominate isoform expressed during OL differentiation. Data were normalized to β-tubulin and represented relative to the respective isoform at day 0 (mean±SEM; two-way ANOVA *$p < 0.05$, **$p < 0.01$, ***$p < 0.001$).

3.4.2 Overexpression of *qkI* promotes the accumulation of *Sirt2* mRNA and expression of SIRT2 protein

In the brainstem of qk^v/qk^v mutant mice, a reduction in SIRT2 protein expression but not *Sirt2* mRNA has been reported in young adult animals (P40) (Zhu et al., 2012). However, little is known about the relationship between QKI and *Sirt2* during OL differentiation. To investigate what role QKI may have in regulating the expression of *Sirt2* during OL differentiation, *qkI* was overexpressed in CG4-OL cells by transfection with pcDNA3.1 vector containing the common coding sequence of the RNA binding domain from QKI-5, QKI-6 and QKI-7. The proliferating CG4-OLs were transfected on day 0 and the cells were harvested 48 h after transfection. The differentiating CG4-OLs were transfected thrice (on day 0, day 2, day 4) and the cells were harvested on day 6. Overexpression of *qkI* increased the expression of QKI protein in both proliferating (growth media; GM; Fig. 3.3A) and differentiating (differentiation media; DM-day 6; Fig. 3.3B) conditions in CG4-OLs. Overexpression of *qkI* promoted the homodimerization of

QKI-His fusion protein, resulting in the appearance of QKI-His fusion protein at 45 kDa. The extent of OL differentiation was analyzed by quantifying the expression of mature OL marker MBP. Expression of *Mbp* mRNA (Fig. 3.3C) increased with induced differentiation reaching a ~60-fold increase by day 6. Consistent with this, the expression of the MBP protein (Fig. 3.3D, E) increased with differentiation from day 4 to day 6. Upregulation of *qkI* increased the accumulation of *Sirt2* mRNA under both proliferating (growth media; GM) (Fig. 3.4A) and differentiating (differentiation media; DM-day 6) conditions (Fig. 3.4B). In GM, *Sirt2.1* and *Sirt2.2* mRNA abundance increased ~2-fold and ~3-fold, respectively; in contrast, *Sirt2.3* abundance was not affected (Fig. 3.4A). In DM, accumulation of all three variants increased ~2-fold in differentiating OLs (Fig. 3.4B). Upregulation of *qkI* also resulted in a corresponding ~1.5 fold increase in SIRT2.1 and SIRT2.2 protein expression under both proliferating (GM; Fig. 3.4C, D) and differentiating (DM; Fig. 3.4E, F) conditions.

A

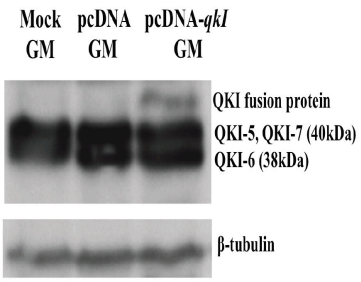
Mock GM
pcDNA GM
pcDNA-qkI GM
QKI fusion protein
QKI-5, QKI-7 (40kDa)
QKI-6 (38kDa)
β-tubulin

B

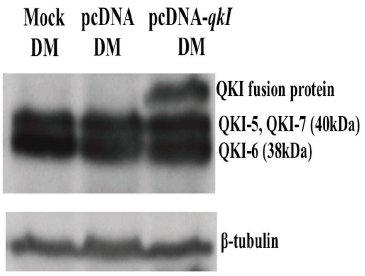
Mock DM
pcDNA DM
pcDNA-qkI DM
QKI fusion protein
QKI-5, QKI-7 (40kDa)
QKI-6 (38kDa)
β-tubulin

C

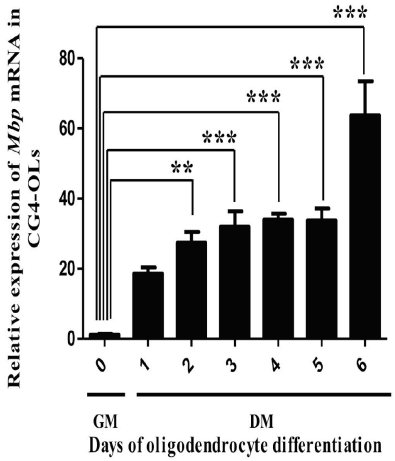
Relative expression of Mbp mRNA in CG4-OLs
***
***
***
***
**
0
20
40
60
80
0 1 2 3 4 5 6
GM
DM
Days of oligodendrocyte differentiation

D

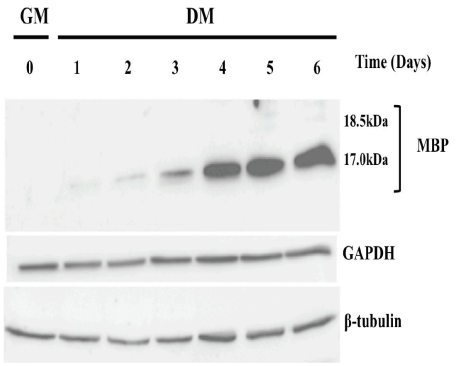
GM
DM
0 1 2 3 4 5 6
Time (Days)
18.5kDa
17.0kDa
MBP
GAPDH
β-tubulin

E

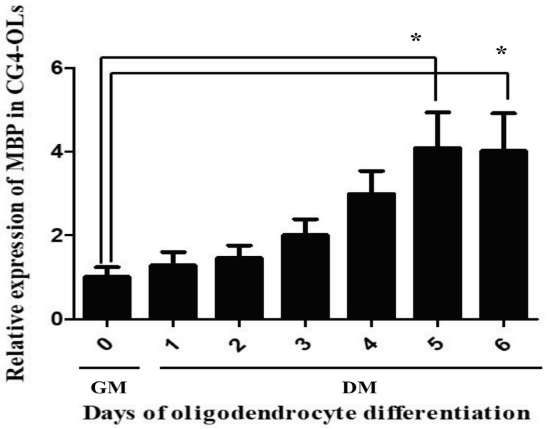
Relative expression of MBP in CG4-OLs
*
*
0
2
4
6
0 1 2 3 4 5 6
GM
DM
Days of oligodendrocyte differentiation

Figure 3.3: Overexpression of *qkI* in CG4-OLs. (A and B) CG4-OLs were transfected with control pcDNA vector or pcDNA-*qkI* vector (containing common coding region of *qkI-5, qkI-6 and qkI-7*). Immunoblot analyses show an increase in the QKI protein expression, 48 h after transfection with pcDNA-*qkI* in GM **(A)** and 6 days after transfection in DM **(B)**. QKI-His fusion protein appeared as homodimer with a molecular mass of 45kDa. CG4-OL cells were allowed to differentiate and whole cell lysates were collected at 24h intervals (day 0, 1, 2, 3, 4, 5 and 6). **(C)** qPCR was carried out to evaluate OL differentiation using OL mature marker *Mbp* (n=3). A gradual increase in *Mbp* mRNA expression was observed over the 6 day experimental timeline. Data were normalized to β-actin and represented relative to day 0 (mean±SEM; one-way ANOVA **p < 0.01, ***p < 0.001). **(D)** Representative immunoblot (n=3) showing a corresponding increase in MBP protein expression over the course of 6 day differentiation.
(E) Densitometric analysis of immunoblots (n=3 biological replicates) showing the increase in MBP expression during OL differentiation. Data were normalized to β-tubulin and represented relative to day 0 (mean±SEM; two-way ANOVA *p < 0.05).

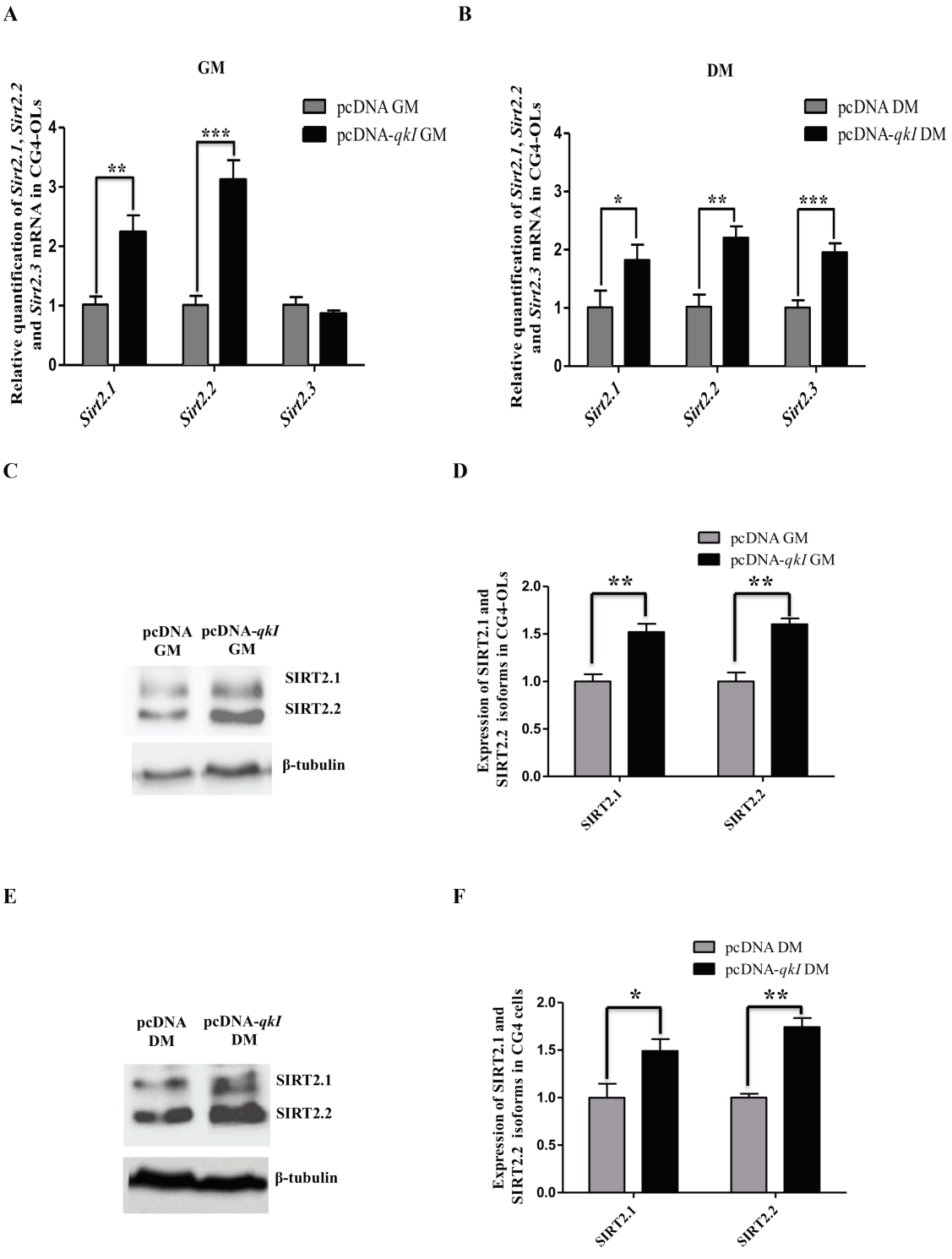
A
GM
pcDNA GM
pcDNA-qkI GM
Relative quantification of Sirt2.1, Sirt2.2 and Sirt2.3 mRNA in CG4-OLs
Sirt2.1
Sirt2.2
Sirt2.3
B
DM
pcDNA DM
pcDNA-qkI DM
C
pcDNA GM
pcDNA-qkI GM
SIRT2.1
SIRT2.2
β-tubulin
D
Expression of SIRT2.1 and SIRT2.2 isoforms in CG4-OLs
E
pcDNA DM
pcDNA-qkI DM
F
Expression of SIRT2.1 and SIRT2.2 isoforms in CG4 cells

Figure 3.4: Overexpression of *qkI* promotes the accumulation of *Sirt2* mRNA and expression of SIRT2 protein in CG4-OLs. CG4-OL cells were transfected with a pcDNA vector containing *qkI* cDNA (common coding region of *qkI-5, qkI-6 and qkI-7,* see materials and methods) under both growth (GM) and differentiation (DM) conditions. Overexpression of *qkI* increased the accumulation of *Sirt2.1* and *Sirt2.2* mRNA only in GM **(A)** whereas accumulation of all three variants of *Sirt2* transcripts (*Sirt2.1, Sirt2.2 and Sirt2.3*) was increased in DM **(B)**. qPCR data (n=3 biological replicates) was normalized to *β-actin* and represented relative to pcDNA control vector (mean±SEM; two-way ANOVA *$p < 0.05$, **$p < 0.01$, ***$p < 0.001$). Representative immunoblots **(C and E)** and densitometric analysis **(D and F)** shows a corresponding increase in SIRT2.1 and SIRT2.2 protein with the overexpression of *qkI*. SIRT2.3 protein was below the limits of detection. Densitometry data (n=3 biological replicates) were normalized to β-tubulin and represented relative to pcDNA control vector (mean±SEM; two-way ANOVA *$p < 0.05$, **$p < 0.01$).

Furthermore, to examine the regulatory function of QKI in primary OLs, I overexpressed *qkI* in primary OLs isolated from the mouse brain (Chen et al., 2007a; Niu et al., 2012). Overexpression of *qkI* increased the expression of QKI protein in both proliferating (growth media; GM; Fig. 3.5A) and differentiating (differentiation media; DM-day 6; Fig. 3.5B) primary OLs. Expression of *Mbp* mRNA (Fig. 3.5C) and protein (Fig. 3.5D, E) increased with induced differentiation in primary OLs. Similar to CG4-OLs, overexpression of *qkI* in primary OLs increased the accumulation of *Sirt2* mRNA under both proliferating (growth media; GM) (Fig. 3.6A) and differentiating (differentiation media; DM-day 6) conditions (Fig. 3.6B). In proliferating primary OLs, upregulation of *qkI* increased the abundance of *Sirt2.1* and *Sirt2.2* mRNA ~2-fold; while, *Sirt2.3* mRNA abundance was not altered (Fig. 3.6A). In DM, abundance of all three variants increased ~3-fold in differentiating primary OLs (Fig. 3.6B). There was a corresponding increase in SIRT2.1 and SIRT2.2 protein expression under both proliferating (Fig. 3.6C, D) and differentiating (Fig. 3.6E, F) conditions after overexpression of *qkI*. Under these experimental conditions, the expression of SIRT2.3 protein isoform was not detectable either with or without *qkI* overexpression (Fig. 3.4C, E and Fig. 3.6C, E). Thus, *qkI* appears to be a positive regulator of SIRT2 protein expression in developing OLs.

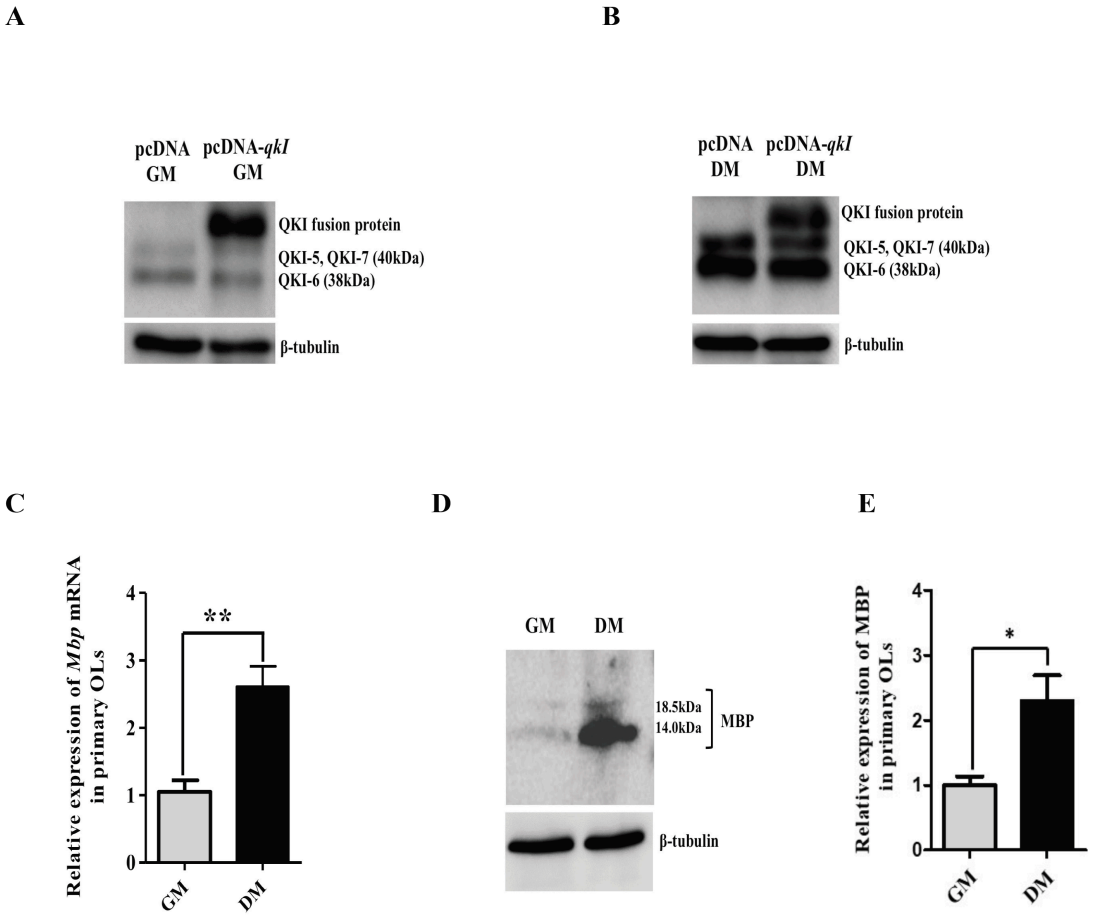

Figure 3.5: Overexpression of *qkI* in primary OLs. (A and B) Primary OLs purified from mixed glial cultures were electroporated with control pcDNA vector or pcDNA-*qkI* vector (containing common coding region of *qkI-5, qkI-6 and qkI-7*) on day 0 and were allowed to proliferate in growth medium (GM) for 48h or differentiate in differentiation medium (DM) for 6 days. Immunoblot analyses show an increase in the QKI protein expression in both GM **(A)** and DM **(B)**. QKI-His fusion protein appeared as homodimer with a molecular mass of 45kDa. *Mbp* mRNA **(C)** and protein **(D)** increased under differentiation conditions. **(C)** qPCR data (n=3) were normalized to *β-actin* and represented relative to day 0 (mean±SEM; unpaired t-test, **$p < 0.01$). **(D)** Representative immunoblot (n=3) showing a corresponding increase in MBP protein expression 6 days after differentiation. **(E)** Densitometric analysis showing the increase in MBP expression during OL differentiation in primary OLs. Data were normalized to β-tubulin and represented relative to day 0 (mean±SEM; two-way ANOVA *$p < 0.05$).

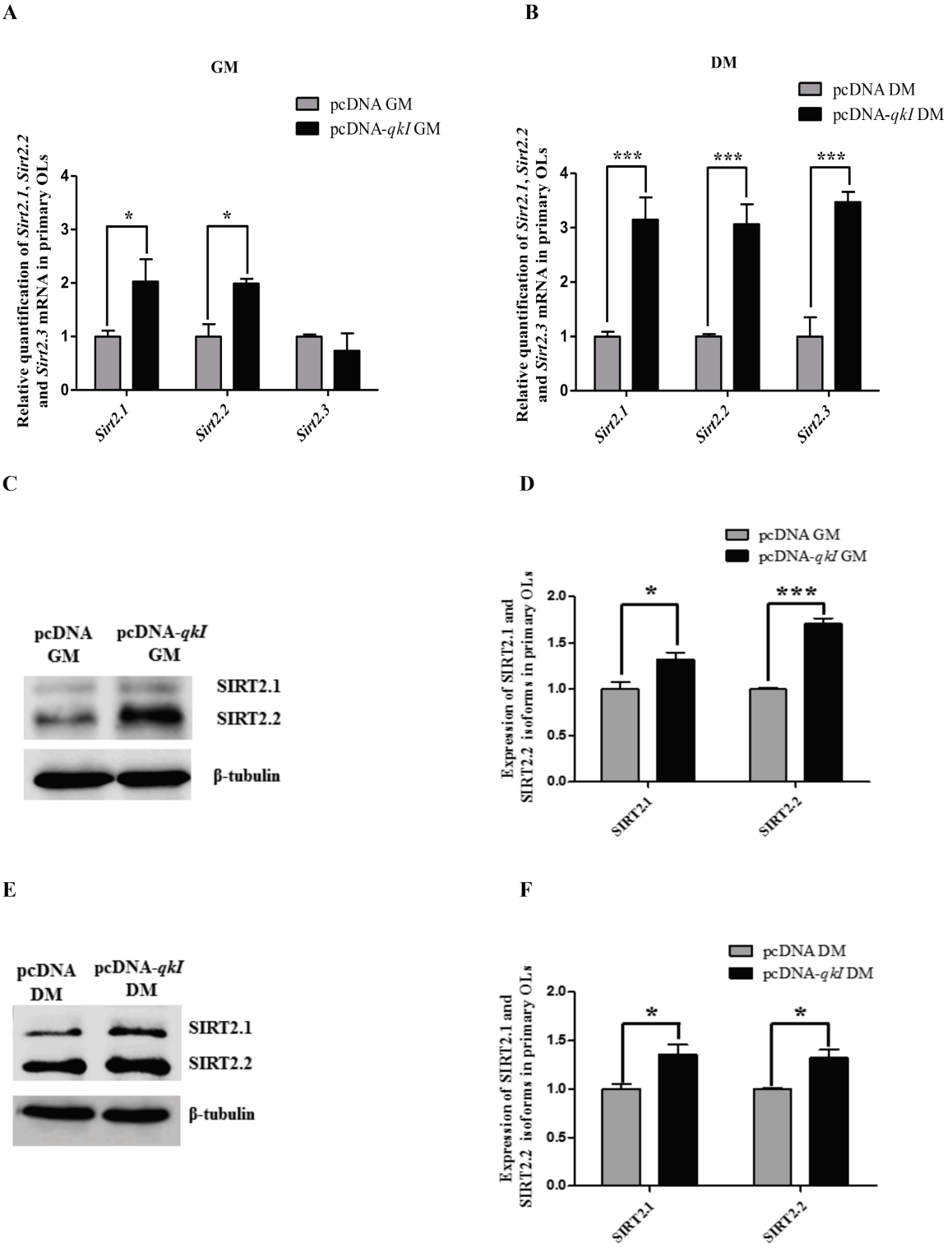
A
GM
pcDNA GM
pcDNA-qkI GM
Relative quantification of Sirt2.1, Sirt2.2 and Sirt2.3 mRNA in primary OLs
Sirt2.1
Sirt2.2
Sirt2.3
B
DM
pcDNA DM
pcDNA-qkI DM
C
pcDNA GM
pcDNA-qkI GM
SIRT2.1
SIRT2.2
β-tubulin
D
Expression of SIRT2.1 and SIRT2.2 isoforms in primary OLs
E
pcDNA DM
pcDNA-qkI DM
F

Figure 3.6: QKI promotes the accumulation of *Sirt2* mRNA and expression of SIRT2 protein in primary OLs. Primary OLs were electroporated with a pcDNA vector containing *qkI* cDNA and cultured under both growth (GM) and differentiation (DM) conditions for 6 days after electroporation. Upregulation of *qkI* increased the accumulation of *Sirt2.1* and *Sirt2.2* mRNA in GM **(A)** while accumulation of all three variants of *Sirt2* transcripts (*Sirt2.1, Sirt2.2 and Sirt2.3*) was increased in DM **(B)**. qPCR data (n=3 biological replicates) was normalized to *β-actin* and represented relative to pcDNA control vector (mean±SEM; two-way ANOVA, *$p < 0.05$, ***$p < 0.001$). Representative immunoblots **(C and E)** and densitometric analysis **(D and F)** shows a corresponding increase in SIRT2.1 and SIRT2.2 protein with the overexpression of *qkI*. SIRT2.3 protein was below the limits of detection. Densitometry data (n=3 biological replicates) were normalized to β-tubulin and represented relative to pcDNA control vector (mean±SEM; two-way ANOVA, *$p < 0.05$, ***$p < 0.01$).

3.4.3 Presence of putative QREs in *Sirt2* transcripts

Using *in silico* analysis, I identified the presence of two putative QREs in *Sirt2* mRNA at the 3′ UTR (Fig. 3.7A). Both putative QREs, AUUAA(C/U) at 1639-1643bp (denoted as QRE-1) and ACUAA(C/U) at 1853-1858bp (denoted as QRE-2) (Fig. 3.7A) in the *Sirt2* mRNA, correspond to the predicted consensus sequences (Wu et al., 2002; Galarneau and Richard, 2005) and are highly conserved (Fig. 3.7A). Thus, 3′ UTR of *Sirt2* mRNA has two putative interaction sites for QKI.

3.4.4 QKI binds to *Sirt2* mRNA to regulate its expression

To determine if QKI directly binds to *Sirt2* mRNA at the putative binding sites, RNA co-immunoprecipitation (RNA co-IP) was carried out using whole cell lysates from CG4-OL under both growth (GM) and differentiating (DM-day 6) conditions. QKI was found to bind *Sirt2* mRNA in both proliferating and differentiating CG4-OLs (Fig. 3.7B, C). In both GM and DM, QKI did not bind with *Gapdh* mRNA (Fig. 3.7B, bottom panel). Further investigation determined that QKI bound to all the three variants of *Sirt2* in differentiating CG4-OLs (Fig. 3.7E), but only bound *Sirt2.1* and *Sirt2.2* in proliferating CG4-OLs (Fig. 3.7D). In addition, interaction of QKI and *Sirt2* mRNA in primary OLs was also examined. QKI was found to interact with *Sirt2* mRNA in both proliferating and differentiating primary OLs (Fig. 3.8A). In proliferating primary OLs, QKI bound only to *Sirt2.1* and *Sirt2.2* mRNA (Fig. 3.8B), while in differentiating primary OLs, QKI bound to all the three variants of *Sirt2* (Fig. 3.8C). Collectively, these data demonstrate that QKI interacts directly with all three variants of *Sirt2* mRNA, presumably via the putative QRE-1 and/or QRE-2 in the 3′ UTR.

A

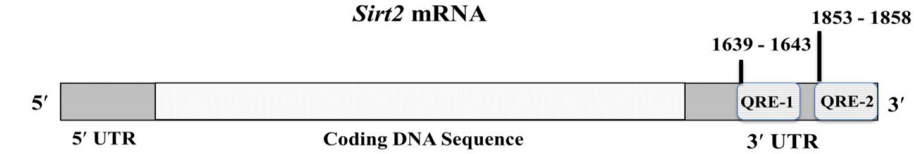

QRE-1

Mouse *Sirt2* 3′UTR	GGCUAAAUCAA--**AUUAAC**CUACCCC-GCAUAGGGGCUGGACUCUACAAAUAGAA	1679
Rat *Sirt2* 3′UTR	AGCUAAAUCAA--**GUUAAU**CUACCCU-GCAUAGGGGCUGGACCCUCCAAAUAUAA	1885
Human *Sirt2* 3′UTR	UAAGUAAACCAUA**CCUAAC**CUACCCCAGUGUGGGUG-UGGGC-CUCUGAAUAUAA	1902

QRE-2

Mouse *Sirt2* 3′UTR	CCUUGCUUAUUAGAAACAAAUUAAAAAACAAAACAAAGCA**ACUAAC**CAUG	1863
Rat *Sirt2* 3′UTR	GCAAGUUGAUUAGAAACAAAUUAAAACUCAGAACAAAGCA**ACUAAA**AAAAAAAAAAAAAA	2059
Human *Sirt2* 3′UTR	CAUUGCUUAUUGGAGACAAAUUAAAAA-----CAAAAACA**ACUAAC**AAUCCGGAAAAAAA	2079

B

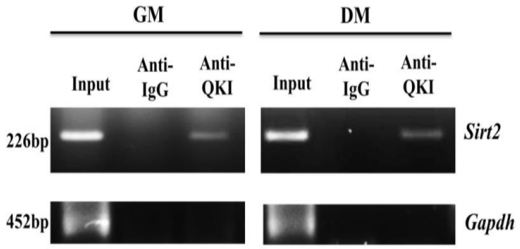

C

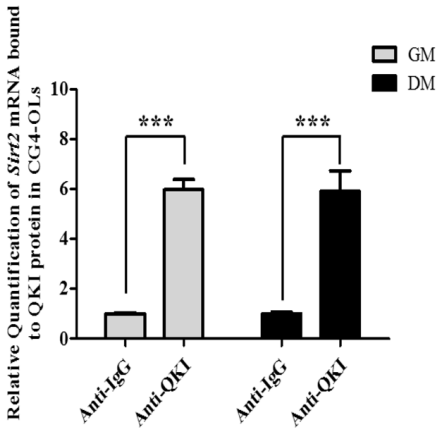

D

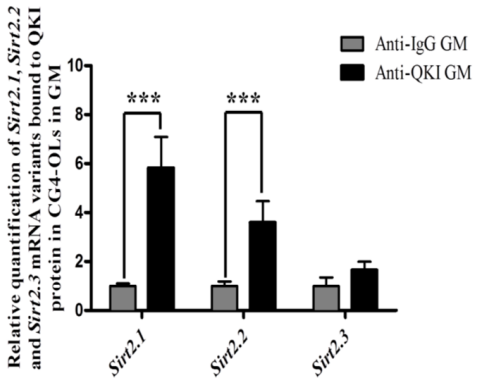

E

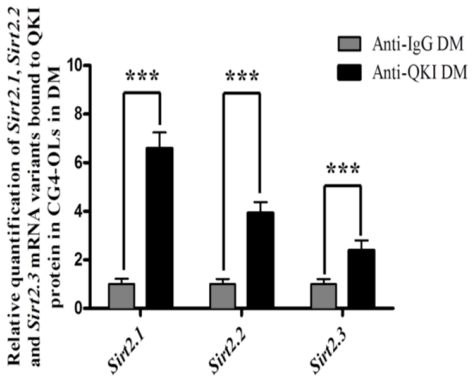

Figure 3.7: Putative binding sites of QKI protein in the *Sirt2* mRNA. (A) Schematic diagram and sequence alignment showing the positions of predicted QKI response elements (QRE), denoted as QRE-1 at 1639-1643bp and QRE-2 at 1853-1858bp, in the 3' UTR of mouse *Sirt2* mRNA. Sequence alignment of the mouse, rat and human *Sirt2* mRNA 3' UTR reveals highly conserved residues for both the QRE-1 and QRE-2 regions (black boxes). **(B and C)** RNA co-immunoprecipitation with anti-QKI antibody using the whole cell lysate from CG4-OL cells show binding of QKI to *Sirt2* mRNA under both growth (GM) and differentiation (DM) conditions. **(B)** RT-PCR products of *Sirt2* and *Gapdh* were detected in a RedSafe stained agarose gel; lanes are as indicated. **(C)** qPCR data (n=3 biological replicates) was normalized to *β-actin* in the input and represented relative to control IgG (mean±SEM; two-way ANOVA ***$p < 0.001$). **(D and E)** QKI binds to *Sirt2.1* mRNA and *Sirt2.2* mRNA under both growth (GM) **(D)** and differentiation (DM) **(E)** conditions whereas binding of QKI to *Sirt2.3* mRNA was only observed under differentiation (DM) conditions in CG4-OLs **(D)**. qPCR data (n=3 biological replicates) were normalized to *β-actin* and represented relative to control IgG (mean±SEM; two-way ANOVA ***$p < 0.001$).

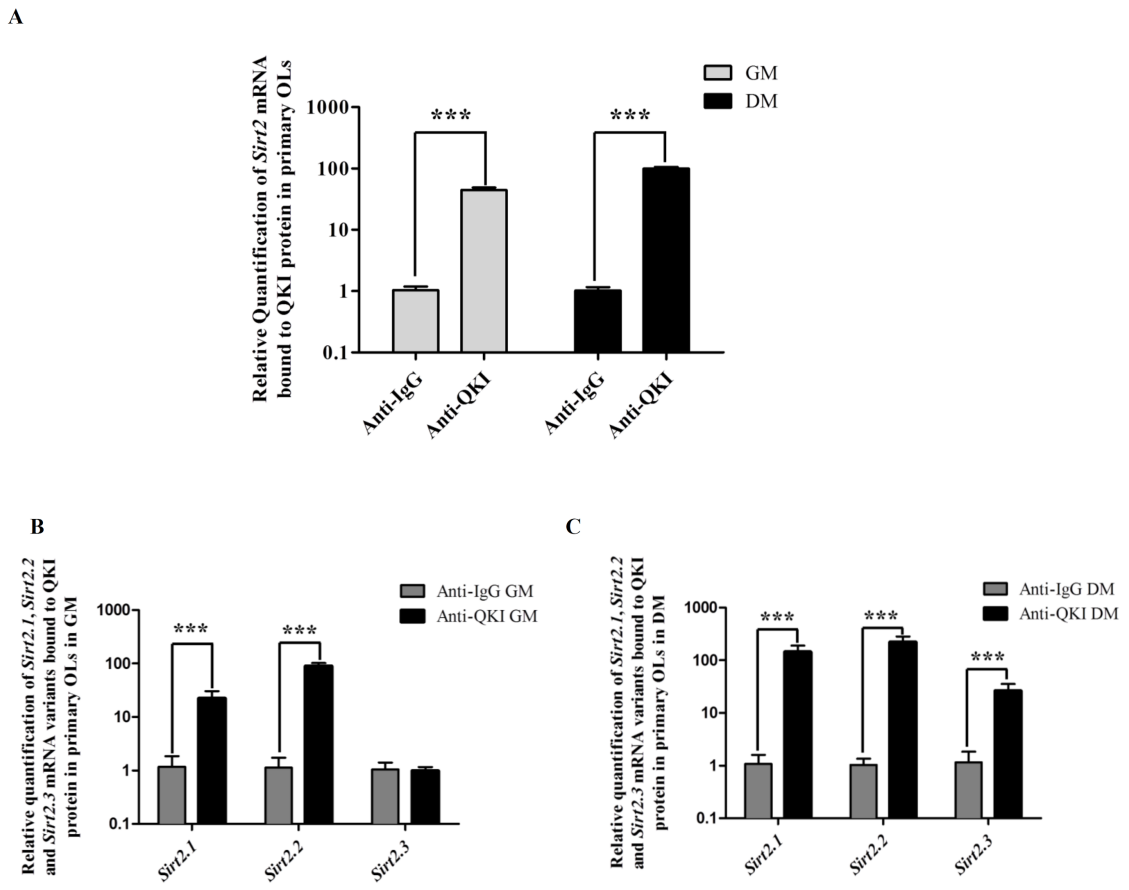

Figure 3.8: QKI interacts with *Sirt2* mRNA in primary OLs. (A) RNA co-immunoprecipitation with anti-QKI antibody using the whole cell lysate from primary OLs shows binding of QKI to *Sirt2* mRNA under both growth (GM) and differentiation (DM) conditions. qPCR data (n=3 biological replicates) was normalized to *β-actin* in the input and represented relative to control IgG (mean±SEM; two-way ANOVA ***$p < 0.001$). **(B and C)** In GM, QKI was bound only to *Sirt2.1* mRNA and *Sirt2.2* mRNA. **(C)** In DM, QKI was bound to all the three variants of *Sirt2* mRNA. qPCR data (n=3 biological replicates) were normalized to *β-actin* and represented relative to control IgG (mean±SEM; two-way ANOVA, ***$p < 0.001$).

3.4.5 QKI binds to 3′ UTR of *Sirt2* mRNA and regulates its expression

To identify the critical QRE site(s) involved in QKI-*Sirt2* interaction, RNA co-IP and luciferase reporter assay systems were used. The *Sirt2* 3′ UTR with wild-type or mutated QREs was cloned downstream to the firefly luciferase and transfected along with pcDNA-QKI. The QRE mutations were as follows (Fig. 3.9A): (i) *Sirt2* 3′ UTR-Mut1 for QRE-1 at 1639bp (AUUAAC→UCGACC) (Fig. 3.9A, B), (ii) *Sirt2* 3′ UTR-Mut2 for QRE-2 at 1853bp (ACUAAC→UCGAGC) (Fig. 3.9A, C), and (iii) *Sirt2* 3′ UTR-Mut1*Mut2 for combined QRE-1 and QRE-2 mutations (Fig. 3.9A, D). RNA co-IP was performed with wild-type or mutated putative QREs of the *Sirt2* 3′ UTR transfected in HEK293T cells with or without *qkI*. RNA co-IP revealed that QKI binds to wild-type and mutated QRE-1 (*Sirt2* 3′ UTR-Mut1) of *Sirt2* mRNA. Mutation of QRE-2 alone (*Sirt2* 3′ UTR-Mut2) or in combination (*Sirt2* 3′ UTR-Mut1*Mut2) prevented the binding (Fig. 3.10A). Luciferase reporter assay was also carried out using wild-type or mutated QREs of the *Sirt2* 3′ UTR cloned downstream to the firefly luciferase, cotransfected in CG4-OL cells together with *qkI*. Overexpression of *qkI* resulted in an increased luciferase activity of *Sirt2* 3′ UTR (Fig. 3.10B). Mutation of QRE-1 (*Sirt2* 3′ UTR-Mut1) also resulted in increased luciferase activity indicating QKI was still able to interact with *Sirt2* 3′ UTR despite the mutation to QRE-1. In contrast, mutation of QRE-2 either alone (*Sirt2* 3′ UTR-Mut2) or double with QRE-1/QRE-2 mutation (*Sirt2* 3′ UTR-Mut1*Mut2) failed to increase the luciferase activity. These results indicate that the nucleotides in QRE-2 (1853-1858bp) are critical for the functional interaction between QKI and *Sirt2*. Thus, QKI binding to *Sirt2* 3′ UTR in the QRE ACUAAC (1853-1858bp) appears to be important for regulating the expression of *Sirt2* during OL development.

A

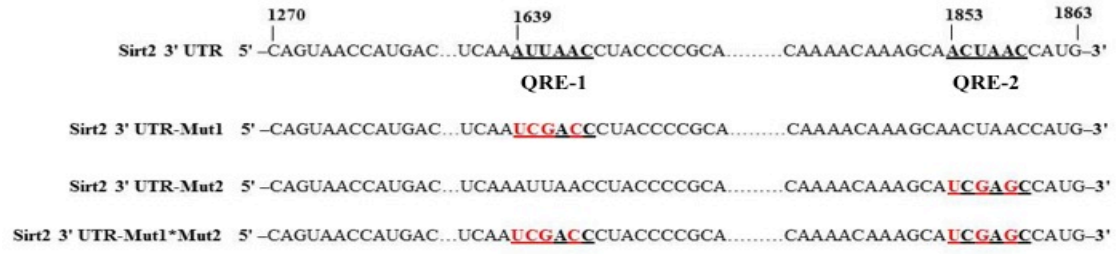

B **QRE-1 at 1639 bp (*Sirt2* 3' UTR-Mut1)**

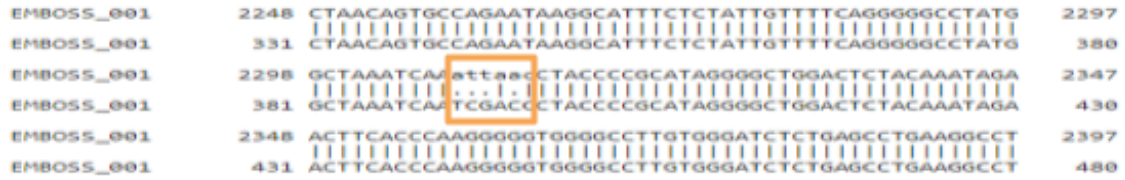

C **QRE-2 at 1853 bp (*Sirt2* 3' UTR-Mut2)**

D **QRE-1*QRE-2 at 1639 bp and 1853 bp (*Sirt2* 3' UTR-Mut1*Mut2)**

Figure 3.9: Site directed mutagenesis of QREs in the 3' UTR of *Sirt2* mRNA. (A) A 593 bp fragment of the *Sirt2* 3' UTR containing putative QKI binding sites was amplified and cloned into pGL3-promoter vector. Site directed mutagenesis of the putative QKI response elements, QRE-1 at 1639 bp (*Sirt2* 3' UTR-Mut1), QRE-2 at 1853 bp (*Sirt2* 3' UTR-Mut2) and both QREs at 1639 bp and 1853 bp (*Sirt2* 3' UTR-Mut1*Mut2) were carried out using QuikChange Lightning kit. The underlined and bold sequences represent putative QREs and the mutated sequences are represented in red. **(B, C and D)** Analysis of sequences using EMBOSS Needle alignment (http://www.ebi.ac.uk/Tools/psa/emboss_needle/nucleotide.html) shows the mutated QREs within the orange box.

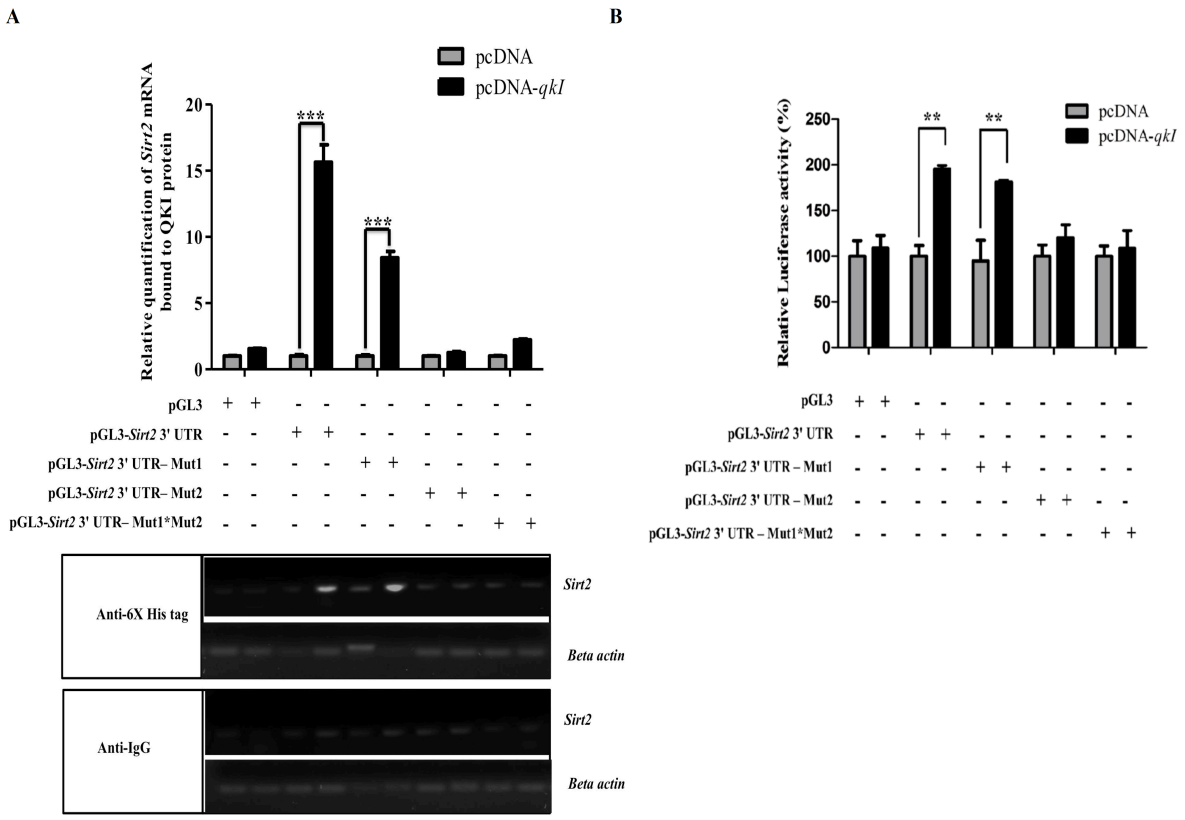

Figure 3.10: QKI interacts with *Sirt2* via the QRE (ACUAAC) at 1853bp in the 3' UTR. (A) HEK293T cells were co-transfected with pcDNA or pcDNA-*qkI* along with pGL3 vector harboring wild-type or mutated QREs in the *Sirt2* 3' UTR, as indicated. RNA co-immunoprecipitation with His tag antibody in these cell extracts reveals high affinity binding of QKI to wild-type or mutated QRE-1 of *Sirt2* 3' UTR but not to QRE-2. qPCR data (top panel) (n=3 biological replicates) was normalized to *β-actin* and represented relative to pcDNA control vector (mean±SEM; two-way ANOVA ***$p < 0.001$). RT-PCR products (bottom panel) were detected in a RedSafe stained agarose gel; lanes are as indicated. **(B)** For luciferase reporter assay, CG4-OL cells were co-transfected with pcDNA or pcDNA-*qkI* (common coding region of *qkI-5, qkI-6 and qkI-7*) along with pGL3 luciferase vector containing wild-type or mutated QREs in the *Sirt2* 3' UTR. Overexpression of *qkI* increased luciferase reporter activity of *Sirt2* 3' UTR and *Sirt2* 3' UTR-Mut1 but not of *Sirt2* 3' UTR-Mut2 or *Sirt2* 3' UTR-Mut1*Mut2. This indicates that QRE-2 at 1853bp is critical for the interaction of QKI with *Sirt2*. Relative luciferase activity (n=4 biological replicates) was normalized to pcDNA control vector co-transfected with pGL3 luciferase vector and represented as percent activity (mean ± SEM; two-way ANOVA, **$p < 0.01$).

3.4.6 QKI stabilizes and protects *Sirt2* mRNA from degradation

QKI regulates myelin gene expression during development, in part by modulating the stability of myelin gene transcripts. To determine if QKI stabilizes *Sirt2* mRNA, a standard mRNA stability assay (Larocque et al., 2005; Doukhanine et al., 2010; Zhao et al., 2006) was used to assess the ability of QKI to protect *Sirt2* transcripts from degradation. Following transfection with pcDNA or pcDNA-*qkI* (48h), actinomycin D was used to inhibit transcription in CG4-OLs under growth conditions (GM) and subsequent degradation of *Sirt2* mRNA was monitored using qPCR. QKI was found to regulate the stability of *Sirt2.1* and *Sirt2.2* variants (Fig. 3.11A, B, D). Overexpression of *qkI* delayed the degradation of *Sirt2.1* (Fig. 3.11A) and *Sirt2.2* (Fig. 3.11B), but not *Sirt2.3* (Fig. 3.11C). The half-life ($t_{1/2}$) of each of the *Sirt2* variants were calculated (Baudouin-Legros et al., 2005) by measuring the reduction in the mRNA levels to 50% from their respective initial mRNA level. *Sirt2.1*, *Sirt2.2* and *Sirt2.3* mRNA $t_{1/2}$ were determined to be 38.6, 23.8, and 61.5 min in CG4-OLs transfected with blank control vector (Fig. 3.11A, B, C) and 78.1, 68.3 and 51.7 min in CG4-OL cells transfected with *qkI*, respectively. Hence, there was ~2 fold and ~2.8 fold increase in $t_{1/2}$'s of *Sirt2.1* and *Sirt2.2* transcripts with *qkI* overexpression, but little difference in the $t_{1/2}$ of *Sirt2.3* mRNA. *Sirt2.2* appears to be the primary functional target of QKI, as >85% of the mRNA transcripts remain protected 30 min after transcription is blocked in CG4-OL cells transfected with *qkI* (Fig. 3.11B) compared to <40% of mRNA transcripts remaining in cells transfected with control vector. Our finding suggests that binding of QKI to *Sirt2.1* and *Sirt 2.2* mRNA increases their stabilization and, in turn, may promote SIRT2.1 and SIRT2.2 protein expression during OL development.

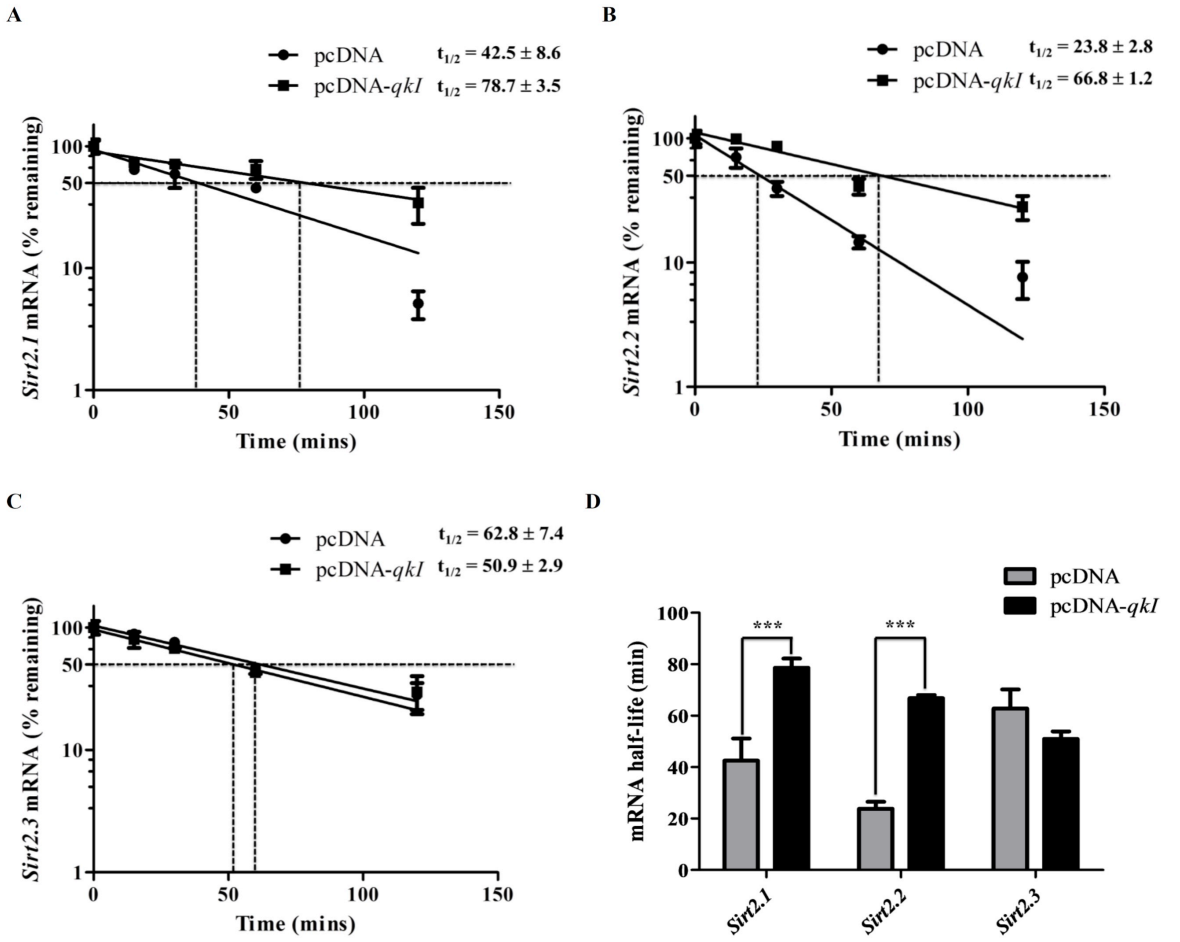

Figure 3.11: QKI stabilizes and protects *Sirt2.1* and *Sirt2.2* mRNA. (A-C) The degradation of *Sirt2* mRNA was monitored in CG4-OL cells transfected with pcDNA and pcDNA-*qkI* in growth conditions. After 48h following transfection, transcription was blocked with actinomycin D and mRNA levels of all the three *Sirt2* variants were determined by qPCR at the indicated time points (0, 15, 30, 60 and 120 min). Overexpression of *qkI* significantly increased the quantity of *Sirt2.2* mRNA remaining at 15 to 120 min after actinomycin D treatment **(B)** and that of *Sirt2.1* mRNA remaining at 120 min after actinomycin D treatment **(A)**. The stability of *Sirt2.3* mRNA was not impacted **(C)**. **(A-C)** qPCR data (n=3 biological replicates) were normalized to *18s rRNA* and are represented as percentage of the *Sirt2* mRNA variant levels measured at time 0 min. (mean±SEM; one phase decay). The half-lives were calculated as the time necessary for each *Sirt2* mRNA variant to reduce to 50% of its initial amount at time 0 min (dashed lines). **(D)** Half-lives of *Sirt2.1*, *Sirt2.2* and *Sirt2.3* mRNA are represented in minutes. (mean±SEM; two-way ANOVA, *p < 0.05, **p < 0.01, ***p < 0.001).

3.5 Discussion

In myelinating OLs, SIRT2 is predominately cytoplasmic, localizing to the paranodal loops (Li et al., 2007a; Werner et al., 2007; Southwood et al., 2007), and is a key regulator of OL development *in vitro* (Ji et al., 2011). As a NAD^+-dependent deactylase, it has a multitude of cellular targets involved in gene transcription (Vaquero et al., 2006; Michan and Sinclair, 2007), proliferation (North and Verdin, 2007b; Vaquero et al., 2006; Inoue et al., 2007; Dryden et al., 2003), cell polarity (Beirowski et al., 2011) and cytoskeletal remodeling (North et al., 2003, Li et al., 2007a, Southwood et al., 2007). We have previously shown that the expression of *Sirt2* drives OL differentiation at the cellular level by enhancing process outgrowth and arborization (Ji et al., 2011), presumably via tubulin deacetylation (North et al., 2003). QKI facilitates proper CNS myelination via post-transcriptional regulation of several transcripts during OL development (Chen et al., 2007b; Larocque et al., 2002; Wu et al., 2002; Li et al., 2000; Zhao et al., 2006a; Zhao et al., 2010; Larocque et al., 2005; Doukhanine et al., 2010; Zhao et al., 2006b; Zearfoss et al., 2011). Interestingly, in qk^v/qk^v mutant mice, there is reduced protein expression of SIRT2, while the expression of *Sirt2* mRNA is not altered in the brain tissue (Zhu et al., 2012; Werner et al., 2007). In addition, it has been reported that QKI indirectly controls the expression of SIRT2 during myelination through co-transport with PLP to the myelin sheath (Zhu et al., 2012; Werner et al., 2007). Although the transport of SIRT2 protein into the myelin sheath is dependent on PLP (Zhu et al., 2012; Werner et al., 2007), the developmental expression of *Sirt2* mRNA and protein is most likely regulated by an alternate mechanism(s) since *Sirt2* is expressed prior to myelin structural proteins both *in vitro* (Zhu et al., 2012; Ji et al., 2011) and *in vivo* (Zhu et al., 2012; Werner et al., 2007; Li et al., 2007a, Southwood et al., 2007). The present study

deciphers the precise molecular interactions governing the expression of *qkI* and *Sirt2* during OL differentiation.

In this study, I found that during OL differentiation, there is coordinated expression of *qkI* and *Sirt2* (Fig. 3.1 and Fig. 3.2) and overexpression of *qkI* increased the expression of SIRT2 (Fig. 3.4 and Fig. 3.6) raising the possibility that QKI may directly modulate *Sirt2* mRNA expression. *In silico* analysis revealed two putative quaking response elements, QRE-1 (AUUAAC) at 1639 bp and QRE-2 (ACUAAC) at 1853 bp in the 3′ UTR of *Sirt2* (Fig. 3.7A), that conform to the predicted core binding sequence ACUAAY (Galarneau and Richard, 2005) or its variant AUUAAY (Wu et al., 2002). A direct interaction of QKI with *Sirt2* transcripts was confirmed by RNA co-IP (Fig. 3.7B, C and Fig. 3.8A). Binding of QKI to *Sirt2* mRNA was observed in both proliferating OLs and differentiating OLs, suggesting that the interaction between QKI and *Sirt2* mRNA is most critical throughout OL development (Fig. 3.7B, C and Fig. 3.8A). Moreover, expression of *Sirt2* drives differentiation at the molecular level by enhancing the expression of MBP (Ji et al., 2011). Thus, the interaction of QKI with *Sirt2* mRNA may be critical in OL differentiation prior to the onset of myelination. Further analysis revealed that the QRE sequence ACUAAC at 1853-1858 bp was essential for the binding of QKI to *Sirt2* mRNA (Fig. 3.10A, B). This reflected the predicted sequence for high affinity binding (Galarneau and Richard, 2005) and was highly conserved across the mammalian *Sirt2* transcripts (Fig. 3.7A). The ability of QKI to bind *Sirt2* mRNA indicates that QKI controls SIRT2 protein expression during OL development through a direct interaction with *Sirt2* transcripts.

A reduction in myelin specific gene transcripts in qk^v/qk^v mice has been shown to be due to post-transcriptional regulation by QKI as transcription rates are not altered (Li et al., 2000). QKI has been implicated in regulating the stability (Larocque et al., 2005; Doukhanine et al.,

2010; Zhao et al., 2006b), splicing (Wu et al., 2002, Zhao et al., 2010), transport (Larocque et al., 2002; Li et al., 2000) and translation (Roth et al., 1985; Sorg et al., 1986) of mRNAs in developing OLs. Though QKI was found to bind all three variants of *Sirt2* (Fig. 3.7D, E and Fig 3.8B, C), my data shows QKI primarily modulates the post-transcriptional stability of the *Sirt2.1* and *Sirt2.2* mRNA (Fig. 3.11A, B) and protects *Sirt2.1 and Sirt2.2* mRNA from degradation (Fig. 3.11). Thus, in addition to regulating major myelin transcripts such as *Mbp* and *Plp,* QKI also controls the stability of *Sirt2* during OL development.

My findings demonstrate that QKI was able to, in some capacity, promote the expression of all three *Sirt2* variants; however, the functional interaction between QKI and *Sirt2.2* appears to be important for proper OL development. Indeed, SIRT2.2 is the most abundant isoform in OLs *in vitro* (Fig. 3.2) and *in vivo* (Zhu et al., 2012), and the main isoform incorporated into the myelin sheath (Werner et al., 2007). While there is efficient binding of QKI to both *Sirt2.1* and *Sirt2.2* transcripts, the interaction between QKI and *Sirt2.2* mRNA is associated with greater stabilization of this transcript (Fig. 3.11B). As all QKI isoforms share a common RNA binding domain (Ebersole et al., 1996) and the *Sirt2* QRE is located in the common 3' UTR, it is still unclear how preferential binding and protection with *Sirt2.2* is achieved. As *Sirt2.2* is the most abundant transcript, possibly due to preferential usage of transcriptional start site (Maxwell et al., 2011) and/or alternative splicing, this increased availability could be the reason for a more prominent functional interaction with QKI. These data, along with an increase in the endogenous expression of both *Sirt2.2* mRNA and protein at early stages of differentiation (Fig. 3.2), are indicative that the regulation of *Sirt2.2* by direct interaction with QKI is critical for proper OL development.

The QUA1 domain in the QKI protein promotes homodimerization, which promotes the ability of QKI to bind to target RNA (Beuck et al., 2012). Overexpression of the common coding region promoted homodimerization of the QKI protein in both CG4-OLs and primary OLs. Interestingly, upregulation of *qkI* increased the accumulation of *Sirt2* mRNA (Fig. 3.4A, B and Fig. 3.6A, B) and expression of SIRT2 protein (Fig. 3.4C-F and Fig 3.6C-F). Moreover, observations using primary OLs further provide evidence of physiological interaction of QKI and *Sirt2* mRNA during OL development *in vivo*. Although a similar interaction was observed in both CG4-OL cell line and primary OLs, the binding affinity was ~10 fold higher in primary OLs (Fig. 3.8). Higher expression levels of QKI isoforms in primary OLs (Fig. 3.5A, B) could serve to increase the interaction. All QKI isoforms contain identical RNA binding and dimerization (QUA1-KH-QUA2) domains (Ebersole et al., 1996; Kondo et al., 1999), and therefore have the ability to bind and stabilize *Sirt2* transcripts. Higher expression levels of QKI isoforms at later stages (i.e. pre-myelinating and myelinating OLs) would stabilize mRNA increasing the number of copies available for translation and promoting the expression of SIRT2 protein. This would serve to tightly control SIRT2 expression during OL differentiation (Fig. 3.12). Further complexity is added by the potential that dimerization (Chen and Richard, 1998; Beuck et al., 2012) and the phosphorylation state (Zhang et al., 2003) of the different QKI isoforms may regulate their activity at various stages of OL development.

Conclusively, the data in this chapter has demonstrated that QKI directly regulates SIRT2 expression in the OLs by binding to the *Sirt2* mRNA at 3′ UTR via a QRE (ACUAAC) at 1853bp. During OL differentiation, QKI increases the stability of *Sirt2* transcripts and the amount of transcript available for translation. This may be particularly important for dictating the timing of SIRT2 protein, as its expression is regulated early in differentiation and can promote

the downstream expression of other myelin proteins (Ji et al., 2011). The expression of QKI isoforms would control the availability of target mRNAs for translation and allow OLs to synchronize the timing of myelin protein expression during development. My finding on the interaction between two key regulators *qkI* and *Sirt2*, during oligodendroglial differentiation sheds further light into this vital aspect of OL development and myelination.

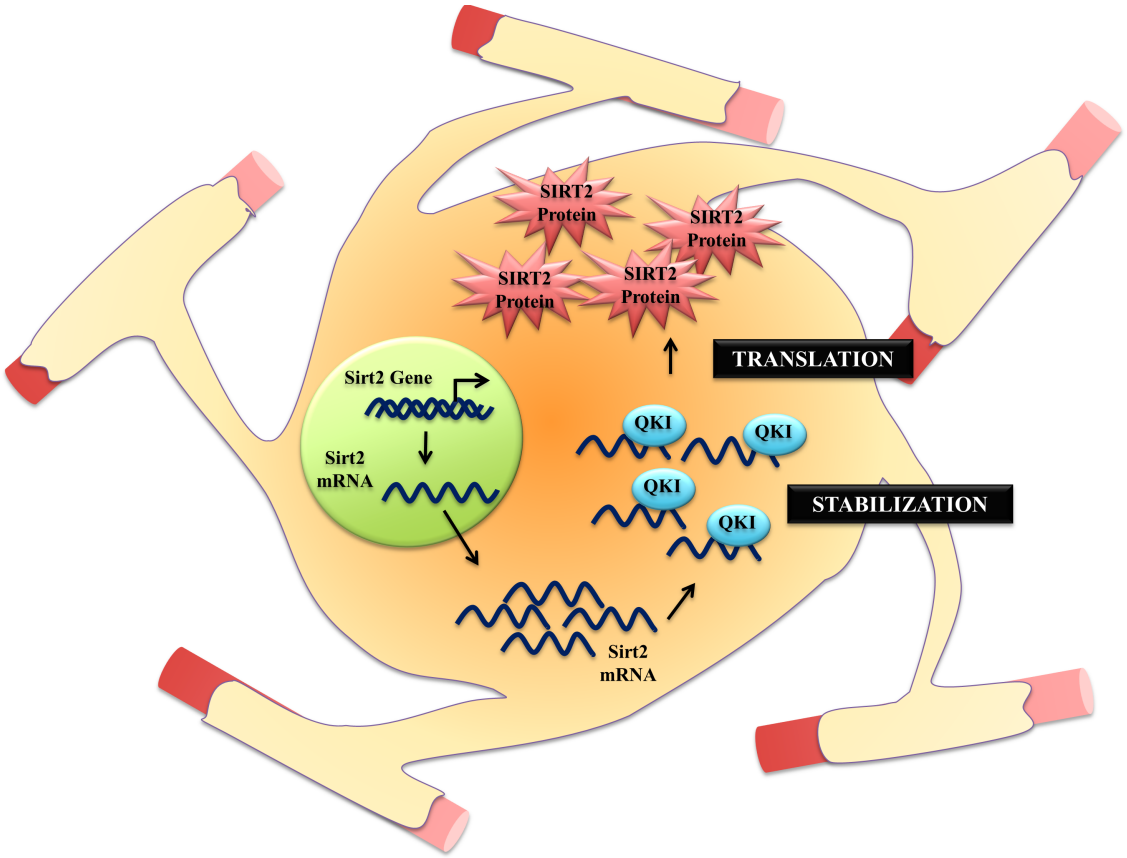

Figure 3.12: Schematic diagram illustrating the interaction of QKI and *Sirt2* in OL development. When the OPCs start to differentiate into post-mitotic OL, there is increased expression of QKI isoforms. Interaction between QKI and *Sirt2* stabilizes the mRNA and promotes the translation of SIRT2 protein facilitating differentiation. This would allow OL cells to accumulate sufficient copies of mRNA but tightly regulate their availability for translation. Thus, an interaction between QKI and *Sirt2* would serve to regulate the timing of OL differentiation for proper CNS myelination.

Preamble to Chapter 4: LOSS OF SIRT2 IMPAIRS MYELINATION AND INCREASES DISEASE SUSCEPTIBILITY IN EXPERIMENTAL AUTOIMMUNE ENCEPHALOMYELITIS (EAE) MOUSE MODEL OF MULTIPLE SCLEROSIS

Rationale: In the previous chapter, I demonstrated the molecular regulation of SIRT2 expression by QKI during OL differentiation. In this chapter, I explored the functional requirement of *Sirt2* during myelination and in MS. Myelinating ability of OLs is crucial for proper development of the CNS and the repair of lesions in MS, making it imperative we learn more about what controls this aspect of their function. In the mammalian CNS, *Sirt2* is primarily expressed in OLs and is a major component of the myelin proteome. However, the role of *Sirt2* in CNS myelination and MS is largely unknown. Here, I have examined the impact of loss of *Sirt2* in myelination and on the disease severity of experimental autoimmune encephalomyelitis (EAE), an animal model of MS using *Sirt2* knockout ($Sirt2^{-/-}$) mice.

Contribution statement

I designed the study, performed experiments and analyzed the data in this chapter. Adil J. Nazarali and J. Ronald Doucette conceived and coordinated the study. Kendra L. Furber and Paul P. R. Iyyanar helped with blinded clinical scoring in EAE study. Glaiza A. Tan helped with tissue sectioning. Bogdan F. Popescu provided human MS brain samples and assisted in histology of paraffin embedded brain tissue. This manuscript is in preparation.

4. LOSS OF SIRT2 IMPAIRS MYELINATION AND INCREASES DISEASE SUSCEPTIBILITY IN EXPERIMENTAL AUTOIMMUNE ENCEPHALOMYELITIS (EAE) MOUSE MODEL OF MULTIPLE SCLEROSIS

4.1 Summary

The myelinating ability of OLs is crucial for proper development of the CNS and efficient repair of lesions in MS. The cellular and molecular mechanisms that control the myelinating ability of OLs remain elusive. SIRT2 is a NAD^+-dependent deacetylase, predominantly expressed in OLs. SIRT2 is upregulated during active myelination and is incorporated into the myelin proteome. However, the role of SIRT2 in myelination and MS is largely unknown. In this study, I hypothesized that *Sirt2* positively regulates CNS myelination and loss of *Sirt2* increases the disease severity of EAE, an animal model of MS. Ultra-structural analyses reveal that the number of myelinated axons is decreased in *Sirt2*$^{-/-}$ mice compared to age-matched wild-type mice. In addition, the expression of myelin structural genes such as *Mbp, Plp* and *Dm20* was decreased in *Sirt2*$^{-/-}$ mice. Deletion of *Sirt2* impairs OL proliferation and differentiation. Loss of *Sirt2* results in increased severity in EAE mouse model in *Sirt2*$^{-/-}$ mice compared to wild-type mice. Furthermore, immunostaining of human MS postmortem brain sections revealed that SIRT2 was absent in MS lesions and its expression reappears in the 'shadow plaques' indicating that it may have an important functional role during remyelination. Taken together, these findings suggest that SIRT2 has a critical role in the myelination of CNS axons and a protective role in the EAE mouse model of MS.

4.2 Introduction

OLs are the glial cells responsible for the formation of myelin sheath in the CNS. OLs originate from OPCs in the VZ/SVZ, migrate and eventually differentiate into myelinating OLs (Baumann and Pham-Dinh 2001; Bergles and Richardson 2015). Myelinating OLs expand their cytoplasmic processes around axons ultimately leading to formation of a multilayered compact myelin sheath (Quarles et al., 2006). Myelination is essential for fast and efficient conduction of action potentials. Impairment of OLs or myelin sheath makes the axons more susceptible to degeneration leading to chronic demyelinating disease such as MS (Hanafy and Sloane, 2011; Miron et al., 2011; Kotter et al., 2011). MS causes neurological disability in adults between 20 to 50 years of age in North America and Europe with a prevalence of 140 and 108 in 100,000, respectively (Multiple Sclerosis International Federation, 2013). Canada has one of the highest incidences of MS in the world (World Health Organization, 2008). Understanding the cellular and molecular mechanisms regulating differentiation of OPCs into myelinating OLs to promote myelination and myelin repair in the CNS is crucial for treatment interventions.

Recently, the sirtuin (SIRTs) family of deacetylases has gained considerable attention for their impact on the regulation of myelination and axonal degeneration (Li et al., 2007a; Suzuki and Koike, 2007). SIRTs are class III NAD^+-dependent protein deacetylases evolutionarily conserved from bacteria to mammals (Brachmann et al., 1995; Frye, 2000; North, et al., 2003). In mammals, seven sirtuins have been identified (SIRT1 to 7) with a conserved 275-amino-acid catalytic core domain (Blander and Guarente, 2004; Frye, 2000). Among them, SIRT2 is predominantly expressed in the cytoplasm of OLs (North et al., 2003). *Sirt2* is reportedly detected throughout the OL lineage, with higher abundance in mature OLs (Werner et al., 2007).

Previously our group has demonstrated that SIRT2 is essential for the process formation and maturation of OLs *in vitro* (Ji et al., 2011).

Expression of SIRT2 increases during the peak period of myelination in the CNS (Southwood et al., 2007) as well as in the PNS (Beirowski et al., 2011). Interestingly, the expression profile of SIRT2 is similar to the expression of myelin markers such as MBP and MPZ in CNS and PNS, respectively (Ji et al., 2011; Beirowski et al., 2011). In addition, studies on myelin proteome revealed that the isoform SIRT2.2 integrates into myelin sheath (Werner et al., 2007) in close proximity to PLP and is localized in paranodal loops (Li et al., 2007a; Southwood et al., 2007). In PNS, knockout of *Sirt2* in Schwann cells resulted in delayed myelin formation with extensive outfoldings in the compact myelin near paranodes (Beirowski et al., 2011). In Schwann cells, SIRT2 deacetylates the master regulator of cell polarity Par-3, decreasing the activity of atypical protein kinase C and thereby regulating myelin formation (Beirowski et al., 2011). However, the role of SIRT2 in CNS myelination and MS has not been investigated.

In an effort to understand the role of *Sirt2* in CNS myelination, I utilized *Sirt2* null (*Sirt2*$^{-/-}$) mice to determine the impact of the loss of function of *Sirt2* on myelin ultrastructure, myelin specific gene expression, OL proliferation and differentiation. Furthermore, to investigate the role of *Sirt2* in the pathogenesis of MS, experimental autoimmune encephalomyelitis (EAE), an established animal model of MS, was induced in *Sirt2*$^{-/-}$ and wild-type mice using MOG_{35-55} peptide. My findings reveal that *Sirt2* plays a critical role in the myelination of axons in CNS and a protective role in the EAE mouse model of MS.

4.3 Materials and Methods

4.3.1 Animals

Breeding pairs of wild-type (Strain name: C57BL/6J; Stock number: 000664) and *Sirt2*$^{-/-}$ mice (Strain name: B6.129-*Sirt2*$^{tm1.1FWa}$/J; Stock number: 012772) were purchased from The Jackson Laboratory. The *Sirt2* null mice were generated using a targeting vector for the mouse *Sirt2* gene with floxed neomycin (neo)- selection cassette to delete exons 5, 6 and part of exon 7 of the *Sirt2* gene. The targeting construct was electroporated into 129S6/SvEvTac-derived TC1 embryonic stem cells. The targeted stem cells were further transiently transfected with Cre recombinase plasmid to remove the neo cassette and subsequently injected into C57BL6/J blastocysts. The resulting chimeric males were bred with 129/Sv females. The progeny of chimera were then backcrossed to C57BL/6 mice for 8 generations to produce homozygous *Sirt2*$^{-/-}$ mice. At The Jackson Laboratory, the resulting mice were bred with C57BL/6J for atleast one generation to establish the colony (https://www.jax.org/strain/012772). Genotyping was carried out using common forward primer (5'-GACTGGAAGTGATCAAAGCTC-3') and specific reverse primer for wild-type (5'-CAGGGTCTCACGAGTCTCATG-3') and *Sirt2* mutant (5'-TCAAATCTGGCCAGAACTTATG-3'). Mice were bred in house at the University of Saskatchewan animal facility in compliance with the University of Saskatchewan's Animal Care Committee guidelines. Animal use was approved by the University of Saskatchewan's Animal Research Ethics Board, and adhered to the Canadian Council on Animal Care guidelines for humane animal use.

4.3.2 Primary OL cell culture

Primary OLs were prepared from the cortices of wild-type or *Sirt2*$^{-/-}$ mouse embryos at E15.5 (Chen et al., 2007a). Briefly, meninges free cerebral cortices were dissected from the embryonic brains and dissociated with Accumax solution (Sigma). The cell suspensions were centrifuged to remove accumax and were resuspended in neurosphere growth medium (DMEM/F12, 25 mg/mL insulin, 100 mg/mL apo-transferrin, 20 nM progesterone, 60 mM putrescine and 30 nM sodium selenite) supplemented with EGF (20 ng/mL) and bFGF (20 ng/mL). The cells were passed through a 70 μm nylon cell strainer and plated on uncoated 100 mm cell culture dishes. After 4 days, neurospheres were passed at 1:3 ratio. Neurospheres were dissociated to generate primary OLs using accumax and plated on poly-D-lysine (Sigma) coated dishes in neurosphere growth medium supplemented with 10 ng/mL human recombinant platelet-derived growth factor (PDGF-AA) and 10 ng/mL basic fibroblast growth factor (bFGF). Differentiation of primary OLs were induced by plating the cells in OL differentiation medium containing 10 ng/mL biotin, 5 μg/mL insulin, 50 μg/mL transferrin, 2 mM glutamine, 30 nM sodium selenite, 0.1% BSA, 10 nM hydrocortisone, 1% penicillin-streptomycin solution, 5 μg/mL *N*-acetyl-L-cysteine and 1% FBS in DMEM/F12.

4.3.3 RNA isolation and qPCR

Total mRNA from the corpus callosum (CC) was isolated using Ambion total RNA miniprep kit (Invitrogen) as per the manufacturer's protocol. First strand cDNA synthesis (reverse transcription) was performed using High-Capacity cDNA Reverse Transcription kit (Applied Biosystems) with random primers. The qPCR was carried out using SYBR select master mix

(Applied Biosystems) in Step one Real Time PCR System (Applied Biosystems) with gene specific primers designed using primer-BLAST tool (Table 4.1).

The relative levels of transcripts were determined by threshold cycle differences ($2^{-\Delta\Delta CT}$) of target normalized to the endogenous control (*β-actin*) as previously described (Doucette et al., 2010).

Table 4.1: Primer sequences used for the relative quantification of myelin specific genes in CC by qPCR

Genes	Primer sequences
Sirtuin2 (Sirt2)	5′-AGCAAGGCACCACTAGCCACC-3′ 5′-TGTTCCTCTTTCTCTTTGGTC-3′
Myelin basic protein (Mbp)	5′-CATGGCTTCCT CCCAAGGCAC-3' 5′-GCCATGGGAGATCCAGAGCGG-3'
Proteolipid protein (Plp)	5′-GGTACAGAAAAGCTAATTGAGACC-3′ 5′-GATGACATACTGGAAAGCATGA-3′
Proteolipid protein and the alternatively spliced isoform of Plp (Plp /Dm20)	5′-GGTACAGAAAAGCTAATTGAGACC-3' 5′-GATGACATACTGGAAAGCATGA-3'
β-actin	5′-ATTGTAACCAACTGGGACG-3' 5'-TTGCCGATAGTGATGACCT-3'

4.3.4 Western blot analyses

Proteins were extracted from CC using RIPA lysis buffer at 4°C. Proteins (20 μg) were separated on 12% SDS-PAGE and Western blot analyses were performed with the following primary antibodies: rabbit polyclonal anti-SIRT2 (1:3000; Sigma) antibody and mouse monoclonal anti-β-tubulin (1:1000; Developmental Studies Hybridoma) antibody. Secondary antibodies utilized were goat anti-rabbit IgG- horse radish peroxidase (HRP) conjugate for SIRT2 and goat anti-mouse IgG- HRP (Biorad) in case of β-tubulin. Blots were developed with Clarity™ Western ECL Substrate (BioRad).

4.3.5 Immunohistochemistry

Wild-type or *Sirt2*$^{-/-}$ mouse brains at P15 were harvested and fixed with 4% paraformaldehyde overnight at 4°C. Fixed brains were cryoprotected in 30% sucrose overnight at 4°C and embedded in Tissue-Tek OCT (Electron Microscopy Sciences). Coronal sections (10 μm) were prepared from the brain of wild-type or *Sirt2*$^{-/-}$ mice. Sections were rehydrated with phosphate buffered saline (PBS) for 15 min and pre-permeabilized with PBS containing 0.4% Triton X-100 for 30 min. Sections were blocked with 10% goat serum in PBS containing 0.4% Triton X-100 for 1 h and incubated with the rabbit polyclonal anti-MBP (Abcam®) antibody overnight at 4°C. The sections were then washed three times and incubated with goat polyclonal anti-rabbit IgG (Alexa Fluor® 594; Molecular Probes®) secondary antibody for 1 h at room temperature and mounted with Prolong Gold anti-fade reagent containing DAPI (Invitrogen®).

4.3.6 BrdU (5-bromo-2′-deoxyuridine) labeling

For OPC proliferation analysis, wild-type or *Sirt2*$^{-/-}$ mouse were injected intraperitoneally with BrdU (100mg/kg; Sigma) at P7. After three hours, the mice were perfused with 4% paraformaldehyde, the brains were dissected out and fixed in 4% paraformaldehyde overnight at 4°C. The percentage of proliferating OPCs was determined by double labeling brain sections with mouse monoclonal anti-Olig2 (Millipore) and rat monoclonal anti-BrdU antibody (Abcam). Coronal sections (10 μm) were rehydrated with PBS for 15 min. The sections were incubated with 1 N HCl for 10 min at 4°C, 2 N HCl for 20 min at 37°C and were neutralized with 0.1 M sodium borate buffer (pH 8.5) for 10 min. Standard immunohistochemistry protocol was followed as mentioned above. Brain sections were imaged using an Olympus VS110 slide scanner (Cameco MS Neuroscience Research Center, Saskatoon). Olig2 and BrdU positive cells in the whole CC region (marked with dashed line in Figure 4.6) were counted from five wild-type and five *Sirt2*$^{-/-}$ mutant brain sections. Cell counts were carried out using Image J software (NIH) (Doucette et al., 2010) and expressed as the percentage proliferating OPCs ($Olig2^{+}/BrdU^{+}$ cells).

4.3.7 Immunocytochemistry

Immunocytochemistry was carried out following the protocol described by Wang et al. (2011). Primary OLs were cultured on a poly-D-lysine coated dish containing coverslips at a density of 2 x 10^2 cells/mm^2. Cells were fixed with 4% paraformaldehyde for 15 min and washed two times with PBS. Cells were blocked with 10% goat serum in PBS containing 0.4% Triton X-100 and incubated with the rabbit polyclonal anti-MBP (Abcam®) antibody overnight at 4°C. The cells were washed three times and incubated with goat polyclonal anti-rabbit IgG (Alexa Fluor® 594;

Molecular Probes®) secondary antibody for 1 h at room temperature. Coverslips were mounted with Prolong Gold anti-fade reagent containing DAPI (Invitrogen®).

4.3.8 Luxol fast blue (LFB) staining

Paraffin embedded human MS brain tissue blocks were sectioned (10 μm) and stained with Luxol fast blue (LFB). Deparaffinized sections were incubated with 0.1% LFB solution overnight at 60°C, washed with 95% alcohol, deionized water and differentiated in 0.05% lithium carbonate for 30-90 s. The slides were then rinsed in 70% alcohol, distilled water and transferred to Harris hematoxylin solution to counterstain with hematoxylin and eosin (HE). The sections were washed in water, acid alcohol (0.5% HCl in 95% alcohol), distilled water and saturated aqueous lithium carbonate. The sections were then stained with eosin subjected to dehydration in a series of ethanol, ethanol/xylene, xylene and finally mounted in DPX mounting media (Sigma).

4.3.9 Electron microscopy (EM)

Postnatal day 15 (P15) *Sirt2*$^{-/-}$ and wild-type mice were anesthetized and perfused with 2.5% glutaraldehyde and 4% paraformaldehyde in 0.1 M sodium cacodylate buffer (Werner et a., 2013). After perfusion, brain was dissected out and post-fixed in the same fixative used for perfusion. Tissue was processed and embedded in Epon resin. The cross-sections of CC from matching areas of *Sirt2*$^{-/-}$ and wild-type brains were visualized using transmission electron microscopy (TEM) (Philips 410LS electron microscope). Electron micrographs from five different fields of view from five different animals were used for the quantification of total number of myelinated axons and myelin thickness. Total numbers of myelinated axons were analyzed using Image J software (National Institutes of Health). Quantification of myelin

thickness was carried out by measuring the diameter of the individual myelin fibers in relation to respective axon diameters using Image-Pro Plus software and represented as g-ratio (ratio of axon diameter to myelin fiber diameter). Axon diameter was obtained by measuring the shortest diameter of each axon.

4.3.10 EAE induction

EAE was induced in 8 week old *Sirt2*$^{-/-}$ and wild-type mice by injecting MOG_{35-55} peptide (200 μg) suspended in complete Freund's adjuvant (CFA) subcutaneously into two different sites on the hind flank on days 0 and 7. Additionally, mice were subjected to intraperitoneal injection with Pertussis toxin on the day of immunization and two days later. A sham control group was immunized with PBS in CFA without antigen subcutaneously. Mice were monitored for body weight and scored daily for clinical disease severity according to a standard EAE grading scale (0, No clinical signs; 1, loss of tail tone; 2, hindlimb weakness; 3, partial hindlimb paralysis; 4, complete hindlimb and forelimb paralysis; and 5, moribund or dead) for 30 days. Brain and spinal cord samples were collected in 10% neutral buffered formalin on day 30 after EAE induction (Miller et al., 2007; Rafalski et al., 2013).

4.3.11 Statistical analysis

Data are presented as mean ± standard error of the mean (SEM). For experiments involving one independent variable, an unpaired t-test was performed. For experiments with two or more independent variables, a two-way analysis of variance was conducted followed by Bonferroni's multiple comparisons post hoc test (Graphpad prism, Prism® Software Corporation), as indicated in the figure legends.

4.4 Results

4.4.1 Confirmation of the loss of Sirt2 expression in *Sirt2*$^{-/-}$ mice

To determine the impact of *Sirt2* in CNS myelination and MS *in vivo*, I used *Sirt2*$^{-/-}$ mice purchased from Jackson Laboratory. The *Sirt2*$^{-/-}$ mice were generated by the targeted insertion of pGK-Neo cassette into exons 5, 6 and part of exon 7 of the *Sirt2* gene. To validate the loss of *Sirt2* expression in the *Sirt2*$^{-/-}$ mice, genotyping was done using specific primers for wild-type (WT) and *Sirt2*$^{-/-}$ mutant alleles (Fig. 4.1A). A complete loss of *Sirt2* mRNA (Fig. 4.1B) and SIRT2 protein (Fig. 4.1C) was observed in the CC of *Sirt2*$^{-/-}$ mice.

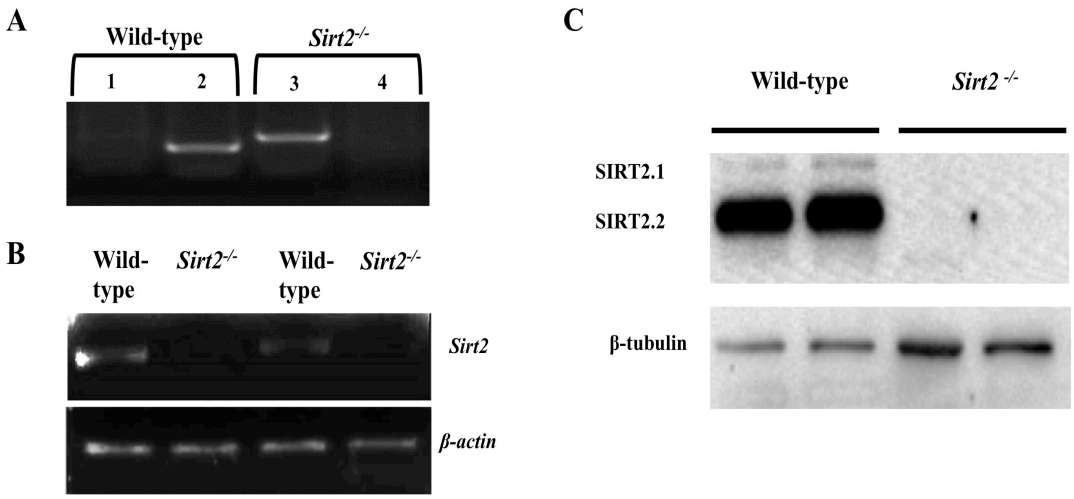

Figure 4.1: *Sirt2*$^{-/-}$ mice show complete loss of *Sirt2* mRNA and protein expression. (A) Genotyping of *Sirt2*$^{-/-}$ mice was performed using primers specific for wild-type (WT; lane 2 and 4) and *Sirt2*$^{-/-}$ mutants (lane 1 and 3). The presence of amplicon at 538 bp (lane 2) and absence of amplicon at 700 bp (lane 1) confirms the WT phenotype, whereas the presence of amplicon at 700 bp (lane 3) and absence of amplicon at 538 bp (lane 4) confirms the *Sirt2* mutant phenotype. **(B)** RT-PCR show the complete absence of *Sirt2* mRNA in the corpus callosum (CC) of *Sirt2*$^{-/-}$ mutants. **(C)** Immunoblots of lysates prepared from the corpus callosum (CC) of *Sirt2*$^{-/-}$ mice show complete absence of the SIRT2 protein.

4.4.2 Hypomyelination in *Sirt2*$^{-/-}$ mice

Our laboratory has previously demonstrated that *Sirt2* promotes process formation and expression of MBP *in vitro* in CG4-OLs (Ji et al., 2011). To determine the effect of loss of function of *Sirt2* on the CNS myelination *in vivo*, TEM technique was employed to examine the CC of wild-type and *Sirt2*$^{-/-}$ mice at P15, a stage at which myelination peaks in rodents. Ultra-structural analysis of myelin in CC showed that the number of myelinated axons was reduced by ~70% in *Sirt2*$^{-/-}$ mice at P15 compared to controls (Fig. 4.2A, B, C). In the wild-type controls, about 63% of axons were myelinated while only 20% of axons were myelinated in the *Sirt2*$^{-/-}$ mice at P15 (Fig. 4.2C). Although the numbers of myelinated axons were decreased in the *Sirt2*$^{-/-}$ mice, the g-ratio analyses (ratio of axon diameter to myelin fiber diameter) revealed an increase in myelin thickness (lower g-ratio, red circles) (Fig. 4.2F). However, the myelin sheath of *Sirt2*$^{-/-}$ mice was uncompacted, which could explain the increased myelin thickness (Fig. 4.2D, E, F). Furthermore, in *Sirt2* null mice, a slight decrease in the myelination of small sized axons was accompanied by a shift in the myelination of large diameter axons (Fig. 4.3A), although not statistically significant. These results suggest that the loss of *Sirt2* results in severe hypomyelination during CNS development *in vivo*.

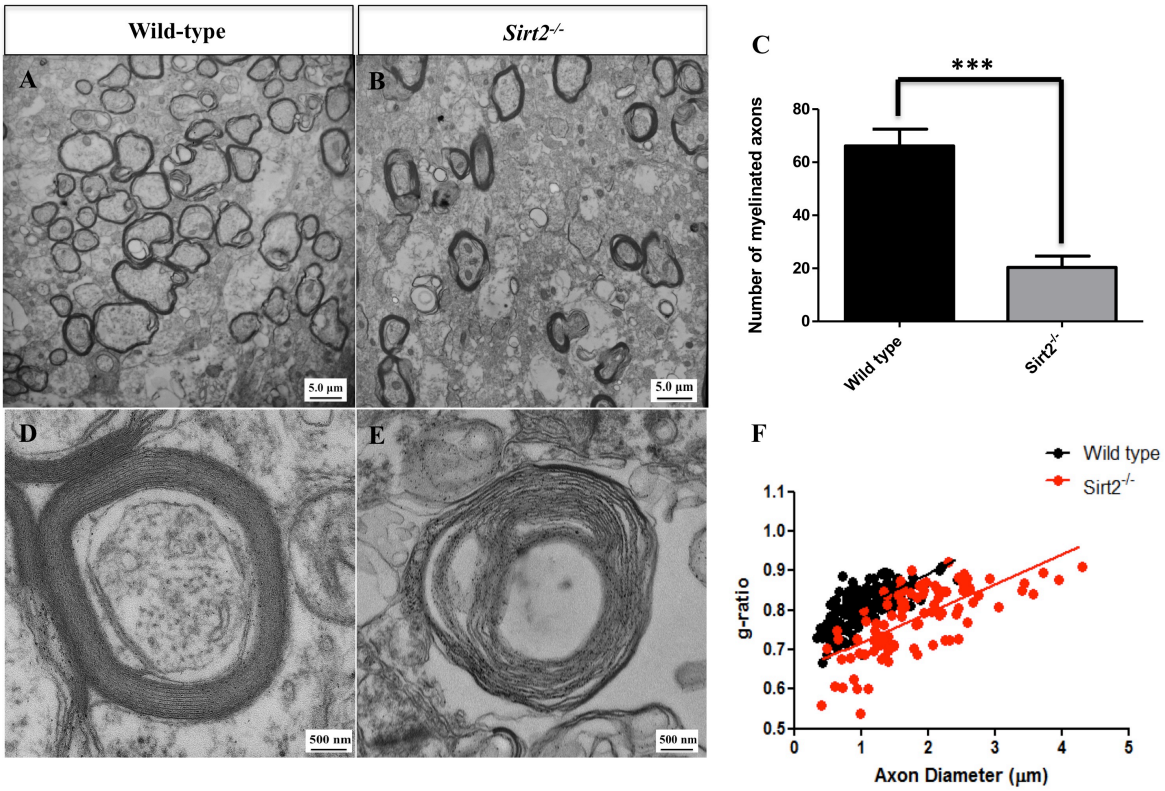

Figure 4.2: Hypomyelination in *Sirt2*$^{-/-}$ mice. (A and **B)** Electron micrographs in the CC sections of *Sirt2*$^{-/-}$ *mice* **(B)** show severe hypomyelination at P15 compared to wild-type controls **(A)**. Scale bar = 5 µm. (**C**) Quantification of the total number of myelinated axons showed a significant reduction in *Sirt2*$^{-/-}$ mice. Data are represented as mean ± SEM. ***P < 0.001, Unpaired t-test (*n* = 5). **(D and E)** Representative image showing uncompact myelin in the *Sirt2*$^{-/-}$ mice compared to wild-type. Scale bar = 500 nm. **(F)** Morphometric quantification of the myelin thickness by g-ratio analyses (ratio of axon diameter to myelin fiber diameter) shows increase in myelin thickness in *Sirt2*$^{-/-}$ mice (red circles) compared to wild-type (black circles).

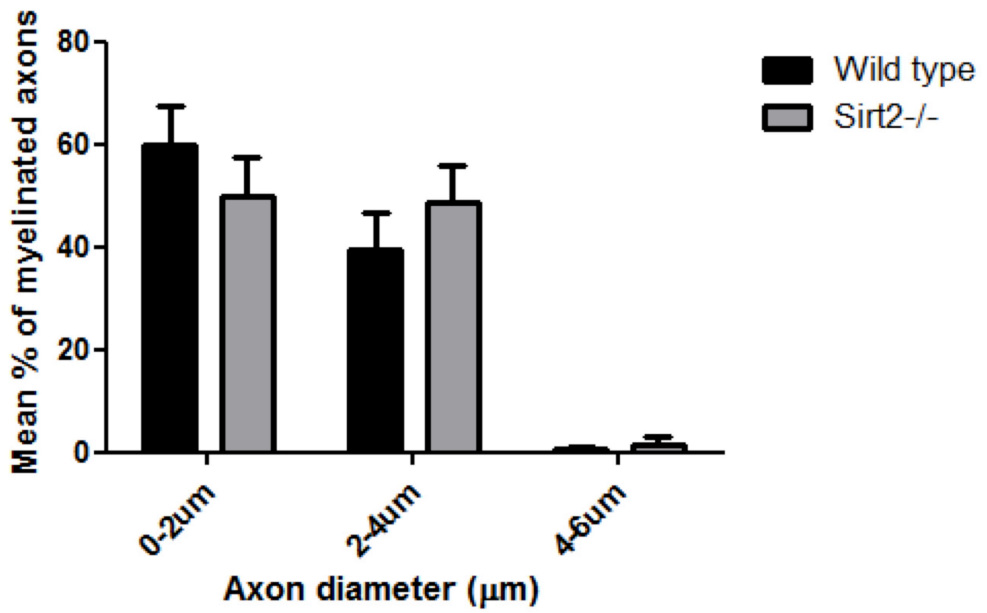

Figure 4.3: Axon calibers in *Sirt2*$^{-/-}$ mice. A. Diameters of all myelinated axons were measured in the CC of P15 *Sirt2*$^{-/-}$ *mice* and WT controls. In the *Sirt2*$^{-/-}$ mice, there is reduction in myelination of small sized axons less than 2 µm in diameter accompanied by a shift to large diameter axons (grey bars).

4.4.3 Loss of *Sirt2* gene impairs the expression of key myelin structural genes

To investigate the impact of loss of *Sirt2* on myelin gene expression, qPCR was performed in *Sirt2*$^{-/-}$ mice during the peak of myelination at P15. Loss of *Sirt2* results in ~50% decreased expression of major myelin transcripts, *Mbp, Plp* and *Plp/Dm20,* which constitute the structural component of myelin sheaths, as compared to wild-type at P15 (Fig. 4.4A, B, C). To determine if the reduction in gene expression persisted in older mice, myelin specific gene expression profiles were assessed at P77. Expression of *Mbp* was reduced ~70% in *Sirt2*$^{-/-}$ mice compared to age matched wild-type controls (Fig. 4.4D), whereas *Plp* and *Plp/Dm20* were reduced ~30% and 20%, respectively, in *Sirt2*$^{-/-}$ mice (Fig. 4.4E, F). In addition, immunostaining of MBP in the rostral CC of *Sirt2*$^{-/-}$ mice (Fig. 4.5B, D) showed reduced expression of MBP compared to the wild-type controls at P15 (Fig. 4.5A and C).

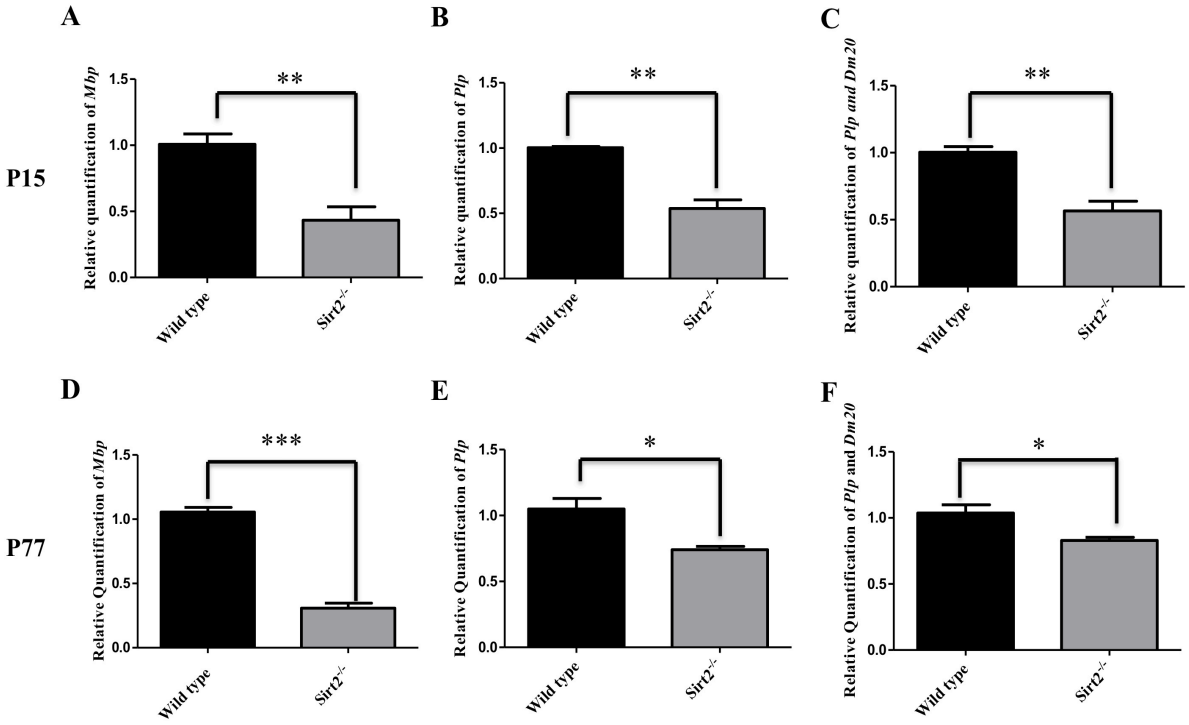

Figure 4.4: Reduced myelin specific gene expressions in *Sirt2*$^{-/-}$ mice. qPCR (n = 3) of RNA isolated from CC of *Sirt2*$^{-/-}$ mice and WT controls shows a significant reduction in the expression of *Mbp, Plp,* and *Plp/Dm20* at P15 **(A, B and C)** and at P77 **(D, E and F).** The bar graphs represent the transcript levels of *Mbp, Plp,* and *Plp/Dm20* relative to wild-type controls. Data represented as mean±SEM; Unpaired t test *p < 0.05, **p < 0.01, ***p < 0.001.

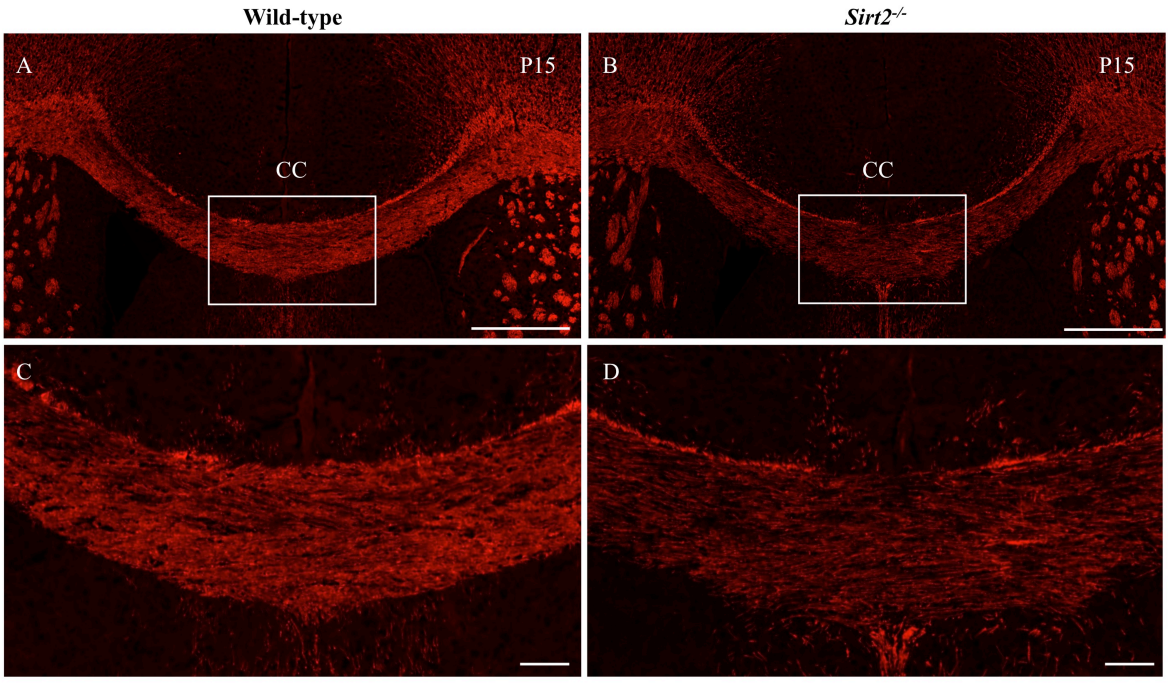

Figure 4.5: Immunohistochemical staining of myelin basic protein (MBP) on coronal sections of P15 brain. (A-D) Immunohistochemical analysis (n = 5) of myelin basic protein (MBP) in coronal sections through the rostral CC of wild-type mice **(A)** and *Sirt2*$^{-/-}$ mice at P15 **(B)**. Scale bar = 200 µm. *Sirt2*$^{-/-}$ mice show reduced expression of MBP in the rostral corpus callosum **(B and D** compared to **A and C)**. Inserts show higher magnification of the boxed region (**C** and **D**). Scale bar, 100 µm.

4.4.4 Loss of *Sirt2* impairs oligodendrogenesis and OL proliferation

To determine if the hypomyelination observed in *Sirt2*$^{-/-}$ mice is due to impaired proliferation of OPCs, the percentage of proliferating OPCs was examined by double labeling brain sections with Olig2, an OPC marker and BrdU, proliferation marker at P7 (Fig 4.6). The total number of Olig2^{+} OPCs was severely reduced by 80% in the *Sirt2*$^{-/-}$ mice (Fig 4.6 B, D, E) compared to wild-type controls (Fig 4.6 A, C, E) in the CC at P7. Similarly, the percentage of proliferating OPCs (BrdU^{+}/ Olig2^{+}) was reduced by 60% in the *Sirt2*$^{-/-}$ mice (Fig 4.6 B, D, G) compared to wild-type controls (Fig 4.6 A, C, G). These results suggest that *Sirt2* plays a critical role in OL cell proliferation during early development.

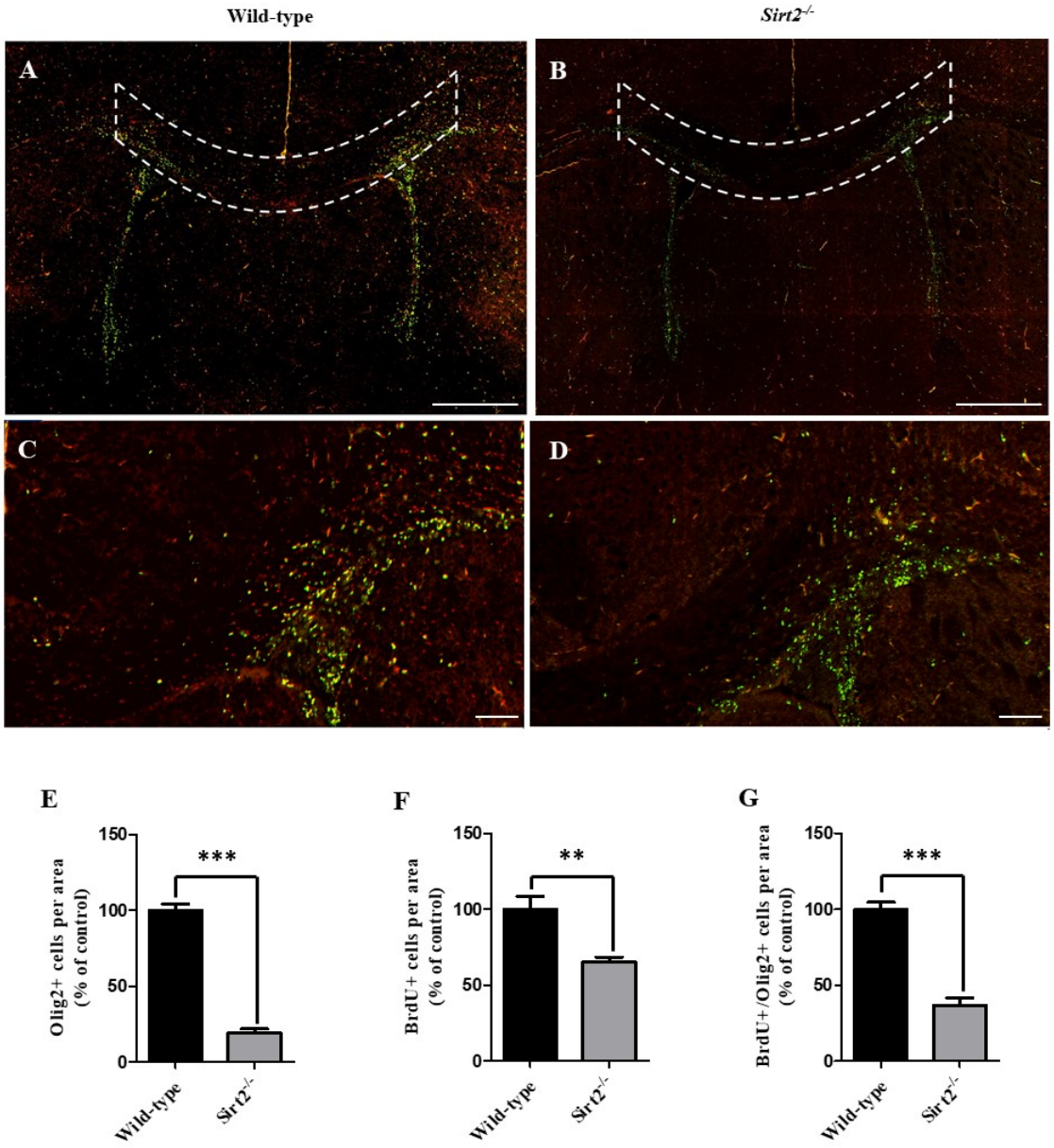

Figure 4.6: Loss of *Sirt2* impairs OPC proliferation. Wild-type and *Sirt2*$^{-/-}$ mice were injected with BrdU (100 mg/kg) intraperitoneally at P7 and brains were harvested after three hours. Brain sections (n = 5) were double labeled with Olig2 (red) and BrdU (green) to quantify the proliferating OPCs. Representative images showing Olig2^{+} and BrdU^{+} cells in the rostral CC (dashed line) of wild-type mice **(A)** and *Sirt2*$^{-/-}$ mice **(B)** at P7. Scale bar, 200 µm. (**C** and **D**) High magnification images show less Olig2^{+} and BrdU^{+} cells in the CC of *Sirt2*$^{-/-}$ mice. Scale bar, 100 µm. Quantification of total number of OPCs (Olig2^{+} cells) **(E)**, total proliferating cells (BrdU^{+} cells) **(F)** and proliferating OPCs (Olig2^{+}/BrdU^{+} cells) **(G)** show reduction in the number of OPCs and proliferating OPCs in the CC of *Sirt2*$^{-/-}$ mice compared to wild-type mice. Mean±SEM; Unpaired t test **p < 0.01, ***p < 0.001.

4.4.5 Loss of *Sirt2* impairs OL differentiation

To examine if loss of *Sirt2* affects OL differentiation, primary OLs isolated from the brains of E15.5 *Sirt2*$^{-/-}$ and wild-type mice were seeded at 0.5 x 10^6 and allowed to differentiate *in vitro* for 6 days. The differentiated cells were stained with MBP to determine the extent of OL differentiation. The number of processes that arised from the *Sirt2*$^{-/-}$ primary OLs were less compared to wild-type primary OLs, indicating that loss of *Sirt2* impairs differentiation of primary OLs (Fig 4.7). This indicates that in addition to OPC proliferation, *Sirt2* plays a critical role in OL differentiation during development.

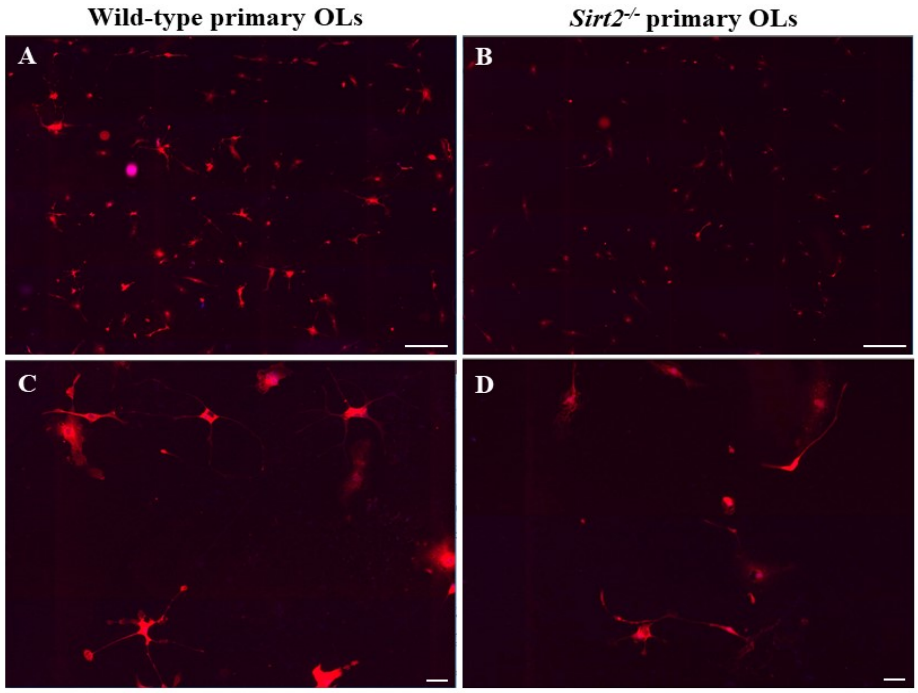

Figure 4.7: Impaired OL differentiation of the primary OLs from *Sirt2*$^{-/-}$ mice. Primary OLs isolated from E15.5 wild-type and *Sirt2*$^{-/-}$ mice (n = 6) were allowed to differentiate for 6 days and immunolabeled for MBP (red) to examine the morphology of differentiated OLs. Representative images showing MBP labeled primary OLs from wild-type **(A)** and *Sirt2*$^{-/-}$ **(B)** mice. Scale bar, 100 µm. Higher magnification images of the differentiated cells from wild-type **(C)** and *Sirt2*$^{-/-}$ **(D)** primary OLs. Scale bar, 50 µm.

4.4.6 Loss of *Sirt2* increases the disease severity of EAE

To examine the impact of loss of function of *Sirt2* on MS, EAE, a mouse model of human MS, was induced by immunizing the *Sirt2*$^{-/-}$ and wild-type mice with MOG_{35-55} peptide (200 μg) emulsified in CFA. A sham control group was immunized with PBS without the antigen. Mice were monitored for weight and scored daily for clinical disease severity according to standard EAE grading scale for 30 days after immunization (Miller et al., 2007). An increase in the clinical disease severity of EAE in the *Sirt2*$^{-/-}$ EAE mice, compared to the wild-type EAE mice, was observed around days 18 to 20 (Fig. 4.8). The sham control group did not develop any clinical disease signs. These results suggest that SIRT2 could plausibly play a protective role in EAE.

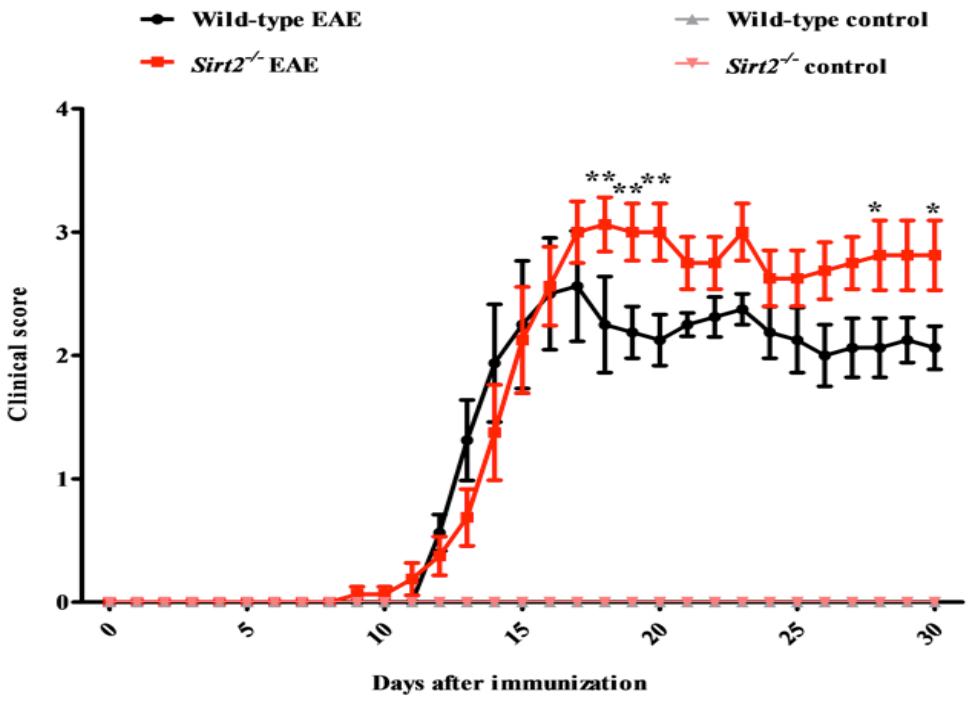

Figure 4.8: Increased severity of EAE in *Sirt2*$^{-/-}$ mice. Eight weeks old *Sirt2*$^{-/-}$ mice (n = 8; red squares) and wild-type mice (n = 8; black circles) were immunized with MOG_{35-55} peptide emulsified in CFA to induce EAE. A sham control group was immunized with PBS without the antigen. The EAE clinical scores were monitored for 30 days. EAE induction increased the disease severity in *Sirt2*$^{-/-}$ mice compared to wild-type mice. (Mean±SEM; Two-way ANOVA followed by Bonferroni's multiple comparison test; *P < 0.05, **P < 0.01).

4.4.7 SIRT2 expressed in the shadow plaques of human MS post-mortem brain and functions in myelin repair

Clinical phenotype in MS is generally associated with active demyelination, which is characterized by the complete loss of myelin and appears as a plaque (Fig. 4.9A, C, G). Remyelinated lesions (shadow plaque) appears in some MS patients with chronic MS. Staining of human MS post-mortem brain sections with luxol fast blue (LFB) sharply demarcated the areas of chronic inactive demyelinated lesions and shadow plaques from the normal appearing white matter based on the amount of myelin density (Fig. 4.9C, E, G). Inactive demyelinated lesions are identified by the presence of macrophages wihout LFB-positive or myelin immunoreactive debris (data not shown). Interestingly, immunostaining of human MS post-mortem brain sections with anti-SIRT2 antibody revealed that the distribution of SIRT2 was absent in the areas of MS lesions and its expression reappears in the 'shadow plaques' similar to LFB (Fig. 4.9B, D, F, H). This indicates that SIRT2 might play a role in remyelination in patients with MS.

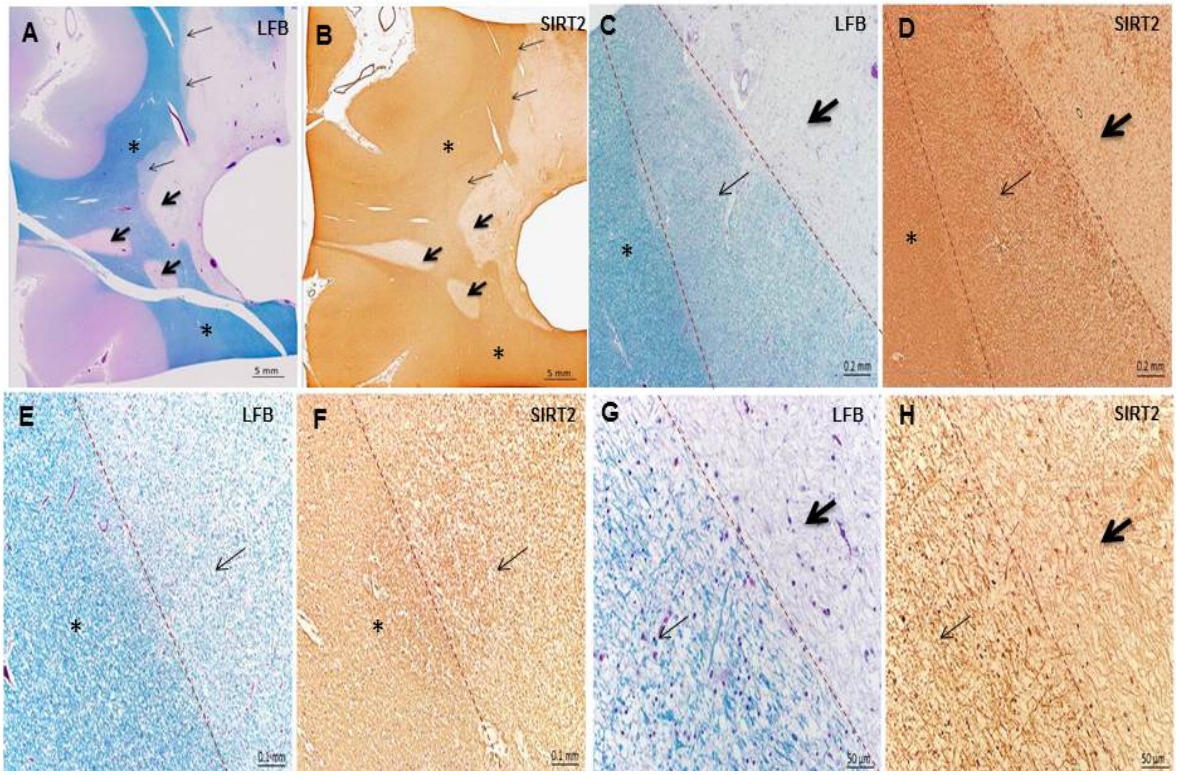

Figure 4.9: Human multiple sclerosis postmortem brain section stained with (A) luxol fast blue (LFB)/hematoxylin and eosin (LFB/HE) and (B) with an antibody against SIRT2. (A) LFB/HE staining reveals the normally myelinated white matter in the brain, indicated by an asterisk. Thick arrows indicate the demyelinated lesions where there is complete absence of LFB staining and thin arrows indicate 'shadow plaques' in which the demyelinated axons are remyelinated (marked by faint myelin staining). **(B)** SIRT2 immunohistochemistry indicates that the distribution of SIRT2 in the white matter is similar to that of LFB staining. **(A and B)** Scale bar, 5 mm. **(C, D, E and F)** The normally appearing white matter, 'shadow plaques' and demyelinated lesions can be clearly distinguished based on the intensity of LFB. The borders are indicated with dashed lines. The expression of SIRT2 reappears in the 'shadow plaques' **(D and F)**. **(G and H)** In lesions where axons are demyelinated there is complete absence of LFB. Sparse staining of SIRT2 in **(H)** (thick arrow) appears to be background staining. Scale bar, 50 μm.

4.5 Discussion

In the CNS, SIRT2 is predominantly expressed in premyelinating and myelinating OLs (North et al., 2003). SIRT2 expression is upregulated during active myelination and is an important component of myelin proteome (Li et al., 2007a; Southwood et al., 2007; Werner et al., 2007). Moreover, *Sirt2* has been demonstrated to play a significant role in the PNS myelination (Beirowski et al., 2011). However, its role in the CNS myelination and disease severity of EAE, a mouse model of human MS is not known. In this study, using *Sirt2*$^{-/-}$ mice I have shown that the loss of *Sirt2* results in hypomyelination with downregulation of myelin specific gene expression and impaired OL development. In addition, EAE induction has demonstrated that the loss of *Sirt2* results in an increased severity of EAE in *Sirt2*$^{-/-}$ mice compared to wild-type mice. My findings demonstrate that SIRT2 may play a crucial role in myelination and a protective role in the EAE mouse model of MS.

SIRT2 is primarily located in paranodal loops where it could potentially play a role in axo-glial interactions and mediate long-term axonal integrity (Li et al., 2007a). In the PNS of *Sirt2*$^{-/-}$ mice, there is a delay in myelin formation by Schwann cells with extensive outfoldings in compact myelin close to paranodes (Beirowski et al., 2011). In this study, ultra-structural analyses with EM reveal that the numbers of myelinated axons are reduced in the CNS of *Sirt2*$^{-/-}$ mice, and their myelin sheath is uncompact. These findings demonstrate the importance of SIRT2 in maintaining the integrity of the myelin sheath. During the peak of myelination, the myelinogenic potential of OLs rapidly increases and OLs synthesize higher amounts of major myelin proteins, lipids, and other cytoskeletal elements (Ishii et al., 2012). SIRT2 is expressed in OLs prior to expression of myelin proteins and continues to be expressed along with myelin proteins in differentiated and mature OLs (Ji et al., 2011; Li et al., 2007a). My findings here

show that the expression of myelin specific genes such as *Mbp* and *Plp* is downregulated in *Sirt2*$^{-/-}$ mice. This failure in the up-regulation of myelin specific genes during active myelination suggests a possible role of *Sirt2* in activating effector molecules and the signaling network that aid in the up-regulation of myelin genes.

Li et al. (2007a) reported that *Sirt2* decelerates OL differentiation, preventing premature maturation by modulating the rate at which OLs differentiate into myelinating glia. These observations were made based on overexpression and knockdown of *Sirt2 in vitro*, which lead to a decrease or increase in the complexity of these arborizations, respectively. However, these researchers also reported that OLs with higher levels of endogenous *Sirt2* expression have more complex cellular arborizations. In addition, postnatal increase in SIRT2 protein in cerebellum and spinal cord from day 0 to 60 coincides with an increase in CNP, a marker of differentiating/myelinating glia (Li et al., 2007a). Hence, *Sirt2* does not appear to be inhibitory to OL differentiation. Furthermore, *Sirt2* was reported to be an early OL differentiation marker in CNS (Southwood et al., 2007). In the present study, the hypomyelination observed in *Sirt2*$^{-/-}$ mice was associated with a defect in OL proliferation and maturation. These results indicate that *Sirt2* promotes the myelinating ability of OLs. This is in agreement with the findings in CG4-OLs that *Sirt2* positively regulates OL differentiation *in vitro* (Ji et al., 2011).

MS is a chronic demyelinating disease of the CNS characterized by multiple focal areas of myelin loss, called lesions or plaques (Noseworthy et al., 2000; Popescu et al., 2013). While remyelination occurs in early and late stages of MS, shadow plaques, sharply circumscribed regions of reduced myelin staining that stain pale blue with LFB, are completely remyelinated lesions that are sometimes present in a subset of patients with MS. In the present study, distribution of SIRT2 was evaluated to understand the involvement of SIRT2 in MS lesions.

Immunostaining of human MS postmortem brain sections reveal that SIRT2 was absent in the areas of demyelinating lesions and its expression reappears in the 'shadow plaques'. Since *Sirt2* promotes OL differentiation (Ji et al., 2011), the reappearance of SIRT2 suggests that it might promote differentiation of OLs and play a role in remyelination. However, increased numbers of biopsies are required to validate the significance of SIRT2 in MS remyelinated lesions. It would be intriguing to investigate the expression of SIRT2 in normal healthy age-matched control brains. In addition, remyelination followed by cuprizone (copper chelator)-induced demyelination would be helpful to identify the impact of SIRT2 in remyelination.

EAE induction in *Sirt2*$^{-/-}$ mice reveals the contribution of *Sirt2* in the pathogenesis of MS. Loss of *Sirt2* results in an increased severity of EAE. Inhibition or loss of function of SIRT2 has been reported to promote microglia activation-mediated inflammation (Pais et al., 2013; Yuan et al., 2016). In addition, SIRT2 interacts and deacetylates p65 subunit of NF-κB, which down-regulates NF-κB-dependent inflammatory genes (Rothgiesser et al., 2010). Inhibition of SIRT2 enhanced neuroinflammation in experimental traumatic brain injury by promoting p65 acetylation and activation of NF-κB-dependent inflammatory genes (Yuan et al., 2016). Hence, SIRT2 might play a protective role in the EAE mouse model of MS possibly by inhibiting microglial activation and inflammation. However, staining brain and spinal cord sections from wild-type and *Sirt2*$^{-/-}$ EAE mice with microglial marker (Iba1) would confirm if loss of *Sirt2* promotes microglial activation in EAE. Further analysis is required to verify if EAE induction in *Sirt2*$^{-/-}$ mice increased the disease severity due to uncompact myelin, which could increase the accessability of MOG in myelin sheath. This could be evaluated by inducing EAE in *Sirt2* overexpressing mice or by using less accessable myelin protein such as MAG to induce EAE.

Together, the results demonstrate that SIRT2 plays a critical role in oligodendrocyte development, myelination, and in the pathogenesis of MS (Fig. 4.10). I anticipate this research will advance the existing knowledge on cellular and molecular mechanisms to identify target molecules that regulate the myelinating ability of OLs in the adult animal leading to the development of potentially new nutrient and pharmacological therapies for MS.

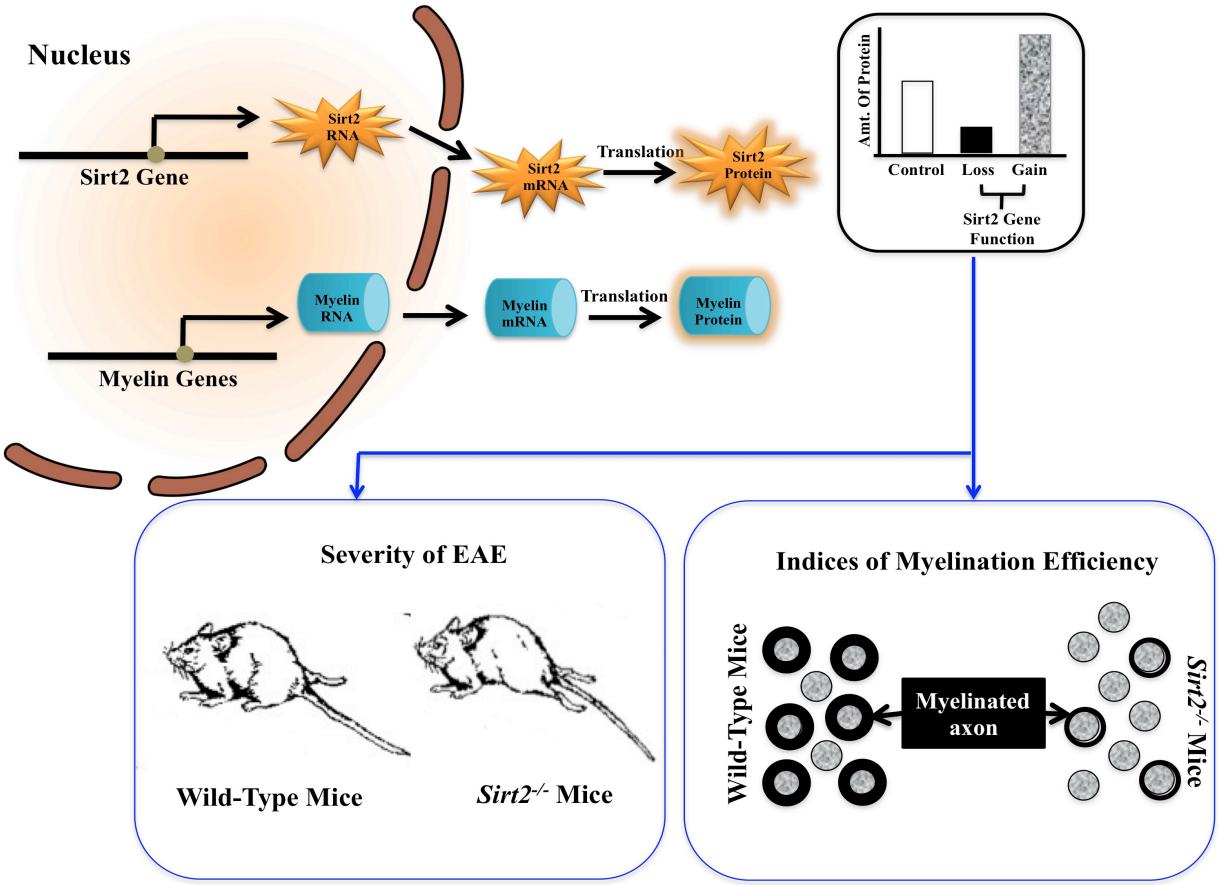

Figure 4.10: Schematic diagram representing the loss of function of *Sirt2* in myelination and disease severity of the EAE mouse model of MS. During early postnatal development, the expression of SIRT2 increases, which positively regulates the expression of myelin specific genes and myelination. Loss of function of *Sirt2* gene impairs myelin gene expression and stability of myelin sheath leading to hypomyelination. Mice lacking *Sirt2* are more susceptible to EAE induction. Thus, *Sirt2* may play a crucial role in myelination and a protective role in the EAE mouse model of MS.

Preamble to Chapter 5: *SIRT2* DOES NOT REGULATE CHOLESTEROL BIOSYNTHESIS DURING OLIGODENDROGLIAL DIFFERENTIATION *IN VITRO* AND *IN VIVO*

Rationale: In the previous chapter, I demonstrated that *Sirt2* plays a critical role in the myelination of axons in the CNS and a protective role in the EAE mouse model of MS. In this chapter, I investigate the plausible targets through which *Sirt2* could regulate myelination. Cholesterol is essential for myelin biogenesis and impairment in cholesterol biosynthesis significantly reduces myelination. SIRT2 has previously been implicated in cholesterol biosynthesis by promoting the nuclear translocation of SREBP-2. Hence, I examined whether the defect in myelination observed in *Sirt2*$^{-/-}$ mice was due to a defect in cholesterol biosynthesis. In this study, I evaluated the role of *Sirt2* in cholesterol biosynthesis in OLs *in vivo* using *Sirt2* null (*Sirt2*$^{-/-}$) mice and *in vitro* using CG4-OL cells and mouse primary OLs.

Publication

Merlin P. Thangaraj, Kendra L. Furber, LaRhonda Sobchishin, Shaoping Ji, J. Ronald Doucette, and Adil J. Nazarali. (2018) "Does Sirt2 Regulate Cholesterol Biosynthesis During Oligodendroglial Differentiation In Vitro and In Vivo?" *Cellular and Molecular Neurobiology*, 38 (1): 329–40. doi:10.1007/s10571-017-0537-6.

Contribution statement: I designed, performed experiments, analyzed data and drafted the manuscript. Adil J. Nazarali and J. Ronald Doucette conceived and coordinated the study. Kendra L. Furber contributed to editing of the manuscript. LaRhonda Sobchishin coded the images for blinded cell counts in Fig. 5.6. Shaoping Ji assisted in experimental design.

5. *SIRT2* DOES NOT REGULATE CHOLESTEROL BIOSYNTHESIS DURING OLIGODENDROGLIAL DIFFERENTIATION *IN VITRO* AND *IN VIVO*

5.1 Summary

SIRT2 is a deacetylase enzyme predominantly expressed in myelinating glia of the CNS. We have previously demonstrated that *Sirt2* expression enhances oligodendrocyte (OL) differentiation and arborization *in vitro*, but the molecular targets of SIRT2 in OLs remain speculative. SIRT2 has been implicated in cholesterol biosynthesis by promoting the nuclear translocation of SREBP-2. I investigated this further in CNS myelination by examining the role of *Sirt2* in cholesterol biosynthesis *in vivo* and *in vitro* employing *Sirt2*$^{-/-}$ mice, primary OL cells and CG4-OL cells. My results here demonstrate that the expression of cholesterol biosynthetic genes in the CNS white matter or cholesterol content in purified myelin fractions did not differ between *Sirt2*$^{-/-}$ and age-matched wild-type mice. Cholesterol biosynthetic gene expression profiles and total cholesterol content were not altered in primary OLs from *Sirt2*$^{-/-}$ mice and in CG4-OLs when *Sirt2* was either down-regulated with RNAi or overexpressed with vector constructs. In addition, *Sirt2* knock-down or overexpression in CG4-OLs had no effect on SREBP-2 nuclear translocation. These results indicate that *Sirt2* does not impact the expression of genes encoding enzymes involved in cholesterol biosynthesis, total cholesterol content or nuclear translocation of SREBP-2 during OL differentiation and myelination.

5.2 Introduction

In the developing CNS, OPCs proliferate and migrate throughout the cortical white matter, such as the CC, and ultimately differentiate into mature, myelinating OLs (Baumann and Pham-Dinh, 2001; Bergles and Richardson, 2015; Nicolay et al., 2007). These differentiating OLs, which are rich in myelin lipids and structural proteins, extend their plasma membranes to wrap axons with compact, multilayered membranous sheath. Proper myelination is critical for rapid signal conduction and long-term axonal survival (Baumann and Pham-Dinh, 2001; Simons and Nave, 2015).

Myelin contains greater than 70% lipids in its dry weight with 25% cholesterol in the total lipid content (Norton and Poduslo, 1973a; Saher and Simons, 2010). In the brain, cholesterol biosynthesis increases during the peak of myelination (Dietschy and Turley, 2004; Jurevics et al., 1997; Jurevics and Morell, 1995; Muse et al., 2001) and cholesterol needed for the myelin biogenesis is primarily derived from the *in situ* biosynthesis in differentiating OLs with little imported via circulation (Jurevics et al., 1997; Jurevics and Morell, 1995). In addition to being a large structural component of myelin membranes, cholesterol may also facilitate transport and sorting of proteins to form compact myelin sheath (Saher and Simons, 2010; Saher et al., 2005; Saher et al., 2009; Simons et al., 2000; Werner et al., 2013). Inactivation or mutation of enzymes involved in the cholesterol biosynthetic pathway in OLs, such as squalene synthase (SQS; Saher et al., 2005) and Hmg-CoA synthase 1 (HMGCS1; Mathews et al., 2014), perturb myelin gene expression and axon ensheathment. Thus, the supply of cholesterol is a rate-limiting factor for proper CNS myelination (Mathews et al., 2014; Mathews and Appel, 2016; Saher et al., 2005).

Two master regulatory transcription factors, sterol regulatory element binding protein (SREBP)-1 and SREBP-2, regulate lipid and cholesterol biosynthesis, respectively (Brown and Goldstein, 1997; Eberlé et al., 2004). SREBP-2 is synthesized as a precursor (125 kDa) and is bound to SREBP cleavage activating protein (SCAP) in the endoplasmic reticulum. Under low sterol levels, SREBP-SCAP complex is exported to the golgi where the cytoplasmic N-terminal active domain of SREBP-2 is cleaved (Sakai et al., 1996; Wang et al., 1994; Yabe et al., 2002; Yang et al., 2002). Subsequently, this mature form (N-terminal domain) of SREBP-2 (68 kDa) translocates to the nucleus and binds to SRE inducing the genes encoding enzymes involved in cholesterol biosynthesis (Amemiya-Kudo et al., 2002; Eberlé et al., 2004; Horton et al., 2002; Horton et al., 2003). The activity of SREBP family of transcription factors is regulated by acetylation and deacetylation of lysine residues within the DNA binding domain, which modulates SREBP activity and downstream target gene expression (Giandomenico et al., 2003; Ponugoti et al., 2010; Walker et al., 2010). However, relatively little is known about the regulatory factors governing SREBP-2 activity and cholesterol biosynthesis during OL differentiation and myelination in the developing CNS.

SIRT2, a NAD^+-dependent deacetylase enzyme has been implicated in cholesterol biosynthesis by facilitating the nuclear translocation of SREBP-2 (Luthi-Carter et al., 2010; Taylor et al., 2011). SIRT2 is primarily expressed in OLs and incorporated into the myelin sheath near paranodal loops (Li et al., 2007a; Werner et al., 2007). *Sirt2* expression promotes process formation and induces myelin gene expression during OL differentiation *in vitro* (Ji et al., 2011). Loss of *Sirt2* in the PNS delays Schwann cell myelin formation via deacetylation of partitioning defective 3 (Par-3), master regulator of cell polarity (Beirowski et al., 2011). In the previous chapter, I demonstrated that *Sirt2* is critical for CNS myelination and myelin specific

gene expression *in vivo*. It was reported that pharmacological inhibition of SIRT2 or deacetylase mutation in *Sirt2* impairs cholesterol biosynthesis by reducing nuclear translocation of SREBP-2 leading to downregulation of several key genes in cholesterol biosynthetic pathways in neuronal cultures (Luthi-Carter et al., 2010). In contrast, Bobrowska et al., (2012) reported no effect on nuclear translocation of SREBP-2 or cholesterol biosynthesis in brain tissue from one month-old *Sirt2*$^{-/-}$ mice. As SIRT2 expression is upregulated dramatically during the peak of myelination (Li et al., 2007a; Southwood et al., 2007; Werner et al., 2007; Zhu et al., 2012), I hypothesize that SREBP-2 may be a target of SIRT2 in CNS white matter when OLs are undergoing active differentiation and myelination.

In the present study, I have used *Sirt2*$^{-/-}$ mutant mice to investigate the role of *Sirt2* in regulating cholesterol biosynthesis in the developing CNS white matter and primary OL cultures. Furthermore, I evaluated the impact of loss or gain of *Sirt2* function in CG4-OLs on the expression of cholesterol biosynthetic genes, cholesterol content and nuclear translocation of SREBP-2.

5.3 Materials and methods

5.3.1 Animals

Sirt2$^{-/-}$ mice (lacking exons 5, 6 and part of exon 7 of the *Sirt2* gene) (Strain name: B6.129-*Sirt2*$^{tm1.1FWa}$/J; Stock number: 012772) and C57BL6/J mice were obtained from the Jackson Laboratory for breeding in house at the University of Saskatchewan. Genotyping was performed using the following primers, Common – 5'-GACTGGAAGTGATCAAAGCTC-3', Wild-type – 5'-CAGGGTCTCACGAGTCTCATG-3', Mutant – 5'-TCAAATCTGGCCAGAACTTATG-3'.

Animal use was approved by the University of Saskatchewan's Animal Research Ethics Board, and adhered to the Canadian Council on Animal Care guidelines for humane animal use

5.3.2 Primary OL cell culture

Primary OLs were isolated from C57BL/6 mice or *Sirt2*$^{-/-}$ mice at P1, as previously described (Chen et al., 2007a; Niu et al., 2012). Briefly, cortices from the neonatal pups were digested with accumax solution (Sigma®) and passed through a 70 μm nylon cell strainer. The filtered cell suspensions were maintained as mixed glial cells in medium containing DMEM/F12, 10% FBS and penicillin-streptomycin solution. After 7 days of culture, mixed glial cells were grown in OL growth medium (OGM) containing 10 ng/mL biotin, 5 μg/mL insulin, 50 μg/mL transferrin, 2 mM glutamine, 30 nM sodium selenite, 0.1% BSA, 10 nM hydrocortisone, 1% penicillin-streptomycin solution and 30% of B104 conditioned medium in DMEM/F12 to enrich OL progenitors. After 14 days of culture, primary OLs were shaken off (at 200 rpm; 37°C) and isolated from the mixed glial cultures. Differentiation was induced in purified primary OLs by plating in OL differentiation medium (ODM) containing 10 ng/mL biotin, 5 μg/mL insulin, 50 μg/mL transferrin, 2 mM glutamine, 30 nM sodium selenite, 0.1% BSA, 10 nM hydrocortisone, 1% penicillin-streptomycin solution, 5 μg/mL *N*-acetyl-L-cysteine and 1% fetal bovine serum (FBS) in DMEM/F12. In some experiments primary OLs were differentiated using 1% delipidated FBS (DLFBS; cholesterol-depleted FBS) to avoid the interference of any external source of cholesterol from the media components. Primary OLs were harvested 6 days after differentiation for RNA extraction and cholesterol assay.

5.3.3 CG4-OL cell culture, small interference RNA, overexpression vector construct and transfection

The CG4-OL cell line was derived from O-A2 progenitors isolated from the rat forebrain (Louis et al., 1992). CG4-OLs were cultured on poly-D-lysine (Sigma) coated tissue culture dishes in growth medium (GM) containing Dulbecco's modified Eagle's medium (DMEM), 50 μg/mL transferrin, 5 μg/mL insulin, 9.8 ng/mL biotin, 50 ng/mL selenium, 1% antibiotic antimycotic solution and 30% B104 conditioned medium (CM) (Ji et al., 2011; Louis et al., 1992; Wang et al., 2011). Differentiation was induced by changing GM to differentiation medium (DM) containing DMEM, 50 μg/mL transferrin, 5 μg/mL insulin, 9.8 ng/mL biotin, 50 ng/mL selenium, 1% antibiotic antimycotic solution and 2% FBS or DLFBS (Ji et al., 2011; Wang et al., 2011) .

Sirt2 siRNA with sense sequence 5′-AGGGAGCAUGCCAACAUAGAU-3′ commercially synthesized (Qiagen®) and pcDNA vector carrying full length *Sirt2* insert have been described previously (Ji et al., 2011). Transfection was carried out with 40 nM of scramble control siRNA or *Sirt2* siRNA and 3 μg of pcDNA-*Sirt2* vector on day 0, day 2, and day 4 using 0.3% Lipofectamine 2000 (Invitrogen®) in serum free / antibiotic free media. Cells were harvested for biochemical analyses after 6 days of differentiation.

5.3.4 RNA isolation, RT-PCR and qPCR

Total RNA was isolated from the CC, primary OLs or CG4-OL cells using Ambion® total RNA miniprep kit (Invitrogen®) as per the manufacturer’s protocol. RNA concentration was determined using NanoVue UV/Visible spectrophotometer (GE Healthcare Life Sciences). First strand cDNA synthesis was performed with 250-500 ng of total RNA using High-Capacity

cDNA Reverse Transcription kit (Applied Biosystems®) with random primers. Final concentration of total RNA for RT-PCR or qPCR was 5-25 ng/μL. RT-PCR was carried out for *Sirt2* in CG4-OLs transfected with *Sirt2* siRNA and pcDNA-*Sirt2* according to Ji et al. (2011). The following primer pairs were used: (i) *Sirt2* forward 5′- TGAATGGCACCTACAGAGAC-3′ and reverse 5′- CAAAGGCATTATGGTAGGGC-3′; and (ii) *β-Actin* forward 5′-ATTGTAACCAACTGGGACG-3′ and reverse 5′-TTGCCGATAGTGATGACCT-3′. The qPCR was carried out using SYBR select master mix in ABI 7300 (Applied Biosystems®) with cDNA samples from CG4-OL cells, primary OLs or corpus callosum of mouse brain. Expression levels of *Srebp-2*, *Hmgcr*, *Sqs*, *Sqle* and *Dhcr7* were quantified using the following primers pairs: (i) *Srebp-2* - forward 5′-TGCAGGTCAAAGTCTCTCCT-3' and reverse 5′-GCAGGACTTGAAAGCTGGT-3'; (ii) *Hmgcr* - forward 5′-CTGGTCCTAGAGCTTTCTCG-3' and reverse 5′-TGCTGTTCTGAGGAGAAGGA-3'; (iii) *Sqs* - forward 5′-GAAGATTCGGAAGGGGCAAG-3' and reverse 5′-CTCAAGTACTGCCAGCTCAG-3'; (iv) *Sqle* forward 5′-TAAGAAATGCGGGGATGTCA-3' and reverse 5′-GAATATCTGAGAAGGCAGCG-3'; and (v) *Dhcr7* forward 5′-TTTATGGCCATGTGACCAAC-3′ and reverse 5′- AACAGGTCCTTCTGATGGTT -3′. Relative quantification of transcripts was determined by threshold cycle differences ($2^{-\Delta\Delta CT}$) of target normalized to the endogenous control *β-actin* as described previously (Doucette et al., 2010).

5.3.5 Immunocytochemistry

Immunocytochemistry was carried out as previously described in (Wang et al., 2011). CG4-OL cells were cultured on coverslips at a density of 2 x 10^2 cells/mm^2. Cells were fixed with 4% paraformaldehyde and rinsed twice with PBS for 10 min. Cells were blocked with 3% skim milk

in PBS containing 0.1% Triton X-100, incubated with the anti-SREBP-2 (Abcam®) antibody overnight at 4°C followed by incubation with Alexa Fluor® 594 (Molecular Probes®) secondary antibody for 1 h at room temperature. Coverslips were mounted with Prolong Gold anti-fade reagent containing DAPI (Invitrogen®) to visualize nuclei. Blinded cell counts were performed (Doucette et al., 2010) using Image J software (NIH). Mean % nuclear SREBP-2 (SREBP-2/DAPI co-localization) was calculated by counting >1500 cells and expressed as a percentage of total cells (DAPI).

5.3.6 Cholesterol assay

Cholesterol assay was carried out using Amplex Red Cholesterol Assay Kit (Invitrogen Molecular Probes®) according to manufacturer's instructions. CG4-OLs and primary OLs were rinsed with 1×PBS and lysed with reaction buffer (Invitrogen®). Cholesterol assay in wild-type and *Sirt2*$^{-/-}$ mice were carried out using purified myelin fractions. Total cholesterol values were normalized to total protein as estimated with the BCA Protein Assay (Pierce®).

5.3.7 Preparation of purified myelin fraction

Myelin was isolated from whole brain of wild-type and *Sirt2*$^{-/-}$ male mice at P15 as described previously (Larocca and Norton, 2007; Norton and Poduslo, 1973b). Briefly, brain was homogenized in ice-cold 0.3 M sucrose solution containing 20 mM Tris-Cl buffer (pH 7.45), 1 mM EDTA, 1 mM DTT, 100 µM phenyl methyl sulfonyl fluoride and 10 µg/mL leupeptin. Brain homogenate was layered over 0.83 M sucrose and centrifuged in an ultracentrifuge at 75,000 x g. Myelin membranes were recovered from the 0.3 M and 0.83 M interface and further purified by two rounds of hypoosmotic shock by resuspension in Tris-HCl buffer, followed by a second

round of centrifugation in a sucrose gradient. Purified myelin was collected from the interface and resuspended in Tris-HCl buffer.

5.3.8 Statistical analysis

All quantitative data were compared using student's t-test (Prism® Software Corporation) and are presented as mean ± standard error of the mean (SEM).

5.4 Results

5.4.1 Cholesterol biosynthesis is not altered in the CNS white matter of *Sirt2*$^{-/-}$ mice

To investigate the role of *Sirt2* in regulating cholesterol biosynthesis *in vivo*, gene expression profiles of key cholesterogenic enzymes were examined in *Sirt2*$^{-/-}$ mice during the period of peak myelination (P15) and in adulthood (P60). Expression levels of *Srebp-2*, *Hmgcr, Sqs, Sqle,* and *Dhcr7* mRNA were not altered in the CC of *Sirt2*$^{-/-}$ mice compared to their age-matched wild-type (WT) controls at P15 (Fig. 5.1A) or P60 (Fig. 5.1B). In addition, total cholesterol content in the purified myelin isolated from the whole brain of *Sirt2*$^{-/-}$ and WT mice did not differ significantly (Fig. 5.1C).

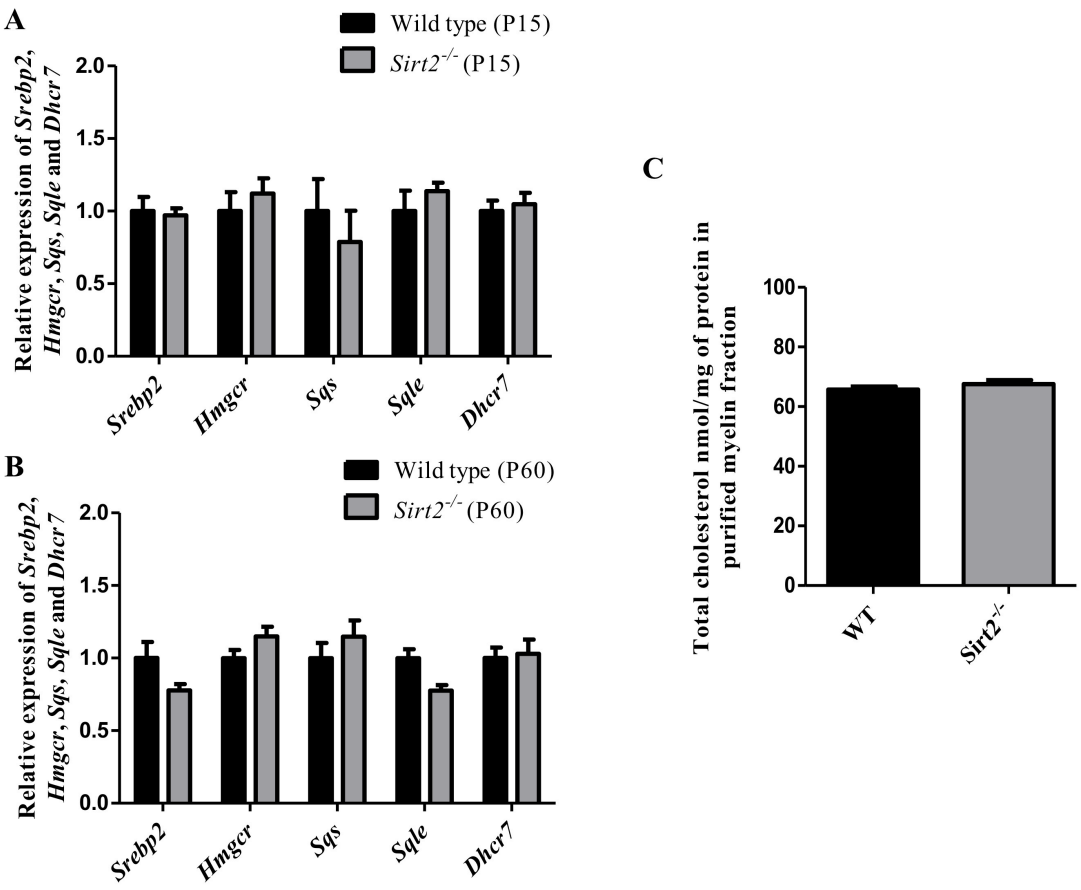

Figure 5.1: Cholesterol biosynthesis is not altered in the CNS white matter of *Sirt2*$^{-/-}$ mice. Quantification of mRNA expression of key cholesterol biosynthetic genes by qPCR at P15 **(A)** and P60 **(B)** showed no difference between in *Sirt2*$^{-/-}$ mice and age matched wild-type (WT) mice. The bar graphs represent the transcript levels of *Srebp2*, *Hmgcr, Sqs, Sqle,* and *Dhcr7* normalized to the housekeeping gene *β-actin* and represented relative to WT controls (n=6). Data represented as Mean ± SEM; unpaired t-test. **(C)** Quantification of total cholesterol content from purified myelin fraction of whole brain at P15 showed no difference between *Sirt2*$^{-/-}$ and WT mice. Protein content in the purified myelin fraction was used to normalize total cholesterol (n=4). Data represented as Mean ± SEM; unpaired t-test.

5.4.2 *Sirt2* does not regulate the cholesterol biosynthesis pathway in OLs

To directly evaluate the impact of *Sirt2* on cholesterol biosynthesis in OLs, progenitor cells were isolated from the neonatal forebrain of *Sirt2*$^{-/-}$ and WT mice followed by differentiation in serum-supplemented media for 6 days. The loss of *Sirt2*$^{-/-}$ in primary OLs did not result in altered expression of *Hmgcr* or *Sqle* when cultured in FBS (Fig. 5.2A) or in DLFBS (Fig. 5.2C). Consistent with this, the total cholesterol content did not differ between *Sirt2*$^{-/-}$ and WT OL cultures (Fig. 5.2B, D).

Furthermore, *Sirt2* was knocked-down or overexpressed in CG4-OL cells during differentiation in media containing either FBS or DLFBS. In *Sirt2*-siRNA treated CG4-OLs, expression of *Sirt2* mRNA was significantly downregulated by ~70% compared to control siRNA treated cells (Fig. 5.3A, B). However, the expression of *Hmgcr, Sqs,* and *Sqle* (Fig. 5.3C, E) and total cholesterol content (Fig. 5.3D, F) were not altered in *Sirt2*-siRNA treated cells. In CG4-OLs transfected with pcDNA-*Sirt2*, expression of *Sirt2* mRNA is significantly upregulated by ~500 fold (Fig. 5.4A, B). Again, neither the expression of *Hmgcr, Sqs,* and *Sqle* (Fig. 5.4C, E) nor the total cholesterol content (Fig. 5.4D, F) was altered in cells overexpressing *Sirt2*.

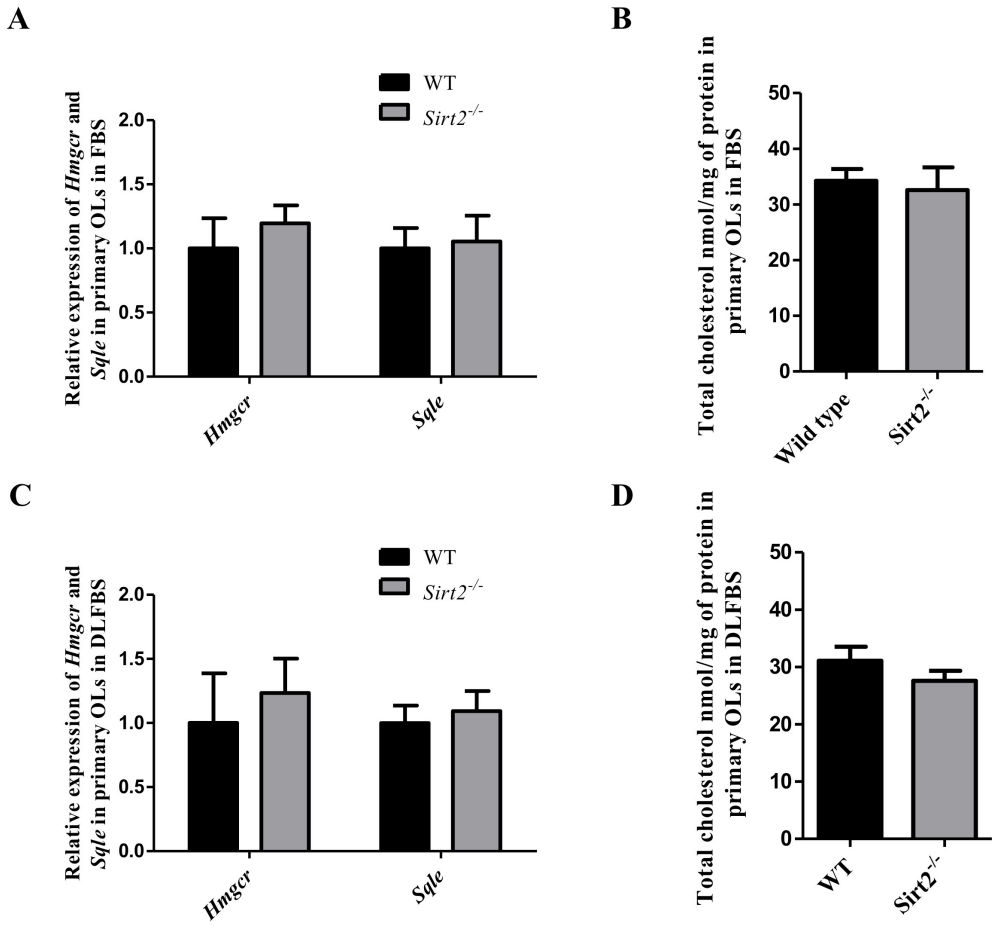

Figure 5.2: Cholesterol biosynthesis is not altered in primary OLs isolated from *Sirt2*$^{-/-}$ mice. Primary OLs isolated from WT and *Sirt2*$^{-/-}$ mice were allowed to differentiate for 6 days. Quantification of mRNA expression levels of *Hmgcr* and *Sqle* by qPCR showed no change in *Sirt2*$^{-/-}$ primary OLs compared to WT primary OLs cultured with FBS (**A**) or with DLFBS (**C**). qPCR data were normalized to the housekeeping gene *β-actin* and represented relative to WT controls (n=6). Mean ± SEM; unpaired t-test; n.s. Quantification of total cholesterol content showed no difference between *Sirt2*$^{-/-}$ and WT primary OLs cultured with FBS **(B)** or with DLFBS **(D)**. Protein content in the cell lysate was used to normalize total cholesterol (n=6). Mean ± SEM; unpaired t-test.

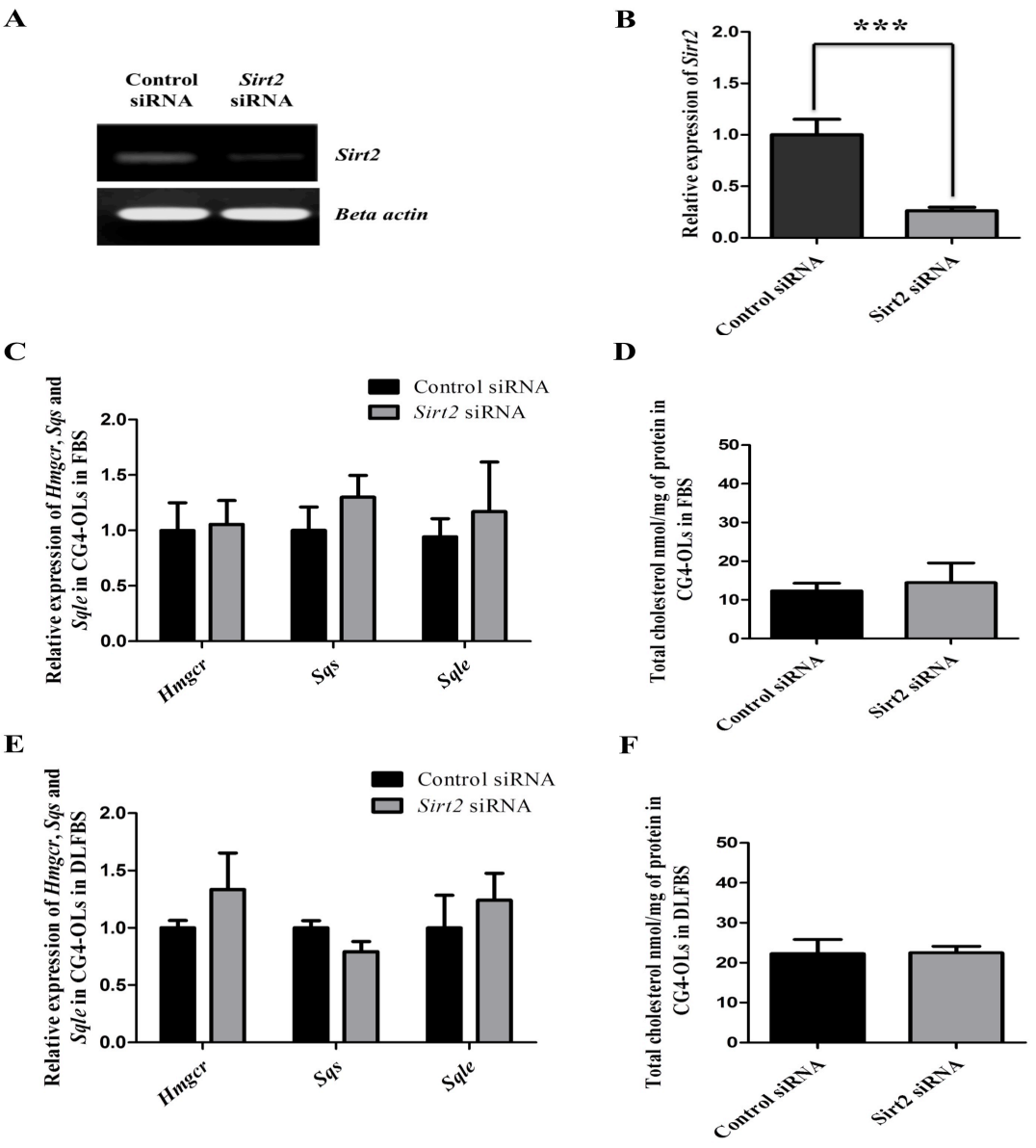

Figure 5.3: Expression of cholesterol biosynthetic genes and total cholesterol content in CG4-OLs after knock-down of *Sirt2*. CG4-OLs were transfected with control siRNA or *Sirt2* siRNA under differentiation conditions. (**A** and **B**) Transfection with *Sirt2* siRNA downregulated the expression of *Sirt2* mRNA after 6 days. qPCR data normalized to *β-actin* and represented relative to control siRNA (n=3). Mean ± SEM; unpaired t-test; ***$p < 0.001$. Knockdown of *Sirt2* did not alter the expression of *Hmgcr*, *Sqs,* and *Sqle* mRNAs in CG4-OL cells differentiated with FBS (**C**) and DLFBS (**E**). qPCR data were normalized to the housekeeping gene *β-actin* and represented relative to control siRNA (n=3). Mean ± SEM; unpaired t-test. Total cholesterol content did not change after knock-down of *Sirt2* in CG4-OL cells differentiated with FBS (**D**) or DLFBS (**F**). Protein concentration in the cell lysate was used to normalize total cholesterol (n=3). Mean ± SEM; unpaired t-test.

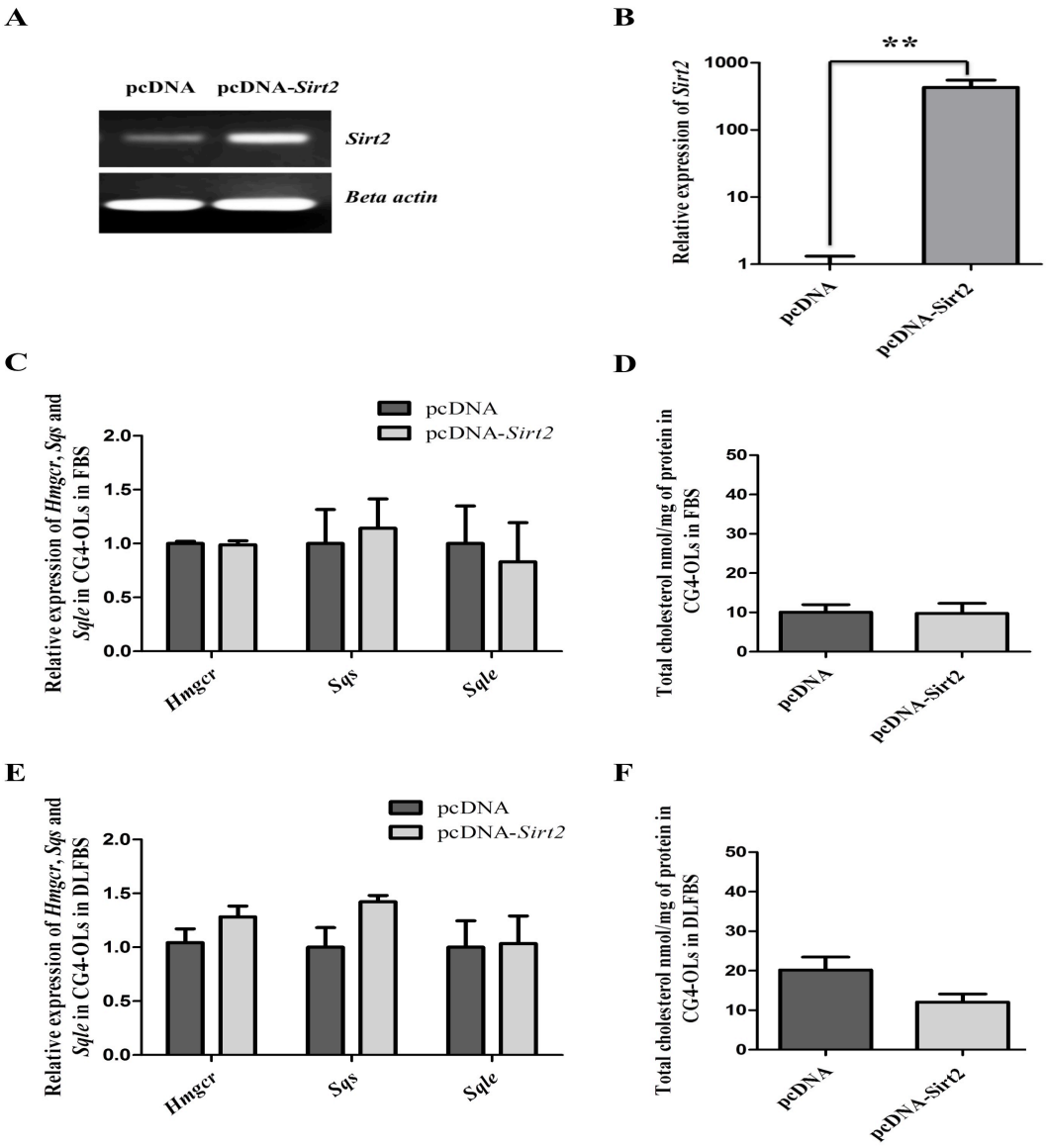

Figure 5.4: Expression of cholesterol biosynthetic genes and total cholesterol content in CG4-OLs overexpressing *Sirt2*. CG4-OLs were transfected with pcDNA or pcDNA-*Sirt2* under differentiation conditions. (**A** and **B**) Overexpression of *Sirt2* displays ~500 fold increase in the *Sirt2* mRNA levels in CG4-OL cells after 6 days. qPCR data normalized to *β-actin* and represented relative to pcDNA control vector (n=3). Mean ± SEM; unpaired t-test; **p < 0.01. Overexpression of *Sirt2* did not alter expression of *Hmgcr*, *Sqs,* and *Sqle* mRNAs in CG4-OL cells differentiated with FBS (**C**) or with DLFBS (**E**). qPCR data were normalized to the housekeeping gene *β-actin* and represented relative to pcDNA vector (n=3). Mean ± SEM; unpaired t-test. Total cholesterol content did not change after overexpression of *Sirt2* in CG4-OL cells differentiated with FBS (**D**) or DLFBS (**F**). Protein content in the cell lysate was used to normalize total cholesterol (n=3). Mean ± SEM; unpaired t-test.

5.4.3 *Sirt2* does not impact nuclear translocation of SREBP-2

Nuclear translocation of SREBP-2 was assessed in CG4-OL cells transfected with *Sirt2*-siRNA or pcDNA-*Sirt2* by immunostaining with SREBP-2 antibody (Fig. 5.5A-B, D-E). SREBP-2 was largely expressed in the perinuclear region of differentiating OLs. Approximately 35-40% of cells also showed nuclear localization of SREBP-2. Knock-down (Fig. 5.5C) or overexpression (Fig. 5.5F) of *Sirt2* did not change the subcellular distribution of SREBP-2 compared to their respective controls.

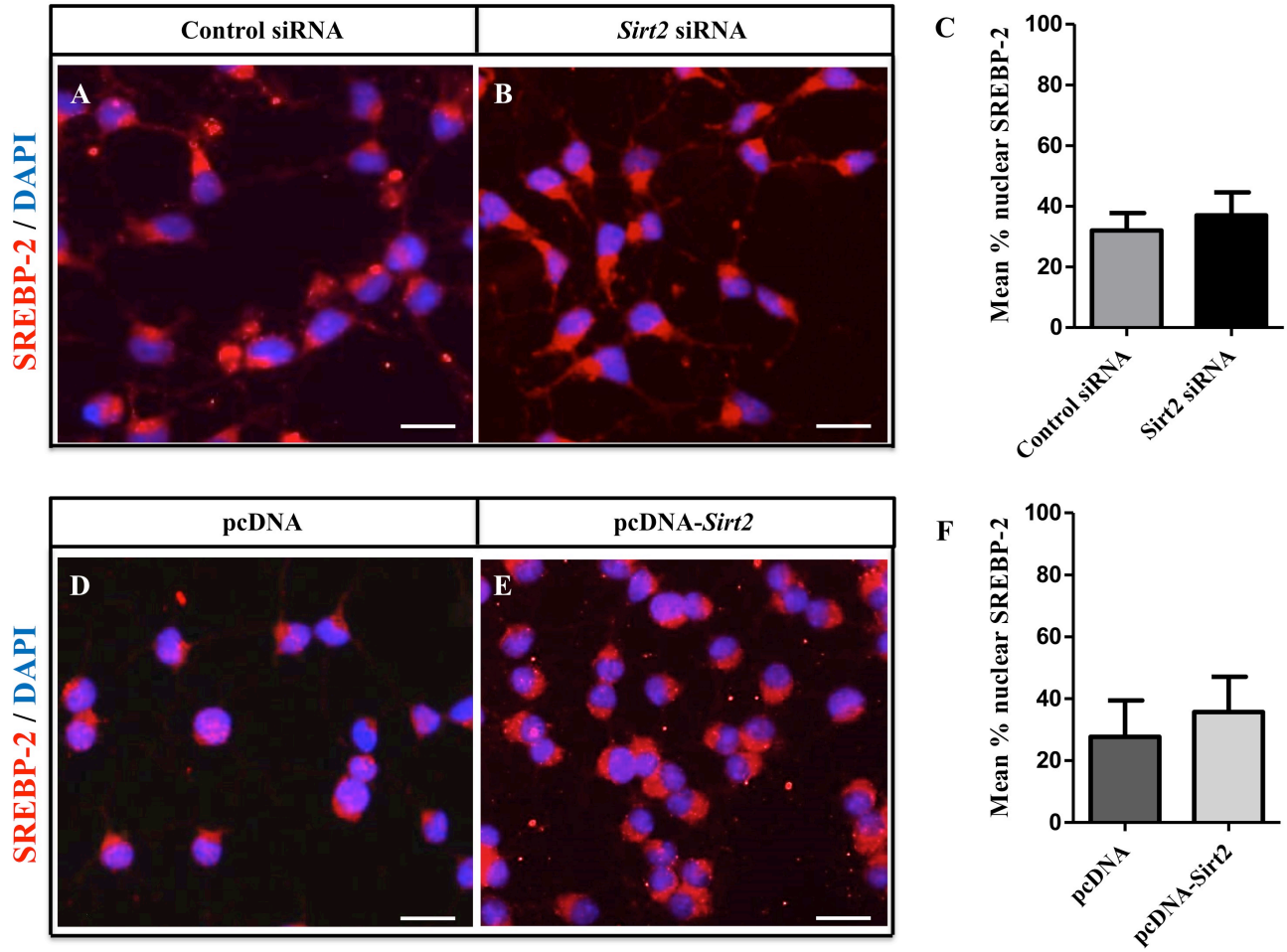

Figure 5.5: *Sirt2* knock-down or *Sirt2* overexpression in CG4-OL cells does not impact the nuclear translocation of SREBP-2. Representative images of CG4-OLs cells transfected with the control siRNA (**A**) and *Sirt2* siRNA (**B**) or pcDNA (**D**) and pcDNA-*Sirt2* (**E**) at day 6 under differentiation conditions. Scale bar, 100 µm. Blinded counts (n=3; >1500 cells) of SREBP-2 (red) expression in the nucleus (DAPI; blue) showed no difference in the subcellular localization of SREBP-2 in CG4-OL cells after *Sirt2* downregulation (**C**) or *Sirt2* overexpression (**F**). Mean ± SEM; unpaired t-test.

5.5 Discussion

Myelin is highly enriched in cholesterol, comprising ~80% of total brain cholesterol (Dietschy and Turley, 2004; Muse et al., 2001). Cholesterol is thought to play a vital role in transport and sorting of the myelin proteins (Saher and Simons, 2010; Saher et al., 2005; Saher et al., 2009; Simons et al., 2000; Werner et al., 2013). Cholesterol-enriched membrane domains in OPCs may also be important for efficient signal transduction to facilitate the differentiation (Mathews and Appel, 2016). Defects in the cholesterol biosynthesis pathway can cause dysmyelination, reduced myelin gene expression, and impaired axon wrapping in both the CNS (Mathews et al., 2014; Mathews and Appel, 2016; Saher et al., 2005) and PNS (Saher et al., 2009; Verheinjen et al., 2009).

SREBP-2 is a key transcription factor that modulates cholesterol biosynthesis. SREBP-2 is synthesized in the endoplasmic reticulum, where it binds to SCAP. Low cellular sterol level induces SREBP-2 processing and translocation to the nucleus where it activates downstream target genes (Horton et al., 2002; Horton et al., 2003). Previous studies using SIRT2 specific inhibitors AGK2, AK-1, and AK-7 were reported to show that the deacetylase activity of SIRT2 impacted sterol biosynthesis by regulating nuclear trafficking of SREBP-2 protein in neuronal cells (Luthi-Carter et al., 2010; Taylor et al., 2011). Overexpression of *Sirt2* increased nuclear translocation of SREBP-2, while overexpression of deacetylase-deficient *Sirt2* (Sirt2H150Y) or pharmacological inhibition of SIRT2 reduced the nuclear translocation of SREBP-2 (Luthi-Carter et al., 2010; Taylor et al., 2011). *In silico* analysis revealed the presence of two lysine residues at K310 and K329 in the DNA binding domain of SREBP-2 (Fig. 5.6A). These lysine residues are highly conserved across various SREBPs of which K283 and K303 in SREBP-1c have been shown to be deacetylated by SIRT1 (Ponugoti et al., 2010; Walker et al., 2010).

Hence, it is possible the two conserved lysine residues in SREBP-2 would be potential deacetylation sites for SIRT2.

Loss of *Sirt2* function in Schwann cells has been shown to delay myelin formation in PNS (Beirowski et al., 2011). *Sirt2* expression is also upregulated during OL differentiation and in CNS myelination (Ji et al., 2011; Li et al., 2007a; Werner et al., 2007; Zhu et al., 2012). Previous work from our lab demonstrates that *Sirt2* expression promotes differentiation in CG4-OLs, including upregulation of MBP expression and enhanced outgrowth of cellular processes (Ji et al., 2011). While α-tubulin has been identified as a primary target of SIRT2 in oligodendroglial cells *in vitro* (Li et al., 2007a), this may not be the case *in vivo* (Bobrowska et al., 2012). Thus, it is postulated that SREBP-2 may be a possible target of SIRT2 during OL differentiation and myelination. This would not only drive sterol synthesis for the formation of myelin membranes (Saher et al., 2005; Mathews et al., 2014) but may indirectly facilitate myelin gene expression (Mathews and Appel, 2016).

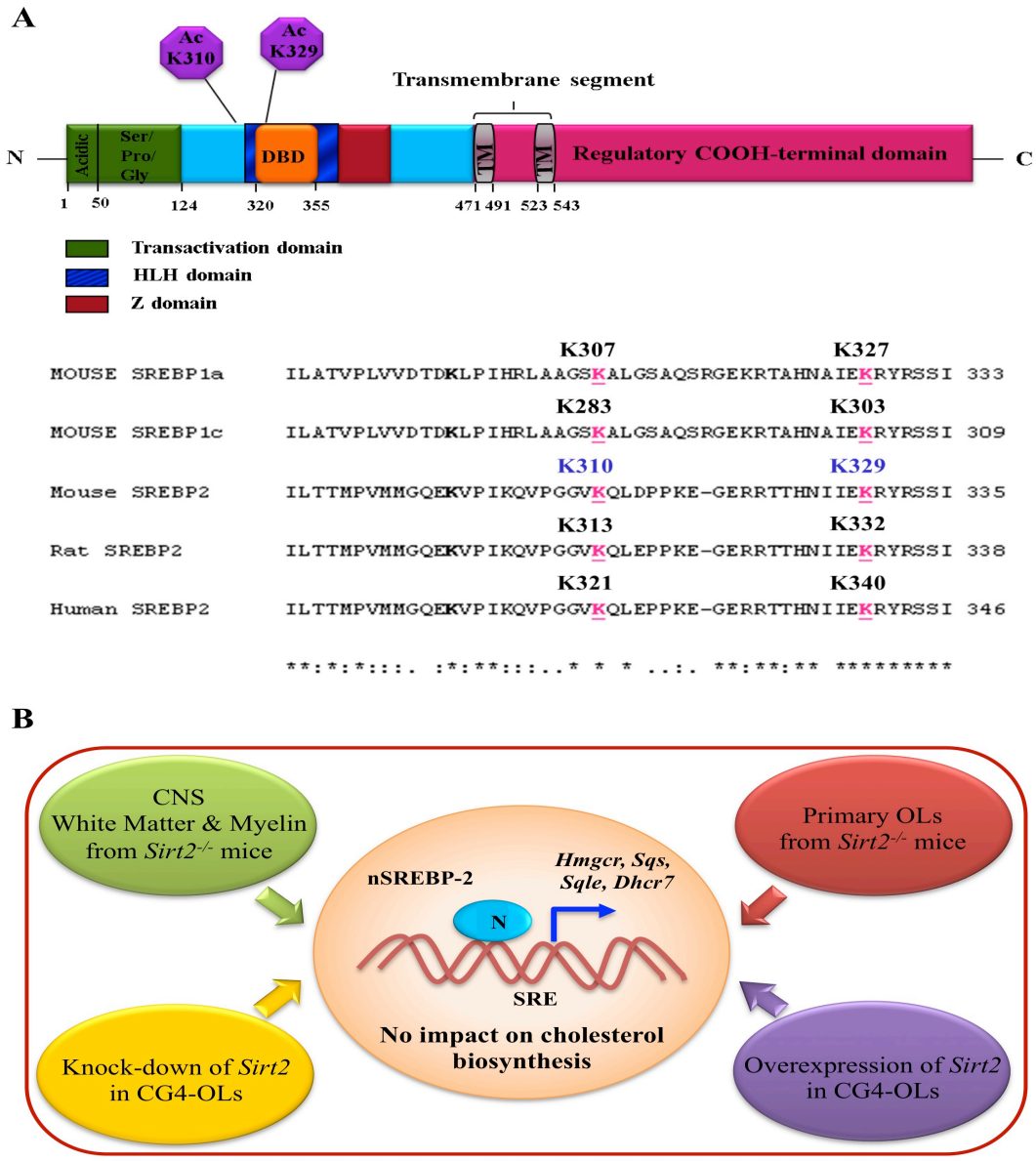

Figure 5.6: Schematic diagram depicting speculative role of *Sirt2* in SREBP-2 nuclear trafficking and cholesterol biosynthesis. (**A**) *In-silico* analysis revealed putative lysine acetylation sites in the DNA binding domain of SREBP-2 protein. Sequence alignment of the conserved lysine residues in mouse, rat and human SREBP proteins with predicted acetylation lysine residues highlighted in red. (**B**) Acetylation/deacetylation regulates nuclear trafficking and activity of mature SREBP-2 (N-terminal fragment). In the nucleus, SREBP-2 binds to sterol responsive element (SRE) and activates the downstream genes encoding enzymes involved in cholesterol biosynthesis. Collectively, our findings show no impact of *Sirt2* expression on the cholesterol biosynthesis pathway indicating that SREBP-2 is not a primary target of SIRT2 during oligodendroglial differentiation.

In the present study, I found no impact of *Sirt2* expression on cholesterol biosynthesis in the CNS white matter *in vivo* and OL cultures *in vitro* (Fig. 5.6B). Although *Sirt2*$^{-/-}$ mice lack *Sirt2* mRNA and SIRT2 protein expression in white matter tracts, the expression level of *Srebp2* or four of the key genes in the biosynthesis pathway were not altered significantly (Fig. 5.1). Furthermore, there was no significant difference in cholesterol content of purified myelin from *Sirt2*$^{-/-}$ and WT mice. Although OLs are thought to be primarily responsible for the production of sterol required for myelin formation, cholesterol derived from extracellular sources may help to maintain the integrity of myelin sheath (Saher et al., 2005; Verheijen et al., 2009). Thus, it is possible that in *Sirt2*$^{-/-}$ mice OLs might depend upon external sources of cholesterol for myelin synthesis *in vivo*. To negate this caveat, primary OL and CG4-OL cultures were differentiated *in vitro* to assess the role of SIRT2 in cholesterol biosynthesis. In mammalian cells, the presence of excess sterol induces feedback regulation by promoting the retention of SREBP-SCAP complex in the endoplasmic reticulum and inhibiting SREBP processing (Wang et al., 1994; Yang et al., 2002). To control the presence of cholesterol in the media, CG4-OLs and primary OLs were cultured in media containing normal serum (FBS) or delipidated serum (DLFBS). The loss of *Sirt2* in primary OLs (Fig. 5.2), as well as knockdown of *Sirt2* or overexpression of *Sirt2* in CG4-OLs (Fig. 5.3 and 5.4), did not alter expression of cholesterol biosynthetic genes and total cholesterol content.

The findings presented here are in agreement with Bobrowska et al., (2012) who did not find a change in the gene expression profile of enzymes involved in cholesterol biosynthesis in the cortex, hippocampus or brain stem of *Sirt2*$^{-/-}$ mice. Unlike neuronal cells (Luthi-Carter et al., 2010; Taylor et al., 2011), knockdown or overexpression of *Sirt2* did not impact nuclear translocation of SREBP-2 in OLs (Fig. 5.5). This discrepancy could be due to the cell type

specific differences in the expression pattern, as *Sirt2* is more abundantly expressed by OLs than other cell types in the CNS (Zhang et al., 2014). Moreover, the predominate isoform in OLs is SIRT2.2 (Zhu et al., 2012), whereas in neurons its SIRT2.1 (Luthi-Carter et al., 2010), which may result in selective deacetylation targets. However, usage of neurons isolated from *Sirt2*$^{-/-}$ and WT mice, as a positive control would confirm that SIRT2 plays role in cholesterol biosynthesis in neurons. In addition, loss of *Sirt2* could activate compensatory sirtuins to restore cholesterol biosynthesis. In summary, I have presented several lines of evidence (Fig. 5.6B) to conclude that *Sirt2* does not impact cholesterol biosynthesis during OL differentiation and myelination in the developing CNS white matter.

6. GENERAL DISCUSSION

This thesis uncovers the molecular mechanism by which the expression of *Sirt2* is regulated during OL development and addresses the functional role of *Sirt2* in CNS myelination and MS. It was previously known that the expression of SIRT2 increases as OLs differentiate (Ji et al., 2011), although the mechanism involved in regulating the expression of SIRT2 during oligodendrogenesis was largely unknown. The RNA binding protein QKI regulates the expression of several myelin-specific transcripts either directly or indirectly for proper OL development and myelination (Chen et al., 2007b; Larocque et al., 2002; Wu et al., 2002; Li et al., 2000; Zhao et al., 2006a; Zhao et al., 2010; Larocque et al., 2005; Doukhanine et al., 2010; Zhao et al., 2006b; Zearfoss et al., 2011). Although SIRT2 protein is absent in qk^{v}/qk^{v} mutant mice (Zhu et al., 2012), it was not known whether QKI directly interacts with *Sirt2* mRNA to modulate OL development. In this study, I have conclusively demonstrated that QKI directly binds to the QRE present at 1853 bp in the 3′UTR of *Sirt2* mRNA (Chapter 3). This interaction stabilizes *Sirt2* mRNA and increases the accumulation and availability of *Sirt2* transcripts for translation. The increase in the expression of QKI during OL differentiation could promote the expression of SIRT2 in premyelinating and myelinating OLs, where it is highly expressed (North et al., 2003). A definitive role for QKI and *Sirt2* interactions in the regulation of myelination *in vivo* remains unclear, but it is plausible that binding of QKI to *Sirt2* mRNA at early stages of OL development is important for regulating the timing of differentiation.

The involvement of *Sirt2* in OL process formation and maturation *in vitro* was identified previously in our lab using CG4-OLs (Ji et al., 2011). However, the role of *Sirt2* in CNS myelination *in vivo* and disease severity of EAE, a mouse model of human MS, remained elusive. To address this, I have used *Sirt2* null mice to determine the impact of loss of *Sirt2* on

myelination and MS. My findings reveal that in the absence of *Sirt2,* the expression of myelin specific genes such as *Mbp* and *Plp* are downregulated in the CNS white matter. In addition, the proliferation and differentiation of OLs in the *Sirt2*$^{-/-}$ mice were impaired (Chapter 4). These findings are in agreement with our previous report (Ji et al., 2011) that *Sirt2* promotes the expression of MBP and cell arborization in CG4-OLs *in vitro*. Electron microscopic analysis revealed a reduction in the number of myelinated axons in *Sirt2*$^{-/-}$ mice with uncompact myelin sheath. This indicates that *Sirt2* plays a critical role in OL development and myelination of axons in the CNS.

The EAE induction study shows that loss of *Sirt2* results in an increased severity of EAE (Chapter 4). This suggests the potentially important contribution of *Sirt2* in the pathogenesis of MS. Recently, EAE models were criticized as some of the therapies developed using EAE models were inefficient in human MS (Longbrake and Racke, 2009; Procaccini et al., 2015). This discrepancy could be due to genetic and environmental factors that contribute to the complexity of MS in humans. Another drawback of the EAE model is that it affects spinal cord white matter primarily with little involvement of brain (Procaccini et al., 2015). In addition to EAE, Theiler's murine encephalomyelitis virus (TMEV) and cuprizone are used to study CNS demyelination. However, EAE is the commonly used animal model of MS because of its immunological and pathological similarity with human MS (Gold et al., 2006; Simmons et al., 2013; Bittner et al., 2014). Immunostaining analysis of human MS postmortem brain sections revealed the presence of SIRT2 in the shadow plaques. This indicates the putative role of SIRT2 in myelin repair. EAE induction using a higher dose of MOG (200 - 300ug) hinders remyelination efficiency with infiltrating macrophages and microglia, and further investigation

using lower doses of MOG (50ug), which induces relapsing-remitting disease course could provide insight on the role of SIRT2 in remyelination.

In neuronal cells, SIRT2 has been demonstrated to play a role in cholesterol biosynthesis by promoting the nuclear translocation of SREBP-2 (Luthi-Carter et al., 2010; Taylor et al., 2011). Cholesterol is essential for myelin formation and defects in cholesterol biosynthesis significantly reduce myelin gene expression and myelination (Mathews et al., 2014; Mathews and Appel, 2016; Saher et al., 2005). I hypothesized that SREBP-2 is a possible target of SIRT2 through which *Sirt2* could regulate myelin gene expression and myelination. However, expression of cholesterol biosynthetic genes and total cholesterol content was not altered in the CNS white matter *in vivo* and OL cultures *in vitro* in the absence of *Sirt2*. Knock-down or overexpression of *Sirt2* in CG4-OLs did not impact nuclear translocation of SREBP-2. Thus, SREBP-2 and the downstream sterol biosynthesis pathway is not regulated by SIRT2 in OLs during CNS myelination (Chapter 5). This finding is consistent with a previous study where no change in the expression of enzymes involved in cholesterol biosynthesis was observed in the whole brain of *Sirt2* knock-out mice (Bobrowska et al., 2012) . However, further analysis on the expression and activity of other sirtuins could give an idea on whether another SIRT plays a compensatory role in the absence of *Sirt2*.

7. FUTURE DIRECTIONS

7.1 QKI-*Sirt2* interaction

QKI post-transcriptionally regulates the expression of several myelin-specific transcripts by modulating target mRNA stability, splicing, localization and translation. In this thesis, I have reported the interaction of QKI with the *Sirt2* mRNA at a common QKI binding site present in the 3' UTR, which promotes the stability of *Sirt2* mRNA. In addition to the two putative QREs in the 3' UTR of *Sirt2* mRNA, I observed the presence of a QRE at intron 2 of *Sirt2* pre-mRNA. Furthermore, presence of putative QRE was reported in the exon 2 of *Sirt2* mRNA (Darbelli et al., 2016), suggesting that QKI may also regulate the splicing of *Sirt2* mRNA, which remains to be explored. The role of QKI in *Sirt2* mRNA splicing could be characterized by generating a *Sirt2* minigene reporter construct containing the genomic DNA starting from exon 1 to exon 4 of the *Sirt2* gene with wild-type putative QREs or mutated putative QREs. Transfection of the *Sirt2* minigene reporter construct with wild-type putative QREs or mutated putative QREs in HEK293T cells followed by RNA co-IP would reveal the involvement of QKI in *Sirt2* mRNA splicing. The functional importance of QKI-*Sirt2* interaction in the regulation of myelination *in vivo* remains unclear. To address this, CRISPR-Cas9 system could be used to mutate or delete the QRE at 1853 bp in the 3′UTR of *Sirt2* mRNA or the whole 3' UTR of *Sirt2* mRNA with guide RNAs. This could uncover the role of QKI-*Sirt2* interaction *in vivo*. Although in practice, the CRISPR-Cas9 system creates off-target deletions, selection of target sites with low GC content (≤ 35%) and designing guide RNAs with 17-18 nucleotides have been reported to reduce off-target effects (Peng et al., 2016).

7.2 *Sirt2* in CNS myelination and MS

In this thesis I have demonstrated the importance of SIRT2 in OL development, myelination and MS using constitutive *Sirt2* knockout mice, in which the target gene is inactivated in a whole animal. However, specific deletion of *Sirt2* in OLs using $Olig2^{cre}$ (immature OLs) or Plp^{cre} (mature OLs) will reveal the stage specific role of *Sirt2* in OL proliferation and differentiation. Given that SIRT2 undergoes incorporation into the myelin sheath near PLP in paranodal loops (Li et al., 2007a; Werner et al., 2007), evaluating the distribution of paranodal proteins, Caspr and Ankyrin G, by immunostaining brain and spinal cord sections from $Sirt2^{-/-}$ mice would give insights into the role of SIRT2 in maintaining the integrity and stability of paranodal junctions. Electron microscopic analysis of longitudinal sections could be used to assess the ultra-structural defects in the organization of paranodal loops. In addition, the role of SIRT2 in axo-glial interactions will be investigated using OL-dorsal root ganglion co-cultures by overexpressing and knocking down *Sirt2 in vitro*. Further, RNA sequencing using the brain samples of $Olig2^{cre}$ or Plp^{cre} *Sirt2* knockout mice could be used to evaluate the downstream targets through which OL-specific SIRT2 regulates myelination and myelin repair. Similarly, proteomic analysis of white matter from wild-type and $Sirt2^{-/-}$ mice would shed light on the functional importance of SIRT2 deacetylase activity in myelin assembly.

EAE induction and clinical scoring revealed the protective role of SIRT2 in a mouse model of MS. Further brain and spinal cord sections from the EAE mouse model could be immunostained for various myelin proteins and inflammatory markers to determine the extent of myelin loss and the severity of inflammation, respectively. Expression of SIRT2 in the shadow plaques of human MS postmortem brain sections indicates a plausible role for SIRT2 in remyelination; however, a definitive role in remyelination is lacking. Cuprizone (copper

chelator)-induced demyelination and cuprizone withdrawal-induced remyelination could be used to study the role of SIRT2 in remyelination. In addition, lower doses of MOG could be utilized to induce a relapsing-remitting EAE disease course to provide further insight into the role of SIRT2 in remyelination.

8. CONCLUSION

Together, these findings suggest that expression of *Sirt2* is regulated by QKI for proper OL development and *Sirt2* positively regulates OPC proliferation, OL differentiation and myelination of axons in CNS. Furthermore, loss of *Sirt2* results in an increased severity in the EAE mouse model of MS. SIRT2 may have an important functional role during remyelination in human MS. However, *Sirt2* is not involved in SREBP-2 dependent cholesterol biosynthesis in OLs. Downstream targets of *Sirt2* remain to be explored to identify potential molecular targets for nutrient and pharmacological interventions that target myelin repair in MS.

REFERENCES

Åberg, K., Saetre, P., Jareborg, N., and Jazin, E. (2006b) Human QKI, a potential regulator of mRNA expression of human oligodendrocyte-related genes involved in schizophrenia. *Proc. Natl. Acad. Sci.* **103**, 7482–7487

Åberg, K., Saetre, P., Lindholm, E., Ekholm, B., Pettersson, U., Adolfsson, R., and Jazin, E. (2006a) Human QKI, a new candidate gene for schizophrenia involved in myelination. *Am. J. Med. Genet. Part B Neuropsychiatr. Genet.* **141B**, 84–90

Ainger, K., Avossa, D., Morgan, F., Hill, S. J., Barry, C., Barbarese, E., and Carson, J. H. (1993) Transport and localization of exogenous myelin basic protein mRNA microinjected into oligodendrocytes. *J. Cell Biol*. **123**, 431–441

Akiyama, K., Ichinose, S., Omori, A., Sakurai, Y., and Asou, H. (2002) Study of expression of myelin basic proteins (MBPs) in developing rat brain using a novel antibody reacting with four major isoforms of MBP. *J. Neurosci. Res.* **68**, 19–28

Amemiya-Kudo, M., Shimano, H., Hasty, A. H., Yahagi, N., Yoshikawa, T., Matsuzaka, T., Okazaki, H., Tamura, Y., Iizuka, Y., Ohashi, K., Osuga, J., Harada, K., Gotoda, T., Sato, R., Kimura, S., Ishibashi, S., and Yamada, N. (2002) Transcriptional activities of nuclear SREBP-1a, -1c, and -2 to different target promoters of lipogenic and cholesterogenic genes. *J. Lipid Res.* **43**, 1220–1235

Amor, S., Baker, D., Groome, N., and Turk, J. L. (1993) Identification of a major encephalitogenic epitope of proteolipid protein (residues 56-70) for the induction of

experimental allergic encephalomyelitis in Biozzi AB/H and nonobese diabetic mice. *J. Immunol.* **150**, 5666–5672

Amor, S., Groome, N., Linington, C., Morris, M. M., Dornmair, K., Gardinier, M. V, Matthieu, J. M., and Baker, D. (1994) Identification of epitopes of myelin oligodendrocyte glycoprotein for the induction of experimental allergic encephalomyelitis in SJL and Biozzi AB/H mice. *J. Immunol.* **153**, 4349–4356

Ascherio, A., and Munger, K. L. (2007) Environmental risk factors for multiple sclerosis. Part I: The role of infection. *Ann. Neurol.* **61**, 288–299

Ascherio, A., Munger, K. L., Lennette, E. T., Spiegelman, D., Hernan, M. A., Olek, M. J., Hankinson, S. E., and Hunter, D. J. (2001) Epstein-barr virus antibodies and risk of multiple sclerosis: A prospective study. *JAMA*. **286**, 3083–3088

Bachstetter, A. D., Webster, S. J., Van Eldik, L. J., and Cambi, F. (2013) Clinically relevant intronic splicing enhancer mutation in myelin proteolipid protein leads to progressive microglia and astrocyte activation in white and gray matter regions of the brain. *J. Neuroinflammation*. **10**, 911

Bae, N. S., Swanson, M. J., Vassilev, A., and Howard, B. H. (2004) Human histone deacetylase SIRT2 interacts with the homeobox transcription factor HOXA10. *J. Biochem.* **135**, 695–700

Baker, D., and Amor, S. (2014) Experimental autoimmune encephalomyelitis is a good model of multiple sclerosis if used wisely. *Mult. Scler. Relat. Disord.* **3**, 555–564

Barbarese, E. (2018) Spatial distribution of myelin basic protein mRNA and polypeptide in Quaking oligodendrocytes in culture. *J. Neurosci. Res.* **29**, 271–281

Barkovich, A. J. (2000) Concepts of myelin and myelination in neuroradiology. *Am. J. Neuroradiol.* **21**, 1099–1109

Barton, D. E., Arquint, M., Roder, J., Dunn, R., and Francke, U. (1987) The myelin-associated glycoprotein gene: Mapping to human chromosome 19 and mouse chromosome 7 and expression in quivering mice. *Genomics*. **1**, 107–112

Baudouin-Legros, M. (2005) Cell-specific posttranscriptional regulation of CFTR gene expression via influence of MAPK cascades on 3'UTR part of transcripts. *AJP Cell Physiol.* **289**, C1240–C1250

Bauer, N. G., Richter-Landsberg, C., and Ffrench-Constant, C. (2009) Role of the oligodendroglial cytoskeleton in differentiation and myelination. *Glia*. **57**, 1691–1705

Baumann, N., and Pham-Dinh, D. (2001) Biology of Oligodendrocyte and Myelin in the Mammalian Central Nervous System. *Physiol. Rev.* **81**, 871–927

Beirowski, B., Gustin, J., Armour, S. M., Yamamoto, H., Viader, A., North, B. J., Michan, S., Baloh, R. H., Golden, J. P., Schmidt, R. E., Sinclair, D. a., Auwerx, J., and Milbrandt, J. (2011) Sir-two-homolog 2 (Sirt2) modulates peripheral myelination through polarity protein Par-3/atypical protein kinase C (aPKC) signaling. *Proc. Natl. Acad. Sci.* **108**, E952–E961

Bénardais, K., Kotsiari, A., Škuljec, J., Koutsoudaki, P. N., Gudi, V., Singh, V., Vulinović, F., Skripuletz, T., and Stangel, M. (2013) Cuprizone [Bis(Cyclohexylidenehydrazide)] is Selectively Toxic for Mature Oligodendrocytes. *Neurotox. Res.* **24**, 244–250

Berard, J. L., Wolak, K., Fournier, S., and David, S. (2010) Characterization of relapsing-remitting and chronic forms of experimental autoimmune encephalomyelitis in C57BL/6 mice. *Glia*. **58**, 434–445

Bergles, D. E., and Richardson, W. D. (2015) Oligodendrocyte Development and Plasticity. *Cold Spring Harb. Perspect. Biol.* 10.1101/cshperspect.a020453

Beuck, C., Qu, S., Fagg, W. S., Jr, M. A., and Williamson, J. R. (2012) Structural analysis of the quaking homodimerization interface. *J. Mol. Biol.* **423**, 766–781

Bittner, S., Afzali, A. M., Wiendl, H., and Meuth, S. G. (2014) Myelin oligodendrocyte glycoprotein (MOG35-55) induced experimental autoimmune encephalomyelitis (EAE) in C57BL/6 mice. *JoVE*. **86**, e51275

Bizzozero, O. A., Pasquini, J. M., and Soto, E. F. (1982) Differential effect of colchicine upon the entry of proteins into myelin and myelin related membranes. *Neurochem. Res.* **7**, 1415–1425

Blakemore, W. F., and Franklin, R. J. M. (2008) Remyelination in experimental models of toxin-induced demyelination. *Curr. Top. Microbiol. Immunol*. 193–212

Blander, G., and Guarente, L. (2004) The Sir2 family of protein deacetylases. *Annu. Rev. Biochem.* **73**, 417–35

Bobrowska, A., Donmez, G., Weiss, A., Guarente, L., and Bates, G. (2012) SIRT2 ablation has no effect on tubulin acetylation in brain, cholesterol biosynthesis or the progression of Huntington's disease phenotypes in vivo. *PLoS One*. **7**, e34805

Bockbrader, K., and Feng, Y. (2008) Essential function, sophisticated regulation and pathological impact of the selective RNA-binding protein QKI in CNS myelin development. *Future Neurol.* **3**, 655–668

Boggs, J. M. (2006) Myelin basic protein: a multifunctional protein. *Cell. Mol. Life Sci.* **63**, 1945–1961

Boison, D., and Stoffel, W. (1989) Myelin-deficient rat: a point mutation in exon III (A----C, Thr75----Pro) of the myelin proteolipid protein causes dysmyelination and oligodendrocyte death. *EMBO J.* **8**, 3295–3302

Boison, D., and Stoffel, W. (1994) Disruption of the compacted myelin sheath of axons of the central nervous system in proteolipid protein-deficient mice. *Proc. Natl. Acad. Sci. U. S. A.* **91**, 11709–11713

Brachmann, C. B., Sherman, J. M., Devine, S. E., Cameron, E. E., Pillus, L., and Boeke, J. D. (1995) The SIR2 gene family, conserved from bacteria to humans, functions in silencing, cell cycle progression, and chromosome stability. *Genes Dev.* **9**, 2888–2902

Bradl, M., and Lassmann, H. (2010) Oligodendrocytes: biology and pathology. *Acta Neuropathol.* **119**, 37–53

Braun, P. E., Sandillon, F., Edwards, A., Matthieu, J. M., and Privat, A. (1988) Immunocytochemical localization by electron microscopy of 2'3'-cyclic nucleotide 3'-phosphodiesterase in developing oligodendrocytes of normal and mutant brain. *J. Neurosci.* **8**, 3057–3066

Brown, M., and Goldstein, J. (1997) SREBP pathway: regulation of cholesterol metabolism by proteolysis of membrane bound transcription factor. *Cell*. **89**, 331–340

Cai, J., Qi, Y., Hu, X., Tan, M., Liu, Z., Zhang, J., Li, Q., Sander, M., and Qiu, M. (2005) Generation of oligodendrocyte precursor cells from mouse dorsal spinal cord independent of Nkx6 regulation and Shh signaling. *Neuron*. **45**, 41–53

Campagnoni, A. T., and Skoff, R. P. (2001) The Pathobiology of Myelin Mutants Reveal Novel Biological Functions of the MBP and PLP Genes. *Brain Pathol.* **11**, 74–91

Campagnoni, A. T., Pribyl, T. M., Campagnoni, C. W., Kampf, K., Amur-Umarjee, S., Landry, C. F., Handley, V. W., Newman, S. L., Garbay, B., and Kitamura, K. (1993) Structure and developmental regulation of Golli-mbp, a 105-kilobase gene that encompasses the myelin basic protein gene and is expressed in cells in the oligodendrocyte lineage in the brain. *J. Biol. Chem.* **268**, 4930–4938

Campagnoni, C. W., Carey, G. D., and Campagnoni, A. T. (1978) Synthesis of myelin basic proteins in the developing mouse brain. *Arch. Biochem. Biophys.* **190**, 118–125

Carson, J. H., Worboys, K., Ainger, K., and Barbarese, E. (1997) Translocation of myelin basic protein mRNA in oligodendrocytes requires microtubules and kinesin. *Cell Motil.* **38**, 318–328

Casaccia-Bonnefil, P., Hardy, R. J., Teng, K. K., Levine, J. M., Koff, A., and Chao, M. V (1999) Loss of p27Kip1 function results in increased proliferative capacity of oligodendrocyte progenitors but unaltered timing of differentiation. *Dev*. **126**, 4027–4037

Casaccia-Bonnefil, P., Tikoo, R., Kiyokawa, H., Friedrich, V., Chao, M. V, and Koff, A. (1997) Oligodendrocyte precursor differentiation is perturbed in the absence of the cyclin-dependent kinase inhibitor p27Kip1. *Genes Dev*. **11**, 2335–2346

Chen, T., and Richard, S. (1998) Structure-function analysis of Qk1: a lethal point mutation in mouse quaking prevents homodimerization. *Mol. Cell. Biol.* **18**, 4863–4871

Chen, Y., Balasubramaniyan, V., Peng, J., Hurlock, E. C., Tallquist, M., Li, J., and Lu, Q. R. (2007a) Isolation and culture of rat and mouse oligodendrocyte precursor cells. *Nat. Protoc.* **2**, 1044–1051

Chen, Y., Tian, D., Ku, L., Osterhout, D. J., and Feng, Y. (2007b) The selective RNA-binding protein quaking I (QKI) is necessary and sufficient for promoting oligodendroglia differentiation. *J. Biol. Chem.* **282**, 23553–23560

Chénard, C. A., and Richard, S. (2008) New implications for the QUAKING RNA binding protein in human disease. *J. Neurosci. Res.* **86**, 233–242

Chernoff, G. F. (1981) Shiverer: an autosomal recessive mutant mouse with myelin deficiency. *J. Hered.* **72**, 128

Chew, L.-J., Coley, W., Cheng, Y., and Gallo, V. (2010) Mechanisms of regulation of oligodendrocyte development by p38 mitogen-activated protein kinase. *J. Neurosci.* **30**, 11011–11027

Choi, Y. H., Kim, H., Lee, S. H., Jin, Y.-H., and Lee, K. Y. (2013) ERK1/2 regulates SIRT2 deacetylase activity. *Biochem. Biophys. Res. Commun.* **437**, 245–249

Colman, D. R., Kreibich, G., Frey, A. B., and Sabatini, D. D. (1982) Synthesis and incorporation of myelin polypeptides into CNS myelin. *J. Cell Biol.* **95**, 598–608

Compston, A., and Coles, A. (2008) Multiple sclerosis. *Lancet*. **372**, 1502–1517

Crawford, A. H., Tripathi, R. B., Richardson, W. D., and Franklin, R. J. M. (2016) Developmental Origin of Oligodendrocyte Lineage Cells Determines Response to Demyelination and Susceptibility to Age-Associated Functional Decline. *Cell Rep.* **15**, 761–773

Dan, L., Klimenkova, O., Klimiankou, M., Klusman, J.-H., van den Heuvel-Eibrink, M. M., Reinhardt, D., Welte, K., and Skokowa, J. (2012) The role of sirtuin 2 activation by nicotinamide phosphoribosyltransferase in the aberrant proliferation and survival of myeloid leukemia cells. *Haematologica*. **97**, 551–559

Darbelli, L., Vogel, G., Almazan, G., and Richard, S. (2016) Quaking regulates Neurofascin 155 expression for myelin and axoglial junction maintenance. *J. Neurosci.* **36**, 4106–4120

Das, C., Lucia, M. S., Hansen, K. C., and Tyler, J. K. (2009) CBP / p300-mediated acetylation of histone H3 on lysine 56. *Nature*. **459**, 113–117

Dautigny, A., Mattei, M.-G., Morello, D., Alliel, P. M., Pham-Dinh, D., Amar, L., Arnaud, D., Simon, D., Mattei, J.-F., Guenet, J.-L., Jollès, P., and Avner, P. (1986) The structural gene coding for myelin-associated proteolipid protein is mutated in jimpy mice. *Nature*. **321**, 867–869

de Ferra, F., Engh, H., Hudson, L., Kamholz, J., Puckett, C., Molineaux, S., and Lazzarini, R. A. (1985) Alternative splicing accounts for the four forms of myelin basic protein. *Cell*. **43**, 721–727

Delarasse, C., Daubas, P., Mars, L. T., Vizler, C., Litzenburger, T., Iglesias, A., Bauer, J., Gaspera, B. Della, Schubart, A., Decker, L., Dimitri, D., Roussel, G., Dierich, A., Amor, S., Dautigny, A., Liblau, R., and Pham-dinh, D. (2003) Myelin / oligodendrocyte glycoprotein – deficient (MOG-deficient) mice reveal lack of immune tolerance to MOG in wild-type mice. *J. Clin. Invest.* **112**, 544–553

Denic, A., Johnson, A. J., Bieber, A. J., Warrington, A. E., Rodriguez, M., and Pirko, I. (2011) The relevance of animal models in multiple sclerosis research. *Pathophysiology*. **18**, 21–29

Dentinger, M. P., Barron, K. D., and Csiza, C. K. (1982) Ultrastructure of the central nervous system in a myelin deficient rat. *J. Neurocytol.* **11**, 671–691

Dietschy, J. M., and Turley, S. D. (2004) Cholesterol metabolism in the central nervous system during early development and in the mature animal. *J. Lipid Res.* **45**, 1375–1397

Doucette, J. R., Jiao, R., and Nazarali, A. J. (2010) Age-related and cuprizone-induced changes in myelin and transcription factor gene expression and in oligodendrocyte cell densities in the rostral corpus callosum of mice. *Cell. Mol. Neurobiol.* **30**, 607–629

Doukhanine, E., Gavino, C., Haines, J. D., Almazan, G., and Richard, S. (2010) The QKI-6 RNA binding protein regulates actin-interacting protein-1 mRNA stability during oligodendrocyte differentiation. *Mol. Biol. Cell*. **21**, 3029–3040

Dryden, S. C., Nahhas, F. A., Nowak, J. E., Goustin, A., and Tainsky, M. A. (2003) Role for human SIRT2 NAD-dependent deacetylase activity in control of mitotic exit in the cell cycle. *Mol. Cell. Biol.* **23**, 3173–3185

Duncan, I. D., Hammang, J. P., and Trapp, B. D. (1987) Abnormal compact myelin in the myelin-deficient rat: absence of proteolipid protein correlates with a defect in the intraperiod line. *Proc. Natl. Acad. Sci.* **84**, 6287–6291

Duncan, I. D., Hammang, J. P., Goda, S., and Quarles, R. H. (1989) Myelination in the jimpy mouse in the absence of proteolipid protein. *Glia*. **2**, 148–154

Eberlé, D., Hegarty, B., Bossard, P., Ferré, P., and Foufelle, F. (2004) SREBP transcription factors: Master regulators of lipid homeostasis. *Biochimie*. **86**, 839–848

Ebersole, T. A., Chen, Q., Justice, M. J., and Artzt, K. (1996) The quaking gene product necessary in embryogenesis and myelination combines features of RNA binding and signal transduction proteins. *Nat. Genet.* **12**, 260–265

Emery, B. (2010) Regulation of oligodendrocyte differentiation and myelination. *Science*. **330**, 779–782

Emery, B., Agalliu, D., Cahoy, J. D., Watkins, T. A., Dugas, J. C., Mulinyawe, S. B., Ibrahim, A., Ligon, K. L., Rowitch, D. H., and Barres, B. A. (2009) Myelin gene regulatory factor is a critical transcriptional regulator required for CNS myelination. *Cell*. **138**, 172–185

Emery, B., and Lu, Q. R. (2015) Transcriptional and epigenetic regulation of oligodendrocyte development and myelination in the central nervous system. *Cold Spring Harb. Perspect. Biol.* 10.1101/cshperspect.a020461

Finnin, M. S., Donigian, J. R., and Pavletich, N. P. (2001) Structure of the histone deacetylase SIRT2. *Nat. Struct. Biol.* **8**, 621–625

Fletcher, D. A., and Mullins, R. D. (2010) Cell mechanics and the cytoskeleton. *Nature*. **463**, 485–492

Flores, A. I., Narayanan, S. P., Morse, E. N., Shick, H. E., Yin, X., Kidd, G., Avila, R. L., Kirschner, D. A., and Macklin, W. B. (2008) Constitutively-active Akt induces enhanced myelination in the central nervous system. *J. Neurosci.* **28**, 7174–7183

Fogarty, M., Richardson, W. D., and Kessaris, N. (2005) A subset of oligodendrocytes generated from radial glia in the dorsal spinal cord. *Development*. **132**, 1951–1959

Freeman, S. A., Desmazières, A., Fricker, D., Lubetzki, C., and Sol-Foulon, N. (2016) Mechanisms of sodium channel clustering and its influence on axonal impulse conduction. *Cell. Mol. Life Sci.* **73**, 723–735

Fritz, R. B., Chou, C. H., and McFarlin, D. E. (1983) Relapsing murine experimental allergic encephalomyelitis induced by myelin basic protein. *J. Immunol.* **130**, 1024–1026

Frohman, E. M., Filippi, M., Stuve, O., Waxman, S. G., Corboy, J., Phillips, J. T., Lucchinetti, C., Wilken, J., Karandikar, N., Hemmer, B., Monson, N., De Keyser, J., Hartung, H., Steinman, L., Oksenberg, J. R., Cree, B. A., Hauser, S., and Racke, M. K. (2005) Characterizing the mechanisms of progression in multiple sclerosis: Evidence and new hypotheses for future directions. *Arch. Neurol.* **62**, 1345–1356

Frye, R. A. (2000) Phylogenetic classification of prokaryotic and eukaryotic Sir2-like proteins. *Biochem. Biophys. Res. Commun.* **273**, 793–798

Fujita, N., Sato, S., Ishiguro, H., Inuzuka, T., Baba, H., Kurihara, T., Takahashi, Y., and Miyatake, T. (1990) The large isoform of myelin-associated glycoprotein is scarcely expressed in the quaking mouse brain. *J. Neurochem.* **55**, 1056–1059

Fujita, N., Sato, S., Kurihara, T., Inuzuka, T., Takahashi, Y., and Miyatake, T. (1988) Developmentally regulated alternative splicing of brain myelin-associated glycoprotein mRNA is lacking in the quaking mouse. *FEBS Lett.* **232**, 323–327

Galarneau, A., and Richard, S. (2005) Target RNA motif and target mRNAs of the Quaking STAR protein. *Nat. Struct. Mol. Biol.* **12**, 691–698

Galarneau, A., and Richard, S. (2009) The STAR RNA binding proteins GLD-1, QKI, SAM68 and SLM-2 bind bipartite RNA motifs. *BMC Mol. Biol.* **10**, 47

Giandomenico, V., Simonsson, M., Grönroos, E., and Ericsson, J. (2003) Coactivator-dependent acetylation stabilizes members of the SREBP family of transcription factors. *Mol. Cell. Biol.* **23**, 2587–2599

Girolamo, F., Ferrara, G., Strippoli, M., Rizzi, M., Errede, M., Trojano, M., Perris, R., Roncali, L., Svelto, M., Mennini, T., and Virgintino, D. (2011) Cerebral cortex demyelination and oligodendrocyte precursor response to experimental autoimmune encephalomyelitis. *Neurobiol. Dis.* **43**, 678–689

Givogri, M. I., Bongarzone, E. R., Schonmann, V., and Campagnoni, A. T. (2001) Expression and regulation of golli products of myelin basic protein gene during in vitro development of oligodendrocytes. *J. Neurosci. Res.* **66**, 679–690

Gold, R., Linington, C., and Lassmann, H. (2006) Understanding pathogenesis and therapy of multiple sclerosis via animal models: 70 Years of merits and culprits in experimental autoimmune encephalomyelitis research. *Brain*. **129**, 1953–1971

Goverman, J., Perchellet, A., and Huseby, E. S. (2005) The role of CD8+ T cells in multiple sclerosis and its animal models. *Curr. Drug Targets - Inflamm. Allergy*. **4**, 239–245

Griffiths, I. R., Scott, I., McCulloch, M. C., Barrie, J. A., McPhilemy, K., and Cattanach, B. M. (1990) Rumpshaker mouse: A new X-linked mutation affecting myelination: Evidence for a defect in PLP expression. *J. Neurocytol.* **19**, 273–283

Griffiths, I., Klugmann, M., Anderson, T., Yool, D., Thomson, C., Schwab, M. H., Schneider, A., Zimmermann, F., McCulloch, M., Nadon, N., and Nave, K.-A. (1998) Axonal swellings and degeneration in mice lacking the major proteolipid of myelin. *Science.* **280**, 1610–1613

Gross, R. H., and Jager, P. L. De. (2011). MS: Epidemiology and Genetics. *Clinical Neuroimmunology,* 71–87

Hafler, D. A., Slavik, J. M., Anderson, D. E., O'Connor, K. C., De Jager, P., and Baecher-Allan, C. (2005) Multiple sclerosis. *Immunol. Rev.* **204**, 208–231

Hafner, M., Landthaler, M., Burger, L., Khorshid, M., Hausser, J., Berninger, P., Rothballer, A., Ascano, M., Jungkamp, A.-C., Munschauer, M., Ulrich, A., Wardle, G. S., Dewell, S., Zavolan, M., and Tuschl, T. (2010) Transcriptome-wide identification of RNA-binding protein and microRNA target sites by PAR-CLIP. *Cell*. **141**, 129–141

Haigis, M. C., and Sinclair, D. A. (2010) Mammalian sirtuins: biological insights and disease relevance. *Annu. Rev. Pathol. Mech. Dis.* **5**, 253–295

Hampton, D. W., Anderson, J., Pryce, G., Irvine, K.-A., Giovannoni, G., Fawcett, J. W., Compston, A., Franklin, R. J. M., Baker, D., and Chandran, S. (2008) An experimental model of secondary progressive multiple sclerosis that shows regional variation in gliosis, remyelination, axonal and neuronal loss. *J. Neuroimmunol.* **201**, 200–211

Han, Y., Jin, Y.-H., Kim, Y.-J., Kang, B.-Y., Choi, H.-J., Kim, D.-W., Yeo, C.-Y., and Lee, K.-Y. (2008) Acetylation of Sirt2 by p300 attenuates its deacetylase activity. *Biochem. Biophys. Res. Commun.* **375**, 576–80

Hanafy, K. A., and Sloane, J. A. (2011) Regulation of remyelination in multiple sclerosis. *FEBS Lett.* **585**, 3821–3828

Harauz, G., and Boggs, J. M. (2013) Myelin management by the 18.5-kDa and 21.5-kDa classic myelin basic protein isoforms. *J. Neurochem.* **125**, 334–361

Hardy, R. J. (1998a) Molecular defects in the dysmyelinating mutant quaking. *J. Neurosci. Res.* **51**, 417–422

Hardy, R. J. (1998b) QKI expression is regulated during neuron-glial cell fate decisions. *J. Neurosci. Res.* **54**, 46–57

Hardy, R. J., Loushin, C. L., Friedrich Jr., V. L., Chen, Q., Ebersole, T. A., Lazzarini, R. A., and Artzt, K. (1996) Neural cell type-specific expression of QKI proteins is altered in quaking viable mutant mice. *J. Neurosci.* **16**, 7941–7949

Hobson, G. M., Huang, Z., Sperle, K., Stabley, D. L., Marks, H. G., and Cambi, F. (2002) A PLP splicing abnormality is associated with an unusual presentation of PMD. *Ann. Neurol.* **52**, 477–488

Hofstetter, H. H., Shive, C. L., and Forsthuber, T. G. (2002) Pertussis toxin modulates the immune response to neuroantigens injected in incomplete Freund's adjuvant: Induction of Th1 cells and experimental autoimmune encephalomyelitis in the presence of high frequencies of Th2 cells. *J. Immunol.* **169**, 117–125

Horton, J. D., Goldstein, J. L., and Brown, M. S. (2002) SREBPs: activators of the complete program of cholesterol and fatty acid synthesis in the liver. *J. Clin. Invest.* **109**, 1125–1131

Horton, J. D., Shah, N. A., Warrington, J. A., Anderson, N. N., Park, S. W., Brown, M. S., and Goldstein, J. L. (2003) Combined analysis of oligonucleotide microarray data from transgenic and knockout mice identifies direct SREBP target genes. *Proc. Natl. Acad. Sci.* **100**, 12027–12032

Hu, Y., Doudevski, I., Wood, D., Moscarello, M., Husted, C., Genain, C., Zasadzinski, J. A. A., and Israelachvili, J. (2004) Synergistic interactions of lipids and myelin basic protein. *Proc. Natl. Acad. Sci. U. S. A.* **101**, 13466–13471

Hudson, L. D., Berndt, J. A., Puckett, C., Kozak, C. A., and Lazzarini, R. A. (1987) Aberrant splicing of proteolipid protein mRNA in the dysmyelinating jimpy mutant mouse. *Proc. Natl. Acad. Sci.* **84**, 1454–1458

Hurwitz, B. J. (2009) The diagnosis of multiple sclerosis and the clinical subtypes. *Ann. Indian Acad. Neurol.* **12**, 226–230

Inoue, T., Hiratsuka, M., Osaki, M., and Oshimura, M. (2007) The molecular biology of mammalian SIRT proteins: SIRT2 in cell cycle regulation. *Cell Cycle*. **6**, 1011–1018

Ishii, A., Fyffe-Maricich, S. L., Furusho, M., Miller, R. H., and Bansal, R. (2012) ERK1/ERK2 MAPK signaling is required to increase myelin thickness independent of oligodendrocyte differentiation and initiation of myelination. *J. Neurosci.* **32**, 8855–8864

Itier, J.-M., Ibáñez, P., Mena, M. A., Abbas, N., Cohen-Salmon, C., Bohme, G. A., Laville, M., Pratt, J., Corti, O., Pradier, L., Ret, G., Joubert, C., Periquet, M., Araujo, F., Negroni, J., Casarejos, M. J., Canals, S., Solano, R., Serrano, A., Gallego, E., Sánchez, M., Denèfle, P., Benavides, J., Tremp, G., Rooney, T. A., Brice, A., and García de Yébenes, J. (2003) Parkin gene inactivation alters behaviour and dopamine neurotransmission in the mouse. *Hum. Mol. Genet.* **12**, 2277–2291

Jacobs, L. D., Wende, K. E., Brownscheidle, C. M., Apatoff, B., Coyle, P. K., Goodman, A., Gottesman, M. H., Granger, C. V, Greenberg, S. J., Herbert, J., Krupp, L., Lava, N. S., Mihai, C., Miller, A. E., Perel, A., Smith, C. R., and Snyder, D. H. (1999) A profile of multiple sclerosis: The New York State Multiple Sclerosis Consortium. *Mult. Scler. J.* **5**, 369–376

Jacque, C., Delassalle, A., Raoul, M., and Baumann, N. (1983) Myelin basic protein deposition in the optic and sciatic nerves of dysmyelinating mutants quaking, jimpy, trembler, mld, and shiverer during development. *J. Neurochem.* **41**, 1335–1340

Jahn, O., Tenzer, S., and Werner, H. B. (2009) Myelin proteomics: Molecular anatomy of an insulating sheath. *Mol. Neurobiol.* **40**, 55–72

Jessen, K. R., and Mirsky, R. (2005) The origin and development of glial cells in peripheral nerves. *Nat. Rev. Neurosci.* **6**, 671–682

Ji, S., Doucette, J. R., and Nazarali, A. J. (2011) Sirt2 is a novel in vivo downstream target of Nkx2.2 and enhances oligodendroglial cell differentiation. *J. Mol. Cell Biol.* **3**, 351–359

Jin, Y. H., Kim, Y. J., Kim, D. W., Baek, K. H., Kang, B. Y., Yeo, C. Y., and Lee, K. Y. (2008) Sirt2 interacts with 14-3-3 β/γ and down-regulates the activity of p53. *Biochem. Biophys. Res. Commun.* **368**, 690–695

Jing, E., Gesta, S., and Kahn, C. R. (2007) SIRT2 regulates adipocyte differentiation through FoxO1 acetylation/deacetylation. *Cell Metab.* **6**, 105–114

Jurevics, H. A, Kidwai, F. Z., and Morell, P. (1997) Sources of cholesterol during development of the rat fetus and fetal organs. *J. Lipid Res.* **38**, 723–33

Jurevics, H., and Morell, P. (1995) Cholesterol for synthesis of myelin is made locally, not imported into brain. *J. Neurochem.* **64**, 895–901

Kamradt, T., Soloway, P. D., Perkins, D. L., and Gefter, M. L. (1991) Pertussis toxin prevents the induction of peripheral T cell anergy and enhances the T cell response to an encephalitogenic peptide of myelin basic protein. *J. Immunol.* **147**, 3296–3302

Kaplan, M. R., Cho, M. H., Ullian, E. M., Isom, L. L., Levinson, S. R., and Barres, B. A. (2001) Differential control of clustering of the sodium channels Nav1.2 and Nav1.6 at developing CNS nodes of Ranvier. *Neuron*. **30**, 105–119

Kaplan, M. R., Meyer-Franke, A., Lambert, S., Bennett, V., Duncan, I. D., Levinson, S. R., and Barres, B. A. (1997) Induction of sodium channel clustering by oligodendrocytes. *Nature*. **386**, 724–728

Kelly, G. S. (2010) A review of the sirtuin system, its clinical implications, and the potential role of dietary activators like resveratrol: part 2. *Altern. Med. Rev.* **15**, 313–28

Kessaris, N., Fogarty, M., Iannarelli, P., Grist, M., Wegner, M., and Richardson, W. D. (2006) Competing waves of oligodendrocytes in the forebrain and postnatal elimination of an embryonic lineage. *Nat. Neurosci.* **9**, 173–179

Klugmann, M., Schwab, M. H., Pühlhofer, A., Schneider, A., Zimmermann, F., Griffiths, I. R., and Nave, K.-A. (1997) Assembly of CNS myelin in the absence of proteolipid protein. *Neuron*. **18**, 59–70

Knapp, P. E., Skoff, R. P., and Redstone, D. W. (1986) Oligodendroglial cell death in jimpy mice: an explanation for the myelin deficit. *J. Neurosci.* **6**, 2813–2822

Kojima, K., Wekerle, H., Lassmann, H., Berger, T., and Linington, C. (1997) Induction of experimental autoimmune encephalomyelitis by CD4+ T cells specific for an astrocyte protein, Sl00ß BT - Advances in Research on Neurodegeneration (Mizuno, Y., Youdim, M. B. H., Calne, D. B., Horowski, R., Poewe, W., and Riederer, P. eds), pp. 43–51, Springer Vienna, Vienna

Kondo, T., Furuta, T., Mitsunaga, K., Ebersole, T. A., Shichiri, M., Wu, J., Artzt, K., Yamamura, K., and Abe, K. (1999) Genomic organization and expression analysis of the mouse qkI locus. *Mamm. Genome*. **10**, 662–669

Kotter, M. R., Stadelmann, C., and Hartung, H.-P. (2011) Enhancing remyelination in disease - Can we wrap it up? *Brain*. **134**, 1882–1900

Krishnamoorthy, G., Saxena, A., Mars, L. T., Domingues, H. S., Mentele, R., Ben-Nun, A., Lassmann, H., Dornmair, K., Kurschus, F. C., Liblau, R. S., and Wekerle, H. (2009) Myelin-specific T cells also recognize neuronal autoantigen in a transgenic mouse model of multiple sclerosis. *Nat. Med.* **15**, 626–632

Lai, C., Brow, M. A., Nave, K. A., Noronha, A. B., Quarles, R. H., Bloom, F. E., Milner, R. J., and Sutcliffe, J. G. (1987) Two forms of 1B236/myelin-associated glycoprotein, a cell adhesion molecule for postnatal neural development, are produced by alternative splicing. *Proc. Natl. Acad. Sci.* **84**, 4337–4341

Lappe-Siefke, C., Goebbels, S., Gravel, M., Nicksch, E., Lee, J., Braun, P. E., Griffiths, I. R., and Nave, K.-A. (2003) Disruption of Cnp1 uncouples oligodendroglial functions in axonal support and myelination. *Nat. Genet.* **33**, 366–74

Larocca, J. N., and Norton, W. T. (2007) Isolation of Myelin. *Curr. Protoc. Cell Biol.* **33**, 3.25.1-3.25.19

Larocque, D., Galarneau, A., Liu, H.-N., Scott, M., Almazan, G., and Richard, S. (2005) Protection of p27Kip1 mRNA by quaking RNA binding proteins promotes oligodendrocyte differentiation. *Nat. Neurosci.* **8**, 27–33

Larocque, D., Pilotte, J., Chen, T., Cloutier, F., Massie, B., Pedraza, L., Couture, R., Lasko, P., Almazan, G., and Richard, S. (2002) Nuclear retention of MBP mRNAs in the quaking viable mice. *Neuron*. **36**, 815–829

Lauriat, T. L., Shiue, L., Haroutunian, V., Verbitsky, M., Ares, M., Ospina, L., and McInnes, L. A. (2008) Developmental expression profile of quaking, a candidate gene for schizophrenia, and its target genes in human prefrontal cortex and hippocampus shows regional specificity. *J. Neurosci. Res.* **86**, 785–796

Levine, J. M., Reynolds, R., and Fawcett, J. W. (2001) The oligodendrocyte precursor cell in health and disease. *Trends Neurosci.* **24**, 39–47

LeVine, S. M., Wong, D., and Macklin, W. B. (1990) Developmental Expression of Proteolipid Protein and DM20 mRNAs and Proteins in the Rat Brain. *Dev. Neurosci.* **12**, 235–250

Levison, S. W., and Goldman, J. E. (1993) Both oligodendrocytes and astrocytes develop from progenitors in the subventricular zone of postnatal rat forebrain. *Neuron*. **10**, 201–212

Li, C., Tropak, M. B., Gerlai, R., Clapoff, S., Abramow-Newerly, W., Trapp, B., Peterson, A., and Roder, J. (1994) Myelination in the absence of myelin-associated glycoprotein. *Nature*. **369**, 747–750

Li, H., Lu, Y., Smith, H. K., and Richardson, W. D. (2007b) Olig1 and Sox10 interact synergistically to drive Myelin basic protein transcription in oligodendrocytes. *J. Neurosci.* **27**, 14375–14382

Li, W., Zhang, B., Tang, J., Cao, Q., Wu, Y., Wu, C., Guo, J., Ling, E.-A., and Liang, F. (2007a) Sirtuin 2, a mammalian homolog of yeast silent information regulator-2 longevity regulator, is an oligodendroglial protein that decelerates cell differentiation through deacetylating alpha-tubulin. *J. Neurosci.* **27**, 2606–2616

Li, Z., Zhang, Y., Li, D., and Feng, Y. (2000) Destabilization and mislocalization of myelin basic protein mRNAs in quaking dysmyelination lacking the QKI RNA-binding proteins. *J. Neurosci.* **20**, 4944–4953

Ligon, K. L., Kesari, S., Kitada, M., Sun, T., Arnett, H. A., Alberta, J. A., Anderson, D. J., Stiles, C. D., and Rowitch, D. H. (2006) Development of NG2 neural progenitor cells requires Olig gene function. *Proc. Natl. Acad. Sci.* **103**, 7853–7858

Lindholm, E., Ekholm, B., Shaw, S., Jalonen, P., Johansson, G., Pettersson, U., Sherrington, R., Adolfsson, R., and Jazin, E. (2001) A schizophrenia-susceptibility locus at 6q25, in one of the world's largest reported pedigrees. *Am. J. Hum. Genet.* **69**, 96–105

Linington, C., Berger, T., Perry, L., Weerth, S., Hinze-Selch, D., Zhang, Y., Lu, H.-C., Lassmann, H., and Wekerle, H. (1993) T cells specific for the myelin oligodendrocyte glycoprotein mediate an unusual autoimmune inflammatory response in the central nervous system. *Eur. J. Immunol.* **23**, 1364–1372

Liu, A., Muggironi, M., Marin-Husstege, M., and Casaccia-Bonnefil, P. (2003) Oligodendrocyte process outgrowth in vitro is modulated by epigenetic regulation of cytoskeletal severing proteins. *Glia*. **44**, 264–274

Liu, Z., Hu, X., Cai, J., Liu, B., Peng, X., Wegner, M., and Qiu, M. (2007) Induction of oligodendrocyte differentiation by Olig2 and Sox10: Evidence for reciprocal interactions and dosage-dependent mechanisms. *Dev. Biol.* **302**, 683–693

Lockhart, P. J., O'Farrell, C. A., and Farrer, M. J. (2004) It's a double knock-out! The quaking mouse is a spontaneous deletion of parkin and parkin co-regulated gene (PACRG). *Mov. Disord.* **19**, 101–104

Longbrake, E. E., and Racke, M. K. (2009) Why did IL-12/IL-23 antibody therapy fail in multiple sclerosis? *Expert Rev. Neurother.* **9**, 319–321

Lorenzetti, D., Antalffy, B., Vogel, H., Noveroske, J., Armstrong, D., and Justice, M. (2004a) The neurological mutant quaking viable is Parkin deficient. *Mamm. Genome*. **15**, 210–217

Lorenzetti, D., Bishop, C. E., and Justice, M. J. (2004b) Deletion of the Parkin coregulated gene causes male sterility in the quaking^{viable} mouse mutant. *Proc. Natl. Acad. Sci. U. S. A.* **101**, 8402 LP-8407

Louis, J. C., Magal, E., Muir, D., Manthorpe, M., and Varon, S. (1992a) CG-4, A new bipotential glial cell line from rat brain, is capable of differentiating in vitro into either mature oligodendrocytes or type-2 astrocytes. *J. Neurosci. Res.* **31**, 193–204

Louis, J.-C., Muir, D., and Varon, S. (1992b) Autocrine inhibition of mitotic activity in cultured oligodendrocyte-type-2 astrocyte (O-2A) precursor cells. *Glia*. **6**, 30–38

Love, S. (2006) Demyelinating diseases. *J. Clin. Pathol.* **59**, 1151–1159

Lu, Q. R., Sun, T., Zhu, Z., Ma, N., Garcia, M., Stiles, C. D., and Rowitch, D. H. (2002) Common developmental requirement for Olig function indicates a motor neuron/oligodendrocyte connection. *Cell*. **109**, 75–86

Lu, Z., Zhang, Y., Ku, L., Wang, H., Ahmadian, A., and Feng, Y. (2003) The quakingviable mutation affects qkI mRNA expression specifically in myelin-producing cells of the nervous system. *Nucleic Acids Res.* **31**, 4616–4624

Lublin, F. D., and Reingold, S. C. (1996) Defining the clinical course of multiple sclerosis. *Neurology*. **46**, 907–911

Lublin, F. D., Reingold, S. C., Cohen, J. A., Cutter, G. R., Sørensen, P. S., Thompson, A. J., Wolinsky, J. S., Balcer, L. J., Banwell, B., Barkhof, F., Bebo, B., Calabresi, P. A., Clanet, M., Comi, G., Fox, R. J., Freedman, M. S., Goodman, A. D., Inglese, M., Kappos, L., Kieseier, B. C.,

Lincoln, J. A., Lubetzki, C., Miller, A. E., Montalban, X., O'Connor, P. W., Petkau, J., Pozzilli, C., Rudick, R. A., Sormani, M. P., Stüve, O., Waubant, E., and Polman, C. H. (2014) Defining the clinical course of multiple sclerosis : The 2013 revisions Defining the clinical course of multiple sclerosis. *Neurology*. **83**, 278–286

Lucchinetti, C., Brück, W., Parisi, J., Scheithauer, B., Rodriguez, M., and Lassmann, H. (2000) Heterogeneity of multiple sclerosis lesions: Implications for the pathogenesis of demyelination. *Ann. Neurol.* **47**, 707–717

Luskin, M. B., and McDermott, K. (1994) Divergent lineages for oligodendrocytes and astrocytes originating in the neonatal forebrain subventricular zone. *Glia*. **11**, 211–226

Luthi-Carter, R., Taylor, D. M., Pallos, J., Lambert, E., Amore, A., Parker, A., Moffitt, H., Smith, D. L., Runne, H., Gokce, O., Kuhn, A., Xiang, Z., Maxwell, M. M., Reeves, S. A., Bates, G. P., Neri, C., Thompson, L. M., Marsh, J. L., and Kazantsev, A. G. (2010) SIRT2 inhibition achieves neuroprotection by decreasing sterol biosynthesis. *Proc. Natl. Acad. Sci. U. S. A.* **107**, 7927–7932

Lyons, D. A., Naylor, S. G., Scholze, A., and Talbot, W. S. (2009) Kif1b is essential for mRNA localization in oligodendrocytes and development of myelinated axons. *Nat. Genet.* **41**, 854–858

Mandler, M. D., Ku, L., and Feng, Y. (2014) A cytoplasmic quaking I isoform regulates the hnRNP F/H-dependent alternative splicing pathway in myelinating glia. *Nucleic Acids Res.* **42**, 7319–7329

Mangiardi, M., Crawford, D. K., Xia, X., Du, S., Simon-Freeman, R., Voskuhl, R. R., and Tiwari-Woodruff, S. K. (2011) An Animal Model of Cortical and Callosal Pathology in Multiple Sclerosis. *Brain Pathol.* **21**, 263–278

Mannara, F., Valente, T., Saura, J., Graus, F., Saiz, A., and Moreno, B. (2012) Passive Experimental Autoimmune Encephalomyelitis in C57BL/6 with MOG: Evidence of Involvement of B Cells. *PLoS One*. **7**, e52361

Marques, S., Zeisel, A., Codeluppi, S., Van Bruggen, D., Mendanha Falcão, A., Xiao, L., Li, H., Häring, M., Hochgerner, H., Romanov, R. A., Gyllborg, D., Muñoz Manchado, A., La Manno, G., Lönnerberg, P., Floriddia, E. M., Rezayee, F., Ernfors, P., Arenas, E., Hjerling-leffler, J., Harkany, T., Richardson, W. D., Linnarsson, S., Castelo-Branco, G., Bruggen, D. Van, Falcão, A. M., Xiao, L., Li, H., Häring, M., Hochgerner, H., Romanov, R. A., Gyllborg, D., Muñoz-manchado, A. B., Manno, G. La, Lönnerberg, P., Floriddia, E. M., Rezayee, F., Ernfors, P., Arenas, E., Hjerling-leffler, J., Harkany, T., Richardson, W. D., Linnarsson, S., Castelo-Branco, G., La Manno, G., Lönnerberg, P., Floriddia, E. M., Rezayee, F., Ernfors, P., Arenas, E., Hjerling-leffler, J., Harkany, T., Richardson, W. D., Linnarsson, S., Castelo-Branco, G., Bruggen, D. Van, Falcão, A. M., Xiao, L., Li, H., Häring, M., Hochgerner, H., Romanov, R. A., Gyllborg, D., Muñoz-manchado, A. B., Manno, G. La, Lönnerberg, P., Floriddia, E. M., Rezayee, F., Ernfors, P., Arenas, E., Hjerling-leffler, J., Harkany, T., Richardson, W. D., Linnarsson, S., and Castelo-Branco, G. (2016) Oligodendrocyte heterogneity in the mouse juvenile and adult central nervous system. *Science.* **352**, 1326–1329

Mathews, E. S., and Appel, B. (2016) Cholesterol Biosynthesis Supports Myelin gene expression and axon ensheathment through modulation of P13K/Akt/mTor signaling. *J. Neurosci.* **36**, 7628–7639

Mathews, E. S., Mawdsley, D. J., Walker, M., Hines, J. H., Pozzoli, M., and Appel, B. (2014) Mutation of 3-hydroxy-3-methylglutaryl CoA synthase I reveals requirements for isoprenoid and cholesterol synthesis in oligodendrocyte migration arrest, axon wrapping, and myelin gene expression. *J. Neurosci.* **34**, 3402–3412

Mathey, E. K., Derfuss, T., Storch, M. K., Williams, K. R., Hales, K., Woolley, D. R., Al-Hayani, A., Davies, S. N., Rasband, M. N., Olsson, T., Moldenhauer, A., Velhin, S., Hohlfeld, R., Meinl, E., and Linington, C. (2007) Neurofascin as a novel target for autoantibody-mediated axonal injury. *J. Exp. Med.* **204**, 2363–2372

Matsushima, G. K., and Morell, P. (2001) The neurotoxicant, cuprizone, as a model to study demyelination and remyelination in the central nervous system. *Brain Pathol.* **11**, 107–116

Matthieu, J.-M., Ginalski, H., Friede, R. L., Cohen, S. R., and Doolittle, D. P. (1980) Absence of myelin basic protein and major dense line in CNS myelin of the mld mutant mouse. *Brain Res.* **191**, 278–283

Matthieu, J.-M., Omlin, F. X., Ginalski-Winkelmann, H., and Cooper, B. J. (1984) Myelination in the CNS of mld mutant mice: Comparison between composition and structure. *Dev. Brain Res.* **13**, 149–158

Matthieu, J.-M., Tosic, M., and Roach, A. (1992) Myelin-deficient mutant mice. An in vivo model for inhibition of gene expression by natural antisense RNA. *Ann. N. Y. Acad. Sci.* **660**, 188–192

Maxwell, M. M., Tomkinson, E. M., Nobles, J., Wizeman, J. W., Amore, A. M., Quinti, L., Chopra, V., Hersch, S. M., and Kazantsev, A. G. (2011) The Sirtuin 2 microtubule deacetylase is an abundant neuronal protein that accumulates in the aging CNS. *Hum. Mol. Genet.* **20**, 3986–3996

Mecha, M., Carrillo-Salinas, F. J., Mestre, L., Feliú, A., and Guaza, C. (2013) Viral models of multiple sclerosis: Neurodegeneration and demyelination in mice infected with Theiler's virus. *Prog. Neurobiol.* **101**–**102**, 46–64

Michalski, J.-P., and Kothary, R. (2015) Oligodendrocytes in a nutshell. *Front. Cell. Neurosci.* **9**, 340

Michan, S., and Sinclair, D. (2007) Sirtuins in mammals: Insights into their biological function. *Biochem. J.* **404**, 1–13

Michishita, E., Park, J. Y., Burneskis, J. M., and Barrett, J. C. (2005) Evolutionarily conserved and nonconserved cellular localizations and functions of human SIRT proteins. *Mol. Biol. Cell*. **16**, 4623–4635

Miller, S. D., Karpus, W. J., and Davidson, T. S. (2007) Experimental autoimmune encephalomyelitis in the mouse. *Curr. Protoc. Immunol./ edited by John E. Coligan ... [et Al.]* **CHAPTER**, Unit-15.1

Milo, R., and Miller, A. (2014) Revised diagnostic criteria of multiple sclerosis. *Autoimmun. Rev.* **13**, 518–524

Miron, V. E., Kuhlmann, T., and Antel, J. P. (2011) Cells of the oligodendroglial lineage, myelination, and remyelination. *Biochim. Biophys. Acta - Mol. Basis Dis.* **1812**, 184–193

Miron, V. E., Rajasekharan, S., Jarjour, A. A., Zamvil, S. S., Kennedy, T. E., and Antel, J. P. (2007) Simvastatin regulates oligodendroglial process dynamics and survival. *Glia*. **55**, 130–143

Mix, E., Meyer-Rienecker, H., Hartung, H. P., and Zettl, U. K. (2010) Animal models of multiple sclerosis-Potentials and limitations. *Prog. Neurobiol.* **92**, 386–404

Morell, P., and Quarles, R. H. (1999) Myelin formation, structure and biochemistry. In: Basic Neurochemistry: Molecular, Cellular, and Medical Aspects, 6 edn, pp. 117–144, Siegel G. J., Agranoff B. W., Albers R. W., Fisher S. K. and Uhler M. D. (eds), Lippincott-Raven, New York

Müller, C., Bauer, N. M., Schäfer, I., and White, R. (2013) Making myelin basic protein -from mRNA transport to localized translation. *Front. Cell. Neurosci.* **7**, 1–7

Multiple Sclerosis International Federation (2013) Atlas of MS 2013: Mapping multiple sclerosis around the world.

Muse, E. D., Jurevics, H., Toews, A. D., Matsushima, G. K., and Morell, P. (2001) Parameters related to lipid metabolism as markers of myelination in mouse brain. *J. Neurochem.* **76**, 77–86

Nadon, N. L., Duncan, I. D., and Hudson, L. D. (1990) A point mutation in the proteolipid protein gene of the “shaking pup” interrupts oligodendrocyte development. *Development*. **110**, 529–537

Narayanan, S. P., Flores, A. I., Wang, F., and Macklin, W. B. (2009) Akt signals through the mammalian target of rapamycin, mTOR, pathway to regulate central nervous system myelination. *J. Neurosci.* **29**, 6860–6870

Nave, K.-A., and Werner, H. B. (2014) Myelination of the nervous system: Mechanisms and functions. *Annu. Rev. Cell Dev. Biol.* **30**, 503–533

Nave, K.-A., Floyd, E. B., and J. Milner, R. (1987) A single nucleotide difference in the gene for myelin proteolipid protein defines the jimpy mutation in mouse. *J. Neurochem.* **49**, 1873–1877

Ndubaku, U., and de Bellard, M. E. (2008) Glial cells: Old cells with new twists. *Acta Histochem.* **110**, 182–195

Nicolay, D. J., Doucette, J. R., and Nazarali, A. J. (2007) Transcriptional control of oligodendrogenesis. *Glia*. **55**, 1287–1299

Nishiyama, A., Lin, X.-H., Giese, N., Heldin, C.-H., and Stallcup, W. B. (1996) Co-localization of NG2 proteoglycan and PDGF α-receptor on O2A progenitor cells in the developing rat brain. *J. Neurosci. Res.* **43**, 299–314

Nishizawa, Y., Kurihara, T., Masuda, T., and Takahashi, Y. (1985) Immunohistochemical localization of 2′,3′-cyclic nucleotide 3′-phosphodiesterase in adult bovine cerebrum and cerebellum. *Neurochem. Res.* **10**, 1107–1118

Niu, J., Wang, L., Liu, S., Li, C., Kong, J., Shen, H. Y., and Xiao, L. (2012) An efficient and economical culture approach for the enrichment of purified oligodendrocyte progenitor cells. *J. Neurosci. Methods*. **209**, 241–249

North, B. J., and Verdin, E. (2007a) Interphase nucleo-cytoplasmic shuttling and localization of SIRT2 during mitosis. *PLoS One*. **2**, e784

North, B. J., and Verdin, E. (2007b) Mitotic regulation of SIRT2 by cyclin-dependent Kinase 1-dependent phosphorylation. *J. Biol. Chem.* **282**, 19546–19555

North, B. J., Marshall, B. L., Borra, M. T., Denu, J. M., and Verdin, E. (2003) The Human Sir2 Ortholog, SIRT2, Is an NAD^+-Dependent Tubulin Deacetylase. *Mol. Cell*. **11**, 437–444

Norton, W. T., and Poduslo, S. E. (1973a) Myelination in rat brain: Changes in myelin composition during brain maturation. *J. Neurochem.* **21**, 759–773

Norton, W. T., and Poduslo, S. E. (1973b) Myelination in rat brain: Method of myelin isolation. *J. Neurochem.* **21**, 749–757

Noseworthy, J. H., Lucchinetti, C., Rodriguez, M., and Weinshenker, B. G. (2000) Multiple sclerosis. *N. Engl. J. Med.* **343**, 938–952

O'Neill, R. C., Minuk, J., Cox, M. E., Braun, P. E., and Gravel, M. (1997) CNP2 mRNA directs synthesis of both CNP1 and CNP2 polypeptides. *J. Neurosci. Res.* **50**, 248–257

Outeiro, T. F., Kontopoulos, E., Altmann, S. M., Kufareva, I., Strathearn, K. E., Amore, A. M., Volk, C. B., Maxwell, M. M., Rochet, J.-C., McLean, P. J., Young, A. B., Abagyan, R., Feany,

M. B., Hyman, B. T., and Kazantsev, A. G. (2007) Sirtuin 2 inhibitors rescue α-synuclein-mediated toxicity in models of Parkinson's disease. *Science.* **317**, 516–519

Pais, T. F., Szegő, É. M., Marques, O., Miller-Fleming, L., Antas, P., Guerreiro, P., de Oliveira, R. M., Kasapoglu, B., and Outeiro, T. F. (2013) The NAD-dependent deacetylase sirtuin 2 is a suppressor of microglial activation and brain inflammation. *EMBO J.* **32**, 2603–2616

Pandithage, R., Lilischkis, R., Harting, K., Wolf, A., Jedamzik, B., Lüscher-Firzlaff, J., Vervoorts, J., Lasonder, E., Kremmer, E., Knöll, B., and Lüscher, B. (2008) The regulation of SIRT2 function by cyclin-dependent kinases affects cell motility. *J. Cell Biol.* **180**, 915–29

Pedraza, L., Huang, J. K., and Colman, D. (2009) Disposition of axonal caspr with respect to glial cell membranes: Implications for the process of myelination. *J. Neurosci. Res.* **87**, 3480–3491

Peng, R., Lin, G., and Li, J. (2016) Potential pitfalls of CRISPR/Cas9-mediated genome editing. *FEBS J.* **283**, 1218–1231

Peritz, T., Zeng, F., Kannanayakal, T. J., Kilk, K., Eiriksdottir, E., Langel, U., and Eberwine, J. (2006) Immunoprecipitation of mRNA-protein complexes. *Nat. Protoc.* **1**, 577–580

Peterson, L. K., and Fujinami, R. S. (2007) Inflammation, demyelination, neurodegeneration and neuroprotection in the pathogenesis of multiple sclerosis. *J. Neuroimmunol.* **184**, 37–44

Pfeiffer, S. E., Warrington, A. E., and Bansal, R. (1993) The oligodendrocyte and its many cellular processes. *Trends Cell Biol.* **3**, 191–197

Pham-Dinh, D., Mattei, M. G., Nussbaum, J. L., Roussel, G., Pontarotti, P., Roeckel, N., Mather, I. H., Artzt, K., Lindahl, K. F., and Dautigny, A. (1993) Myelin/oligodendrocyte glycoprotein is a member of a subset of the immunoglobulin superfamily encoded within the major histocompatibility complex. *Proc. Natl. Acad. Sci.* **90**, 7990–7994

Ponugoti, B., Kim, D. H., Xiao, Z., Smith, Z., Miao, J., Zang, M., Wu, S. Y., Chiang, C. M., Veenstra, T. D., and Kemper, J. K. (2010) SIRT1 deacetylates and inhibits SREBP-1C activity in regulation of hepatic lipid metabolism. *J. Biol. Chem.* **285**, 33959–33970

Popescu, B. F. G., Pirko, I., and Lucchinetti, C. F. (2013) Pathology of multiple sclerosis: Where do we stand? *Contin. Lifelong Learn. Neurol.* **19**, 901–921

Popko, B., Puckett, C., Lai, E., Shine, H. D., Readhead, C., Takahashi, N., Hunt, S. W., Sidman, R. L., and Hood, L. (1987) Myelin deficient mice: Expression of myelin basic protein and generation of mice with varying levels of myelin. *Cell*. **48**, 713–721

Procaccini, C., De Rosa, V., Pucino, V., Formisano, L., and Matarese, G. (2015) Animal models of multiple sclerosis. *Eur. J. Pharmacol.* **759**, 182–191

Quarles, R. H., Macklin, W. B., and Morell, P. (2006) Myelin formation, structure, and biochemistry. Basic Neurochemistry (eds. G.J. Siegel, et al.) 7th Edition, Elsevier, 51-71

Rafalski, V. A., Ho, P. P., Brett, J. O., Ucar, D., Dugas, J. C., Pollina, E. A., Chow, L. M. L., Ibrahim, A., Baker, S. J., Barres, B. A., Steinman, L., and Brunet, A. (2013) Expansion of oligodendrocyte progenitor cells following SIRT1 inactivation in the adult brain. *Nat. Cell Biol.* **15**, 614–624

Ramakrishnan, G., Davaakhuu, G., Kaplun, L., Chung, W.-C., Rana, A., Atfi, A., Miele, L., and Tzivion, G. (2014) Sirt2 deacetylase is a novel AKT binding partner critical for AKT activation by insulin. *J. Biol. Chem.* **289**, 6054–6066

Readhead, C., and Hood, L. (1990) The dysmyelinating mouse mutations shiverer (shi) and myelin deficient (shi^{mld}). *Behav. Genet.* **20**, 213–234

Remahl, S., and Hildebrand, C. (1990) Relation between axons and oligodendroglial cells during initial myelination I. The glial unit. *J. Neurocytol.* **19**, 313–328

Roach, A., Takahashi, N., Pravtcheva, D., Ruddle, F., and Hood, L. (1985) Chromosomal mapping of mouse myelin basic protein gene and structure and transcription of the partially deleted gene in shiverer mutant mice. *Cell*. **42**, 149–155

Rosenbluth, J., and Bobrowski-Khoury, N. (2013) Structural bases for central nervous system malfunction in the quaking mouse: Dysmyelination in a potential model of schizophrenia. *J. Neurosci. Res.* **91**, 374–381

Rosenbluth, J., Nave, K.-A., Mierzwa, A., and Schiff, R. (2006) Subtle myelin defects in PLP-null mice. *Glia*. **54**, 172–182

Roth, H. J., Hunkeler, M. J., and Campagnoni, A. T. (1985) Expression of myelin basic protein genes in several dysmyelinating mouse mutants during early postnatal brain development. *J Neurochem*. **45**, 572–580

Rothgiesser, K. M., Erener, S., Waibel, S., Lüscher, B., and Hottiger, M. O. (2010) SIRT2 regulates NF-κB-dependent gene expression through deacetylation of p65 Lys310. *J. Cell Sci.* **123**, 4251–4258

Roussel, G., Neskovic, N. M., Trifilieff, E., Artault, J.-C., and Nussbaum, J.-L. (1987) Arrest of proteolipid transport through the Golgi apparatus in Jimpy brain. *J. Neurocytol.* **16**, 195–204

Ryder, S. P., and Williamson, J. R. (2004) Specificity of the STAR/GSG domain protein Qk1 : Implications for the regulation of myelination. *RNA*. **10**, 1449–1458

Saher, G., and Simons, M. (2010) Cholesterol and myelin biogenesis. In: Harris J. (eds) Cholesterol binding and cholesterol transport proteins: Structure and function in health and disease *Subcellular biochemistry* (Harris, J. R. ed), Springer, Dordrecht, **51**, 489–508

Saher, G., and Stumpf, S. K. (2015) Cholesterol in myelin biogenesis and hypomyelinating disorders. *Biochim. Biophys. Acta - Mol. Cell Biol. Lipids*. **1851**, 1083–1094

Saher, G., and Stumpf, S. K. (2015) Cholesterol in myelin biogenesis and hypomyelinating disorders. *Biochim. Biophys. Acta - Mol. Cell Biol. Lipids*. **1851**, 1083–1094

Saher, G., Brügger, B., Lappe-Siefke, C., Möbius, W., Tozawa, R. I., Wehr, M. C., Wieland, F., Ishibashi, S., and Nave, K. A. (2005) High cholesterol level is essential for myelin membrane growth. *Nat. Neurosci.* **8**, 468–475

Saher, G., Quintes, S., and Nave, K. A. (2011) Cholesterol: A novel regulatory role in myelin formation. *Neuroscientist*. **17**, 79–93

Saher, G., Quintes, S., Möbius, W., Wehr, M. C., Krämer-Albers, E.-M., Brügger, B., and Nave, K.-A. (2009) Cholesterol regulates the endoplasmic reticulum exit of the major membrane protein P0 required for peripheral myelin compaction. *J. Neurosci.* **29**, 6094–6104

Sakai, J., Duncan, E. A., Rawson, R. B., Hua, X., Brown, M. S., and Goldstein, J. L. (1996) Sterol-regulated release of SREBP-2 from cell membranes requires two sequential cleavages, one within a transmembrane segment. *Cell*. **85**, 1037–1046

Sanders, B. D., Jackson, B., and Marmorstein, R. (2010) Structural basis for sirtuin function: What we know and what we don't. *Biochim. Biophys. Acta*. **1804**, 1604–1616

Scolding, N. J., Frith, S., Linington, C., Morgan, B. P., Campbell, A. K., and Compston, D. A. S. (1989) Myelin-oligodendrocyte glycoprotein (MOG) is a surface marker of oligodendrocyte maturation. *J. Neuroimmunol.* **22**, 169–176

Sidman, R. L., Dickie, M. M., and Appel, S. H. (1964) Mutant mice (quaking and jimpy) with deficient myelination in the central nervous system. *Science.* **144**, 309–311

Sidorova-Darmos, E., Wither, R. G., Shulyakova, N., Fisher, C., Ratnam, M., Aarts, M., Lilge, L., Monnier, P. P., and Eubanks, J. H. (2014) Differential expression of sirtuin family members in the developing, adult, and aged rat brain. *Front. Aging Neurosci.* **6**, 333

Silva, D. F., Esteves, A. R., Oliveira, C. R., and Cardoso, S. M. (2017) Mitochondrial metabolism power SIRT2-dependent deficient traffic causing Alzheimer's-disease related pathology. *Mol. Neurobiol.* **54**, 4021–4040

Simmons, S. B., Pierson, E. R., Lee, S. Y., and Goverman, J. M. (2013) Modeling the heterogeneity of multiple sclerosis in animals. *Trends Immunol.* **34**, 410–422

Simons, M., and Nave, K.-A. (2015) Oligodendrocytes: Myelination and axonal Support. *Cold Spring Harb. Perspect. Biol.* 10.1101/cshperspect.a020479

Simons, M., and Trajkovic, K. (2006) Neuron-glia communication in the control of oligodendrocyte function and myelin biogenesis. *J. Cell Sci.* **119**, 4381–4389

Simons, M., Krämer, E.-M., Thiele, C., Stoffel, W., and Trotter, J. (2000) Assembly of myelin by association of proteolipid protein with cholesterol- and galactosylceramide-rich membrane domains. *J. Cell Biol.* **151**, 143–154

Singh, P., Hanson, P. S., and Morris, C. M. (2017) Sirtuin-2 protects neural cells from oxidative stress and is elevated in neurodegeneration. *Parkinsons. Dis.* 10.1155/2017/2643587

Skoff, R. P. (1995) Programmed cell death in the dysmyelinating mutants. *Brain Pathol.* **5**, 283–288

Smolders, I., Smets, I., Maier, O., vandeVen, M., Steels, P., and Ameloot, M. (2010) Simvastatin interferes with process outgrowth and branching of oligodendrocytes. *J. Neurosci. Res.* **88**, 3361–3375

Snaidero, N., and Simons, M. (2017) The logistics of myelin biogenesis in the central nervous system. *Glia*. **65**, 1021–1031

Snaidero, N., Möbius, W., Czopka, T., Hekking, L. H. P., Mathisen, C., Verkleij, D., Goebbels, S., Edgar, J., Merkler, D., Lyons, D. A., Nave, K. A., and Simons, M. (2014) Myelin membrane wrapping of CNS axons by PI(3,4,5)P3-dependent polarized growth at the inner tongue. *Cell*. **156**, 277–290

Soldán, M. M. P., and Pirko, I. (2012) Biogenesis and significance of central nervous system myelin. *Semin Neurol.* **32**, 009–014

Song, J., O'connor, L. T., Yu, W., Baas, P. W., and Duncan, I. D. (1999) Microtubule alterations in cultured taiep rat oligodendrocytes lead to deficits in myelin membrane formation. *J. Neurocytol.* **28**, 671–684

Sorg, B. A., Smith, M. M., and Campagnoni, A. T. (1987) Developmental expression of the myelin proteolipid protein and basic protein mRNAs in normal and dysmyelinating mutant mice. *J. Neurochem.* **49**, 1146–1154

Sorg, B. J. A., Agrawal, D., Agrawal, H. C., and Campagnoni, A. T. (1986) Expression of myelin proteolipid protein and basic protein in normal and dysmyelinating mutant mice. *J. Neurochem.* **46**, 379–387

Southwood, C. M., Peppi, M., Dryden, S., Tainsky, M. A., and Gow, A. (2007) Microtubule deacetylases, SirT2 and HDAC6, in the nervous system. *Neurochem. Res.* **32**, 187–195

Stolt, C. C., Rehberg, S., Ader, M., Lommes, P., Riethmacher, D., Schachner, M., Bartsch, U., and Wegner, M. (2002) Terminal differentiation of myelin-forming oligodendrocytes depends on the transcription factor Sox10. *Genes Dev.* **16**, 165–170

Suzuki, K., and Koike, T. (2007) Mammalian Sir2-related protein (SIRT) 2-mediated modulation of resistance to axonal degeneration in slow Wallerian degeneration mice: a crucial role of tubulin deacetylation. *Neuroscience*. **147**, 599–612

Takahashi, N., Roach, A., Teplow, D. B., Prusiner, S. B., and Hood, L. (1985) Cloning and characterization of the myelin basic protein gene from mouse: one gene can encode both 14 kd and 18.5 kd MBPs by alternate use of exons. *Cell*. **42**, 139–148

Takahashi, N., Sakurai, T., Davis, K. L., and Buxbaum, J. D. (2011) Linking oligodendrocyte and myelin dysfunction to neurocircuitry abnormalities in schizophrenia. *Prog. Neurobiol.* **93**, 13–24

Tang, B. L., and Chua, C. E. L. (2008) SIRT2, tubulin deacetylation, and oligodendroglia differentiation. *Cell Motil. Cytoskeleton*. **65**, 179–182

Tang, X., Beesley, J. S., Grinspan, J. B., Seth, P., Kamholz, J., and Cambi, F. (1999) Cell cycle arrest induced by ectopic expression of p27 is not sufficient to promote oligodendrocyte differentiation. **279**, 270–279

Tanno, M., Sakamoto, J., Miura, T., Shimamoto, K., and Horio, Y. (2007) Nucleocytoplasmic shuttling of the NAD+-dependent histone deacetylase SIRT1. *J. Biol. Chem.* **282**, 6823–6832

Taylor, D. M., Balabadra, U., Xiang, Z., Woodman, B., Meade, S., Amore, A., Maxwell, M. M., Reeves, S., Bates, G. P., Luthi-Carter, R., Lowden, P. A. S., and Kazantsev, A. G. (2011) A brain-permeable small molecule reduces neuronal cholesterol by inhibiting activity of sirtuin 2 deacetylase. *ACS Chem. Biol.* **6**, 540–546

Thompson, A. J., Kermode, A. G., MacManus, D. G., Kendall, B. E., Kingsley, D. P., Moseley, I. F., and McDonald, W. I. (1990) Patterns of disease activity in multiple sclerosis: clinical and magnetic resonance imaging study. *Br. Med. J.* **300**, 631–634

Tompkins, S. M., Padilla, J., Dal Canto, M. C., Ting, J. P.-Y., Van Kaer, L., and Miller, S. D. (2002) De novo central nervous system processing of myelin antigen is required for the initiation of experimental autoimmune encephalomyelitis. *J. Immunol.* **168**, 4173–4183

Tosic, M., Dolivo, M., Amiguet, P., Domanska-Janik, K., and Matthieu, J.-M. (1993) Paralytic tremor (pt) rabbit: a sex-linked mutation affecting proteolipid protein-gene expression. *Brain Res.* **625**, 307–312

Trapp, B. D., Bernier, L., Andrews, S. B., and Colman, D. R. (1988) Cellular and subcellular distribution of 2′,3′-cyclic nucleotide 3′-phosphodiesterase and its mRNA in the rat central nervous system. *J. Neurochem.* **51**, 859–868

Tripathi, R. B., Clarke, L. E., Burzomato, V., Kessaris, N., Anderson, P. N., Attwell, D., and Richardson, W. D. (2011) Dorsally and ventrally derived oligodendrocytes have similar electrical properties but myelinate preferred tracts. *J. Neurosci.* **31**, 6809–6819

Tsai, H. H., Niu, J., Munji, R., Davalos, D., Chang, J., Zhang, H., Tien, A. C., Kuo, C. J., Chan, J. R., Daneman, R., and Fancy, S. P. J. (2016) Oligodendrocyte precursors migrate along vasculature in the developing nervous system. *Science.* **351**, 379–384

Tsunoda, I., Kuang, L.-Q., Libbey, J. E., and Fujinami, R. S. (2003) Axonal injury heralds virus-induced demyelination. *Am. J. Pathol.* **162**, 1259–1269

Tsunoda, I., Tanaka, T., Saijoh, Y., and Fujinami, R. S. (2007) Targeting inflammatory demyelinating lesions to sites of Wallerian degeneration. *Am. J. Pathol.* **171**, 1563–1575

Tuohy, V. K., Lu, Z., Sobel, R. A., Laursen, R. A., and Lees, M. B. (1989) Identification of an encephalitogenic determinant of myelin proteolipid protein for SJL mice. *J. Immunol.* **142**, 1523–1527

Tyler, W. A., Jain, M. R., Cifelli, S. E., Li, Q., Ku, L., Feng, Y., Li, H., and Wood, T. L. (2011) Proteomic identification of novel targets regulated by the mammalian target of rapamycin pathway during oligodendrocyte differentiation. *Glia*. **59**, 1754–1769

Uschkureit, T., Spörkel, O., Stracke, J., Büssow, H., and Stoffel, W. (2000) Early onset of axonal degeneration in double (plp−/−mag−/−) and hypomyelinosis in triple (plp−/− mbp−/−mag−/−) mutant mice. *J. Neurosci.* **20**, 5225–5233

Vallstedt, A., Klos, J. M., and Ericson, J. (2005) Multiple Dorsoventral Origins of Oligodendrocyte Generation in the Spinal Cord and Hindbrain. *Neuron*. **45**, 55–67

Vaquero, A., Scher, M. B., Lee, D. H., Sutton, A., Cheng, H.-L., Alt, F. W., Serrano, L., Sternglanz, R., and Reinberg, D. (2006) SirT2 is a histone deacetylase with preference for histone H4 Lys 16 during mitosis. *Genes Dev.* **20**, 1256–1261

Verheijen, M. H. G., Camargo, N., Verdier, V., Nadra, K., de Preux Charles, A.-S., Médard, J.-J., Luoma, A., Crowther, M., Inouye, H., Shimano, H., Chen, S., Brouwers, J. F., Helms, J. B., Feltri, M. L., Wrabetz, L., Kirschner, D., Chrast, R., and Smit, A. B. (2009) SCAP is required for timely and proper myelin membrane synthesis. *Proc. Natl. Acad. Sci. U. S. A.* **106**, 21383–21388

Voelter-Mahlknecht, S., Ho, A.D., & Mahlknecht, U. (2005). FISH-mapping and genomic organization of the NAD-dependent histone deacetylase gene, Sirtuin 2 (Sirt2). *Int J Oncol.* 27, 1187–1196

Wahl, S. E., McLane, L. E., Bercury, K. K., Macklin, W. B., and Wood, T. L. (2014) Mammalian target of rapamycin promotes oligodendrocyte differentiation, initiation and extent of CNS myelination. *J. Neurosci.* **34**, 4453–4465

Walker, A. K., Yang, F., Jiang, K., Ji, J. Y., Watts, J. L., Purushotham, A., Boss, O., Hirsch, M. L., Ribich, S., Smith, J. J., Israelian, K., Westphal, C. H., Rodgers, J. T., Shioda, T., Elson, S. L., Mulligan, P., Najafi-Shoushtari, H., Black, J. C., Thakur, J. K., Kadyk, L. C., Whetstine, J. R., Mostoslavsky, R., Puigserver, P., Li, X., Dyson, N. J., Hart, A. C., and Näär, A. M. (2010) Conserved role of SIRT1 orthologs in fasting-dependent inhibition of the lipid/cholesterol regulator SREBP. *Genes Dev.* **24**, 1403–1417

Wang, E., Dimova, N., Sperle, K., Huang, Z., Lock, L., McCulloch, M. C., Edgar, J. M., Hobson, G. M., and Cambi, F. (2008) Deletion of a splicing enhancer disrupts PLP1/DM20 ratio and myelin stability. *Exp. Neurol.* **214**, 322–330

Wang, F., and Tong, Q. (2009) SIRT2 suppresses adipocyte differentiation by deacetylating FOXO1 and enhancing FOXO1's repressive interaction with PPARγ. *Mol. Biol. Cell*. **20**, 801–808

Wang, F., Nguyen, M., Qin, F. X.-F., and Tong, Q. (2007) SIRT2 deacetylates FOXO3a in response to oxidative stress and caloric restriction. *Aging Cell*. **6**, 505–514

Wang, M., Doucette, J. R., and Nazarali, A. J. (2011) Conditional Tet-regulated over-expression of Hoxa2 in CG4 cells increases their proliferation and delays their differentiation into oligodendrocyte-like cells expressing myelin basic protein. *Cell. Mol. Neurobiol.* **31**, 875–886

Wang, X., Sato, R., Brown, M. S., Hua, X., and Goldstein, J. L. (1994) SREBP-1, a membrane-bound transcription factor released by sterol-regulated proteolysis. *Cell*. **77**, 53–62

Wang, Y.-P., Zhou, L.-S., Zhao, Y.-Z., Wang, S.-W., Chen, L.-L., Liu, L.-X., Ling, Z.-Q., Hu, F.-J., Sun, Y.-P., Zhang, J.-Y., Yang, C., Yang, Y., Xiong, Y., Guan, K.-L., and Ye, D. (2014) Regulation of G6PD acetylation by SIRT2 and KAT9 modulates NADPH homeostasis and cell survival during oxidative stress. *EMBO J.* **33**, 1304–1320

Warf, B. C., Fok-Seang, J., and Miller, R. H. (1991) Evidence for the ventral origin of oligodendrocyte precursors in the rat spinal cord. *J. Neurosci.* **11**, 2477–2488

Werner, H. B., Krämer-Albers, E. M., Strenzke, N., Saher, G., Tenzer, S., Ohno-Iwashita, Y., De Monasterio-Schrader, P., Möbius, W., Moser, T., Griffiths, I. R., and Nave, K. A. (2013) A critical role for the cholesterol-associated proteolipids PLP and M6B in myelination of the central nervous system. *Glia*. **61**, 567–586

Werner, H. B., Kuhlmann, K., Shen, S., Uecker, M., Schardt, A., Dimova, K., Orfaniotou, F., Dhaunchak, A., Brinkmann, B. G., Mobius, W., Guarente, L., Casaccia-Bonnefil, P., Jahn, O., and Nave, K.-A. (2007) Proteolipid protein is required for transport of sirtuin 2 into CNS myelin. *J. Neurosci.* **27**, 7717–7730

Willard, H. F., and Riordan, J. R. (1985) Assignment of the gene for myelin proteolipid protein to the X chromosome: implications for X-linked myelin disorders. *Science.* **230**, 940–942

Wis´niewski, H., and Morell, P. (1971) Quaking mouse: ultrastructural evidence for arrest of myelinogenesis. *Brain Res.* **29**, 63–73

World Health Organization (2008) Atlas: Multiple Sclerosis Resources in the World 2008.

Wu, G., Song, C., Lu, H., Jia, L., Yang, G., Shi, X., and Sun, S. (2014) Sirt2 induces C2C12 myoblasts proliferation by activation of the ERK1/2 pathway. *Acta Biochim. Biophys. Sin.* **46**, 342–345

Wu, J. I., Reed, R. B., Grabowski, P. J., and Artzt, K. (2002) Function of quaking in myelination: regulation of alternative splicing. *Proc. Natl. Acad. Sci. U. S. A.* **99**, 4233–4238

Wu, J., Zhou, L., Tonissen, K., Tee, R., and Artzt, K. (1999) The quaking I-5 protein (QKI-5) has a novel nuclear localization signal and shuttles between the nucleus and the cytoplasm. *J. Biol. Chem.* **274**, 29202–29210

Xie, W., Song, C., Young, N. L., Sperling, A., Xu, F., Sridharan, R., Conway, A., Garcia, B. A., Plath, K., Clark, A., and Grunstein, M. (2009) Histone H3 lysine 56 acetylation is linked to the core transcriptional network in human embryonic stem cells. *Mol. Cell*. **33**, 417–427

Xin, M., Yue, T., Ma, Z., Wu, F., Gow, A., and Lu, Q. R. (2005) Myelinogenesis and axonal recognition by oligodendrocytes in brain are uncoupled in Olig1-null mice. *J. Neurosci.* **25**, 1354 -1365

Xu, Y., Li, F., Lv, L., Li, T., Zhou, X., Deng, C.-X., Guan, K.-L., Lei, Q.-Y., and Xiong, Y. (2014) Oxidative stress activates SIRT2 to deacetylate and stimulate phosphoglycerate mutase. *Cancer Res.* **74**, 3630–3642

Yabe, D., Xia, Z.-P., Adams, C. M., and Rawson, R. B. (2002) Three mutations in sterol-sensing domain of SCAP block interaction with insig and render SREBP cleavage insensitive to sterols. *Proc. Natl. Acad. Sci. U. S. A.* **99**, 16672–16677

Yang, T., Espenshade, P. J., Wright, M. E., Yabe, D., Gong, Y., Aebersold, R., Goldstein, J. L., and Brown, M. S. (2002) Crucial step in cholesterol homeostasis: Sterols promote binding of SCAP to INSIG-1, a membrane protein that facilitates retention of SREBPs in ER. *Cell.* **110**, 489–500

Yuan, F., Xu, Z.-M., Lu, L.-Y., Nie, H., Ding, J., Ying, W.-H., and Tian, H.-L. (2016) SIRT2 inhibition exacerbates neuroinflammation and blood–brain barrier disruption in experimental traumatic brain injury by enhancing NF-κB p65 acetylation and activation. *J. Neurochem.* **136**, 581–593

Zearfoss, N. R., Clingman, C. C., Farley, B. M., McCoig, L. M., and Ryder, S. P. (2011) Quaking regulates Hnrnpa1 expression through its 3' UTR in oligodendrocyte precursor cells. *PLoS Genet.* **7**, e1001269

Zhang, Y., Chen, K., Sloan, S. A., Bennett, M. L., Scholze, A. R., O'Keeffe, S., Phatnani, H. P., Guarnieri, P., Caneda, C., Ruderisch, N., Deng, S., Liddelow, S. A., Zhang, C., Daneman, R., Maniatis, T., Barres, B. A., and Wu, J. Q. (2014) An RNA-sequencing transcriptome and

splicing database of glia, neurons, and vascular cells of the cerebral cortex. *J. Neurosci.* **34**, 11929–11947

Zhang, Y., Lu, Z., Ku, L., Chen, Y., Wang, H., and Feng, Y. (2003) Tyrosine phosphorylation of QKI mediates developmental signals to regulate mRNA metabolism. *EMBO J.* **22**, 1801–1810

Zhao, L., Ku, L., Chen, Y., Xia, M., Lopresti, P., and Feng, Y. (2006a) QKI binds MAP1B mRNA and enhances MAP1B expression during oligodendrocyte development. *Mol. Biol. Cell*. **17**, 4179–4186

Zhao, L., Mandler, M. D., Yi, H., and Feng, Y. (2010) Quaking I controls a unique cytoplasmic pathway that regulates alternative splicing of myelin-associated glycoprotein. **107**, 19061–19066

Zhao, L., Tian, D., Xia, M., Macklin, W. B., and Feng, Y. (2006b) Rescuing qk^{v} dysmyelination by a single isoform of the selective RNA-binding protein QKI. *J. Neurosci.* **26**, 11278–11286

Zhu, H., Zhao, L., Wang, E., Dimova, N., Liu, G., Feng, Y., and Cambi, F. (2012) The QKI-PLP pathway controls SIRT2 abundance in CNS myelin. *Glia*. **60**, 69–82

Zilberman, Y., Ballestrem, C., Carramusa, L., Mazitschek, R., Khochbin, S., and Bershadsky, A. (2009) Regulation of microtubule dynamics by inhibition of the tubulin deacetylase HDAC6. *J. Cell Sci.* **122**, 3531–3541